RNI No. MAHENG / 2017 / 74063
VOLUME 4 (Issue I) July - Dec 2020

ISSN No. 2581-5911
BI-ANNUAL SUBSCRIPTION : Rs. 2000/-

G P GLOBALIZE RESEARCH JOURNAL OF CHEMISTRY

CODEN : GPGRAG

Abstracted in
Chemical Abstracts (CAS), USA

International Scientific Indexing (ISI)
Impact Factor 1.022

International Society for Research Activity Journal
Impact Factor 0.615

International Institute of Organized Research (I2OR)
Impact Factor 1.405

GAURANG PUBLISHING

GAURANG PUBLISHING GLOBALIZE
PRIVATE LIMITED

RNI No. MAHENG/2017/74063

ISSN (Print) No. 2581–5911
CODEN : GPGRAG

Volume 4 Issue 1 ❖ July – December 2020

G P GLOBALIZE RESEARCH JOURNAL OF CHEMISTRY

Abstracted in Chemical Abstracts (CAS), USA
International Scientific Indexing (ISI) Impact Factor 1.022 (2019-2020)
International Institute of Organized Research (I2OR) Impact Factor 1.405
ISRA Journal Impact Factor 0.615

Supported by **ASSOCIATION OF CHEMISTRY TEACHERS**, the National Registered Organisation of Chemistry Educators of India
Registration No. Maharashtra Government, Mumbai, 922, 2010 G.B.B.S.D. dated 08.04.2010.
Website: www.associationofchemistryteachers.org

GAURANG PUBLISHING GLOBALIZE PRIVATE LIMITED, MUMBAI
CIN No. U22130MH2016PTC287238
UAN - MH19D0008178

Published by:
Gaurang Publishing Globalize Private Limited, Mumbai
1, Plot 72, Pandit M.M.M. Marg, Tardeo, Mumbai 400 034.
Email: gpglobalize@gmail.com ❖ www.gpglobalize.in
Tel: +91 9969392245
CIN No. U22130MH2016PTC287238

ISSN (Print) No: 2581-5911
CODEN : GPGRAG

Printed at: Nil Creation, Girgaum, Mumbai - 400 004, India.

GP GLOBALIZE RESEARCH JOURNAL OF CHEMISTRY

An International Peer Reviewed Journal of Chemistry

RNI No: MAHENG/2017/74063 **ISSN (Print) No: 2581-5911**
ISI Impact Factor 1.022 (2019-2020) **CODEN : GPGRAG**

Printed and Published by Gaurang Rajan Pendurkar on behalf of Gaurang Publishing Globalize Private Limited and printed at NIL CREATION, Shop No. 7, 35/55, Bandu Gokhale Path, Mugbhat Cross Lane, Jivanji Maharaj Chawl (Shree Swami Samarth Nagar), Girgaon, Mumbai 400004 and published at Gaurang Publishing Globalize Private Limited 1, Plot 72, P M M M Marg, Tardeo, Mumbai-400034.

Editor-in-Chief Dr. D.V. Prabhu.

Editorial Board

Editorial Board

Editorial Board

Editorial Board

G P GLOBALIZE RESEARCH JOURNAL OF CHEMISTRY

RNI No: MAHENG/2017/74063 **ISSN No. (Print): 2581-5911**
ISI Impact Factor 1.022 (2019-2020) **CODEN : GPGRAG**

GUIDELINES TO AUTHORS

GP Globalize Research Journal of Chemistry is an international peer reviewed journal which publishes full length research papers, short communications, review articles and book reviews covering all areas of Chemistry including Environmental Chemistry. G P Globalize Research Journal of Chemistry is a biannual journal published in English in print and online versions.

(1) Manuscript Preparation

a) Page Layout: A4 (21 cm x 29.7 cm) leaving 2.5 cm margin on all sides of the text. All the text should be in Times New Roman font, double spaced and pages should be numbered consecutively.

b) Use MS word (2003-2007) for text and TIFF, JPEG or Paint for figures.

c) The first page should contain title in bold, 14 point size, name/s of author/s in bold, 12 point size, affiliation/s-address, email id and contact number in 11 point size, abstract-up to 200 words in 11 point size, keywords-between 5 to 10 keywords in 11 point size.

d) Main Text- The paper should be divided into the following sections:

Introduction, Materials and Methods, Results and Discussion, Conclusions, Acknowledgement and References.

Tables and Figures of good resolution (600 dpi) should be numbered consecutively and given in the order of their appearance in the text and should not be given on separate pages.

e) References- References should be cited in the text as superscript numbers in order of appearance.

References at the end of the paper should be listed in serial order to match their order of appearance in the text. Names of journals should be in italics and volume number should be in bold.

Reference to papers e.g. Ganesh R.S., Pravin S. and Rao T.P., 2005, *Talanta,* **66,** 513.

Reference to books e.g. Lee J.D., 1984, A New Course in Inorganic Chemistry, 3rd ed., ELBS and Van Nostrand Reinhold (UK) Co. Ltd., p.268-269.

f) Abbreviations should be explained at first appearance in the text.

g) Nomenclature should be as per **IUPAC** guidelines.

h) SI units should be used throughout.

(2) Manuscript Submission

Manuscripts should be submitted online at dvprabhu48@gmail.com. The paper will be accepted for publication after review. All correspondence should be made to the Editor- in-Chief at dvprabhu48@gmail.com.

(3) Proofs

Galley proofs will be sent online to the corresponding author on request and should be returned to the Editorial office within seven working days.

(4) Plagiarism

GP Globalize Research Journal of Chemistry is committed to avoid plagiarism and ensure that only original research work is published. The journal follows a Zero Tolerance Policy on Plagiarism.

The Editorial Board and panel of reviewers will check and prevent plagiarism in the manuscripts submitted for publication.

(5) Copyright

Publication of a paper in GP Globalize Research Journal of Chemistry automatically transfers copyright to the publisher. Authors can share free eprints of their published papers with fellow researchers.

(6) Circulation and Subscription Rates

The Journal is published twice a year - January and July

Subscription rates are as follows:

Library/Institutional Charges (In India)	Rs. 2000/-
Individual Charges (In India)	Rs. 2000/-
Library/Institutional Charges (Outside India)	US $ 100
Individual Charges (Outside India)	US $ 100

Subscription Charges:
Review of research papers is done free of charge. There is no charge for processing of manuscripts. Subscription to the Journal is welcome.

Mode of Payment:

Demand draft/Multicity cheque payable at Mumbai in favour of **"Gaurang Publishing Globalize Pvt. Ltd. Mumbai"**

For Online Payment:

Name of the Bank	**:**	**Axis Bank**
Branch Name	**:**	**Tardeo, Mumbai (MH)**
Account No.	**:**	**916020066451552**
IFSC Code	**:**	**UTIB0001345**

For further details please contact:

Dr. D.V. Prabhu, Editor-in-Chief,
Email: dvprabhu48@gmail.com
Mobile: 09870 226 899

Mr. Rajan Pendurkar, Managing Editor,
Email: gpglobalize@gmail.com
Mobile: 09969 392 245

A Request to Authors

We thank you for sending your research paper to G P Globalize Research Journal of Chemistry (RNI No. MAHENG/2017/74063 ISSN No. (Print): 2581-5911, CODEN : GPGRAG).

Review and processing of research papers is done free of charge.

You are requested to send a DD/Multicity Cheque for Rs. 2000/- in favour of ***"Gaurang Publishing Globalize Pvt. Ltd., Mumbai"*** *payable at Mumbai,* ***as subscription charges.***

We would appreciate if you help us in our efforts to promote academic excellence.

G P GLOBALIZE RESEARCH JOURNAL OF CHEMISTRY

RNI No: MAHENG/2017/74063 **ISSN No. (Print): 2581-5911**
ISI Impact Factor 1.022 (2019-2020) **CODEN : GPGRAG**

Volume 4 Issue 1 ❄ July - December 2020

CONTENTS

CONTENTS

RNI No. MAHENG/2017/74063
ISSN No. (Print) 2581-5911
ISI Impact Factor 1.022 (2019-2020)

Enhanced Photodegradation Efficiency of Cerium loaded ZnS using Solar Light

K. Meena[1], Gomathy Jayamani[1], M. Swaminathan[2] M. Shanthi[1*]
[1] Department of Chemistry, Annamalai University,
Annamalainagar 608 002, Tamil Nadu, India
[2] Nanomaterials Laboratory, Department of Chemistry,
Kalasalingam Academy of Research and Education, Krishnankoil, India
[*]**Email: shanthimsm@gmail.com; m.swaminathan@klu.ac.in**

Abstract
The Cerium loaded ZnS (Ce-ZnS) nanocatalyst was successfully synthesized by a simple hydrothermal method and characterized by X-ray diffraction (XRD), diffuse reflectance spectra (DRS), photoluminescence spectra (PL) and X-ray photo electron spectroscopy (XPS). The photocatalytic activity of Ce-ZnS was investigated for the degradation of naphthol blue black (NBB) dye in aqueous solution using solar light. Cerium loading shifts the absorbance of ZnS to the entire visible region. Ce-ZnS is found to be more efficient than ZnS, TiO_2 (anatase), nano ZnO and ZnO at pH 7 for the mineralization of NBB dye under solar light. The influence of operational parameters such as the amount of photocatalyst, dye concentration and initial pH on photomineralization of NBB has been analyzed and discussed. The mineralization of NBB dye has been confirmed by COD measurements. The catalyst is found to be reusable. The mechanism of degradation of NBB dye by Ce-ZnS is proposed.

Keywords: *Ce-ZnS, Solar photocatalysis, Naphthol Blue Black, dye degradation*

Introduction

Textile effluent is known to have a strong colour, large amount of suspended solids, fluctuating pH and high chemical oxygen demand (COD).[1] Synthetic textile dyes can be structurally different and even a very low concentration of dyes in effluent is highly visible and undesirable.[2] Discharge of these dyes is undesirable not only for aesthetic reasons, but also because they may decrease the absorption of light by water, plants and phytoplankton reducing photosynthesis and the oxygenation of water.[3] Many azo dyes and their intermediate products are toxic and mutagenic (carcinogenic) to aquatic life and humans and they may also contain certain levels of heavy metals that breach environmental standards.[4] Due to large scale production, they can cause considerable environmental pollution and pose a risk to health[5]. Reactive textile dyes are extensively used for dyeing of textiles, and about 20-40% of these dyes are lost in the effluents. They exhibit a wide variability in chemical structure, primarily based on substituted aromatic and heterocyclic groups. A large

number of reactive dyes are azo compounds containing an azo bond (-N=N-). Since reactive dyes are highly soluble in water, their removal from wastewater is very difficult by conventional coagulation and activated sludge processes.[6-8]

Actually several physical, chemical and biological technologies are being evaluated for the treatment of textile wastewater. Advanced oxidation processes (AOP), particularly heterogeneous photocatalysis offer a new route for the oxidative degradation of organic compounds. In this process, a non-toxic semiconductor catalyst is employed as a photocatalyst. In recent years, the semiconductor metal oxides and metal sulphides are widely used as green photocatalysts in the field of wastewater remediation.[9-13]

One of the approaches to improve the photocatalytic activity of nanoparticles is doping. The optical, electrical and catalytic properties of the doped nanoparticles have been of great interest to researchers. The doped nanomaterials have been largely studied in recent years due to their widespread applications in various devices such as sensors, solar cells, lasers, photocatalysts, photodetectors, IR detectors, colour television and light emitting diodes.[14-19]

Rare elements are used as dopants to improve the luminescence and catalytic properties of nanoparticles because they have the special 4f-4f intra shell transition. In the present study, cerium (Ce) is one of the rare elements, used as a dopant to synthesize Ce doped ZnS nanoparticles. ZnS is one of the important semi-conducting materials. It is transparent in the visible spectral region having excitation binding energy of 40 meV.[20] Induced sub-band gap transitions in ZnS occur at energies in the visible range that allows the optical detection of traps, radioactive recombination centers and surface states.

Naphthol Blue Black (NBB) dye was selected as a model pollutant as it has the largest consumption among all acidic dyes. It is an industrially important acidic diazo dye, which has a high photo and thermal stability.

Photodegradation of pollutants using semiconductor modified catalyst with solar light can make it an economically viable process since solar energy is an abundant natural energy source. We can trap solar energy and utilize it. When the process is carried out using solar radiation, it becomes a green chemical process. In the present work, the photocatalytic activity of cerium doped ZnS nanocatalyst towards NBB dye degradation using solar light is studied.

Materials and Methods

Naphthol blue black (NBB) dye, obtained from Colour Chem., Pondicherry was used as received. Zinc nitrate hexahydrate (99%), sodium sulfide (99%), cerium ammonium sulfate (99%) were obtained from Himedia Chemicals. Nano ZnO obtained from Aldrich, ZnO (HiMedia) and TiO_2 (Merck) were used as received. Ferrous ammonium sulfate (Qualigens 98.5%), Potassium dichromate (SD Fine Chem. 99.5%), Silver sulfate (AR-HiMedia), Mercury sulfate (Merck) were used as received for COD analysis. AnalaR grade reagents H_2O_2, $K_2S_2O_8$, $KBrO_3$, Na_2CO_3 and NaCl (Merck) were used as received. Double distilled water was used to prepare experimental solutions. The pH of the solution before irradiation was adjusted using H_2SO_4 / NaOH.

Preparation of Cerium doped ZnS

Cerium loaded ZnS was prepared by hydrothermal method. 0.6 M zinc nitrate hexahydrate and 0.06 M sodium sulfide in deionized water were prepared separately. Equal volumes of the two solutions were mixed and the mixture was stirred for 2h to get zinc sulfide. To this ZnS suspension, 100 mL of ceric ammonium sulfate (CAS, 0.003 M) solution was added, stirred for 4h and sonicated for 2h. Then the mixture

was treated hydrothermally in a teflon lined stainless steel autoclove at 115^{0}C for 6 h. The precipitate obtained (Ce-ZnS) was filtered, washed thoroughly with distilled water, dried at 100^{0}C in an air oven for 2h. The dried Ce-ZnS catalyst was collected and used for further analysis. This catalyst contained 23.6 wt% of Cerium. Catalysts with 14.2, 18.9, 28.3, 33.0 wt % of Cerium-ZnS were prepared using the same procedure. ZnS was prepared using a similar procedure without the addition of ceric ammonium sulfate (CAS).

Analytical methods

Powder X-ray diffraction patterns of ZnS and Ce-ZnS catalysts were obtained using a Equinox 1000 Inel diffractometer equipped with a Cu tube for generating CuK_α radiation (wavelength 1.5406 A°) at 40 kV, 25 mA. Peak positions were compared with standard files to identify the crystalline phases. A Shimadzu UV 2600 UV-vis spectrophotometer was used to record the UV-visible diffuse reflectance spectra (DRS) of the catalysts. Photoluminescence (PL) spectra at room temperature (Excitation wavelength 300 nm) were recorded using a Perkin Elmer LS 55 fluorescence spectrometer. UV spectral measurements were done using UV-1650 PL Shimadzu UV-visible spectrophotometer. The pH of the solution was measured by ELICO (LI-LOT model) digital pH meter. X-ray photoelectron spectra of the catalyst was recorded in an ESCA-3 mark II spectrometer using AIK_α (1486.6 eV) as the radiation source.

Irradiation Experiments

For the photolysis experiment, the dye solution (NBB dye) of desired molar ratio was freshly prepared from the stock solution of the dye. NBB dye stock solution was used as synthetic waste water. All photocatalytic experiments were carried out under similar conditions on sunny days between 11 am and 2 pm. An open borosilicate glass tube of 50 mL capacity, 40 cm height and 20 mm diameter was used as the reaction vessel. The suspension was magnetically stirred in the dark for 30 min to attain adsorption-desorption equilibrium between dye and Ce-ZnS. Irradiation was carried out in open-air conditions. 50 mL of dye solution with Ce-ZnS was continuously aerated by a pump to provide oxygen and for the complete mixing of reaction solution. After dark adsorption, the first sample was taken. At specific time intervals, 2-3 mL of the sample was withdrawn and centrifuged to separate the catalyst. 1 mL of the centrifugate was suitably diluted and its absorbance at 318 nm was measured to monitor the dye concentration. Absorbance at 318 nm represents the aromatic part of NBB dye and its decrease indicates the degradation of dye.

Solar light intensity measurements

Solar light intensity was measured at intervals of 30 minutes and the average light intensity over the duration of each experiment was calculated. The sensor was always set in the position of maximum intensity. The intensity of solar light was measured using LT Lutron Lx-10/A Digital Lux Meter and the intensity was 1250x100± 100 lux. The intensity was found to be nearly constant during the experiments.

Chemical oxygen demand (COD) measurements

COD was determined using the following procedure. The dye sample was refluxed with $HgSO_4$ and known volumes of standard $K_2Cr_2O_7$, $AgSO_4$ and H_2SO_4 for 2h and titrated against standard ferrous ammonium sulphate (FAS) using ferroin as indicator. A blank titration was carried out using distilled water instead of dye sample. COD was determined by using the following equation:

$$COD=\frac{(\text{Blank titre value-Dye sample titre value})\times\text{normality of FAS}\times 8\times 1000}{\text{Volume of the sample}} \quad \text{.....(1)}$$

Results and Discussion

Characterization of Catalyst

Primary analysis of photocatalytic degradation of NBB dye with different Cerium loaded ZnS catalysts was carried out under solar light at 90 min of irradiation. The % degradation values of NBB dye for 14.2, 18.9, 23.6, 28.3 and 33.0 wt % of Cerium loading were 63.6, 78.4, 88.5, 71.2 and 52.1 respectively. The catalyst loaded with 23.6 wt % of cerium shows a higher degradation percentage. 23.6 wt % of cerium in the catalyst was found to be the optimum concentration.

The XRD patterns of bare ZnS and Ce-ZnS are shown in Fig.1. For the bare ZnS (Fig. 1(a)) diffraction peaks at 28.3, 47.6, and 56.2 correspond to (111), (220) and (311) planes of zinc blende structure which is one of the commonly available phases of ZnS.[21] In the Ce-ZnS system (Fig.1b) there is one new peak obtained with 2θ value of 28.9 corresponding to Ce^{4+} in CAS.[22] This confirms the loading of cerium. Broadening of the peak of Ce-ZnS indicates the reduction of crystallite size (22.3 nm) when compared to that of the bare ZnS (32.7 nm). The crystalline sizes of ZnS and Ce-ZnS were determined using Debye-Scherrer equation.

$$D=\frac{K\lambda}{\beta \cos \theta} \quad \text{.....(2)}$$

where D is the crystal size of the catalyst, K is a dimensionless constant (0.9), λ is the wavelength of X-ray, β is the full width at half maximum (FWHM) of the diffraction peak and è is the diffraction angle.

The diffuse reflectance spectra of bare ZnS and Ce-ZnS are given in Figs. 2(a) and (b) respectively. There is no significant change in absorbance in the UV range but there is a slight increase in absorbance from 400 nm to the entire visible region in Ce loaded ZnS. Dopant cerium extends the absorbance of ZnS to the entire visible region, which increases its visible light activity.

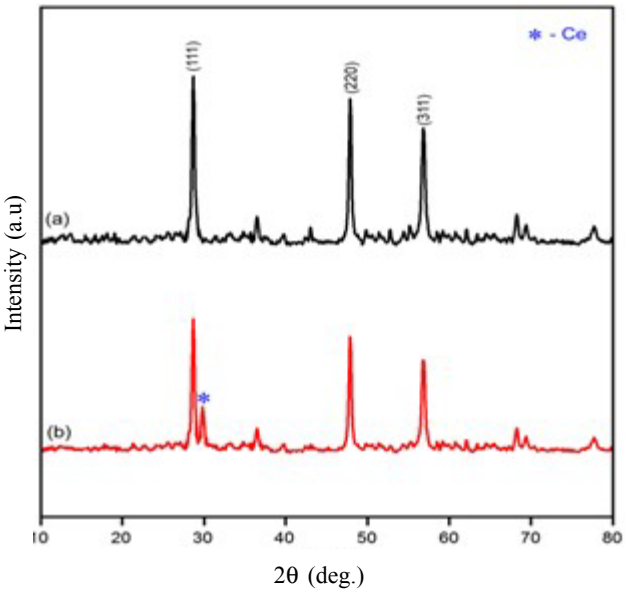

Fig.1. XRD patterns of a) bare ZnS and b) 23.6 wt % Ce-ZnS

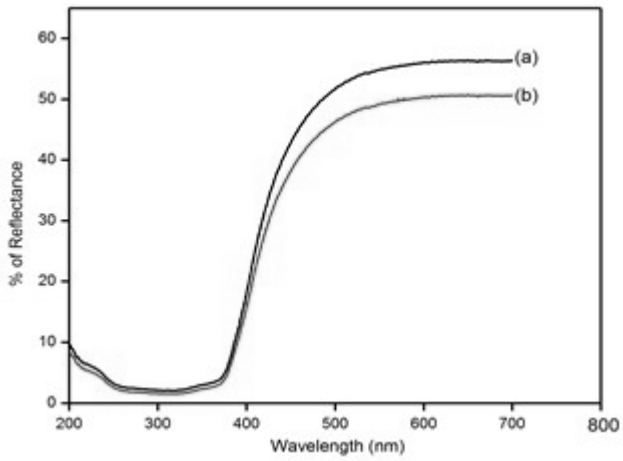

Fig. 2. DRS of a) bare ZnS and 23.6 wt % Ce-ZnS

In addition, the UV-vis spectra in the diffuse reflectance mode (R) were transformed to the Kubelka-Munk function F(R) to separate the extent of light absorption from scattering. The band gap value is obtained from the plot of the modified Kubelka-Munk function $(F(R)E)^{½}$ *vs* the energy of the absorbed light (E)

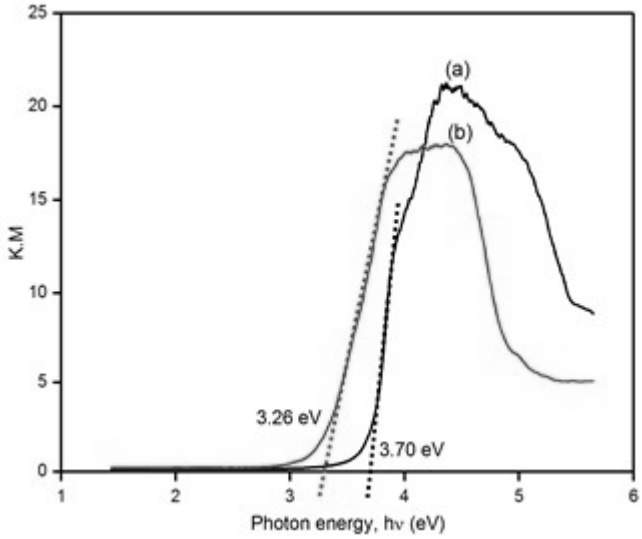

Fig. 3. KM plot of a) bare ZnS and b) 23.6 wt% Ce-ZnS

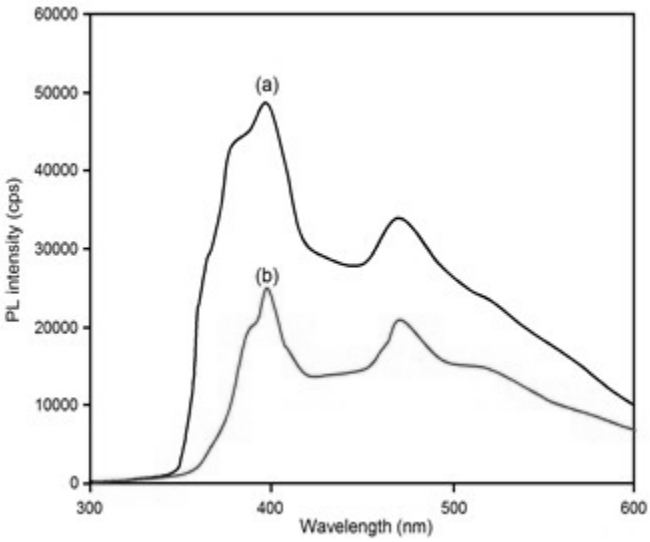

Fig. 4. PL spectra of a) bare ZnS and b) 23.6 wt% Ce-ZnS

(Fig. 3). The band gap energies of bare ZnS and Ce-ZnS were found to be 3.70 and 3.26 eV respectively.

Photoluminescence spectra of bare ZnS and Ce-ZnS are shown in Figures 4 (a) and (b) respectively. The photoluminescence occurs due to electron-hole recombination. The bare ZnS gave two emissions at 397 and 470 nm. The doping of Ce does not shift the emission wavelength of ZnS but the intensity of PL emission is less as compared to that of bare ZnS. This is because of suppression of recombination of electron-hole pairs by Ce, which enhanced the photocatalytic activity of the catalyst. In order to know the chemical state of Zn, S and Ce present in the catalyst, the XPS of the catalyst was taken. The XPS survey spectrum (Fig. 5a) of Ce-ZnS indicates the peaks of elements Zn, S and Ce. The binding energy peaks of Ce $3d_{5/2}$ and Ce $3d_{3/2}$ (Fig. 5b) observed at 885 and 904 eV, correspond to Ce^{4+}.[23] Zn $2p_{3/2}$ and Zn $2p_{1/2}$ occurred at 1022.2 eV and 1045.1 eV respectively (Fig. 5c), which confirmed the presence of Zn(II) in the catalyst. The S 2p peak of samples located at 169.1 eV (Fig. 5d) indicated the presence of the S^{2-}.[24]

Photodegradability of NBB dye

The photodegradability of NBB dye with different photocatalysts under solar light is shown in Fig. (6). 9.5% decrease in dye concentration occurred due to adsorption by Ce-ZnS in the absence of solar light (curve-c). The dye is resistant to self photolysis (curve-b). Simultaneous irradiation and aeration in the presence of Ce-ZnS catalyst caused 94.9 %degradation (curve-a) in 150 min. Based on these observations, we can say that both solar light and catalyst are needed for effective degradation of the NBB dye. When ZnS, TiO_2, Nano ZnO and ZnO were used under the same conditions 83.8 (curve-d), 77.6 (curve-e) 74.7 (curve-f) and 62.8 (curve-g) percentages of degradation occurred, respectively. This shows that Ce-ZnS is more efficient in NBB dye degradation than other catalysts.

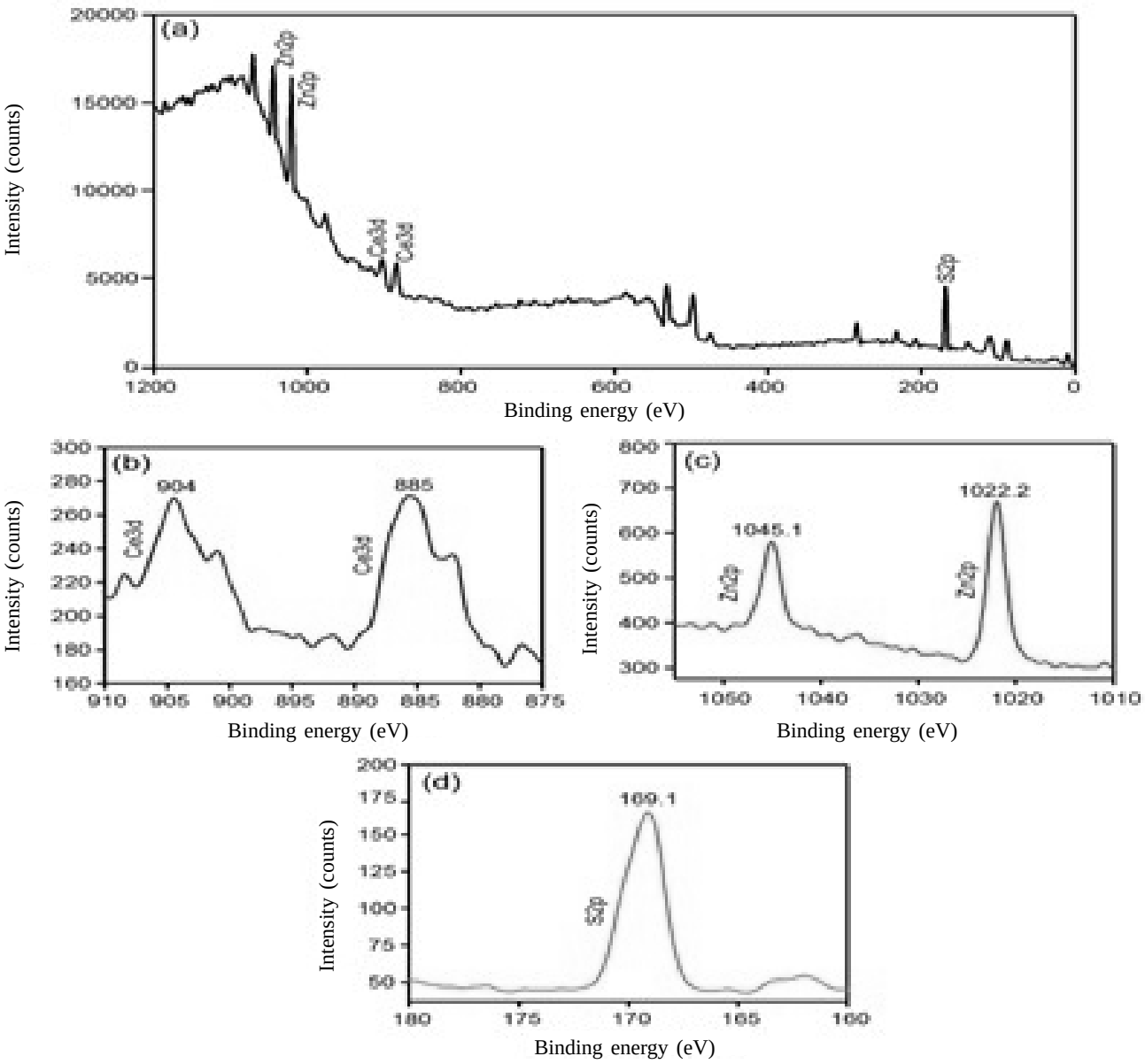

Fig. 5. XPS of 23.6 wt% Ce-ZnS: a) survey spectrum, b) Ce3d peak, c) Zn2p peak and S2p peak

Effect of Operational Parameters

Effect of catalyst weight

The amount of catalyst is one of the main parameters for degradation studies. In order to avoid the use of excess catalyst, it is necessary to find out the optimum loading for efficient removal of pollutant. Several authors have investigated the reaction rate as a function of catalyst loading in photocatalytic degradation process.[25-27] The effect of catalyst weight (Ce-ZnS nanoparticles) on the percentage removal of NBB dye was investigated from 50 to 150 mg/50 mL of the catalyst.

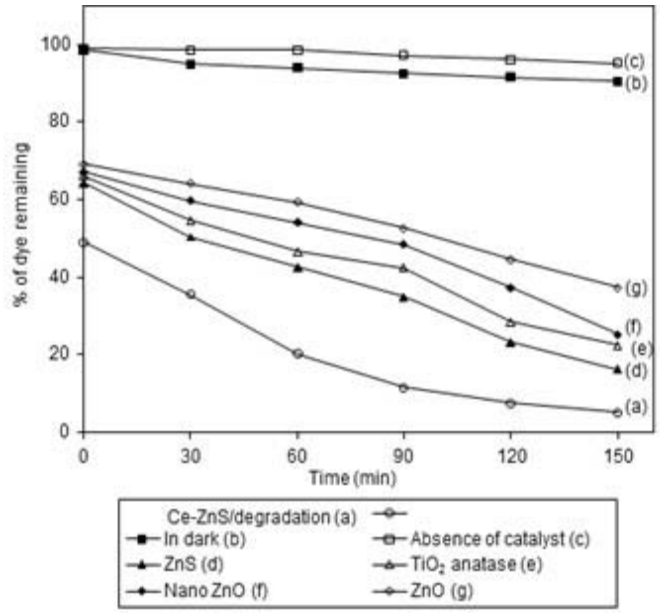

Fig. 6. Photodegradability of NBB dye using solar/Ce-ZnS nanoparticles: [NBB] = $2x10^{-4}$ mol/L, pH = 7.0±0.1, Ce-ZnS nanoparticles = 100 mg/50 mL, airflow rate = 8.1 mL s^{-1}, I_{solar} = 1250 x 100 ± 100 lux.

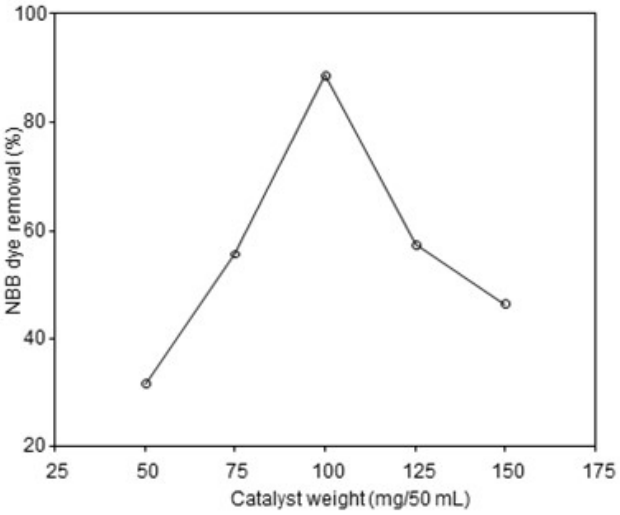

Fig. 7. Effect of catalyst weight on the photocatalytic degradation of NBB using solar light: [NBB] = $2x10^{-4}$ mol/L, pH = 7.0 ± 0.1, airflow rate = 8.1 mL s^{-1}, irradiation time = 90 min, I_{solar} = 1250 x 100 ± 100 lux.

The results are shown in Fig. 7. The results clearly show that the increase of catalyst weight from 50 to 100 mg increases the dye degradation from 31.5 to 88.5% using Ce-ZnS under solar light in 90 minutes.

This is due to an increase in the number of catalyst particles, which increases the absorption of photons and adsorption of pollutant (dye) molecules. Further increase of Ce-ZnS loading (above 100 mg/50 mL) decreases the removal rate. Increase of the catalyst loading beyond 100 mg/50 ml may cause screening effect. These effects reduce the specific activity of the catalyst. At high loading of catalyst, particle aggregation may also reduce the catalytic activity. The optimum amount of catalyst loading is found to be 100 mg/50 mL of the degradation of NBB dye.

Effect of solution pH

The solution pH plays an important role in the photo catalytic degradation process of various pollutants.[28,29] The effect of pH on the photodegradation of NBB dye was studied in the pH range 3-11 and the results are shown in Fig.8. The degradation efficiency is high at pH 7 and decreases when the pH is above or below 7. Hence the optimum pH for the efficient removal of NBB dye on Ce-ZnS is 7. In acidic pH range, the removal efficiency is less and it is due to the dissolution of ZnS. ZnS can react with acids to produce corresponding salts at low acidic pH values. Degradation efficiency of a catalyst depends on the adsorption of dye molecules. An experiment to verify dark adsorption of NBB dye under different pH was carried out. The percentages of adsorption at pH 3,5,7,9, and 11 were found to be 21.5, 36.2, 52.3, 43.4 and 31.2 respectively after the attainment of adsorption equilibrium (30 min). Maximum adsorption was observed at pH 7. Hence, the higher degradation efficiency is due to the strong adsorption of NBB dye on the catalyst surface.

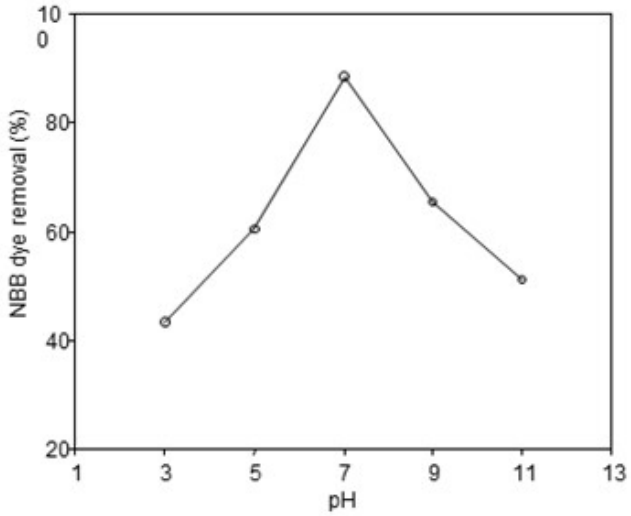

Fig. 8. Effect of initial pH on the degradation of NBB using solar light/Ce-ZnS nanoparticles: [NBB] = 2x10^{-4} mol/L, Ce-ZnS nanoparticles = 100 mg/50 mL, airflow rate = 8.1 mL s^{-1}, irradiation time = 90 min, I_{solar} = 1250 x 100 ± 100 lux.

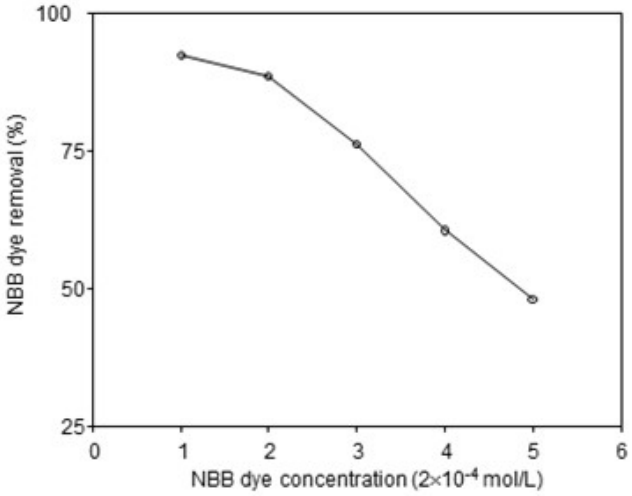

Fig. 9. Effect of various initial dye concentrations on the degradation of NBB using solar light/Ce-ZnS nanoparticles: pH = 7.0±0.1, Ce-ZnS nanoparticles = 100 mg/50 mL, airflow rate = 8.1 mL s^{-1}, irradiation time = 90 min, I_{solar} = 1250 x 100 ± 100 lux.

Effect of initial dye concentration

The effect of various initial dye concentrations on the degradation of NBB dye on Ce-ZnS catalyst surface has been investigated. Increase of dye concentration from 1 to 5x10^{-4} mol/L decreases the degradation from 92.4 to 48.2 % in 90 min of solar light irradiation time (Fig.9). The possible explanation for this behaviour is at high initial dye concentration, the path length of photon entering into the solution also decreases. Thus, the photocatalytic degradation efficiency decreases, but at low concentration, the reverse effect is observed thereby increasing the number of photons absorbed by the catalyst.[30] The large amount of adsorbed dye may also have a competing effect on the adsorption of oxygen and OH^- onto the surface of catalyst.

Stability of the catalyst

The stability of the catalyst Ce-ZnS was tested for the degradation of NBB dye in solar light. Fig.10 shows the degradation of NBB dye using the same Ce-ZnS nanocatalyst for 3 consecutive runs. About 94.9% of

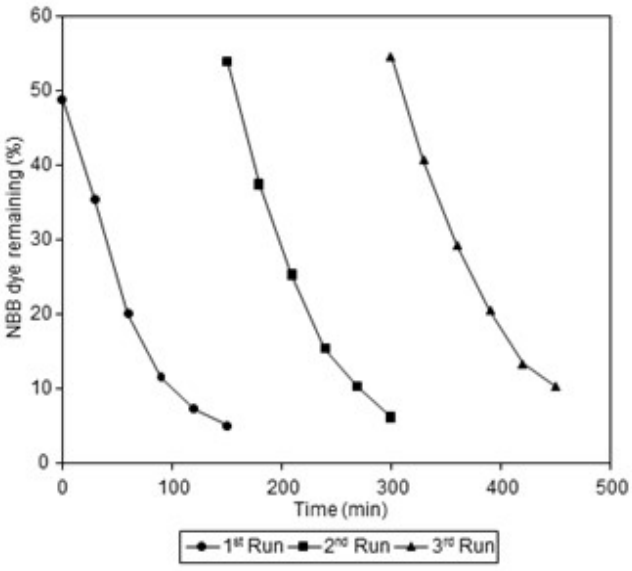

Fig. 10. Catalyst reusability: [NBB] = 2x10^{-4} mol/L, pH = 7.0±0.1, Ce-ZnSnanoparticles = 100 mg/50 mL, airflow rate = 8.1 mL s^{-1}, irradiation time = 90 min, I_{solar} = 1250 x 100 ± 100 lux

dye removal took place at 150 min, in the first run. In the second and third runs, the dye degradation percentages are 93.8 and 89.7 respectively. Even in the third run, the catalyst shows 89.7 % degradation efficiency. This shows that the catalyst is found to be more stable and reusable under solar light.

COD Analysis

To confirm the mineralization of NBB dye, the degradation was also analyzed by COD values. The percentage of COD reduction after 150 min of irradiation was 89% (Table 1), which indicates that the complete mineralization of dye had occurred. Mineralization of NBB dye was also revealed by the formation of CO_2 during photodegradation. Carbon dioxide formation was tested by passing the gas evolved during photodegradation into lime water.

Table 1. COD removal rate by Ce–ZnS nanoparticles

[NBB]=210^{-4} mol/L, Ce-ZnSnanoparticles=100 mg/50mL

pH = 7.0±0.1, I_{solar} = 1250 x 100 ± 100 lux

Time (min)	COD reduction (%)
0	0
90	56
150	89

Mechanism of dye degradation

The photocatalytic process is initiated by the illumination of a semiconductor catalyst (Ce-ZnS) with radiation of energy higher than the band gap energy of the semiconductor. This irradiation generates electrons (e^-) and holes (h^+) in the conduction band (CB) and valence band (VB) respectively as shown in Scheme 1. In general, these electron-holes recombined to decrease the catalytic activity of semiconductor. But the presence of Cerium (Ce) traps the electron from CB of ZnS, which suppresses the electron-hole recombination. The oxygen adsorbed on the surface of photocatalyst can trap the photogenerated electrons[31] and the electron transfer to O_2 may be the rate-determining step in semiconductor photocatalysis[32]. Nevertheless, Ce^{4+} easily traps the photoexcited electron in the system of Ce-loaded ZnO catalyst. Ce^{4+} ion, as a Lewis acid, has higher ability in trapping the electron than oxygen molecule (O_2) [33]. The trapped electrons are transferred to the adsorbed O_2 synergistically to form superoxide radicals, so that the recombination between electrons and holes is reduced. The highly reactive superoxide radical anion and hydroxyl radical are used for the degradation of pollutant.

$$Ce^{4+} + e^- \rightarrow Ce^{3+}$$
$$Ce^{3+} + O_2 \rightarrow O_2^{\bullet -} + Ce^{4+}$$

Therefore it can be seen that the Ce 4f level in Ce-ZnS plays an important role in the interfacial charge transfer and inhibition of electron-hole recombination, which facilitates increase the photocatalytic activity of Ce-ZnS photocatalyst.

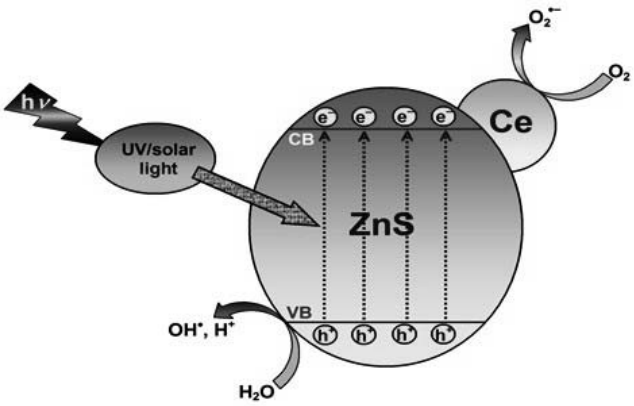

Dye / Dye^+ + $O_2^{\leftarrow}$ → Mineral acids + $Co_2\uparrow$ + H_2O
Dye / Dye^+ + ^+HO → Mineral acids + $Co_2\uparrow$ + H_2O

Scheme 1. Mechanism of degradation of NBB dye by Ce-ZnS

Conclusions

We have prepared Ce-ZnS catalyst by hydrothermal method. The presence of Cerium is evidenced by XRD and XPS. Dopant Cerium decreases the crystallite size and increases the visible light absorbance. Ce-ZnS nano

catalyst possesses high solar photocatalytic activity for the degradation of NBB dye under optimized reaction conditions. Ce^{4+} ion, as a Lewis acid, traps the electrons and transfers them to the adsorbed O_2 synergistically to form superoxide radicals, so that the recombination between electrons and holes is reduced, as revealed by photoluminescence spectra. This research work is relevant to water treatment and the results can make important changes in industrial effluent treatment. The dyeing industries can utilize the results for the design of more efficient effluent treatment plants.

References

1. Forgacs E., Cserhati, T., and Oros G., 2004, *Environ. Int.*, **30**, 953.
2. Meric S., Kaptan D., and Olmez T., 2004, *Chemosphere*, **54**, 435.
3. Ozdemir O., Armagan B., Turan M., and Celik M.S., 2004, *Dyes and Pigments*, **62**, 49.
4. Lawless D., Serpone N., and Meisel D., 1991, *J. Phys. Chem.*, **95**, **(13),** 5166.
5. Fang X., and Wu J., 1999, *Radiation Phys. Chem.*, **55**, **(4),** 465.
6. Nigam P., Armour G., Banat I.M., Singh D., and Marchat R., 2000, *Bio. Technol.*, **72(3)**, 219.
7. Van der zee F.P., Lettinga G. and Filed J.A., 2001, *Chemosphere*, **44**, 1169.
8. Karacakaya P., Kilic N.K., Duygu E. and Donmez G., 2009 *J. Hazard. Mater*., **172**, 1635.
9. Sobana N., Krishnakumar B. and Swaminathan M., 2013, *Mater. Sci. Semicon. Proc.*, **16,** 1046.
10. Neppolian B., Choi H.C., Sakthivel S., Arabindoo B. and Murugesan V., 2002, *J. Hazard. Mater. B.*, **89**, 303.
11. Kansal S.K., Singh M., and Sud D., 2007, *J. Hazard. Mater.*, **147**, 581.
12. Lizama C., Freer J., Baeza J. and Mansilla H.D., 2002, *Catal. Today*, **76**, 235.
13. Akyol A., Yatmaz H.C., and Bayramoglu M., 2004, *Appl. Catal. B.*, **54**, 19.
14. Ong H.C. and Chang R.P.H., 2001, *Appl. Phys. Lett.*, **79**, 3612.
15. Kar S. and Biswas S., 2008, *J. Phys. Chem*. C, **112**, 11144.
16. Kripal R. and Kumar Gupta A., 2010, *Chalcogenide Lett.*, **7**, 203.
17. Klimov V.I., Ivanov S.A., Nanda J., Achermann M., Bezel I., McGuire J.A. and Piryatinski A., 2007, *Nature*, **447**, 441.
18. Green A.A. and Hersam M.C., 2008, *Nano Lett.*, **8**, 1417.
19. Toyama T., Hama T., Adachi D., Nakashizu Y. and Okamoto H., 2009, *Nanotechnol.*, **20**, 055203.
20. Kumar V., Ntwaeaborwa Q.M., Soga T., Dutta V. and Swart H.C., 2017, *ACS Photonics*, **4**, 2613.
21. Gunbat M., Horoz S., Sahin O. and Ekinci A., 2018, *Digest J. Nanomater. Biostruct*., **13**, 799.
22. Subash B., Krishnakumar B., Pandiyan V., Swaminathan M. and Shanthi M., 2012, *Sep. Purif. Technol.*, **96**, 204.
23. Preisler E.J., Marsh O.J., Beach R.H., and McGill T.C., 2001, *J. Vac. Sci. Technol B*, **19**, 1611.
24. Vdovenkova T., Vdovenkov A. and Tornqvist R., 1999, *Thin Solid Films*, **332**, 343.

25. San N., Hatipoglu A., Kocturk G., and Cinar Z., 2001, *J. Photochem. Photobiol*. A, **139**, 225.

26. Gouvea C.A.K., Wypych F., Moraes S.G., Duran N., Nagata N. and Zamora P.P., 2000, *Chemosphere*, **40**, 433.

27. Saquib M. and Muneer M., 2002, *Dyes and Pigments*, **53**, 237.

28. Krishnakumar, B., Selvam, K., Velmurugan, R. and Swaminathan, M., 2010, *Desalination water treatment*, **24**, 132.

29. Shanthi M. and Kuzhalosai V., 2012, *Indian J. Chem.*, **51(A),** 428.

30. Dhatshanamurthi P., Subash B., Senthilraja A., Kuzhalosai V., Krishnakumar B. and Shanthi M., 2013, *J. Nano Sci., Nanotechnol.,* **13**, 1.

31. Mills A. and McGrady M., 2008, *J. Photochem. Photobiol. A*, **193**, 228.

32. Mura G.M., Ganadu M.L., Lombardi P., Lubinu G., Branca M. and Maida V., 2002, *J. Photochem. Photobiol. A*, **18**, 199.

33. Coronado J.M., Maira A.J., Martinez-Arias A., Conesa J.C., and Soria J., 2002, *J. Photoche. Photobiol. A*, **150**, 213.

RNI No. MAHENG/2017/74063
ISSN No. (Print) 2581-5911
ISI Impact Factor 1.022 (2019-2020)

Effect of Treated Calcium Carbonate on the Total Protein Content of Natural Rubber Latex Films

A.R. Ruhida*[1] and A. Hassan[2]
[1] Malaysian Rubber Board, 50450 Kuala Lumpur, Malaysia.
[2] Department of Chemistry, University of Malaya, 50603 Kuala Lumpur, Malaysia.
Email: ruhida@lgm.gov.my; Ahassan@um.edu.my

Abstract
Calcium carbonate as a filler was treated with stearic acid in chloroform medium at various concentrations (0.5%, 1.0%, 3.0%, 4.0%, 5.0% and 7.0%) and evaluated to understand the mechanism of the interaction involved between stearic acid and treated $CaCO_3$ in chloroform medium. The reduction of extractable protein (EP) content in NR latex films filled with treated filler, was evaluated. The treated filler was characterised and monitered using Thermogravimetric Analyzer (TGA), Fourier Transform Infra-red (FTIR), and Field Emission Scanning Electron Microscope (FESEM) to detect the presence of stearic acid on the surface of filler particles. The percentages of nitrogen (N) and EP content were measured using Automatic Analyser and UV microplate reader. The treated $CaCO_3$ were characterised using FTIR and TGA. The percentages of nitrogen (N) for original and aged samples using 3.0% treated $CaCO_3$ were similar at 0.71% and 0.72% respectively. All the uncorrected and corrected EP content results for original samples were lower as compared to the untreated filler. The corrected EP content of unaged samples produced lower EP content as compared to uncorrected EP content.

Keywords: *Natural Rubber, Treated Calcium Carbonate, Stearic Acid, Total Protein Content, Nitrogen Content*

Introduction

The use of commercial filler such as calcium carbonate ($CaCO_3$) in the making of natural rubber latex (NRL) dipped products, particularly natural rubber (NR) latex gloves has increased due to high demand[1,2]. Therefore, the filler is usually added to NR products due to the high price of NR latex and to address the shortage of latex. $CaCO_3$ was favoured probably because of its lower cost[3,4]. It is known that dry rubber or elastomers, various chemical ingredients like additives and fillers are added to rubber to produce a new class of materials. The combination of these rubber or elastomer additives leads to new desirable properties and ability to improve the mechanical properties like tensile strength, surface hardness etc.[3-5]. Problems of Latex allergy and total protein content cannot be resolved by adding the fillers in NR latex. Hence it is predicted that treating fillers might be able to resolve these problems. Many studies on the treated or coated surface of filler with fatty acids have been done and used in rubber. A fatty acid like stearic acid produced a monolayer of a hydrophobic

organic molecule which attaches on the filler surface. This monolayer was bonded to the NR rubber particles (hydrophobic) to obtain the NR latex film. The bonded monolayer has a strong influence on the final properties of the NR latex film because this film represents the interface between the two phases of the heterogeneous material. It also determines the particle-particle as well as the particle-matrix interactions and controls the buildup of the interphase[6].

The stearic acid content on the surface of the treated filler can be detected and identified by Thermogravimetric Analyser (TGA) and Fourier Transform Infra-red (FTIR) as suggested by Thomas and Clouse[7,8]. Thermogravimetric analysis (TGA) is a simple technique which is used to determine the amount of organic material on the surface of calcium carbonate. It is reported that thermal analysis can differentiate between chemisorbed, intercalate (local bilayer), and free acid molecules, which may be present on the surface of fillers[6,9]. The calcium carbonate surface also can be treated with the solution of acid in a nonpolar solvent, as mentioned by Hansen et al.[10]. Hansen et al reported that if calcium carbonate was wetted with distilled water before it was put into n-decane plus stearic acid solution, the water film on the calcite surface altered the adsorption of acid on the mineral surface. The modification of the $CaCO_3$ surface by a variety of surface modifiers has been extensively studied, Fatty acids like stearic acid alter the wetting and dispersion behaviour of $CaCO_3$ particles [11]. Therefore, the objectives of this research were to identify and measure the presence of stearic acid on the surface of $CaCO_3$ as filler using TGA and FTIR instruments. Besides, the percentage of nitrogen (N) and extractable protein (EP) contents of NR latex films filled with the treated filler were measured using Automatic Analyser and UV microplate reader. All the values of EP content are reported as uncorrected and corrected EP.

Materials and Methods

The raw NR field latex was collected from the selected plant clones from Kota Tinggi Research Station, Johor, Malaysia, before processing into NR latex concentrate. The chemicals were manufactured by Merck while $CaCO_3$ (Z80) as filler that was mixed into NR latex compounds was of commercial grade and was manufactured by Zancarb.

Preparation of treated $CaCO_3$ with stearic acid

The surface of $CaCO_3$ was treated with stearic acid in chloroform medium at concentrations of 0.5, 1.0, 3.0, 4.0, 5.0 and 7.0 by (w/v %) Approximately 10g of 50% commercial $CaCO_3$ dispersion was weighed and mixed with 100mL of distilled water. Then, it was placed in the water-bath for about 30 minutes at 50°C and 10mL of an appropriate amount of dissolved stearic acid in chloroform medium, was added into the $CaCO_3$ suspension. The $CaCO_3$ suspension was stirred at 4000 rpm for 15 minutes. After that, the suspension was centrifuged at 8000 rpm for 8 minutes before the semi-solid slurry was collected and washed with distilled water. Then, it was dried in an oven at 50°C for 24 hours before grinding. The ground treated filler was prepared by mixing 50% $CaCO_3$, 1.0% dispersing agent and 49% distilled water with vigorous stirring for 30 minutes. Then, the filler dispersion was poured into a 500mL plastic bottle containing about 50 pebbles of various sizes for dispersing and grinding the ingredients when the bottle was shaken on the milling machine.

Preparation of NR latex films with treated $CaCO_3$

For further investigation, NR latex films were prepared only at one $CaCO_3$ loading, i.e. 30 pphr. Table 1 shows the formulations used for diferent contents of stearic acid based on the procedure that was reported.[12].

Table 1. Formulation of NR latex compounds with treated $CaCO_3$ at various concentrations of Stearic acid

Components	Concentration (pphr)
Latex concentrate, 60 %	100
Potassium hydroxide, 10 %	0.1
Potassium laurate, 20 %	0.5
Sulphur dispersion, 50 %	1.5
Zinc dibutyl dithiocarbamate (ZBuD), 33.3 %	1.0
Zinc oxide, 50 %	0.5
Wingstay L, 40 %	1.0
Treated $CaCO_3$ dispersion, 20%	30

Characterisation techniques

1. TGA measurements

The treated $CaCO_3$ in powders and NR latex films have been evaluated by TGA. A test sample of about 15mg was used for each test run, heated from 50°C until 850°C in nitrogen gas with a scan rate of 20°C min^{-1}. The percentage of weight loss of materials were analysed as a function of temperature. The analysis ended at about 850°C, when no further decrease in weight was observed. The thermograms from the TGA analysis illustrate the results of polymer, treated $CaCO_3$ and ash contents [13].

2. FTIR identifications

The treated $CaCO_3$ in the form of powder, dispersions and NR latex films at various concentrations of stearic acid was evaluated by FTIR Nicolet iZ10 Module according to the MRB test method [14]. The FTIR spectra were generated by the absorption of electromagnetic radiation in the frequency range 400 - 4000 cm^{-1} by organic molecules.

3. Surface morphology analysis

The surface morphology of treated $CaCO_3$ in NR latex films at various concentrations was evaluated using Field Emission Scanning Electron Microscope (FESEM), JEOL JSM-840 model-6211 to observe and monitor changes in the surface morphology of $CaCO_3$ particles before and after treatment. The specimen surface was coated with gold of 2.5 μm thickness prior to testing to prevent charging.

4. Total protein content measurement

The total protein content of treated $CaCO_3$ in NR latex films was evaluated according to the percentage of nitrogen (N) and extractable protein (EP) content. The protein of NR is usually related to nitrogen content by a formula, as stated in RRIM Test Method B7[15-17]. The samples were aged by heating in the oven at 70°C for 7 days before analysis. In nitrogen (N) content analysis, about 10g of original and aged NR latex films were creped at least 10 times by using small scale milling to ensure that the samples were well homogenised before analysis by Automatic Analyser. All the crepe samples, together with the standard, namely 2,5-bis(5-tert-butyl-2-benzoxazolyl) thiophene (BBOT) used for nitrogen analysis, were weighed[18]. The total protein content was determined by the Rubber Research Institute of Malaysia Test Method B7[17,19]. The EP content from NR latex films was extracted and the assay was measured based on the ASTM D5712 test method[20]. The process involved sample preparation, protein extraction, precipitation of proteins in the extracts, solubilising the protein precipitate in sodium hydroxide, complexing the proteins with copper reagent (uncorrected), replacing copper reagent with distilled water (corrected) and measuring the absorbance of reduced Folin at 750nm, by UV Microplate Reader. The results were analysed using an ovalbumin calibration curve with reference to μg/g of NR latex film[15,21,22].

Results and Discussion

Characterisation of $CaCO_3$

$CaCO_3$ as a commercial filler was treated with stearic acids in chloroform ($CHCl_3$) medium to identify and measure the ability of stearic acid to attach on the surface of $CaCO_3$ particles and to find out the optimum content of stearic acid to be used. TGA and FTIR analyses were

used for this purpose. Figure 1 shows the mean value of treated $CaCO_3$ content with stearic acid in powder form at various concentrations in chloroform medium. No significant difference in the amount of treated $CaCO_3$ at 0.5% and 1.0% concentrations was observed as compared to Control 1 (untreated filler). This indicates that the stearic acid might be attached to $CaCO_3$ and might be permanently bonded. From 3.0% until 7.0%, there was a small amount of stearic acid detected. For example, Figure 2 shows stearic, attached on treated $CaCO_3$ at 1.0% and 4.0% concentrations. From the thermogram, the presence of stearic acid in filler was confirmed since the treated fillers degrade at the higher temperature (806ºC and 810ºC) as compared to pure $CaCO_3$ (802ºC) [23].

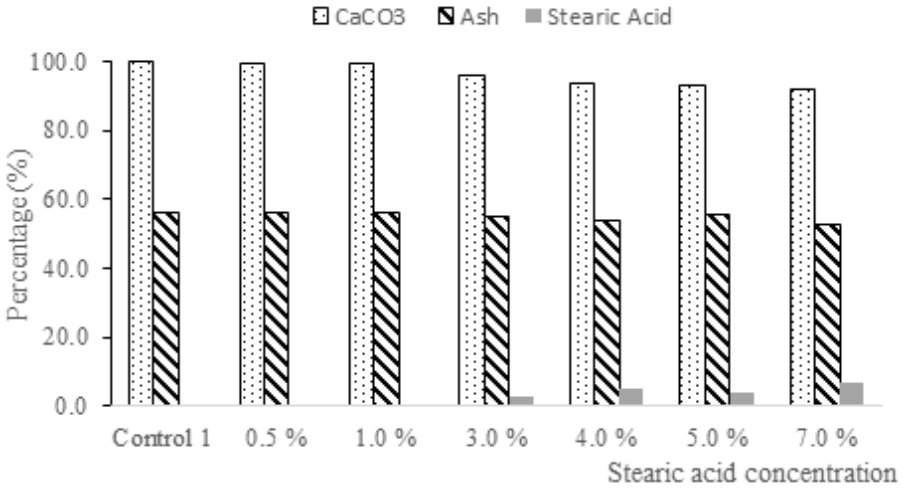

Fig. 1. $CaCO_3$, ash and stearic acid contents in powder form as determined by TGA analysis

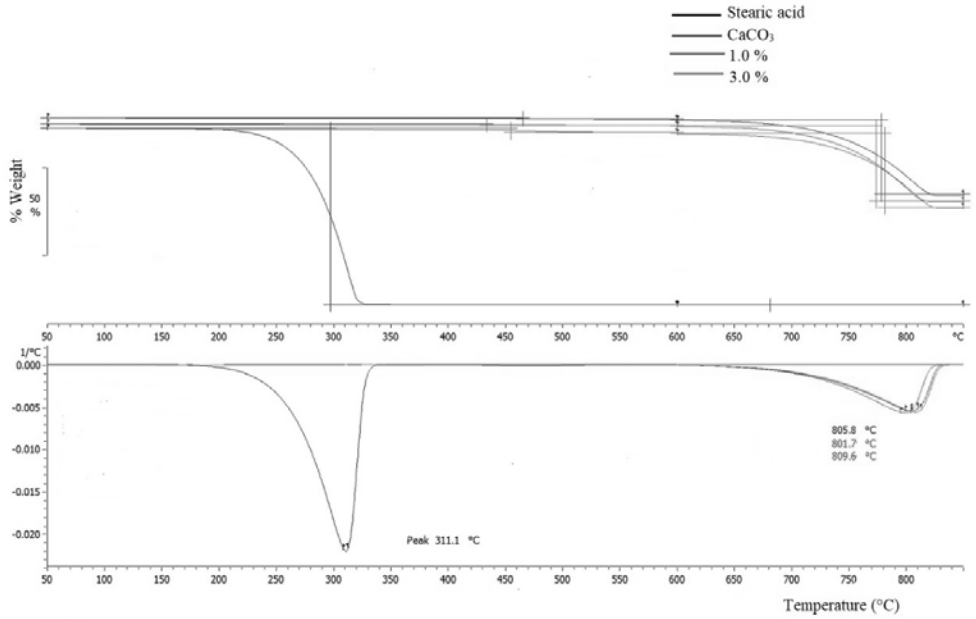

Fig. 2. TGA thermograms of stearic acid, $CaCO_3$ and treated $CaCO_3$ at 1.0% and 3.0% concentrations

FTIR identification

Figure 3 shows the FTIR spectra of treated $CaCO_3$ dispersions to identify the presence of stearic acid on the surface of $CaCO_3$ particles. Based on Figure 4, it was observed that the strong and sharp peaks occurred in the range 1500cm^{-1} to 1400cm^{-1} of Control 1 (untreated filler at 30pphr), Control 2 (without filler) and 0.5% treated $CaCO_3$. It was also observed that a strong and broad peak occurred at 1.0%, 3.0% and 7.0% treated $CaCO_3$, a weak and broad peak was obtained at 4.0%, and 5.0% $CaCO_3$. Nevertheless, at 1375cm^{-1}, it was observed that a small, strong peak was observed at Control 1 (untreated filler) and small and weak peaks at 1.0% and 3.0% treated $CaCO_3$. However, a broad and weak peak occurred at 4.0% treated filler. At 1025cm^{-1}, strong broad peaks were observed for Control 1 (untreated filler), Control 2 (without filler) and 0.5%, 4.0% and 5.0% treated filler. Small strong peaks at 875 cm^{-1} were found at 1.0%, 3.0% and 7.0% treated fillers. It was assumed that the peaks obtained at 875cm^{-1} corresponding to attachment of stearic acid, while the peaks at 835cm^{-1} and 1429cm^{-1} indicate the presence of $CaCO_3$[24]. The small weak peak of natural rubber was observed at about 900cm^{-1} [25,26].

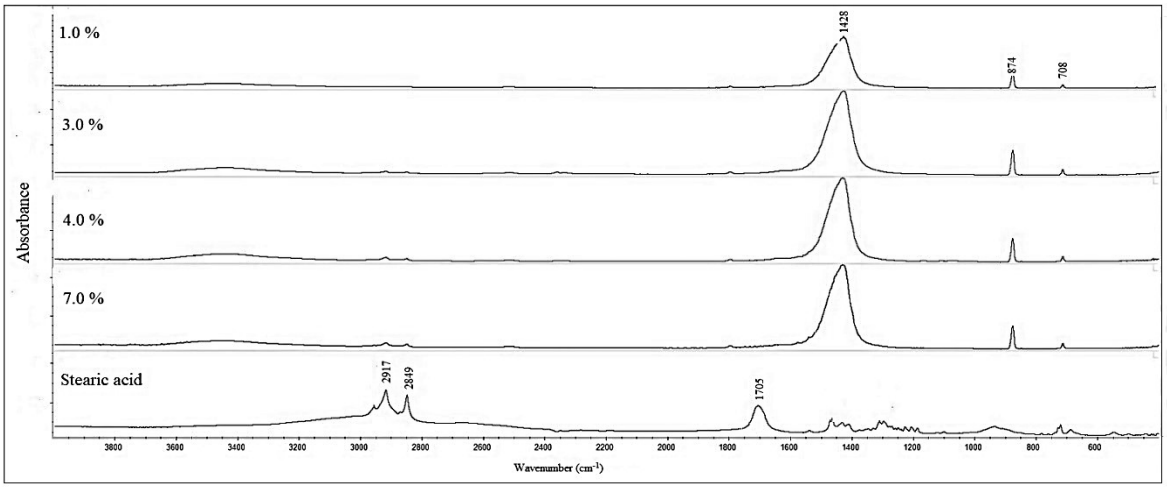

Fig. 3. The FTIR spectrum of treated $CaCO_3$ in dispersion form at 1.0%, 3.0%, 4.0% and 7.0% concentrations as compared to pure stearic acid

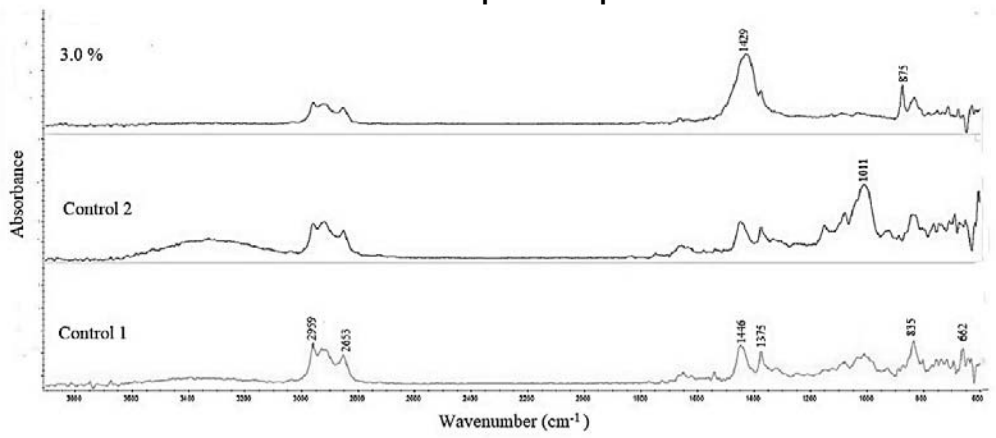

Fig. 4. The spectrum of NR latex films Control 1, Control 2 and 3.0% treated $CaCO_3$

Total protein content

The total protein contents of treated fillers in NR latex films at various concentrations of stearic acid were determined based on the percentage (%) of nitrogen (N) and extractable protein (EP) contents. These were carried out before and after ageing with the additional parameter at EP with and without correction.

Determination of nitrogen content

Figure 5 shows the percentage of nitrogen (N) content of original and aged NR latex films with treated $CaCO_3$ at various concentrations of stearic acids. Overall, the results of the percentage of nitrogen (N) content film at 30 pphr (Control 1, untreated) for the original samples were higher as compared to aged treated samples. It is difficult to identify the trends of the nitrogen (N) content due to the inconsistency of results produced. It was found that original treated samples at 0.5%, 4.0% and 7.0% treated $CaCO_3$ in NR latex films, showed higher results compared to aged treated samples. However, at 1.0% and 5.0% treated $CaCO_3$ in NR latex films showed opposite results. In addition, at 3.0% of treated $CaCO_3$, the percentage of nitrogen (N) of original and aged samples produced a similar value of 0.71% and 0.72%, respectively. The nitrogen content was presumed to be related to the presence of a protein in the rubber and indicates the presence of some residual nitrogenous components probably amino-acids bonded directly to polyisoprene molecules[27]. According to the study by Dalrymple and Audley, the total nitrogen content of NR glove prepared from standard latices was twice that of the film 'free' of non-protein nitrogen[28].

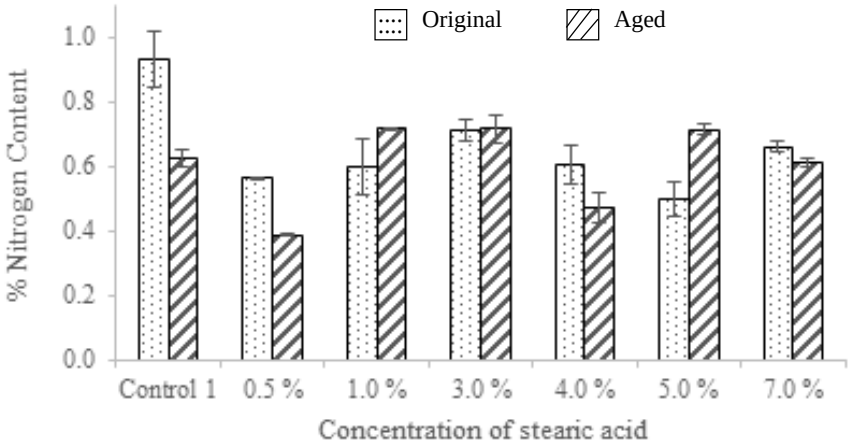

Fig. 5. The percentage of nitrogen content (N) of original and aged NR latex films filled with treated $CaCO_3$ at various concentrations of stearic acids

Extractable protein content

Figures 6 and 7 show the non-corrected and corrected EP contents for original and aged NR latex films. Figure 6 shows that the non-corrected EP content for the original samples was higher than that of aged samples except at 4.0% concentration. However, no significant differences were observed in the values of original and aged samples for the non-corrected EP content at 3.0% concentration. It was also observed that there was a reduction of EP content from Control 1 until 3.0% concentrations and a slight reduction from 3.0% until 7.0% concentrations. This indicates that the stearic acid may be bonded to $CaCO_3$.

In Figure 7, it was observed that the results of corrected EP contents for the original and aged films were

inconsistent. The corrected EP content of original for films at 0.5%, 4.0% and 7.0% should higher results as compared to aged samples. However, the corrected EP content of aged samples at 1.0%, 3.0% and 5.0% showed higher results as compared to original samples with the highest value at 417.4 µg/g (3.0% treated). This observation was probably due to the contribution of chemicals interference from the rubber chemicals in the latex compounds[21,29]. The test method provides an optional method to correct absorbance values for samples whose values were suspected to be affected by the interfering non-proteinaceous substances present in samples. The corrected method was based on the reaction with Folin reagent in the presence of distilled water that was replaced by the copper (Cu^{+2}) reagent. Therefore, there was no complex formation of protein with copper reagent. Under normal conditions, the Cu^{2+} ion binds with protein to form complexes that subsequently reduce Folin reagent, resulting in the development of a blue coloured solution that absorbs at 750nm.[29]

The treated $CaCO_3$ was predicted to reduce the EP content. The uncorrected and corrected EP content for both original and aged NR latex films were analysed, as shown in Figures 8 and 9, respectively. From Figure 8, as expected, the non-corrected EP content of original NR latex films was higher compared to corrected EP content due to the removal of chemical interference during the complex formation with protein. It was also found that all the uncorrected and corrected EP contents of treated samples were lower as compared to Control 1 (untreated filler).

For aged samples (Figure 9), it was found that the results of non-corrected EP content at 1.0%, 3.0% and 5.0% concentrations were lower as compared to the corrected EP content. The reduction might be due to the presence of stearic acid on the treated $CaCO_3$ as well as the contribution of heating during the ageing process. However, the opposite results were observed at other concentrations (Control 1, 0.5%, 4.0% and 7.0%). It was theoretically proved that the corrected EP should give lower results compared to the uncorrected aged sample since the interferences have been removed at the correction stage [20]. Therefore, further study needs to be explored in order to rectify this phenomenon.

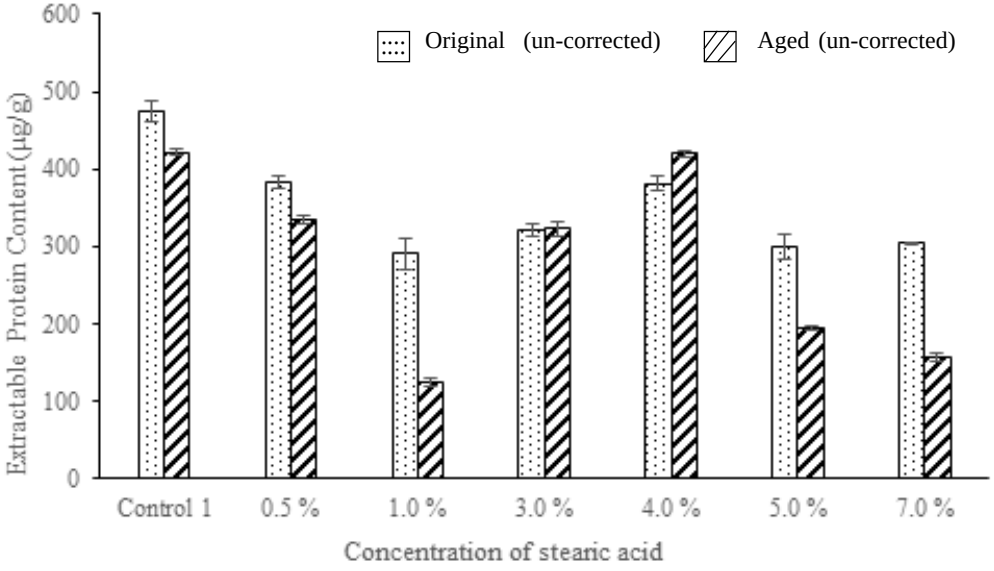

Fig. 6. The non-corrected EP contents of original and aged NR latex films filled with treated $CaCO_3$

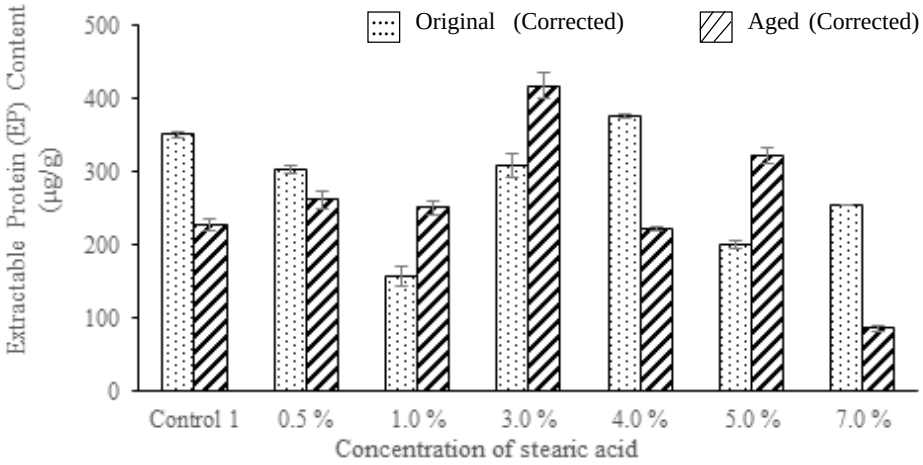

Fig. 7. The corrected EP contents of original and aged NR latex films filled with treated $CaCO_3$

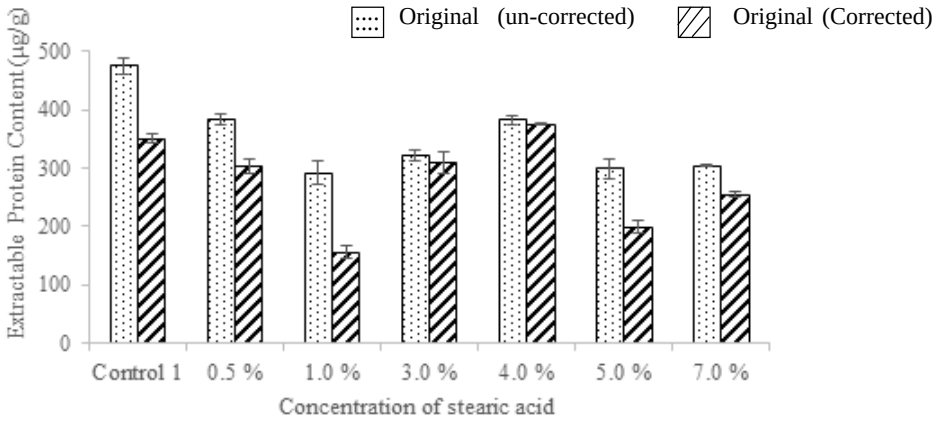

Fig. 8. The un-corrected and corrected EP contents of original NR latex films filled with treated $CaCO_3$

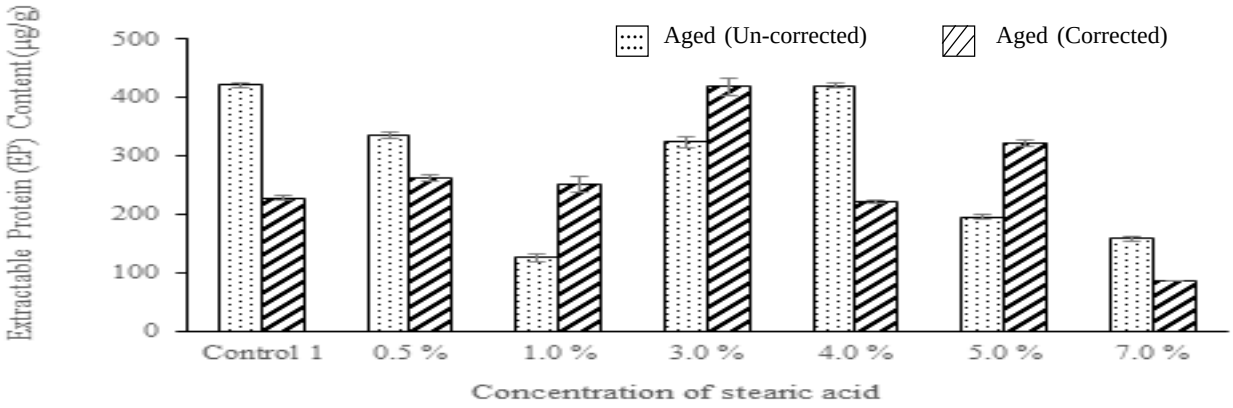

Fig. 9. The un-corrected and corrected EP contents of aged NR latex films filled with treated $CaCO_3$

The surface morphology of NR latex films with treated $CaCO_3$

Figure 10 shows the surface morphology of NR latex films filled with treated $CaCO_3$ at Control 1 (untreated filler), 1.0%, 3.0% and 7.0% of stearic acid concentrations by using FESEM. It was observed that surface morphology of NR latex film without filler showed a smooth surface as compared to Control 1 (untreated filler) and other NR latex film with treated fillers. However, the surface morphology at 1.0% showed a better and smooth surface as compared to 3.0%, and 7.0% treated $CaCO_3$ (rougher and coarser). It is also observed that there was no agglomeration of treated filler occurred on the surface of fillers.

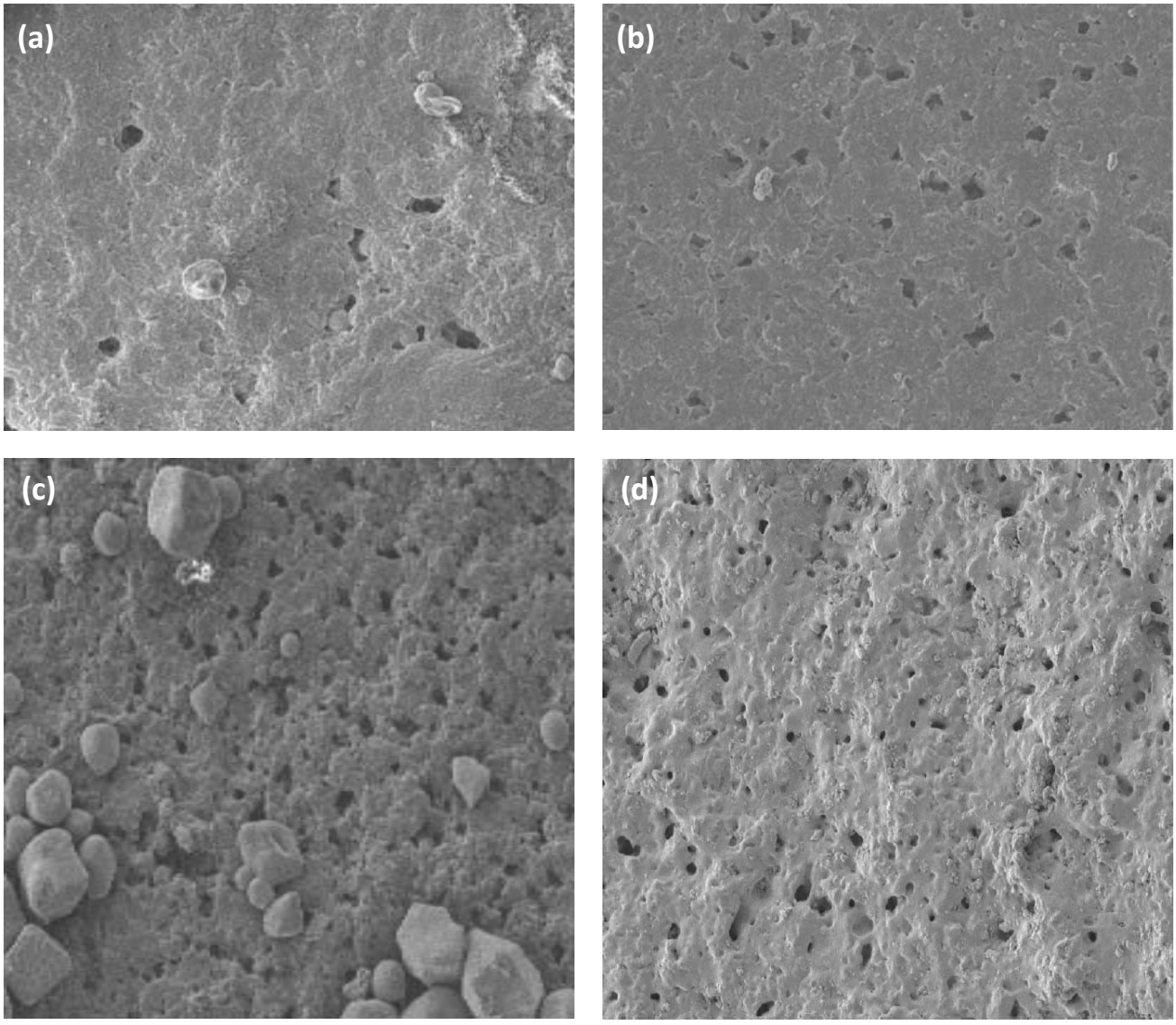

Fig. 10. The surface morphology of NR latex films (a) Control 1 (b) 1.0% (c) 3.0% (d) 7.0% of treated filler at certain concentrations of stearic acid at 2000x magnification

Conclusions

By treating $CaCO_3$ with stearic acid in chloroform medium at various concentrations, it can be concluded that the composition of stearic acid in filler can be characterised using TGA. From FTIR analysis, the composition of stearic acid was identified at 0.5%, and 1.0% concentration using observable peaks at 875cm^{-1}, which indicated the attachment of stearic and to the filler. In addition, the occurrences of peaks at 835cm^{-1} and 1429cm^{-1} indicated the presence of stearic acid, which was not attached to the filler. The percentage of nitrogen (N) for original and aged samples at 3.0% treated $CaCO_3$ showed similar results (0.71% and 0.72% respectively). It was also found that all the un-corrected and corrected EP content results for original samples were lower as compared to the Control 1 (untreated filler). The corrected original samples have a lower value of EP content as compared to uncorrected samples.

Acknowledgement

The authors thank the University of Malaya, Malaysia as the research done in this paper was funded by grant UM PPP (PG261-2015B). This study is part of the PhD research project in collaboration with the Malaysian Rubber Board (MRB). The authors would also like to thank the Malaysian Rubber Board for the supply of latex and facilities.

References

1. Manroshan, S. and Baharin, A., 2005, *J. Appl. Polym. Sci*. **96(5)**, 1550-1556. http://dx.doi.org/10.1002/app.21595

2. Ramli, R., Jaapar, J., Singh, M. S. J., and Yatim, A.H.M., 2014, *Advances in Environmental Biology*, 2714-2723.

3. Barrera, C.S., Soboyejo, A.B., and Cornish, K., 2018, *Rubber Chem. Technol.* **91(1)**, 79-96. http://dx.doi.org/10.5254/rct.82.83716.

4. Nor, N. M. and Othman, N., 2016, *Procedia Chemistry*, **19**, 351-358. http://dx.doi.org/1016/j.proche.2016.03.023.

5. Sarma, A. D., Le, H. H., Das, A., Wießner, S., Stöckelhuber, K. W., Bhowmick, A. K. and Heinrich, G., 2018, *Polymer*, **150,** 64-71. http://dx.doi.org/10.1016/j.polymer. 2018.07.013.

6. Osman, M.A. and Suter, U.W., 2002, *Chemistry of Materials*, **14(10),** 4408-4415. http://dx.doi.org/10.1021/cm021222u.

7. Thomas, M.M., Clouse, J.A. and Longo, J.M., 1993, *Chemical Geology*, **109(1-4),** 201-213. http://dx.doi.org/10.1016/0009-2541(93)90070-Y.

8. Nabinejad, O., Debnath, S., Rahman M. and Davies, I., 2015, *Journal of Thermal Analysis and Calorimetry*, **122(1)**, 227-233. http://dx.doi.org/10.1007/s10973-015-4681-2.

9. Mihajloviæ, S., Sekuliæ, Ž, Dakoviæ, A., Vuèiniæ, D., Jovanoviæ, V. and Stojanoviæ, J., 2009, *Ceramics–Silikáty*, **53(4)**, 268-275.

10. Hansen, G., Hamouda, A. A. and Denoyel, R., 2000, *Colloids and Surfaces A: Physicochemical and Engineering Aspects*, **172(1-3),** 7-16. http://dx.doi.org/10.1016/S0927-7757(99)00498-7.

11. Song, E., Kim, D., Kim, B. J. and Lim, J., 2014, *Colloids and Surfaces A: Physicochemical and Engineering Aspects*, **461,** 1-10. http://dx.doi.org/10.1016/j.colsurfa.2014.07.020.

12. Ruhida, A.R. and Aziz, H., 2016, 3rd Advanced Materials Conference 2016., Langkawi, Kedah, Malaysia.

13. MRB Test Method., UPB/P/010., Thermogravimetric analysis of rubbers and rubber related, 2010.

14. MRB Test Method, UPB/P/011, Polymer type(s) by FTIR Spectroscopy in 2010.

15. Norhayati, M., 2005, *MRB Rubber Technology Developments*,**5,** 27-30.

16. Eng, A.H., Kawahara, S. and Tanaka, Y., 1993, *J. Nat. Rubb. Res.*, **8(2)**, 109-113.

17. Ng, Y.T., 1992, RRIM test methods for standard Malaysian rubbers. Rubber Research Institute Malaysia, Kuala Lumpur, 1-4.

18. MRB Test Method. UPB/P/04. Rubber and rubber products- Determination of carbon, nitrogen and sulphur, 2007.

19. Chaikumpollert, O., Yamamoto, Y., Suchiva, K. and Kawahara, S., 2012, *Colloid and Polymer Science*, **290(4),** 331-338. http://dx.doi.org/ 10.1007/s00396-011-2549-y.

20. ASTM D5712-10 Standard test method for analysis of aqueous extractable protein in natural rubber and its products using the modified Lowry method, 2010.

21. Hasma, H., Nurul Hayati, Y., Lau, C. H., Ruhida, A. R. and Amir Hashim, M.Y., 2004, *Journal of Rubber Research*, **7(1)**, 56-70.

22. Ong, E.L., 2014, Recent Technical Surveillance of Extractable Protein Content of Latex Condoms. Latex 2004. 3rd two-day conference on synthetic emulsion, natural latex and latex based products, 2014, Hamburg, Germany: Rapra Technology Ltd.

23. Devamani, R.H.P., Deepa, N. and Gayathri, J., 2016, *International Journal of Innovative Science, Engineering & Technology*, **3(1)**, 87-89.

24. Croitoru, C., Pascu, A., Roata, I. C. and Stanciu, E.M., 2017, June, IOP Conference Series: Materials Science and Engineering, IOP Publishing., **209(1)**, 012041. http://dx.doi.org/10.1088/1757-899X/209/1/012041

25. Mente, P., Motaung, T.E. and Hlangothi, S.P., 2016, *Polymer*, **2(1),** 1-19. http://dx.doi.org/10.4172/2471-9935.100015.

26. Reig, F. B., Adelantado, J. G. and Moreno, M.M., 2002, *Talanta*, **58(4)**, 811-821. http://dx.doi.org/ 10.1016/S0039-9140(02)00372-7.

27. Marinho, J.R., and Tanaka, Y., 2000, *Journal of Rubber Research*, **3(4)**, 193-199.

28. Dalrymple, S.J. and Audley, B.G., 1992, *Rubber developments*, ***45*(2)**, 51-60.

29. Mok, K.L., Norhayati, M., Rosmahani, C. I., Hasma, H. and Nurul Hayati, Y., 2005, *MRB Rubber Technology Developments*. **5(1)**, 3-7.

RNI No. MAHENG/2017/74063
ISSN No. (Print) 2581-5911
ISI Impact Factor 1.022 (2019-2020)

Ion Chromatography-Instrumentation and Applications

Deepak Parab, Uvaraj Mani and Sriram Balachandran
Metrohm India Limited, Metrohm Siri Towers, Fourrts Avenue,
Annai Indira Nagar, Chennai 600096, India
Email: deepak.parab@metrohm.in

Abstract
Ion chromatography (IC), a branch of chromatography deals with the separation and quantification of ionic components (inorganic hydrophilic cations, anions, and organic anions). Though it operates on the separation principle, with identification and quantification, it is used more as an analytical technique. In the last two decades, advancements in column materials and detector technologies integrated with digitalization have made ion chromatograph a prominent analytical tool for separation and quantification of component ions from ultra-trace level (parts per billion to percentage level. Use of hyphenated techniques like IC-MS, IC-ICP-MS is also increasing to cater to speciation studies.

Keywords: *Ion Chromatography, Ionic Components, Identification, Quantification*

Introduction

Ion chromatography was introduced in 1975 by Small, Stevens and Baumann as a new analytical method. Ion chromatography is a subset of liquid chromatography which is a process that allows the separation of ions and polar molecules based on their charge. Similar to liquid chromatography, ion chromatography utilizes a liquid mobile phase, separation column and a detector to measure the species eluted from the column. Normally in ion chromatography, both mobile phase and stationary phases are ionic in nature. Conductivity detector is widely used for most of the applications. Other detectors like electrochemical and UV-Vis are also used based on the application. Ion chromatography can be coupled with MS and ICP-MS for better selectivity and sensitivity. Ion exchange chromatography can be applied to the determination of ionic solutes, such as inorganic anions, cations, transition metals and organic acids/bases. It can also be used for almost all kinds of charged molecules including proteins, amino acids and carbohydrates using different detection techniques. Based on the polarities of the stationary phase (column) and the mobile phase (eluent), Ion chromatography is further divided into Ion exchange, Ion pair and Ion exclusion chromatography. In the ion exchange and ion exclusion chromatography, both the stationary phase and the mobile phase are ionic in nature, whereas in the ion pair, the stationary phase is non-polar, while the mobile phase remains polar/ionic. The separation in ion exchange chromatography is based on different affinities for the exchanger of analyte ion and competing ion.

$$E^+(stat) + A^+(mob) \leftrightarrow C^+(stat) + E^+(mob)$$

$$K_c = \frac{[C^+]_{stat} \times [E^+]_{mob}}{[E^+]_{stat} \times [C^+]_{mob}}$$

Components of Ion Chromatograph: The schematic of ion chromatograph is shown below.

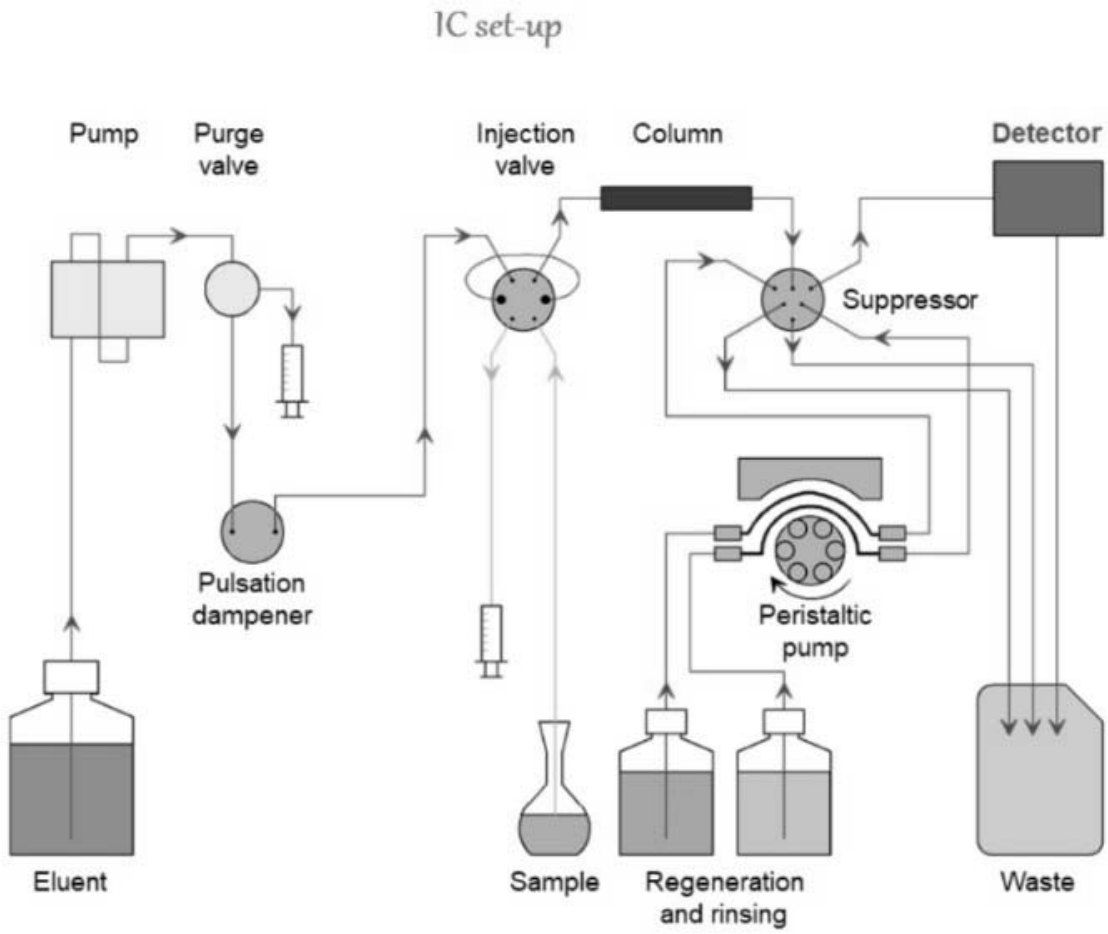

Fig. 1. Schematic diagram of Ion Chromatography

Eluents: The mobile phase or the eluent is responsible for carrying the sample through the injector, column, its separation and elution. It carries the competing ion which exchanges with the analyte ion for the sites available in column whereby effecting the elution. The composition, concentration, pH and flow rate influence the separation of component ions.

Pump: Unlike HPLC, the construction of pump is made using PEEK (Poly ethyl ether ketone). Dual piston pump with variable flow rates (typically 0.001 to 20mL) are available. Multiple pumps or eluent dosing systems are available. In gradient applications, use of low pressure system, where eluent flow is due to gravity and mixing is done using valves, or high pressure gradient where

more than one pump or a pump along with dosing systems are used.

Pulsation dampener is used to absorb the pressure variation caused by the very small difference due to flow or switching off the valves.

Inline filter: Generally a 2 µm filter is connected in between pulsation dampener and injector as a preventive measure to eliminate foreign particles (if any) entering the analytical line from the pump.

Injector: It is the component from where the samples are introduced into the analytical system. Although six port injector is the one which is commonly used, ten port injectors are also in use where inline sample preparation is carried out. Injector made of Rhodyne is used in the case of HPLC whereas PEEK material is used for its construction in ion chromatography.

Injector picture

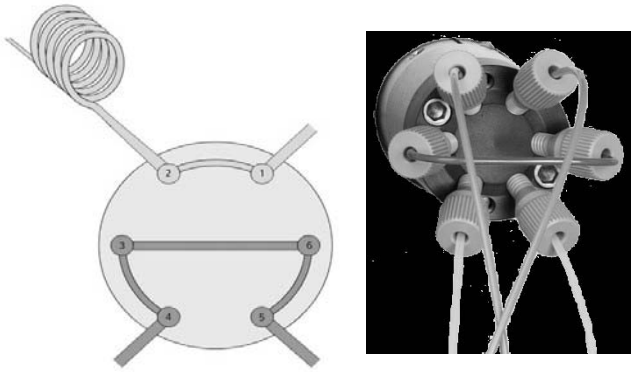

Fig. 2. Injector setup in ion chromatography schematic and actual injector

Guard column: A preventive column with the same packing material as that of the analytical column but with less capacity, is connected prior to column in order to reduce the risk of contamination of analytical column from sample.

Sample: A variety of industry samples like environmental protection, organic, pharmaceutical, petroleum, plastics, photographic, food, stimulants, beverages, flavours, biochemical, fertilizers, base materials, cosmetics, detergents, textiles, paper, ceramics, paints, lacquers, mineral resources, cement, different kind of power plants make use of ion chromatograph as a suitable analytical technique for their analytical needs.

Analytes like alkali, alkaline earth, transition metals, post transition metals, halides, oxy halides, organic acids, sugar, sugar alcohols, amino acids, amines, amides, ammonia, electrochemically active components are conveniently separated, identified and quantified using ion chromatograph.

Stationary Phase: The stationary phase in ion chromatography is mostly organic materials like poly styrene divinyl benzene, polymethacrylate, Hydoxy-ethylmethacrylate and polyvinyl alcohol. The ionic exchanger contains sulphonic ($SO_3^-H^+$) or carbonic (COO^-H^+) group in case of cation separation and quaternary ammonium groups, alkyl amines, alkyl amines with acrylate type cross linking for anion separation. They are linked with the base resin through a spacer group usually an ethyl group. Inorganic columns based on silica are also used for the separation of cations. Columns with such packing material with different capacities are available. The selection of the column for an analysis depends on how many components are to be separated, analyte ion concentration, eluent composition, pH of the sample and speed of analysis.

Detectors: Many detectors like conductivity, electrochemical and UV-Vis are used for the detection among out of which the conductivity detector is widely used.

Conductivity Detection: Conductivity measurement is widely used in ion chromatography. In conductivity detection, an electric filed is applied between the two electrodes often referred as a cell with a known cell

constant (***l/a***) where *l* represents the distance between the parallel plates and ***a*** denotes its area of cross section. Ions migrate in the field and the electrical resistance of the solution is measured. From the electrical resistance, conductivity is calculated using the formula $k = 1/R*(K_c)$ where K_c is the cell constant. Two factors namely reduction in background conductivity and increase in analyte sensitivity decides whether single column or two column technique needs to be used for the analysis. Use of dual column technique needs to be avoided when precipitation occurs as a result of exchange reaction. In the direct conductivity detection, the competing ion carrying the same charge as the analyte ion which competes for the ion exchanger in the column. The charge and size of the analyte influences the elution pattern. Higher the charge, greater will be the interaction with the ion exchange group of stationary phase and hence more is the retention. Smaller the size of the ion, greater will be solvation and shorter will be retention time. Retention time can also be modified by adjusting the pH of the eluent. In a styrene divinyl benzene based column with sulphonic acid as an exchanger, sodium carbonate and bi carbonate as eluent, phosphate (HPO_4^-) will elute before sulphate (SO_4^{2-}) whereas sulphate can be eluted before phosphate when pH of the eluent is raised to 12. Here, (HPO_4^{2-}) gets converted to PO_4^{3-}.

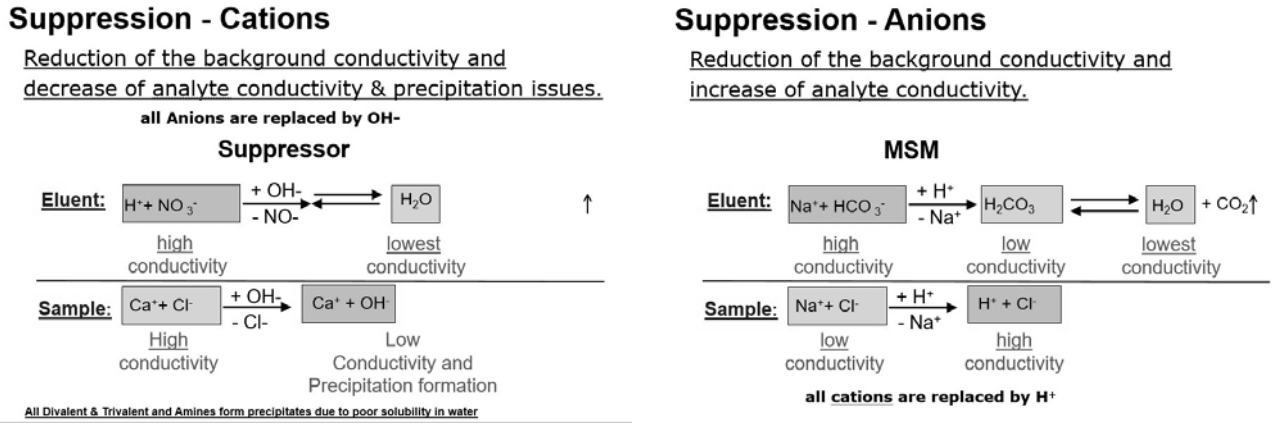

Fig. 3. Illustration of effect of suppressor on cation exchange and anion exchange chromatography

UV-Vis Detection: There are many ways in which UV-Vis detector is used. There are methods available for direct detection, indirect detection, detection with pre column derivatization and post column derivatization. In direct detection, the analyte ion will be chromophoric in nature whereas in the indirect detection, the eluent will be absorbing while the analyte will not be sensitive. In the post column derivatization, the analyte ions, after separation by the column will be allowed to react with post column reagent (a complexing agent, ligand). For the detection of transition and post transition metals, UV-Vis detection is used. This detector is very useful for analysing analytes in trace levels in the presence of large excess of other ions often referred as matrix elimination.

Direct UV-Vis detection: Ions which absorb strongly in the ultra violet region are analysed. This technique is very useful in quantifying ions which are at low level in presence of large excess of similar ions e.g. separation of nitrite, nitrate in presence of high concentrations of chloride, phosphate which do not absorbs UV.

Indirect UV-Vis detection: In this technique, analyte ions which do not absorb can be quantified along with ions which absorb by using an eluent

(8-Hydroxyquinoline). The analyte which does not absorb provides a negative peak and the analyte which absorb produces a peak in the positive direction. Aluminium and iron are analysed in complicated sample matrix.

UV-VIS detection with Post column derivation: In this technique, after separation, the analyte ions are allowed to react with a complexing agent (ligand), called post column reagent to form a complex which gets absorbed. Transition metals and lanthanides are analysed by this technique.

Table 1. Absorption wavelength for some of the analytes

Analyte	λ max	Analyte	λ max
F^-	<< 190nm	Br^-, NO_3^-	214nm
CH_3COO^-	≤190nm	SO_4^{2-} ,HPO_4^{2-}	≤190nm
Cl^-	≤190nm	Anions after PCR	>300nm
NO_2^-	210nm	Cations after PCR	>300nm
BrO_3^-	195nm		

Electrochemical detector: Electrochemical detector is the commonly used detector when analyte of interest undergoes oxidation or reduction and is electro-chemically active. In coulometry, all the analyte ions are oxidised or reduced at a fixed potential. In voltammetry, measurement of current due to redox reaction is measured against a potential in a defined range. In amperometry, current due to redox reaction at constant applied potential is measured and is widely used in ion chromatography. Detector of trace levels of iodide in brine is a typical application wherein iodide (electrochemically active), in large excess of chloride (electrochemically inactive) is determined without any interference. Many organic compounds like sugar, sugar alcohols, anions such as nitrite, nitrate, cyanide, sulphide, sulphite, amino acids are quantified using this detector.

Mechanism

Ion exchange mechanism: In ion exchange mechanism, the charge of the column will be opposite to that of the charged exchanger. For example, for exchange of cations, the charge of the column will be negative. Initially the competing ion in the eluent or mobile phase interacts with the ion exchanger and reaches an equilibrium called column equilibration. When the sample with anayte cations is injected, they replace the competing ion from the column and interact with the column. As the eluent is continuously pumped into the system, the competing ions push the analyte ions thereby eluting them. Elution or separation in ion exchange depends on two factors namely charge and size of ions. Higher the charge of the analyte, greater is its tendency to interact with the ion exchanger and hence higher will be its retention. Thus, the elution order is monovalent followed by divalent and trivalent ions. For analytes with same charge, size will influence the retention pattern. Smaller the size, higher will be solvation layer around it and hence interaction will be low due to reduction in effective charge. For common cations and anions, the retention time increases from left to right as given below.

Cations: Li^+, Na^+, NH_4^+, K^+, Mg^{2+}, Ca^{2+}.

Anions- F^-, $HCOO^-$, CH_3COO^-, BrO_3^-, Cl^-, NO_2^-, Br^-, ClO_4^-, NO_3^-, HPO^{2-}, SO_4^{2-}

However, by addition of a complexing agent like Pyridine-2,6-dicarboxylic acid, the elution of Mg and Ca can be reversed owing to the decrease in effective charge after the complexation of Calcium with the ligand.

Ion exclusion: Ion exclusion chromatography is mainly used for the separation of weak acids or bases In ion

exclusion method, a completely sulfonated cation exchanger whose sulfonic acids groups are electrically neutral and protons as counter ions, is frequently used as a packing material. In aqueous eluents the functional groups are hydrated. The hydrated shell is limited by an imaginary negatively charged membrane (Donnan membrane). It is only possible using uncharged, non-dissociated molecules such as water. Organic acids can be separated if strong mineral acids such as sulfuric acid are used as a mobile phase. Due to their low pK_a value, organic acids are almost completely present in a non-dissociated form in strongly acidic eluent medium. They can pass through the Donnan membrane and can be adsorbed at the stationary phase, whereas the sulfate ions of the completely dissociated sulfuric acid are excluded. The moment organic acid is ionised (inside the Donnan membrane), it will be pushed out from the Donnan membrane layer and thus eluted. The elution pattern depends on the dissociation constant of the organic acid. Higher the dissociated constant, faster will be the ionisation and hence faster will be its elution.

Ion pair: In ion pair mechanism, the column will be non-polar like C18. An ion pair reagent is added to the eluent; this consists of anionic or cationic surfactants such as tetra alkyl ammonium salts or n-alkyl sulfonic acids. Together with the oppositely charged analyte ions, the ion pair reagent forms an uncharged ion pair, which can be retarded at the stationary phase by hydrophobic interactions. Separation is possible because of the formation of the ion pairs and their different degrees of adsorption. Here, the elution order depends on the polarity of the molecules. Anionic and cationic surfactants are the common analytes separated and quantified using this mechanism.

Materials and Method

Determination of anions and oxy halides: An anion exchange column having Polyvinyl alcohol with quaternary ammonium group and Sodium carbonate and sodium bicarbonate as the eluent is used with suppressor. 50 mmol/L sulphuric acid is used as the suppressor regeneration solution and ultra-pure water as the rinsing solution.

Hazardous anions (reference) like Fluoride, Arsenic, Oxy halides like Bromate which is a suspected human carcinogen are separated and quantified along with the common anions like chloride, nitrate sulphate etc. As per WHO guidelines, although fluoride concentration up to 7.0 mg/L is beneficial, an excess of it in the range above 1.5 mg/L is harmful, while the bromate concentration should be less than 10 µg/L.

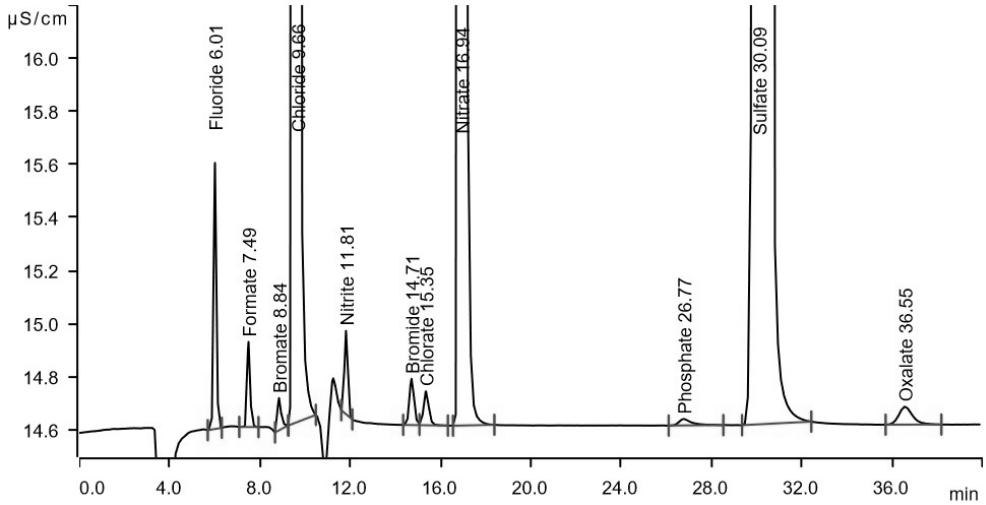

Fig. 4. Chromatogram showing anion separation

Determination of cations, hydrazine and morpholine in trace levels:

Morpholine is a common additive, in parts per million concentration in power plants as a corrosion inhibitor. It mixes well with water because of similar volatility and thereby adjusts the pH which helps in corrosion prevention. Hydrazine is used in steam cycles as an oxygen scavenger to control the concen-tration of dissolved oxygen in an effort to reduce corrosion.

In the determination of cations, hydrazine and morpholine using non-suppressed conductivity detection. Metrosep C3 column is used with Nitric acid with oxalic acid as eluent. The polyvinyl alcohol based column functio-nalised with carboxyl group has a 30µmol exchange capacity and is compatible with organic solvents like acetonitrile and acetone in different proportions. Apart from alkali metals, alkaline earth metals, certain amines and transition metals can also be analysed.

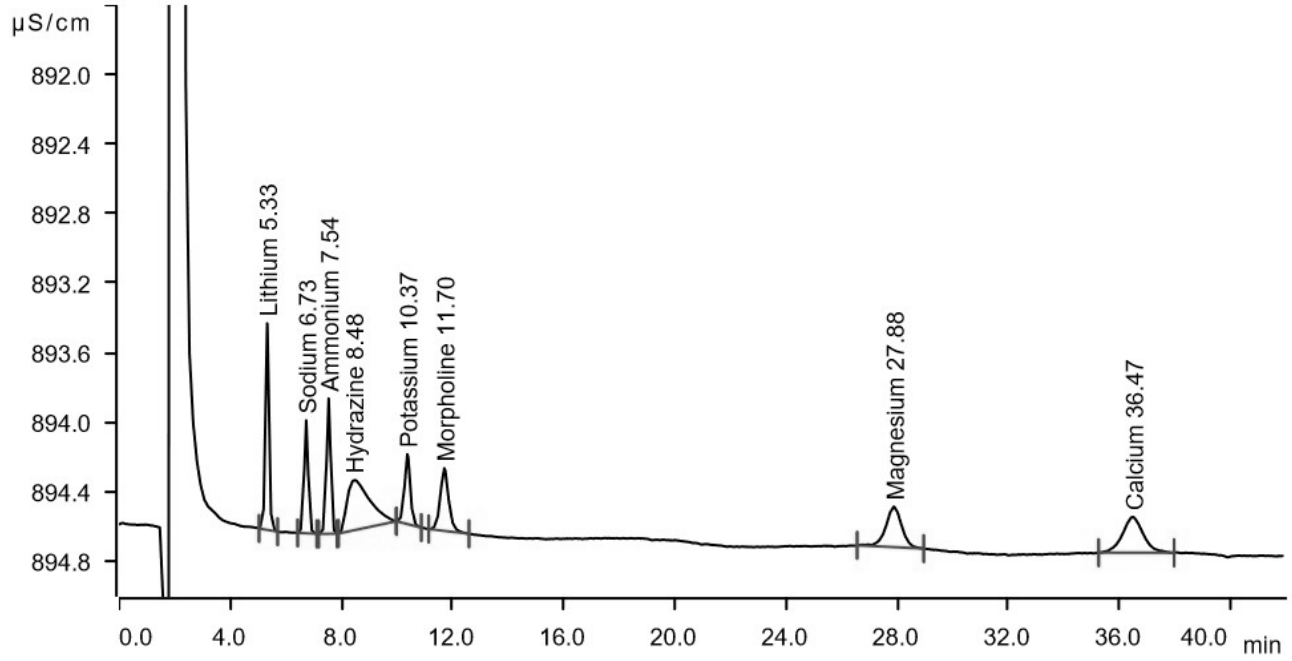

Fig. 5. Chromatogram showing separation of Hydrazine, Morpholine along with common cations

Determination of Organic acids:

Formate, acetate, propionate, isobutyrate, butyrate, isovaleriate, valeriate and capronate can be determined by ion exclusion chromatography with suppressed conductivity detection after Inline Dialysis by using a column of polystyrene divnyl benzene with sulphonic acid exchanger.

Dialysis is the process of separating molecules in solution by the difference in their rates of diffusion through a semipermeable membrane. Inline Dialysis separates not only particles from their analytes, but also colloids, oil components and large molecules. A nylon or cellulose acetate membrane with pore size 0.2µm is used. One membrane can be used for analysis of many samples.

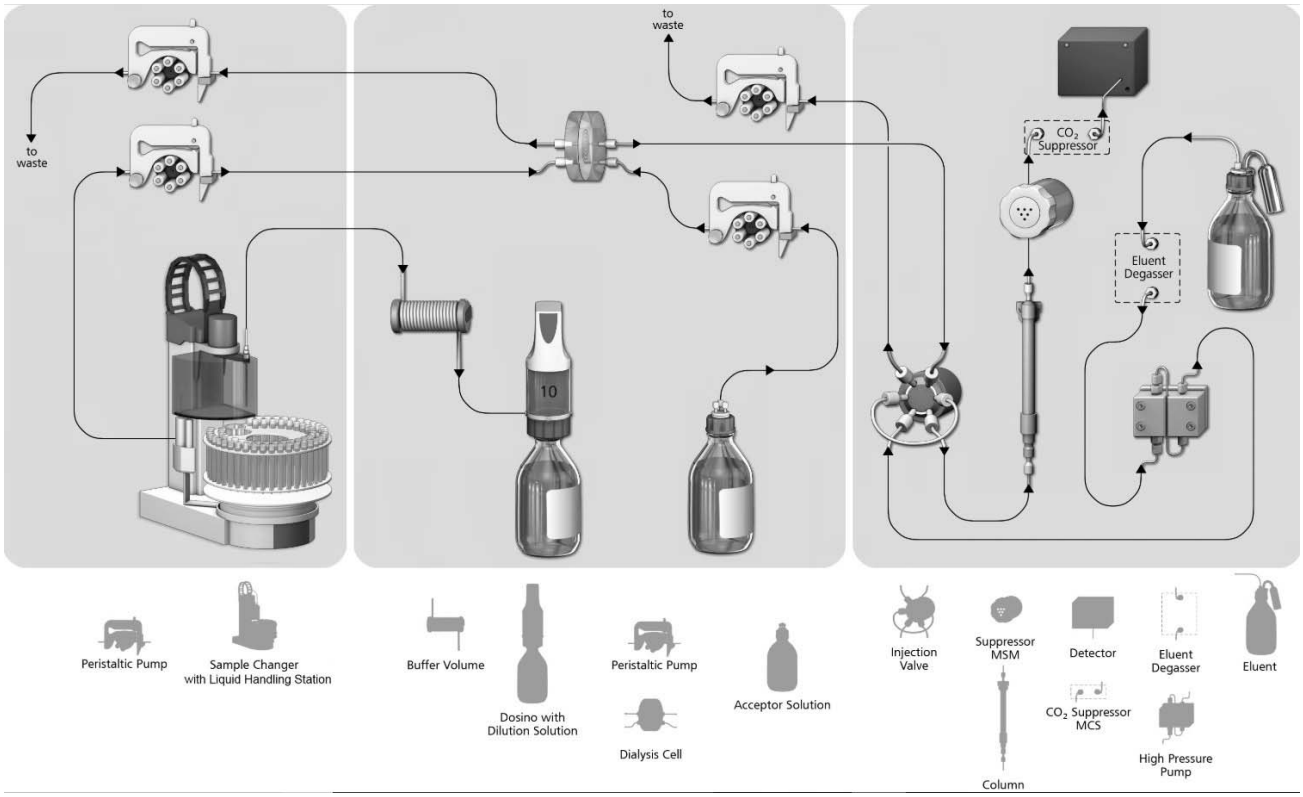

Fig. 6. Automated inline dialysis set up

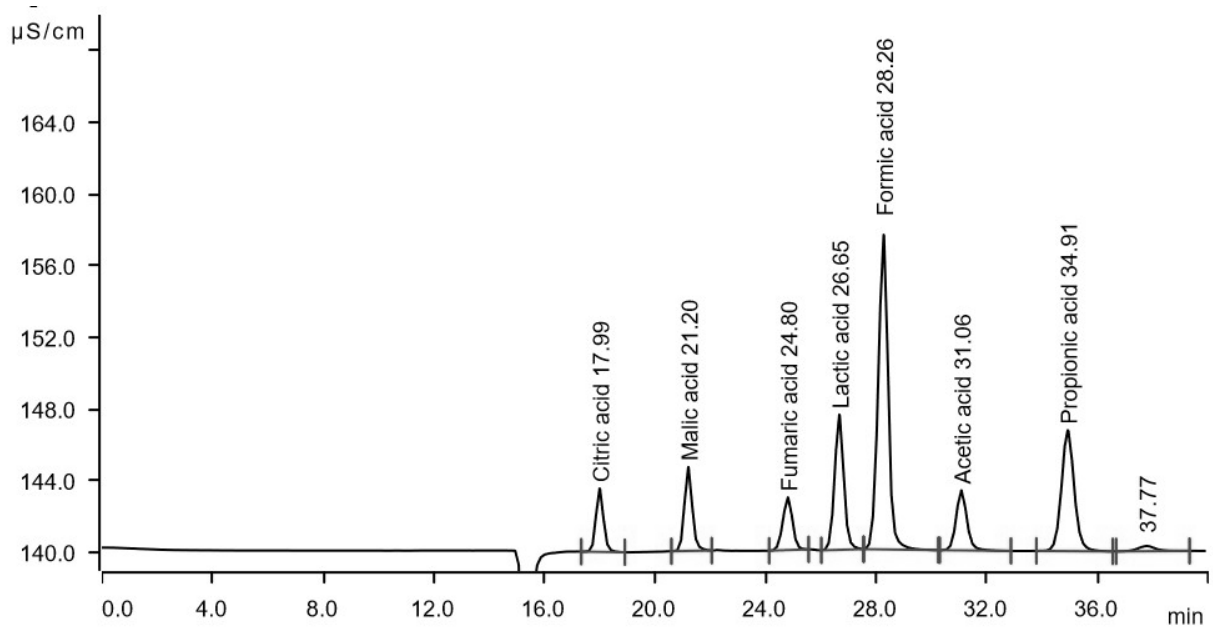

Fig. 7. Chromatogram showing separation of organic acids

Xylose, xylotriose, xylotetrose and xylopentose in xylose derivatives can be determined using an anion exchange column with Polystyrene divinylbenzene copolymer with quaternary ammonium groups using a gradient separation.

Xylose is a monosaccharide of the aldopentose type consisting of five carbon atoms and an aldehyde functional group. Xylose is a sugar isolated from wood. D-Xylose is a sugar widely used as a diabetic sweetener in food and beverage, Xylose has also been used as a diagnostic agent to observe malabsorption.

Metrosep Carb 2 - 250/4.0, the high-capacity anion exchanger column is particularly suitable for the determination of carbohydrates using alkaline eluents and pulsed amperometric detector. The base material is made of styrene-divinylbenzene copolymer which is stable in the range of pH = 0 to pH = 14 and separates monosaccharides and disaccharides. It is also suitable for the analysis of sugar alcohols, anhydrous sugars, amino sugars, etc.

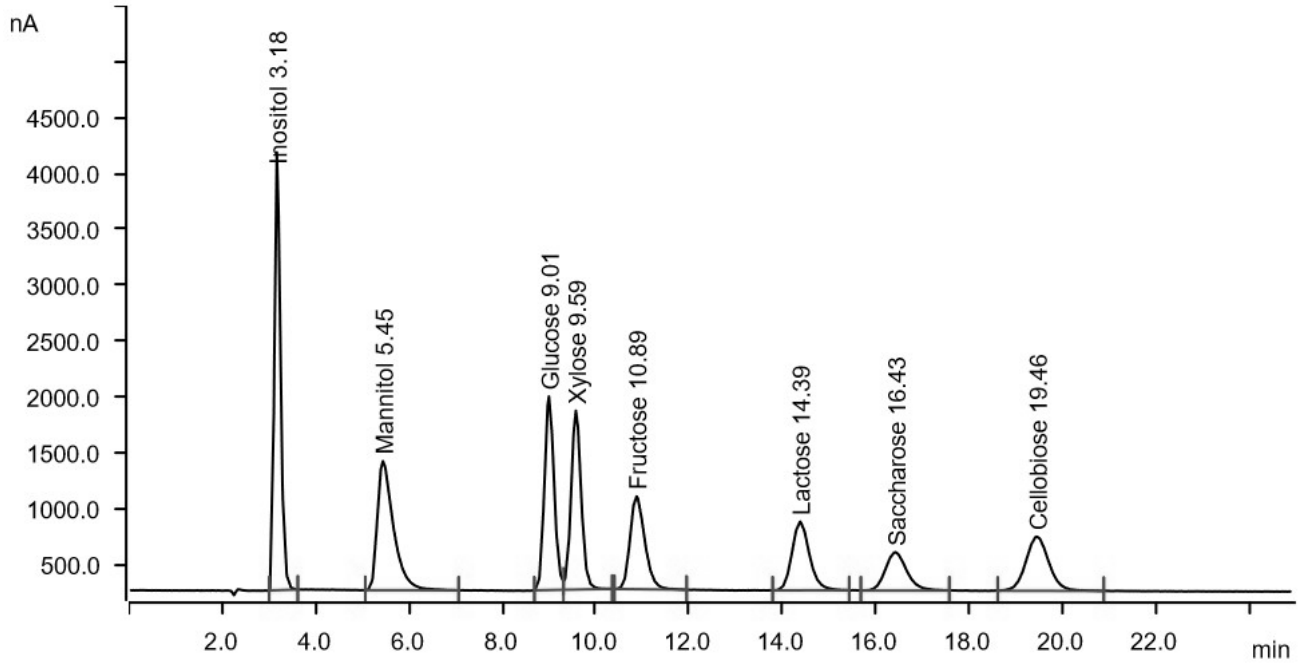

Fig. 8. Chromatogram showing separation of carbohydrates

Determination of amino acids in Desmopressin by UV Vis Detector:

Desmopressin is used to control the amount of urine produced by kidneys. Normally, the amount of urine is controlled by a certain substance in the body called vasopressin. Desmopressin is a man-made form of vasopressin and is used to replace low levels of vasopressin. This medication helps to control increased thirst and excess urination and thus helps prevent dehydration.

The determination of amino acids in Desmopressin is carried out as per EP method. The binary gradient is performed with a 940 Professional IC Cation Gradient. The PCR reaction takes place at 120°C in the Professional Reactor and the components are detected with the Professional UV/VIS detector.

Metrosep Amino Acids 1 - 100/4.0 is the standard separation column for amino acids. The column matrix is sulfonated polystyrene-divinylbenzene. The determination of amino acids is accomplished by means of photometric detection following a post-column reaction with ninhydrin.

Metrosep Amino Acids 1 - 100/4.0 permits the separation of up to 44 amino acids including all the naturally occurring amino acids.

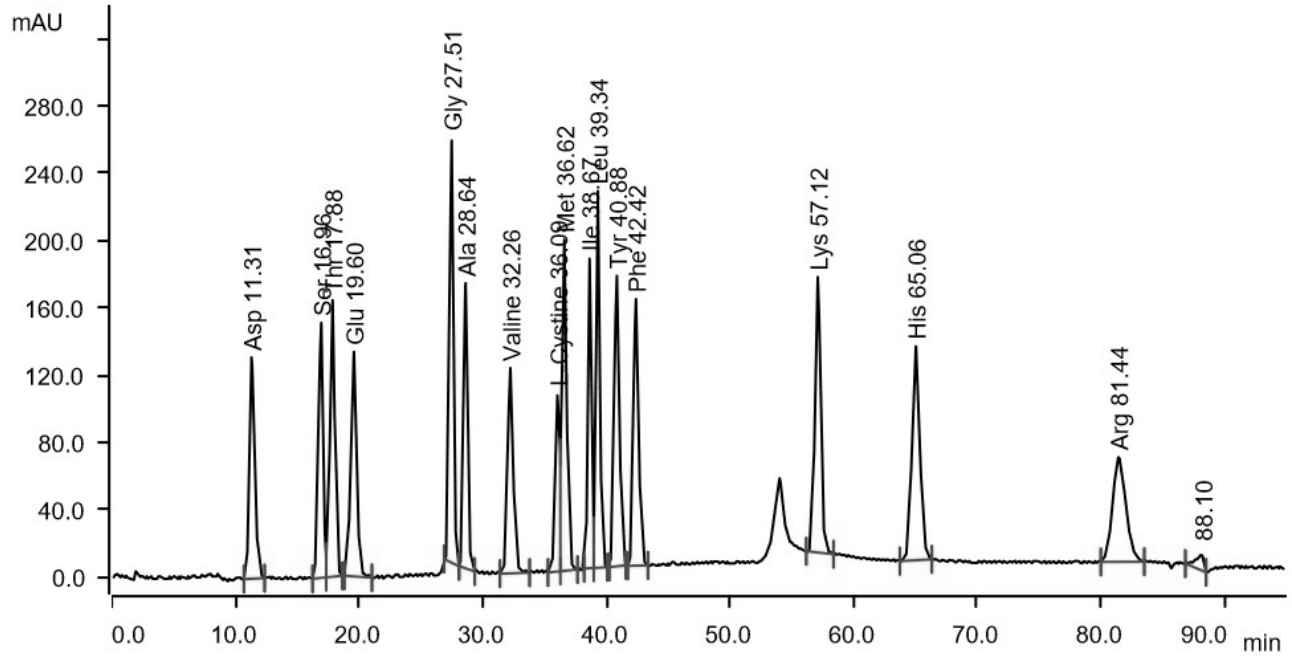

Fig. 9. Chromatogram showing amino acid separation

Conclusions

Ion chromatography is a very useful analytical in quantifying a variety of analytes like anions, cations, amines, organic acids, sugars, sugar alcohols, amino acids in samples from pharmaceutical, food, petrochemical, environmental semiconductors, fertilizers, explosives, textiles, paper, ceramics, cements, minerals, chemicals, solvents, thermal and nuclear power plants. The speed of analysis, ability to analyse multiple analytes in a single analysis, capacity to analyse ions from parts per billion to percentage level, detection of trace level of analytes in presence of large excess of other similar analytes, flexibility in use of inline sample preparation modules like ultra filteration, dialysis, matrix elimination, pre concentration, partial loop techniques, use of different detectors like conductivity, UV-VIS, amperometry, ability to connect with other advanced techniques like IC ICP AES IC ICP MS have made ion chromatography the most promising, reliable and economical analytical tool.

References

1. Ramajeevan Ganeshjeevan, Raghavan Chandrasekar, Subramanian Yuvaraj and Ganga Radhakrishnan., 2003, *Journal of Chromatography* **A, 988**, 157-165.

2. P. Chandra Mouli, S. Venkata Mohan, S. Jayaraman Reddy., 2003, *Journal of Hazardous Materials,* **B99**, 217-228.

3. Rajmund Michalski, *Journal of Chromatographic Science*, **48**, August 2010.

4. Jonathan Bruce, 2002, *Journal of Automated Methods & Management in Chemistry*, **24(4)**, 127-130

5. Thyagarajan Shanmugam, Joseph Selvaraj and Uvaraj Mani., 2019, *Journal of Chromatographic Science,* **57(10)**, 939-943.

6. Caterina Giuriati, Silvano Cavalli, Alfredo Gorni, Denis Badocco and Paolo Pastore, 2004, *Journal Chromatography A*, **1023,** 105-112.

7. Colenutt, B.A. and Trenchard P.J., 1985, *Environmental Pollution (Series B),* **10,** 77-96.

8. EPA 300.1 Part A and Part B : Determination of inorganic anions in drinking water by Ion Chromatography

9. EPA 314.0 : Determination of perchlorate in drinking water by Ion Chromatography

10. EPA 218.7 : Determination of dissolved hexavalent chromium by means of Ion Chromatography (post-column reaction and VIS detection)

11. DIN EN ISO 14911 : Water quality – Determination of dissolved lithium, sodium, ammonium, potassium, manganese, calcium, magnesium, strontium and barium using Ion Chromatography – Method for water and waste water

12. DIN 38405-7 : Determination of cyanide in slightly polluted water by Ion Chromatography

13. DIN EN ISO 15061 : Determination of dissolved bromate in drinking water

14. ASTM D 7319-07 : Standard test method for determination of total and potential sulfate and inorganic chloride in fuel ethanol by direct injection suppressed Ion Chromatography

15. ASTM D4327-03 : Standard test method for anions in water by chemically suppressed Ion Chromatography

16. ASTM D5257-03 : Standard test method for dissolved hexavalent chromium in water by Ion Chromatography.

RNI No. MAHENG/2017/74063
ISSN No. (Print) 2581-5911
ISI Impact Factor 1.022 (2019-2020)

Synthesis of Chlorinated N-glucopyranosyl Thiocarbamides and 1,2,4-Dithiazolidines and Study of their Antimicrobial Activity

Aruna Hardas[1*] and Priti Tayade (Gosavi)[2]
[1] Department of Chemistry, S.F.S. College, Seminary Hills, Nagpur 440006, Maharashtra, India
[2] Innovation Centre, Raman Science Centre, Nagpur 440018, Maharashtra, India
*** Email: arunahardas777@gmail.com; gosavipriti@gmail.com**

Abstract
The present study deals with the chorination of N-glucopyranosyl thiocarbamide and 1,2,4 dithiazolidine. Chlorination of the compound under study is important due to its pharmacological activities. Targeted chlorinated compounds were divided into two series. Series I is 1-tetra –O-acetyl –β-D glucopyranosyl -3-mono/di/tri chloro phenyl thiocarbamide and series II is 3-phenyl/p-chlorophenyl-4-mono/di/tri chloro phenyl -5-tetra-O-acetyl-β-D-glucopyranosylimino-1,2,4-dithiazolidine. The characterization techniques such as IR spectroscopy, NMR spectroscopy and Mass spectroscopy were used for the analysis of the chlorinated compounds. All chlorinated compounds were examined for their antimicrobial activities against gram *(-) E.coli and* gram *(+) staphylococcus aureus. Compound 3-p-chlorophenylimino-4-p-chloro phenyl 5-tetra-o-acetyl-β-D-glucopyranosyl imino-1,2,4 dithiazolidine (IIa) and 3 p-chlorophenylimino-4 (2, 4 dichloro) phenyl 5-tetra-o-acetyl-β-D-glucopyranosyl imino-1,2,4 dithiazolidine (IIb) were found to be most effective over a wide range of time period particularly for 24h, 48h and 72 h.*

Keywords: *Chlorination of N-gluconosyl thiocarbamide, Chlorination of dithiazolidine, Mass fragmentation pattern, NMR, Antimicrobial activities.*

Introduction

Synthesis of 1,2,4-dithiazolidines and its pharmacological activities have been reported earlier[1-9] 1,2,4-dithiazolidines have been found to have potential anti-inflammatory and antitumor activity properties as they downregulate the NF-kB transcription factor[10].

In our previous study, we have reported the synthesis of 1-tetra –O-acetyl –β-D glucopyranosyl –phenyl thiocarbamide and 3-phenyl-4-phenyl -5-tetra-O-acetyl-β-D-glucopyranosylimino-1,2,4-dithiazolidine from glucose as starting material.

The present study deals with chlorination of two series of N-glucosylated compounds. Targeted Series (I) is 1-tetra –o-acetyl –β-D glucopyranosyl -3-mono/di/tri chloro phenyl thiocarbamide and Series (II) is 3-phenyl/p-chlorophenyl-4-mono/di/tri chloro phenyl -5-tetra-O-acetyl-β-D-glucopyranosylimino-1,2,4-dithiazolidine.

Furthermore, their antimicrobial activities have been studied along with effect of chlorination site on antimicrobial activity.

Materials and Methods

Synthesis of tetra-o-acetyl β-D-glucopyranosyliso-thiocyanate

The compound tetra-o-Acetyl β-D glucopyranosyl isothiocyanate was synthesized[9, 11]. A solution of 20 g of tetra-O-Acetyl- β-D-glucopyranosyl bromide in 150 mL Xylene was prepared. 16 g of lead isothiocyanate was added with refluxing for 3hr. Agitation by means of shaking was provided. The solution was cooled and the compound was obtained by filtration and further purification.

Synthesis of chlorinated thiocarbamide and 1,2,4-dithiazolidine

Interaction between tetra-O-acetyl- β-D-glucopyranosyl isothiocyanate and appropriate chloroaniniline results in the respective chlorinated compounds.

Synthesis of 1-p-chlorophenyl-3-tetra –O-acetyl –β-D-glucopyranosyl –thiocarbamide. (Ia)

In a typical synthesis, 0.02M i.e. 7.8 g of tetra-o-acetyl-β-D glucopyranosyl isothiocyanate in 50mL benzene was dissolved. 0.02M i.e. 2.52 g of p-chloro-aniline in 20 mL benzene was prepared separately. Both the reactants were added together and allowed to reflux in a boiling water bath for 3 hours. Benzene was removed by distillation. A sticky mass was triturated several times with petroleum ether. A granular solid with yield of 5 g was obtained. The compound was crystallized by using aqueous alcohol denoted as **(Ia)**.

Reaction

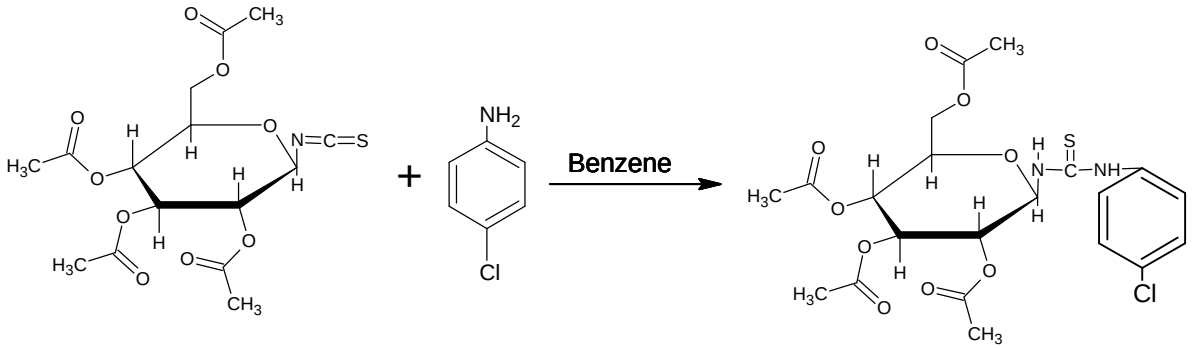

2,3,4,6 tetra-O-acetyl-β–D glucopyranosyl isothiocynate

p-chloro aniline

(1-p-chloro) phenyl-3 tetra-O-acetyl-β–D-glucopyranosyl thiocarbamide (Ia)

Synthesis of 1-(2,4 dichloro) phenyl-3-tetra-O-acetyl - β-D-glucopyranosyl thiocarbamide.(Ib)

0.02 M solution of 2,4-dichloro aniline i.e. 3.24 g in 20 mL benzene was prepared. A separate 0.02 M solution of tetra-o-acetyl –β-D-glucopyranosyl isothiocyanate i.e. 7.8 g in 40 mL benzene was prepared. Both the reactants were allowed to mix. The mixture was refluxed for 3 hours. The solvent was removed by distillation. A sticky mass was obtained as product, which was triturated several times with petroleum ether. A granular solid was obtained **(Ib)**. The material was crystallized by using ethanol and water. The yield of material was found to be 4.5 g. The melting point of material was found to be 178°C.

Reaction

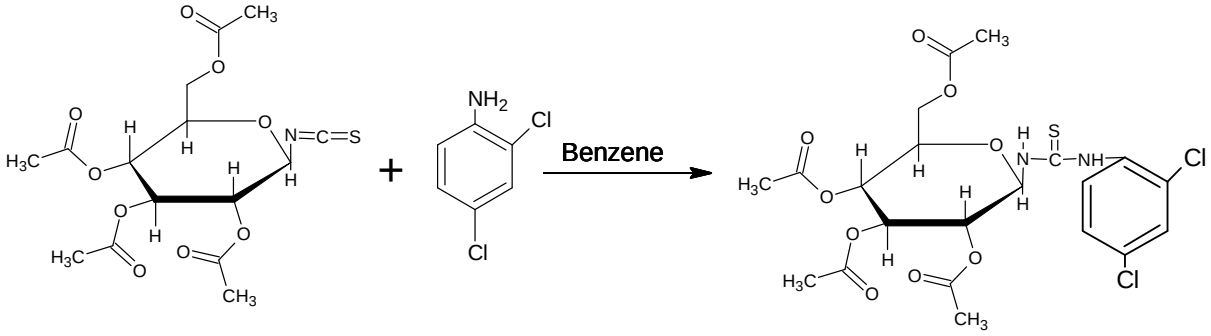

2,3,4,6 tetra-O-acetyl-β–D glucopyranosyl isothiocynate

2,4-di-chloro aniline

1-(2,4-di-chloro) phenyl-3 tetra-O-acetyl-β–D-glucopyranosyl thiocarbamide

Synthesis of 1-(3,4 dichloro) phenyl -3-tetra-O-acetyl - β-D-glucopyranosyl –thiocarbamide. (Ic)

0.02 M solution of 3,4 dichloro aniline in benzene i.e. 3.24 g in 20 mL was prepared. A separate 0.02 M solution of tetra-o-acetyl- β-D- glucopyranosyl isothiocyanate in benzene (7.8 g in 40 mL) was prepared. Both the reactants are allowed to mix and refluxed for 3 hours in a boiling water bath. Benzene was removed by dry distillation method. A sticky mass was obtained, which was triturated several times by using petroleum ether. The obtained granular mass was crystallized by using ethanol and water. The crystalline product was denoted as **Ic**.

Reaction

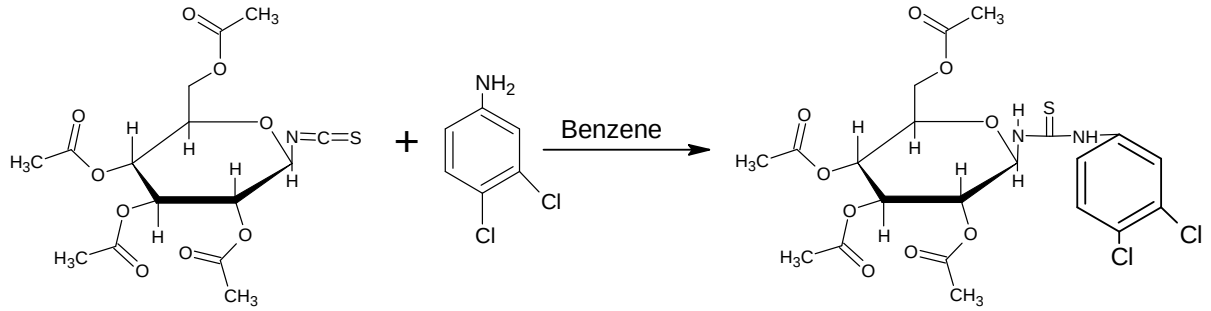

2,3,4,6 tetra-O-acetyl-β–D glucopyranosyl isothiocynate

3,4-di-chloroaniline

1-(3,4 di-chloro) phenyl-3 tetra-O-acetyl-β–D-glucopyranosyl thiocarbamide

Synthesis of 1-(2,4,6 trichoro) phenyl -3-tetra-O-acetyl - β-D-glucopyranosyl –thiocarbamide. (Id)

0.02 M solution of 2,4,6-trichloro aniline in benzene i.e. 3.93 g in 20 mL was prepared. A separate 0.02 M solution of tetra-o-acetyl- β-D- glucopyranosyl isothiocyanate in benzene (7.7 g in 40 mL) was prepared. Both the reactants were allowed to mix and refluxed for 3 hours in a boiling water bath. Benzene was removed by dry distillation method. A sticky mass was obtained, which was triturated several times by using petroleum ether. The obtained granular mass was crystallized by using ethanol and water. The crystalline product was denoted as **Id**.

Reaction

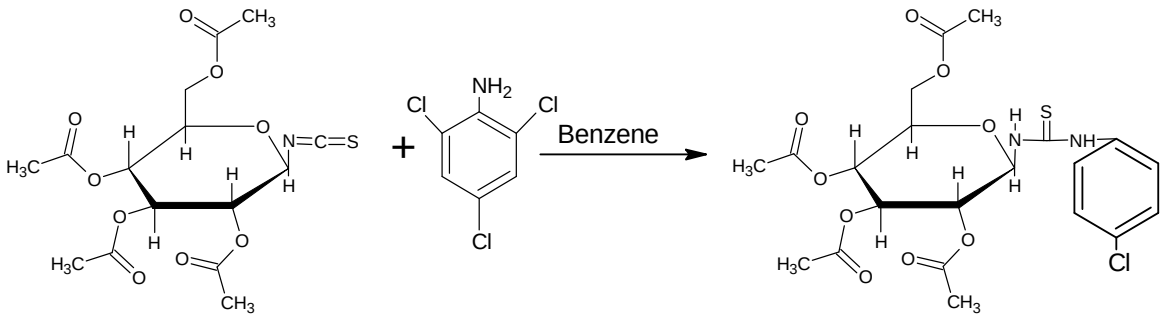

2,3,4,6 tetra-O-acetyl-β–D glucopyranosyl isothiocynate

2,4,6-tri-chloroaniline

1-(2,4,6-trichoro) phenyl-3 tetra-O-acetyl-β–D-glucopyranosyl thiocarbamide

Synthesis of 3-p-chlorophenylimino-4-p-chloro phenyl 5-tetra-O-acetyl-β-D-glucopyranosyl imino-1,2,4 dithiazolidine (IIa)

A suspension of finely powdered 1-p-chloro phenyl-3-tetra-o-acetyl- β-D- glucopyranosyl thiocarbamide (**Ia**) was prepared by adding 5.16 g in 20 mL of benzene. A separate solution of N-p-chloro phenyl –S-chloro thiocarbamide by adding 2.45 g in 10 mL benzene was prepared. A suspension of **Ia** was added to the solution of N-p-chloro phenyl –S-chlorothiocarbamide and refluxed for 4 hours in a water bath. A brisk reaction with evolution of Hydrogen chloride was noticed. The remaining suspended solid was removed by filtration. The solvent was removed by dry distillation. An oily residue was obtained, which was triturated several times by using petroleum ether. The granular solid was crystallized by using ethanol and water. **(IIa)**

Reaction

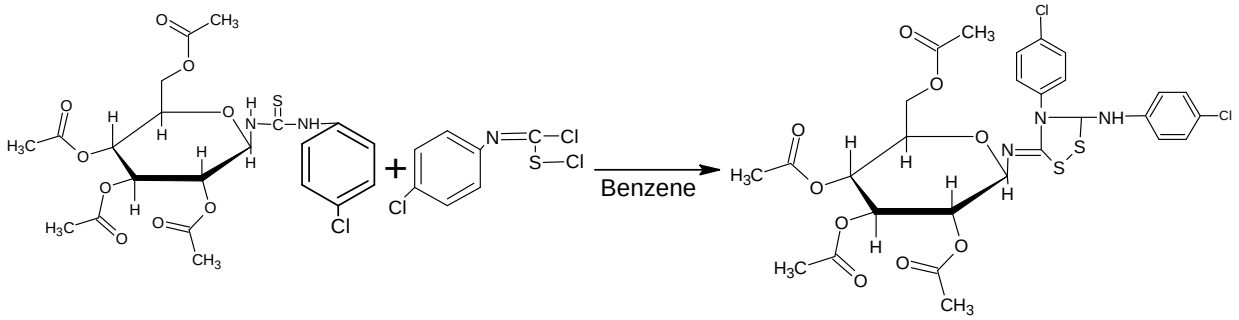

1-(p-chloro) phenyl-3 tetra-O-acetyl-β–D-glucopyranosyl thiocarbamide

s-chloro-N-p-chlorophenyl isothiocarbamoyl chloride

3-p-chlorophenyl imino-4-p-chlorophenyl-tetra-O-acetyl-β–Dglucopyranosyl imino-1,2,4-dithiazolidine (IIa)

Synthesis of 3 p-chlorophenylimino-4 (2, 4 dichloro) phenyl -5-tetra-O-acetyl-β-D-glucopyranosyl imino-1,2,4 dithiazolidine (IIb)

A suspension of finely powdered 1-(2,4-dichloro) phenyl-3-tetra-O-Acetyl-β-D-glucopyranosyl thiocarbamide **(Ib)** was prepared by adding 5.51 g of **Ib** in 20 mL of benzene. A separate solution of N-p-chloro phenyl –S-chlorothiocarbamide by adding 2.45 g in 10 mL benzene was prepared. A suspension of **Ib** was added to the solution of N-p-chloro phenyl –S-chlorothiocarbamide

and refluxed for 4 hours in a water bath. A brisk reaction with evolution of Hydrogen chloride was noticed. The remaining suspended solid was removed by filtration. The solvent was removed by dry distillation. An oily residue was obtained, which was triturated several times by using petroleum ether. The granular solid was crystallized by using ethanol and water. **(IIb)**

Reaction

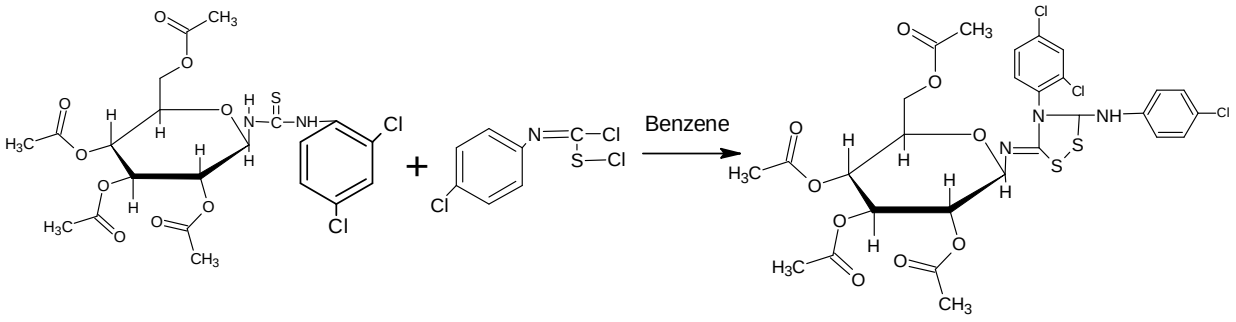

1-(2,4-di-chloro) phenyl-3 tetra-O-acetyl-β–D-glucopyranosyl thiocarbamide

s-chloro-N-p-chlorophenyl isothiocarbamoyl chloride

3-p-chlorophenyl imino-4-(2,4-dichloro) phenyl-tetra-O-acetyl-β–Dglucopyranosyl imino-1,2,4-dithiazolidine (IIb)

Synthesis of 3- p-chlorophenylimino-4(3,4 dichloro) phenyl -5-tetra-O-acetyl-β-D-glucopyranosyl imino-1,2,4 dithiazolidine(IIc)

A suspension of finely powdered 1-(3,4-dichloro) phenyl-3-tetra-O-Acetyl-β-D-glucopyranosyl thiocarbamide **(Ic)** was prepared by adding 5.51 g of Ib in 20 mL of benzene. A separate solution of N-p-chloro phenyl –S-chlorothiocarbamide by adding 2.45 g in 10 mL benzene was prepared. A suspension of **Ic** was added to the solution of N-p-chloro phenyl –S-chlorothiocarbamide and refluxed for 4 hours in a water bath. A brisk reaction with evolution of Hydrogen chloride was noticed. The remaining suspended solid was removed by filtration. The solvent was removed by dry distillation. An oily residue was obtained, which was triturated several times by using petroleum ether. The granular solid was crystallized by using ethanol and water. **(IIc)**

Reaction

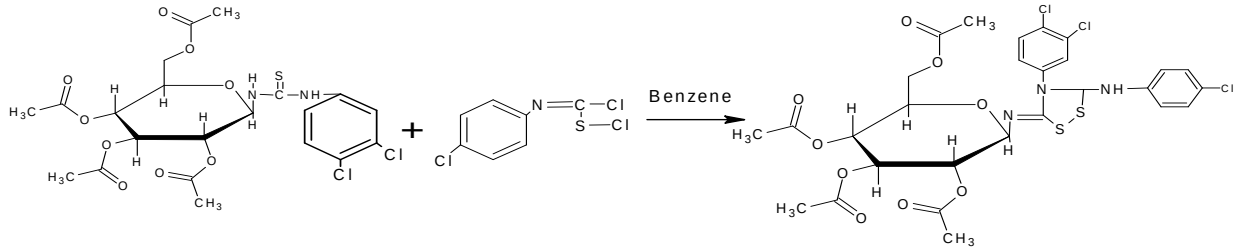

1-(3,4-di-chloro) phenyl-3 tetra-O-acetyl-β–D-glucopyranosyl thiocarbamide

s-chloro-N-p-chlorophenyl isothiocarbamoyl chloride

3-p-chlorophenyl imino-4-(3,4-dichloro)phenyl-tetra-O-acetyl-β–D glucopyranosyl imino-1,2,4-dithiazolidine (IIc)

Synthesis of 3 p-chlorophenylimino-4(2,4,6 trichloro) phenyl 5-tetra-O-acetyl-β-D-glucopyranosyl imino-1,2,4 dithiazolidine (IId)

A suspension of finely powdered 1-(2,4,6-trichloro) phenyl-3-tetra-O-Acetyl-β-D-glucopyranosyl thiocarbamide

(Id) was prepared by adding 5.58 g of **Ib** in 20 mL of benzene. A separate solution of N-p-chloro phenyl –S-chlorothiocarbamide by adding 2.45 g in 10 mL benzene was prepared. A suspension of **Id** was added to the solution of N-p-chloro phenyl –S-chlorothiocarbamide and refluxed for 4 hours in a water bath. A brisk reaction with evolution of Hydrogen chloride was noticed. The remaining suspended solid was removed by filtration. The solvent was removed by dry distillation. An oily residue was obtained, which was triturated several times by using petroleum ether. The granular solid was crystallized by using ethanol and water. **(IId)**

Reaction

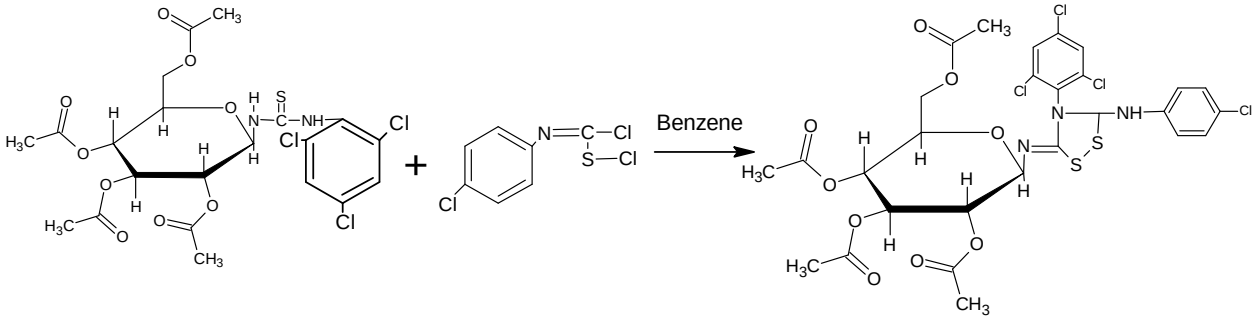

1-(2,4,6-tri-chloro) phenyl-3 tetra-O-acetyl-β–D-glucopyranosyl thiocarbamide

s-chloro-N-p-chlorophenyl isothiocarbamoyl

3-p-chlorophenyl imino-4-(2,4,6-tri-chloro)phenyl-tetra-O-acetyl-β –Dglucopyranosyl imino-1,2,4-dithiazolidine (IId)

Synthesis of 3-phenylimino-4 –p-chloro phenyl 5-tetra-O-acetyl-β-D-glucopyranosyl imino-1,2,4 dithiazolidine (IIe)

A suspension of finely powdered 1-p-chloro phenyl-3-tetra-O-Acetyl-β-D-glucopyranosyl thiocarbamide **(Ia)** was prepared by adding 5.58 g of **Ia** in 20 ml of benzene. A separate solution of N- phenyl –S-chlorothiocarbamoyl chloride by adding 2.45 g in 10 mL benzene was prepared. A suspension of **Ia** was added to the solution of N-phenyl-S-chloroisothiocarbamide and refluxed for 4 hours in a water bath. A brisk reaction with evolution of Hydrogen chloride was noticed. The remaining suspended solid was removed by filtration. The solvent was removed by dry distillation. An oily residue was obtained, which was triturated several times by using petroleum ether. The granular solid was crystallized by using ethanol and water. **(IIe)**

Reaction

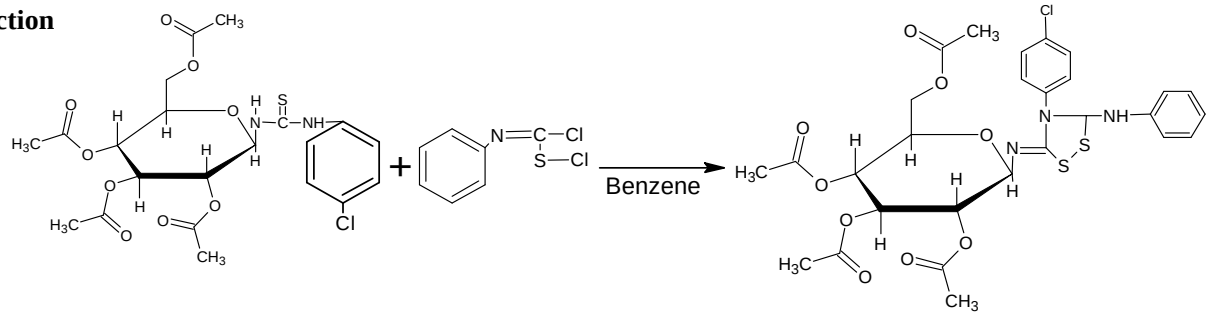

(1-p-chloro) phenyl-3 tetra-O-acetyl-β–D-glucopyranosyl thiocarbamide

s-chloro-N-phenyl isothiocarbamoyl chloride

3-p-phenyl imino-4-p-chlorophenyl -tetra-O-acetyl-β–Dglucopyranosyl imino-1,2,4-dithiazolidine (IIe)

Synthesis of 3 p-chlorophenylimino-4- phenyl 5-tetra-O-acetyl-β-D-glucopyranosyl imino-1,2,4 dithiazolidine (IIf)

A suspension of 1-phenyl-3-tetra-O-acetyl-â-D-glucopyranosyl-thiocarbamide was prepared by adding 9.6 g i.e. 0.02 M in 40 mL of benzene. A separate solution of N-p-chlorophenyl –S-chloroisothiocarbamoyl chloride by adding 4.18 g in 20 mL of benzene was prepared. Both the solutions were mixed and refluxed for 4h. An oily residue was obtained which was further purified. The solid obtained was crystallized by using ethanol and water. **(IIf)**

Reaction

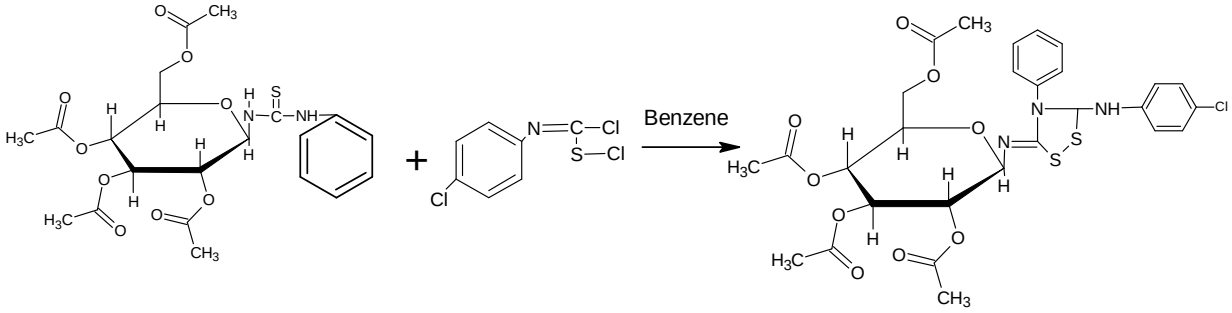

1-phenyl-3 tetra-O-acetyl-β–D-glucopyranosyl thiocarbamide

s-chloro-N-p-chlorophenyl isothiocarbamoyl Chloride

3-p-chlorophenyl imino-4-phenyl -tetra-O-acetyl-β–Dglucopyranosyl imino-1,2,4-dithiazolidine (IIf)

Synthesis of 3 -phenylimino-4(2,4 dichloro) phenyl 5-tetra-O-acetyl-β-D-glucopyranosyl imino-1,2,4 dithiazolidine (IIg)

A suspension of finely powdered 1-(2,4-dichloro) phenyl-3-tetra-O-Acetyl-β-D-glucopyranosyl thiocarbamide **(Ib)** was prepared by adding 5.51 g in 20 mL of benzene. A separate solution of N- phenyl –S-chlorothiocarbamoyl chloride by adding 2.06 g in 20 mL benzene was prepared. A suspension of **Ib** was added to the solution of N-p-chloro phenyl –S-chlorothiocarbamide and refluxed for 4 hours over a water bath. A brisk reaction with evolution of Hydrogen chloride was noticed. Gradually solid went into the solution. Remaining suspended solid was removed by filtration. The solvent was removed by dry distillation. An oily residue was obtained, which was triturated several times by using petroleum ether. The granular solid was crystallized by using ethanol and water. We denoted this material as **IIg.**

Reaction

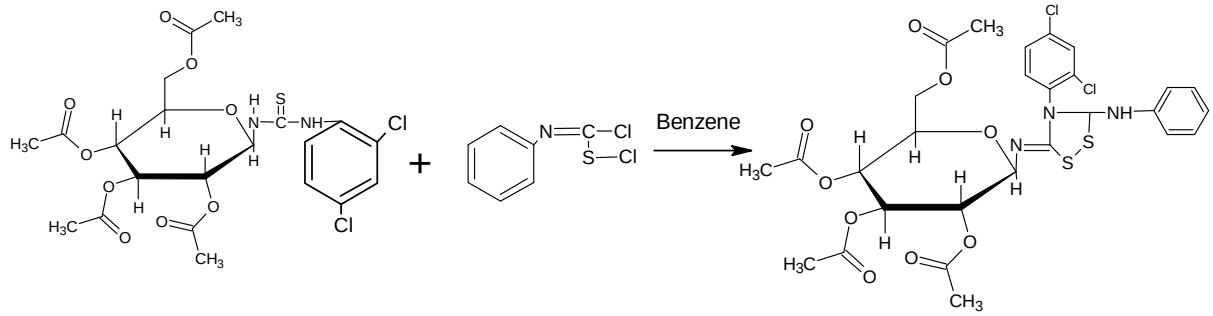

1-(2,4-di-chloro) phenyl-3 tetra-O-acetyl-β–D-glucopyranosyl thiocarbamide

s-chloro-N-phenyl isothiocarbamoyl chloride

3-phenyl imino-4-(2,4-dichloro)phenyl-tetra-O-acetyl-β–Dglucopyranosyl imino-1,2,4-dithiazolidine (IIg)

Synthesis of 3 -phenylimino-4(3,4 dichloro) phenyl 5-tetra-O-acetyl-β-D-glucopyranosyl imino-1,2,4 dithiazolidine(IIh)

A benzene solution of N-phenyl-S-chloro-isothiocarbamoyl chloride, i.e. 2.06 g in 10 mL was added to the suspension of 1-(3,4 –dichloro)-phenyl -3-tetra-O-acetyl –β-D-glucopyranosyl thiocarbamide, **(Ic)** i.e. 5.51 g in 20 **ml** benzene. The reactants were refluxed for 4 hours in a water bath. A brisk reaction with evolution of Hydrogen chloride was noticed. The remaining suspended solid was removed by filtration. The solvent was removed by dry distillation. An oily residue was obtained, which was triturated several times by using petroleum ether. The granular solid was crystallized by using ethanol and water. **(IIh)**

Reaction

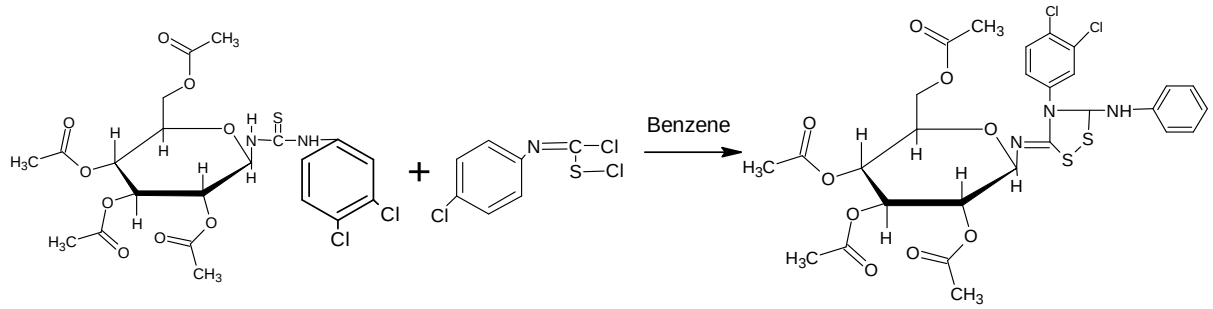

1-(3,4-di-chloro) phenyl-3 tetra-O-acetyl-β–D-glucopyranosyl thiocarbamide

s-chloro-N-p-chlorophenyl isothiocarbamoyl

3-p-chlorophenyl imino-4-(3,4,-di-chloro)phenyl-tetra-O-acetyl-β–Dglucopyranosyl imino-1,2,4-dithiazolidine (IIh)

Antimicrobial activity

The stains used for testing antimicrobial activity of synthesized chlorinated compounds were gram (+) *staphylococcus aureus and* gram (-) *E.Coli*.

Preparation of nutrient broth medium

The nutrient broth medium was prepared by dissolving 2.6 g nutrient broth (commercial grade) having composition; peptone 5.0 g/L, sodium chloride 5.0 g/L, beef extract 1.5 g/L, yeast extract 1.5 g/L in 200 ml of distilled water. The pH of the nutrient composition at 25°C was 7.4 ± 0.2. The nutrient mixture was sterilized in an autoclave.

Preparation of stock solution

The stock solutions of compounds **Ia to Id** and **IIa to IIh** were prepared by dissolving 30 mg of each sample in 5 mL dimethyl sulphoxide. These stock solutions were also sterilized in an autoclave.

Sterilization of glassware

Glasswares were carefully sterilized in an autoclave.

Inoculation

To the sterilized test tubes, 5 mL nutrient broth was transferred by pipette. To each test tube, stock solutions (0.1 mL) of **Ia to Id** and **IIa to IIb** were added. The resultant system was then inoculated with *Staphylococcus Aureus*. The second set of systems containing 5 mL nutrient broth sample were inoculated with *E. coli*. Two reference systems were also prepared with 5 mL nutrient broth and 1mL dimethyl sulphoxide. The reference systems were also inoculated with *Staphylococcus aureus* and *E. Coli* respectively.

Incubation

The two sets of systems were kept in an incubator at 37°C at different time intervals ranging from 24 to 72 h. and after each time interval, the growth of micro-organism was recorded with respect to the standard.

Results and Discussion

Melting point and yield

Melting points of all chlorinated products are enlisted along with yield in **Table 1**.

Table 1: Physical properties of Chlorinated Compounds

Sr. No	Compound	*m.p. (°C)	Yield (g)	Solubility					
				Water	Petroleum ether	Alcohol	Acetone	$CHCl_3$	C_6H_6
1	Ia	162	5	X	X	√	√	√	√
2	Ib	178	4.5	X	X	√	√	√	√
3	Ic	135	4.5	X	X	√	√	√	√
4	Id	160	6.5	X	X	√	√	√	√
5	IIa	190	3.5	X	X	√	√	√	√
6	IIb	174	3.2	X	X	√	√	√	√
7	IIc	223	3.4	X	X	√	√	√	√
8	IId	140	3	X	X	√	√	√	√
9	IIe	-	-	X	X	√	√	√	√
10	IIf	-	-	X	X	√	√	√	√
11	IIg	145	4.5	X	X	√	√	√	√
12	IIh	205	4.5	X	X	√	√	√	√

* m.p. melting point

Solubility

Solubility behavior of thiocarbamide series and dithiazolidine series is shown in **Table 1**. Compounds from Series II i.e. dithiazolidine compounds were found to be soluble in dioxane, dimethyl formamide and dimethyl sulphoxide in addition to the solvents mentioned in **Table 1**.

Effect of concentrated Sulfuric acid and alkaline plumbite solution

Chlorinated compounds of Series I and Series II showed charring effect on treatment with concentrated sulphuric acid.

Chlorinated compounds of Series I on boiling with alkaline plumbite solution showed desulpharisation but not the chlorinated compounds of Series II.

Specific Rotation

Specific rotation of compounds from Series II are shown below.

Specific rotation $[\alpha]^{30}$ of compound **IIa** was found to be +136.40 (0, 0.16 in chloroform)

Specific rotation $[\alpha]^{30}$ of compound **IIb** was found to be -141.290 (0, 0.12 in chloroform)

Specific rotation $[\alpha]^{30}$ of compound **IIc** was found to be -122.7 (0, 0.12 in chloroform)

Specific rotation $[\alpha]^{30}$ of compound **IId** was found to be -126.67 (0, 0.13 in chloroform)

Specific rotation $[\alpha]^{30}$ of compound **IIg** was found to be +120.35 (0, 0.12 in chloroform)

Specific rotation $[\alpha]^{30}$ of compound **IIh** was found to be +156.085 (0, 0.13 in chloroform)

Elemental analysis

The elemental composition obtained from analysis was N=5.23, S=6.00 for **(Ia)**. The molecular formula of **Ia** was estimated to be $C_{21}H_{25}N_2SO_9Cl$.

Ib had the elemental composition N=5.03, S=5.60. Molecular formula of the compound was estimated to be $C_{21}H_{24}N_2SO_9Cl_2$.

Ic had the elemental composition N=4.93, S=5.45. Molecular formula of compound was estimated to be $C_{21}H_{24}N_2SO_9Cl_2$

Id had the elemental composition N=4.52, S=5.24. Molecular formula of compound was estimated to be $C_{21}H_{23}N_2SO_9Cl_3$

The compound **IIa** had elemental composition of C=48.70, H=4.82, N=6.23, S=9.18. The molecular formula of compound **IIa** was found to be $C_{28}H_{27}N_3S_2O_9Cl_2$.

The compound **IIb** had elemental composition of C=46.38, H=4.45, N=5.86, S=8.69. The molecular formula of compound **IIb** was estimated to be $C_{28}H_{26}N_3S_2O_9Cl_3$.

The compound **IIc** had elemental composition of C=4.93, S=8.28. The molecular formula of compound **IIc** was estimated to be C28H26N3S2O9Cl3.

The compound **IId** had elemental composition of N=4.2, S=8.27. The molecular formula of compound **IId** was estimated to be C28H25N3S2O9Cl4

The compound **IIg** had elemental composition of N=5.91, S=9.03. The molecular formula of compound **IIg** was estimated to be C28H27N3S2O9Cl2.

The compound **IIh** had elemental composition of N=5.72, S=9.13. The molecular formula of compound **IIg** was estimated to be C23H27N3S2O9Cl2

Table 2. Absorption peaks obtained from IR analysis for Chlorinated Thiocarbamides (Series I)

Absorption peak observed (cm^{-1})	Absorption corresponding group
IR absorption peaks Ia	
3340	N-H stretching
1360	C-N stretching
1535	Phenyl nucleous
1210	C=S stretching
890	β-D-glucopyranosyl ring
1030	Aryl chloride
IR absorption peaks for Ib	
3340	N-H stretching
1370	C-N stretching
1550	Phenyl nucleous
1240	C=S stretching
900	β-D-glucopyranosyl ring
1040	Aryl chloride
IR absorption peaks for Ic	
3340	N-H stretching
1370	C-N stretching
1525	Phenyl nucleous
1220	C=S stretching
890	β-D-glucopyranosyl ring
1030	Aryl chloride

Absorption peak observed (cm^{-1})	Absorption corresponding group
IR absorption peaks for Id	
3340	N-H stretching
1360	C-N stretching
1530	Phenyl nucleous
1220	C=S stretching
895	β-D-glucopyranosyl ring
1030	Aryl chloride

Table 3. Absorption peaks obtained from IR analysis for chlorinated 1,2,4 -dithiazolidines (Series II)

Absorption peak observed(cm^{-1})	Absorption corresponding group
IR absorption peaks for IIa	
1735	C=O stretching
1600	C=N stretching
1350	C-N stretching
690	C-S stretching
480	S-S stretching
890	β-D-glucopyranosyl ring
1030	Aryl chloride
IR absorption peaks for IIb	
1735	C=O stretching
1600	C=N stretching
1350	C-N stretching
690	C-S stretching
480	S-S stretching
890	β-D-glucopyranosyl ring
1030	Aryl chloride
IR absorption peaks for IIc	
1735	C=O stretching
1550	C=N stretching
1350	C-N stretching
690	C-S stretching
480	S-S stretching
890	β-D-glucopyranosyl ring
1030	Aryl chloride
IR absorption peaks for IId	
1735	C=O stretching
1600	C=N stretching
1360	C-N stretching
790	C-S stretching
480	S-S stretching
890	β-D-glucopyranosyl ring
1030	Aryl chloride

Absorption peak observed(cm^{-1})	Absorption corresponding group
IR absorption peaks for IIg	
1740	C=O stretching
1590	C=N stretching
1330	C-N stretching
690	C-S stretching
460	S-S stretching
898	β-D-glucopyranosyl ring
1030	Aryl chloride
IR absorption for IIh	
1735	C=O stretching
1600	C=N stretching
1330	C-N stretching
690	C-S stretching
470	S-S stretching
898	β-D-glucopyranosyl ring
1030	Aryl chloride

NMR spectral analysis

The NMR spectrum of **Ia** distinctly showed the signals due to NH proton at δ 3.0 ppm, aromatic protons at δ 7.5 ppm, It also showed the signals due to pyranosyl ring at δ 4-4.5 ppm and δ 4.65 -5.3 ppm.

The NMR spectrum of **Ib** distinctly showed the signals due to N-H proton at δ 3.3 ppm, aromatic proton at δ 7.5 ppm, acetyl proton at δ 2.02 and protons of pyranosyl ring at δ 4-4.5 and δ 4.8-5.5 ppm.

The NMR spectrum of **Ic** distinctly showed the signals due to N-H proton at δ 3.2 ppm, aromatic proton at δ 7.5 ppm, acetyl proton at δ 1.8 ppm and protons of pyranosyl ring at δ 3.8-4.3 and δ 4.7-5.3 ppm.

The NMR spectrum of **Id** distinctly showed the signals due to N-H proton at δ 2.9 ppm, aromatic proton at δ 7.5 ppm, acetyl proton at δ 1.8 ppm and protons of pyranosyl ring at δ 3.8-4.3 and δ 4.7-5.3 ppm.

The NMR spectrum of **IIa** distinctly showed the signals due to aromatic proton at δ 6.60-7.5 ppm, acetyl proton at δ 2.05 ppm. It also showed the signals due to proton off pyronosyl ring at δ 3.8- 4.2 and δ 4.6-5.3 ppm.

The NMR spectrum of **IIb** distinctly showed the signals due to aromatic proton at δ 6.7-7.4 ppm, acetyl proton at δ 2.05 ppm. It also showed the signals due to proton of pyronosyl ring at δ 3.8- 4.2 and δ 4.6-5.3 ppm.

The NMR spectrum of **IIc** distinctly showed the signals due to aromatic proton at δ 6.7-7.5 ppm, acetyl proton at δ 2.05 ppm. It also showed the signals due to proton of pyronosyl ring at δ 3.7- 4.4 and δ 4.6-5.3 ppm.

The NMR spectrum of **IId** distinctly showed the signals due to aromatic proton at δ 6.7-7.5 ppm, acetyl proton at δ 2.05 ppm. It also showed the signals due to proton of pyronosyl ring at δ 3.7- 4.4 and δ 4.6-5.3 ppm.

The NMR spectrum of **IIg** distinctly showed the signals due to aromatic proton at δ 6.7-7.5 ppm, acetyl proton at δ 2.05 ppm. It also showed the signals due to proton of pyronosyl ring at δ 3.9- 4.2 and δ 4.6-5.2 ppm.

The NMR spectrum of **IIh** distinctly showed the signals due to aromatic proton at δ 6.7-7.5 ppm, acetyl proton at δ 1.9 ppm. It also showed the signals due to proton of pyronosyl ring at δ 3.9- 4.2 and δ 4.6-5.2 ppm.

Mass spectral analysis

When anti-microbial activity was observed, **IIa** and **IIb** showed good activities hence mass spectral analysis was carried out for products **IIa** and **IIb**. Important fragments along with molecular ion peak and abundance of respective fragments are enlisted in **Table 4** for **IIa** and **IIb**.

Table 4. Mass spectral analysis of Chlorinated Dithazolidines with fragments and relative abundance

Sr. No.	Ion	m/e	Relative abundance
IIa			
1	M+	684	1.3%
2	M-4H+	680	9.3%
3	TAGN-C=S=S-N	453	2.1%
4	M-C14H8N3S2Cl2)++ =TAG	330	27.5%
5	(M-C15H9NS2O9)=p-ClPhN-C=Np-ClPh	263	10.4%
6	(M-C21H23N2O9Cl)=pClPhN=C-S-S	200	9.7%
7	(M-C21H23N2O9SCl)=p-ClPhN=C=S	169	100%
8	TAG-2CH3COOHCH2=CO	169	
9	(M-C22H23N2S2O9Cl)=p-ClPhN	127	
10	(TAG-3CH3COH, CH2=CO	109	
IIb			
1	M+	714	Not located
2	(M-ClPh-N=C=S,Cl)	514	1.9 %
3	(M-C12H7NCl3) TAGN—C=S=S-N	453	0.8%
4	(M-C14H7N3Cl3S2)=TAG	330	11.4%
5	TAG-CH3COO-	278	3.7%
6	TAG-AcOCH=O	243	1.0%
7	(M-C22H23N2O9Cl2)=p-ClPhN-C-S-S	202	29.6%
8	(M-C2123N2O9SCl2)=p-ClPh-N=C=S	168	52.6%
9	TAG-2CH3COOHCH2=CO	168	52.6%
10	M-C22H33N2O9S2Cl2=p-ClPhN	126	
11	TAG-3CH3COOH, CH2C=O	108	

The probable fragmentation patterns of molecular ions are shown in Schemes I and II for **IIa** and **IIb** respectively.

Mass fragmentation pattern for **IIa** is shown in **Scheme 1** below:

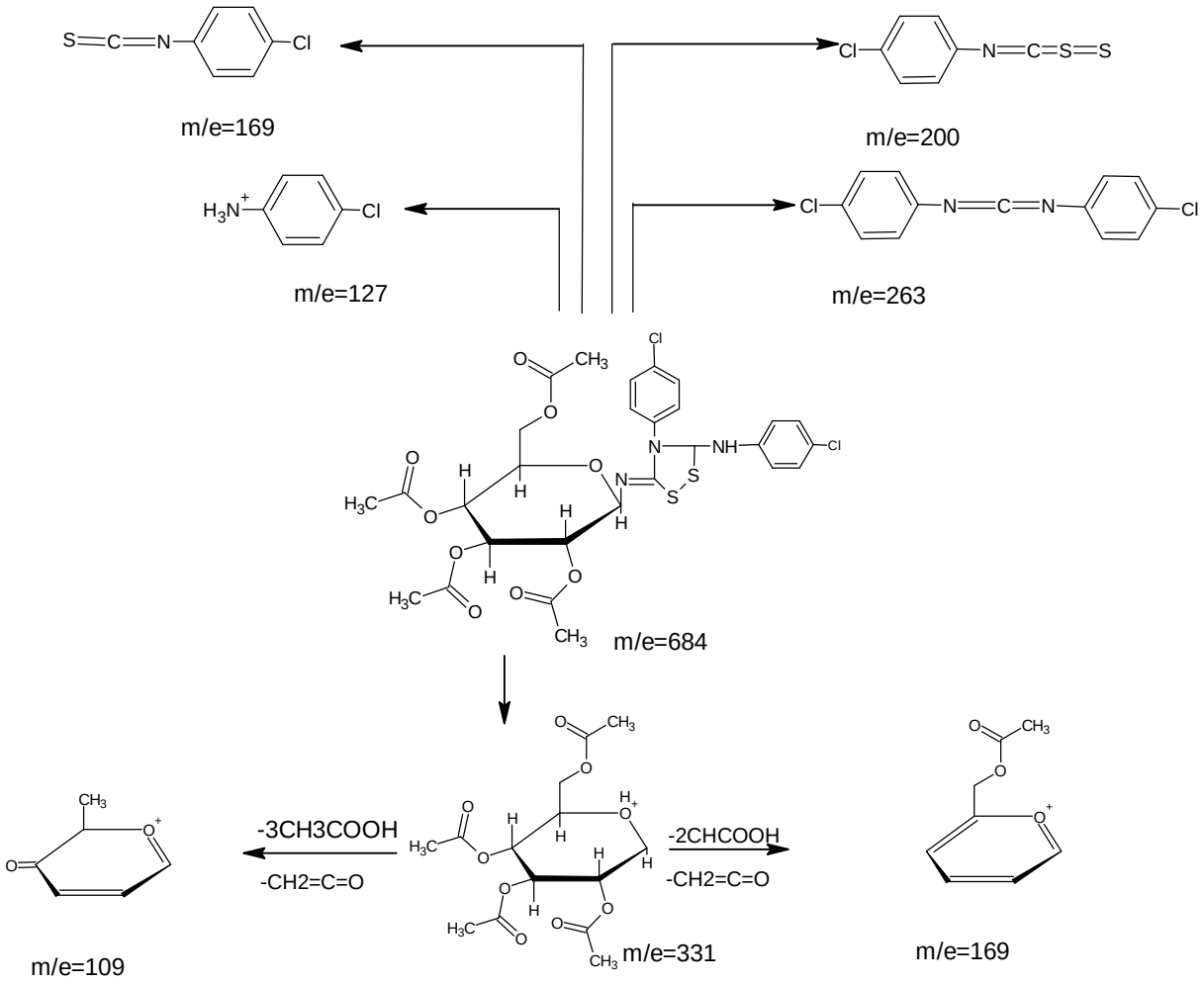

Scheme 1

Mass fragmentation pattern for **IIb** is shown in **Scheme 2** below.

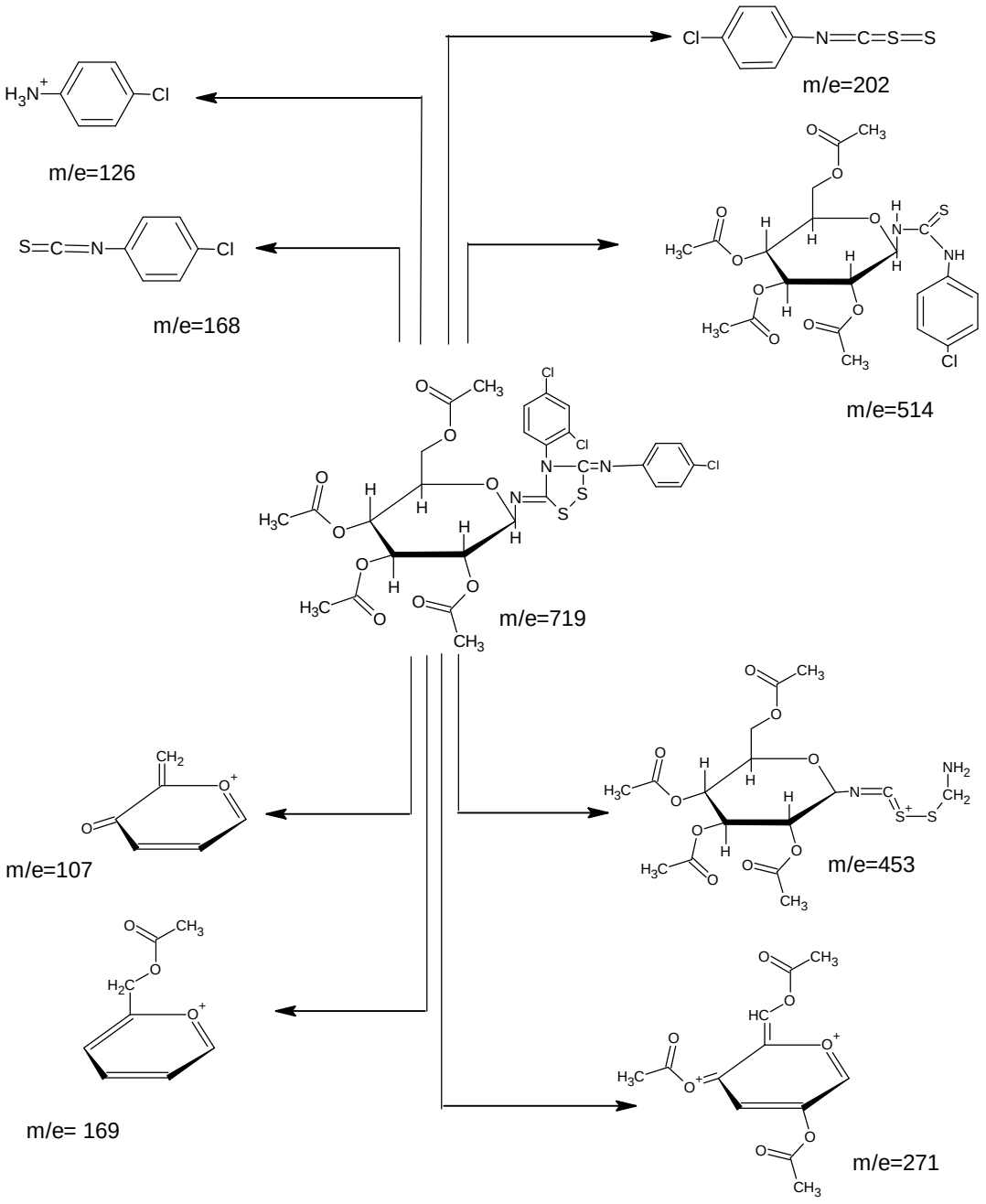

Scheme 2

Results and Discussion on Antimicrobial activity

Antimicrobial activities for the chlorinated compounds of Series I and Series II were done.

Antimicrobial activity of chlorinated thiocarbamide and 1,2,4-ditiazolidone

The antimicrobial activities of the synthesized chlorinated thiocarbamide and 1,2,4-dithiazolidine have been investigated in vitro. The strains used for screening were gram (-) *E.coli* and gram (+) *staphylococcus aureus*. The screening was carried out for the durations of 24 h, 48h and 72h. Detail antimicrobial study for all chlorinated thiacarbamide and 1,2,4-dithiazolidine compounds are shown in Table 5.

Table 5. Antimicrobial activities of Chlorinated Thiocarbamides and 1,2,4-dithiazolidines

Sr. No.	Name of compound	24h		48h		72h	
		Staphylococcus aureus	E.coli	Staphylococcus aureus	E.coli	Staphylococcus aureus	E.coli
	Chlorinated thiocarbamide compounds						
	Ia	-	-	-	-	-	-
	Ib	-	-	-	-	-	-
	Ic	+	-	+	-	+	-
	Id	-	-	-	-	-	-
	Chlorinated 1,2,4 dithiazolidine compounds						
	IIa	+	+	+	+	+	+
	IIb	++	++	++	++	++	++
	IIc	-	-	-	-	-	-
	IId	-	+	-	+	-	+
	IIe	+	-	-	-	-	-
	IIf	+	-	-	-	-	-
	IIg	-	-	-	-	-	-
	IIh	-	-	-	-	-	-

Out of the compounds from Series I i.e chlorinated thiocarbamide, 1-(3,4 dichloro) phenyl -3-tetra-o-acetyl –β-D-glucopyranosyl thiocarbamide showed better antimicrobial activity. Similarly, it has been observed that in the case of chlorinated compounds from Series II, the chlorination at phenyl of 3rd position is not found to be effective. Instead chlorination of phenyl at 4th position has been found to be most effective with respect to antimicrobial activity.

Conclusions

N-glucopyranosyl thiocarbamide and 1,2,4 dithiazolidine have been successfully chlorinated to 1-tetra –o-acetyl –β-D glucopyranosyl -3-mono/di/tri chloro phenyl thiocarbamide (Series I) and to 3-phenyl/p-chlorophenyl-4-mono/di/tri chloro phenyl -5-tetra-O-acetyl-β-D-glucopyranosylimino-1,2,4-dithiazolidine (Series II) respectively. Synthesized chlorinated compounds have been analyzed by using several characterization tools namely, IR spectroscopy, NMR and mass spectroscopy.

Schematic fragmentation patterns have been obtained. The chlorinated compounds have been exposed for antimicro bacterial activities. Compound 3-p-chlorophenylimino-4-p-chloro phenyl 5-tetra-o-acetyl-β-D-glucopyranosyl imino-1,2,4 dithiazolidine **(IIa)** and 3 p-chlorophenylimino-4 (2, 4 dichloro) phenyl 5-tetra-o-acetyl-β-D-glucopyranosyl imino-1,2,4 dithiazolidine **(IIb)** have been found to be most effective over a wide range of time period (24h, 48h and 72 h). It can be concluded that mono and dichloro substitution at phenyl ring at 4^{th} position of 1,2,4 dithiazolidine is effective as compared to chlorine substitution at other site.

Acknowledgement

Authors acknowledge CDRI, Lucknow, India for spectral analysis of samples. Authors also acknowledge their affiliated institutes/organizations for permission to publish the work. Authors acknowledge Department of Chemistry, RTM Nagpur University for facilities, chemicals and apparatus.

References

1. Kharate R.M., Deohate P.P. and Berad B.N., 2009, *Int. J. Chem. Sci*., **7**, 2843.

2. Agrawal P.T. and Deshmukh S.P., 2009, *J. Indian Chem. Soc*., **86**, 645.

3. Makawa H.R. and Malani A.H., 2017, *IOSR Journal of Applied Chemistry (IOSR-JAC)*, **10**, 76.

4. Fuloria N.K., Singh V., Shaharyar M. and Ali M., 2008, *Asian J. Chem.*, **20**, 6457.

5. Singh P.K. and Singh R., 2001, *Indian J. Hetero. Chem*., **10**, 311.

6. Yadgire A.V., Barate D. L. and Deshmukh S.P., 2011, *Rasayan J. Chem*., **4**, 780.

7. Thorat S.M., Dhumale J. P. and Deshmukh S. P., 2011, *Indian J. Hetero. Chem*., **20**, 277-278.

8. Deohate, P., 2012, *Der Pharma Chemic.,* **4**, 2368.

9. Hardas, A. Tayade (Gosavi) P., 2018, *Asian J. Chem*., **30**, 2310.

10. Manna P., Singh R, Narang, K.K., Manna, S.K., 2005, *Indian J. Chem*., **44B**, 1880.

11. Wurtzer, S. Compain, Benech, S.H., Hance, A.J. and Clavel F., **2005** *J. Virol*., **79**, 14815.

RNI No. MAHENG/2017/74063
ISSN No. (Print) 2581-5911
ISI Impact Factor 1.022 (2019-2020)

Kinetics and Mechanism of Hydrolytic Dephosphorylation of Mono-2-nitro-4-chloro Aniline Phosphate

Archana Singh
Department of Chemistry,
B. K. Birla College of Arts, Science and Commerce (Autonomous),
Kalyan (West), Thane, Maharashtra, India
Email: dr.archanasingh30@gmail.com

Abstract
Due to C-N-P linkages in nucleotides, the role of organic phosphate ester in biochemistry was recognized quite early. The synthesis of Mono-2-nitro-4-chloro Aniline Phosphate ester was carried out using CTABr as catalyst and investigation of the kinetics of hydrolysis of compound was studied in the acid range 0.1 to 7 M at 50 (+/-5)°C. Allen's modified method has been employed for quantitative results. The first order rate coefficients have been determined in the above acid range. Solvent and concentration effect studies and Arrhenius parameters have also been calculated indicating bimolecular mode of hydrolysis with P-N bond fission.

Keywords: *Kinetics, Solvent effect studies, Arrhenium parameters.*

Introduction

Organic phosphates are of great importance due to their wide range of applications in various branches of Chemistry[1]. Organic phosphates have been of great importance to humans and plants due to their biochemical functions[2]. Aryl phosphoramidates with a variety of substituent have shown significant applications in industries[3]. In particular, they are found to be of great use in the synthesis of pyrophosphates, employed as flame proofing agents[4], corrosion inhibitors[5], fuel additives and insecticides. These compounds consist of linkages like C-O-P, C-N-P, C-S-P etc. The investigation of the kinetics and mechanism of the hydrolysis of these compounds has been reported in various acid and buffer media[6,7]. Various methods for quantitative studies have been employed for the study of kinetics of hydrolysis. The study of the synthesis and susceptibility of disubstituted Phenyl Phosphoramidate[8] was limited and it was felt that these compounds need to be examined more rigorously as they are significant for various biological phenomenon. Mono-2-nitro-4-chloro Aniline Phosphate ester is one such compound having C-N-P linkage whose synthesis by using CATBr was reported for the first time by Singh et. al.[9] Although, its synthesis has been carried by different techniques these are few reports of the kinetic investigations of hydrolysis of this compound. The kinetics and mechanism of hydrolytic dephosphorylation of synthesized Mono-2-nitro-4-chloro Aniline Phosphate was carried out in acid range 0.1 to 7 M at 50 (+/-5)°C. Allen's modified method[10] used for quantitative analysis has been reported in this paper.

Materials and Methods

2-nitro-4-chloro Aniline was dissolved in dry benzene followed by gradual addition of phosphorous oxy chloride and a cationic micelle, Cetyl trimethyl ammonium bromide (CTABr) with shaking till a homogenous mixture was formed. The reaction mixture was refluxed in an oil bath (90-100^{o}C) for about 4 hours. The compound was obtained in the form of sticky brown colored residue which was further extracted. The extracted residue was treated with 2% Barium hydroxide solution to convert it into the corresponding Barium salt. The formation of the mono ester was confirmed by elemental analysis, UV visible absorption and IR spectra. Kinetic study of hydrolysis of Phosphate ester in the acid range 0.1 to 7 M at 50 (+/-5)^{o}C, was carried out spectrophotometrically using Allen's modified method. The procedure involves the estimation of inorganic phosphate from the ester during the course of its hydrolysis. Single cell type Spectonic-20 photoelectric colorimeter was used for the measurement of optical density. The rate data obtained includes the effects of different variables used to understand the stability and reactivity of contributing species during hydrolysis.

The elemental composition in weight percentage of the monoesters was observed to be 18.06% for C, 1.16% for H and 7.20% for N and 7.95 for P which is in agreement with the theoretically calculated values i.e. 18.56% for C, 1.03% for H, 7.22% for N, 7.99% for P confirming the formation of monoester.

The intense UV absorption peaks were found at 455 nm, 275 nm and 253 nm wavelengths, indicating the aromatic character of the compound and extended conjugation due to the presence of -NO_2 and –Cl groups.

The IR spectral data showed the characteristics peaks at 3307 cm^{-1}, 2920 cm^{-1} , 1636 cm^{-1}, 1569 cm^{-1}, 1557 cm^{-1}, 1538 cm^{-1}, 1441 cm^{-1}, 1510 cm^{-1}, 1336 cm^{-1}, 1240 cm^{-1}, 1107 cm^{-1}, 900 cm^{-1} and 721 cm^{-1} indicating the presence of NH stretching, aromatic CH Stretching, NH bending vibrations, C=C bending vibrations, Asymmetric and Symmetric stretching-NO_2, P=O, -P-O, P-N and P-Cl-C bonding.

Results and Discussion

The rate coefficient was found to be of first order (Table 1) by conducting the kinetic studies at varied neutral electrolyte concentration.

Table 1. Observed rate-coefficients for the hydrolysis of Mono-2-nitro-4-chloro Aniline Phosphate

Sr. No.	HCl (M)	2 + log C_H+	k_e (obsd) 10^3 min^{-1}	4 + log k_e
1	0.1	1.00	3.63	1.56
2	0.5	1.70	4.35	1.64
3	1.0	2.00	5.30	1.72
4	2.0	2.30	5.77	1.76
5	3.0	2.48	4.74	1.68
6	4.0	2.60	15.86	2.20
7	4.5	2.65	13.87	2.14
8	5.0	2.70	12.18	2.09
9	6.0	2.78	11.8	2.07
10	7.0	2.84	9.79	1.99

From Table 1, it is evident that there is regular increase in the value of the observed rate (k_e (obsd) min^{-1}) with the rise in acid molarities, keeping the ionic strength constant. The rising slope of the linear curve (Figure 1) indicates positive ionic strength effect leading to the contribution of the conjugate acid species of the present monoamidate during hydrolysis.

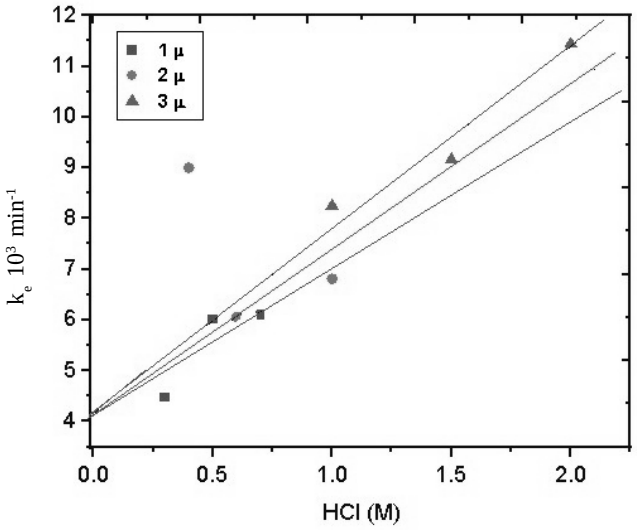

Fig. 1. Hydrolysis of Mono 2-nitro-4-chloro Aniline Phosphate at Constant Ionic Strength

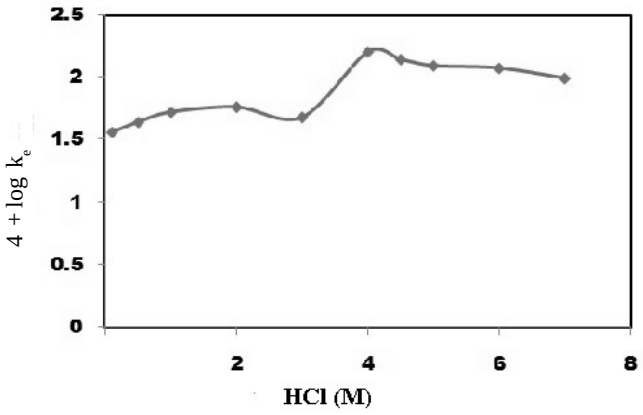

Fig. 2. Acid-Log rate profile for Hydrolysis of 2-nitro-4-chloro Aniline Phosphate.

The linear curves are based on the second empirical term of the Debye Huckel equation.

$$k = k_o \exp b\mu \quad \text{(i)}$$

This can be further modified for the conjugate acid form of this ester as

$$k_H = k_{Ho}{}^{+} \exp b_{H+} \mu \quad \text{(ii)}$$

In higher acid range, due to the involvement of water, the above equation can be further modified as:

$$k_H = k_{Ho}{}^{+} \exp b_{H+}\mu \quad \text{(iii)}$$

Figure 2 shows acid molarities vs (4 + log k_e) curve indicating that the neutral form operates between 0. 1 to 3 M HCl. The contribution of conjugate acid species exists in the acid range 4.5 to 7 with maximum rate at 4M HCl, showing the moderate basic nature of the monoester.

In concentrated acid media (more than 4M), the mono-protonated species solely contributes towards the calculated rates. The Hammet correlation (Figure 3A) with slope = 0.31 indicates the involvement of water molecule in the rate determining stage of hydrolytic degradation. Yates and McCleland correlation[11] comprising Hammett value (slope=0.24) and based on the activity of water, corresponds to slope=3.33 (Figure 3B) indicating the involvement of actual number of water molecules during hydrolysis. The bimolecular nature of reaction is further supported by Zucker-Hammett plot[12] (slope = 1.38).

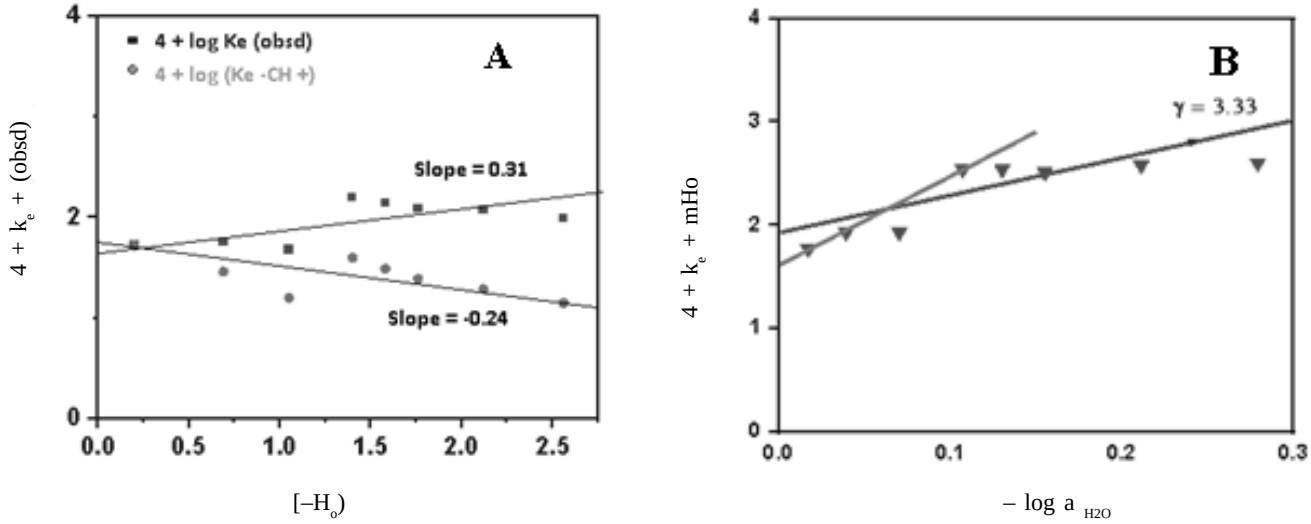

Fig. 3. A. Hammett plot, B. Yates and McCleland plot

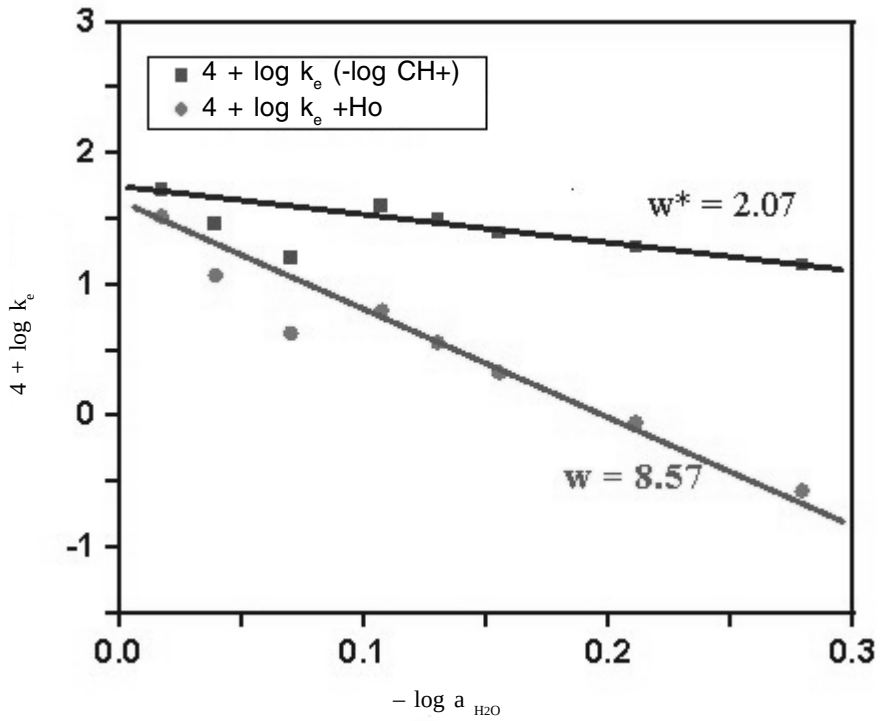

Fig. 4. Bunnet Plot for Mono-2-nitro-4-chloro Aniline Phosphate ester

Further kinetic studies were conducted at different temperature and various thermodynamic parameters[14] were calculated for 4.5M HCl. The entropy of activation was calculated to be -27.31 e. u. suggesting the formation of expanded transition states with water for both the reactive forms. The frequency factor 'A' was calculated to be 13.67 X 10^8 S^{-1} which is quite high and can be assigned to interaction of the solvent with the reactant during bimolecular hydrolysis. The activation energy is found to be 26.36 kJ mol^{-1}. This is in agreement with the large activation energy (E ≥ 20 kJ mol^{-1}) for hydrolysis. Due to the presence of phosphorous, the nucleophilic attack leads to P-N bond fission. The liberation of free Aryl Amine also supports the P-N bond fission of the obtained monoester during hydrolytic degradation.

Conclusions

The monoester of 2-nitro-4-chloro Aniline phosphate was synthesized by dissolving 2-nitro-4-chloro aniline in dry benzene followed by gradual addition of phosphorous oxy chloride and a cationic micelle, Cetyl trimethyl ammonium bromide (CTABr). The formation of the compound was confirmed by elemental analysis, UV absorption spectra and IR spectral data analysis. Kinetic studies have been conducted at various neutral electrolyte concentrations and rate coefficient was determined to be of first order. The mono-protonated species solely contributes towards the calculated rates in the concentrated acid media i.e. more than 4M. The Hammet correlation and Yates and McCleland correlation indicate the involvement of water molecules during hydrolysis. The Zucker-Hammett plot shows the bimolecular nature of reaction. The kinetic studies conducted at different temperature for 4.5M HCl shows that the entropy of activation is -27.31 e. u and the frequency factor 'A' is 13.67 X 10^8 S^{-1} supporting bimolecular hydrolysis. The activation energy is found to be 26.36 kJ mol^{-1} which is in agreement with the large activation energy (E ≥ 20 kJ mol^{-1}) for hydrolysis.

References

1. Grob, D., 1950, *Ann. Intern. Med*., **32(6)**, 1229-1234.
2. Gryaznov, S.M., Lloyd, D.H., Chen, J.K., Schultz, R.G., DeDionisio, L.A., Ratmeyer, L. and Wilson, W.D., 1995, **92(13)**, 5798-5802
3. Agrawal, S., Goodchild, J., Civeira, M.P., Thornton, A.H., Sarin, P.S. and Zamecnik P.C., 1988, PNAS, **85(19)**, 7079-7083.
4. Keun, Jang. Hyoun and Park Hong-Soo, 1994, *J. of Korean Oil Chemists Soc*., **2(1)**, 45-52.
5. Xiang Gao, Shaotong Liu, Haifeng Lu, Feng Gao and Houyi Ma, 2015, *Ind. Eng. Chem. Res.*, **54(7)**, 1941-1952.
6. Moller K.M., 1955, *Biochem et Biophysics Acta.*, **90(162)**, 243-245.
7. Rathlev T. and Rosen Berg, 1956, *Arch. Biochem. Biophysics*, **65**, 319-322.
8. Chanley J.D. and Feageson Edward, 1958, *J. Am. Chem. Soc*., **80**, 2686-2687.
9. Archana Singh and Shashi Prabhu, 1996, *Asian Journal of Chemistry*, **8(1)**, 129-133.
10. Allen RJL, 1940,. *Biochem. J.*, **34**, 858-860.
11. Yates, K. and McCleland, R.A., 1967, *J. Am. Chem. Soc*., **89**, 2686-2688.
12. Hammet, L.P. and Zucker, L., 1939, *J. Am. Chem. Soc*., **61**, 2779-2785.
13. Bunnet, J.F., 1961, *J. Am. Chem. Soc*., **83**, 4956-4958.
14. Arrhenius S., 1988, *Z. Phys. Chem*., **2**, 495; 1889, **4**, 244; 1899, **28**, 317.

RNI No. MAHENG/2017/74063
ISSN No. (Print) 2581-5911
ISI Impact Factor 1.022 (2019-2020)

An Improved Liquid Chromatographic Method for the Determination of Trace Level Iodide in Human Urine Samples using Amperometric Detection

Deepak Parab, Uvaraj M., Surendiran A and Sriram B.
Metrohm India Private Limited, Chennai, Tamil Nadu, India.
Email: deepak.parab@metrohm.in

Abstract

Iodine is an essential micronutrient for human growth, metabolism and regulation of thyroid hormones in humans as well as animals. The determination of urinary iodide concentration is a valuable tool in epidemiological studies of iodine supplementation, particularly in diagnosing and controlling iodine deficiency. Because of the difficulty of directly measuring dietary iodine intake, serum and urinary iodide concentrations are usually used as an index of iodine intake. Also the measurement of iodine in urine is useful for the diagnosis of transient thyroid dysfunction and iodine induced hyperthyrosis. Urine iodide concentration is recommended by World Health Organization (WHO) as the single indicator of iodine nutrition. Existing colorimetric analysis based on Sandell-Kolthoff reaction requires sample pretreatment like acid digestion and its sensitivity is also limited. Iodide concentrations usually in the range of parts per billion in biological materials such as urine or serum, demands a method with high sensitive detection. Methods like ICP-MS provides high sensitivity and accurate results, but the cost of the equipment along with running cost makes it unaffordable for the epidemiological assays of a large sample population. Although use of HPLC with ion pair reagents is used for iodide detection, one needs salts along with buffering agents, organic modifiers and specific pH conditions. This method is not popular due to several limitations. The proposed method making use of ion (liquid) chromatography with amperometric detector and an anion separation column is rapid, rugged and does not requires any prior sample pretreatment like acid or alkaline digestion or any special reagents. It is sufficient if samples are passed through C-18 sample preparation cartridge to remove the bulk organic moiety and filtration through a 0.2µ filter to remove any particulate matter. LOD of the proposed method is 2 ppb and LOQ is 10 ppb.

Keywords: *Ion exchange chromatography, Iodide content, human urine, Amperometric detection, Ion exchange column.*

Abbrevations

WHO	–	World Health Organization
ICP-MS	–	Inductively Coupled Plasma Mass Spectrometry
IC	–	Ion Chromatography
DC	–	Direct Current
PAD	–	Pulse Amperometric Detection
flexIPAD	–	Flexible Pulse Amperometric Detection
CV	–	Cyclic Voltammetry
mV	–	Millivolts
MΩ	–	Megaohms
IC	–	C18 – Ion chromatography Carbon 18
RT	–	Retention Time
nA	–	Nanoampere
LOD	–	Limit of Detection
LOQ	–	Limit of Quantification
SNR	–	Signal to noise ratio
ppm	–	parts per million
ppb	–	parts per billion
RSD	–	Relative Standard Deviation
Ag	–	Silver
Ag/AgCl	–	Silver/Silver chloride

Introduction

Iodine deficiency disorders (IDDs) are a global health problem. According to WHO over two billion people are at risk worldwide[1]. As per World health organization guidelines, the recommended iodine intake per day is 150 mcg (microgram) (Table 1). Iodine deficiency can lead to swelling of the thyroid gland, known as goiter, and hypothyroidism, which can cause fatigue, muscle weakness and weight gain. Iodine is an essential component of the thyroid hormones thyroxine (T4) and triiodothyronine (T3). Thyroid hormones regulate many important biochemical reactions, including protein synthesis and enzymatic activity, and are critical determinants of metabolic activity. They are also required for proper skeletal and central nervous system development in fetuses and infants.

Iodine is an essential micronutrient. The source of iodine in body is only through diet and is absorbed by the gastrointestinal tract as its inorganic ion iodide. So determination of iodide concentration in the body provides information about iodine nutrition. It is assumed that an equilibrium exists between the amount of iodine intake (absorbed) and the inorganic iodide like sodium iodide or potassium iodide excreted in the urine. Hence determination of iodide in urine is an important test.

Although iodized cooking salts are the leading sources of iodine (>15 ppm) [6] in food, other sources are sea food, iodine in processed foods[2] drinking water[3], cows' milk, infant formula[4] and vegetables[5]. 90% of the iodine consumed gets excreted in urine[7]. In iodine analysis, sample collection is an important step and care needs to be taken to avoid contamination. Also no preservatives are required as iodide is stable in the urine matrix and evaporation is prevented by refrigerating the samples. There are a number of methods available for analysing iodide in salt as well as in urine samples. This includes manual methods using sophisticated analytical instrumentation techniques. Based on the Sandell-Kolthoff reaction, most colorimetric assay methods for urinary iodine (UI) determination that have been developed require pretreatment of urine sample. The sample has to undergo acid digestion where inorganic iodate and organically bound iodide get converted to iodine and the catalyst. Cerium (IV) is reduced to Cerium (II) by arsenic trioxide. Typical detection limit is upto 20 parts per billion (µg/L). Sample preparation involves use of chloric acid digestion and dry digestion with alkaline ashing. Later, the chloric acid was replaced with ammonium persulfate and with modifications, the detection limit was further improved.

Haldimann et. al.[9] presented an ICP-MS method for the determination of urinary iodide making use of isotope dilution using Iodine-129. Although it offers precise results and can be easily automated, the high cost of the equipment and running cost with need of skilled personnel are hindrances for its wide use in the industry for epidemiological assay of a large sample population. Analysis using ion selective electrode is a cost effective solution besides having the advantage of quicker analysis. An iodide concentrations from 1.3 ppb to 126 ppm can be measured between pH of 0 to 14. There can be interferences with certain concentrations of Cl^-, Br^-, CN, S^{2-}, $S_2O_3^{2-}$ and potassium nitrate is used as the ionic strength adjuster solution[8]. However, when applied to the measurements in physiological fluids, the chances are that these electrodes are fouled by formation of coating with contaminants and hence require frequent cleaning, polishing and conditioning. Even with ionophore based ion selective electrodes, because of the use of polymeric membrane matrix, the contamination and frequent cleaning are the main issues. A technique making use of ion pair reagent with reverse phase method in HPLC[10] is widely used for detection of iodine in urine. Need for use of many chemicals, besides ion pair reagents and organic solvents with specific pH are the limitations of this method. Also, the effect of these ion pair reagents on the electrode surface needs to be studied. The method proposed operates by ion exchange

mechanism using commonly available salts as the eluent, separating the analyte by anion exchange column and detection as iodide (anion) and quantification using an Silver electrode against silver / silver chloride reference system. It is even more economical and convenient when the bulkier ion pair reagent is used and the associated issues like adsorption on the metal electrodes and cleaning are avoided.

Materials and Methods

Apparatus

A 930 Compact IC flex Ion Chromatography instrument from Metrohm (Herisau, Switzerland) along with 858 Professional IC Sample Processor was used. 945 Professional Detector Vario Amperometry detector with a three electrode setup was used. Ag (silver) electrode was used as a working electrode. Ag/AgCl was used as a reference electrode and stainless steel was used as an auxiliary (counter) electrode. There are four measuring modes (DC, PAD, flexIPAD and CV) available for different applications. The analysis was carried out with DC mode with 150 mV potential applied between Ag tip (silver working electrode) and Ag/AgCl reference electrode. These instruments were controlled and data acquisition was done through the MagIC Net 3.0 software (Figure 1). High pressure dual piston pump was used to deliver eluent at the flow rate of 0.7 mL/min. Metrosep A Supp 5 - 150/4.0 medium capacity ion exchange column, which is based on a polyvinyl alcohol polymer with quaternary ammonium groups as functional group was used for the separation of iodide. The column temperature was maintained at 40°C for good sensitivity. 20 µL Sample and standard were injected into ion chromatograph system.

Chemicals and reagents

All solutions were prepared using ultrapure water (> 18 MΩ) purified by an Elga Purelab Flex 1 system (Elga Veolia, UK). Sodium carbonate (Merck EMSURE), Sodium bicarbonate (Sigma Aldrich), Acetone (Merck HPLC grade) and Potassium iodide (Sigma Aldrich) were used.

Eluent preparation

Eluent: 3.8 mmol/L Sodium carbonate and 1.2 mmol/L sodium bicarbonate in 2% acetone

Standard: Iodide standard stock solution of 1000 ppm was prepared dissolving potassium iodide salt in ultrapure water. All the lower level standards were prepared by diluting the standard stock solution with ultrapure water.

Sample preparation: The urine samples were collected from volunteers and was filtered through 0.2 µm Nylon filter paper. The filtered sample solution were passed through sample preparation cartridge IC - C18 to remove high organic content from urine sample. The prepared sample solutions were directly injected into the ion chromatograph system.

Results and Discussion

Method Specificity

Blank and Standard solutions were injected to check the specificity. In blank solution analysis, no peak was observed at the retention time (RT) of iodide. This shows that the method is specific (Figure 2).

Linearity

Iodide standard concentrations of 2, 5, 10, 25 and 50 ppb were prepared by diluting 0.5 ppm stock iodide standard with ultrapure water. The prepared low-level concentrations were injected to check the linearity (Figure 3).

A regression line was obtained by plotting peak area ((nA) × minutes) of the iodide using the least square method. The relationship between peak response and concentration was found to be linear between the ranges of 2 to 50 ppb of iodide, with the coefficient of determination (r^2) of 0.9991 (Figure 4).

Limits of detection and quantification (LOD & LOQ)
Based on the linearity of calibration and the response of the iodide ion under the given chromatographic conditions, the limit of detection (LOD) was calculated as 2 ppb and the limit of quantification (LOQ) was calculated as 10 ppb. The calculation was done based on signal-to-noise ratio (SNR) value. The signal-to-noise ratio (SNR) was 4.9 for LOD and 24.2 for LOQ (Figure 6). In general, a SNR value of more than 3 is considered as LOD and more than 10 is considered as LOQ.

Repeatability studies
10 ppb iodide standard was injected eighteen times continuously and the RSD was found to be less than 3% (Figure 7, Peak Area (Peak response) values shown in Table 2). Iodide standard 10 ppb was injected as check standard once in every four hours in between the sample injection and the relative standard deviation for twelve hours was found to be less than 5% (Figure 8). This shows the suitability of the method used. Samples were also injected in multiple numbers (n=5) and the RSD values were found to be less than 2%. The ion chromatogram of the urine sample from a representative volunteer is shown in Figure 9 and the results are shown in Tables 3 and 4.

Reproducibility Studies
10 ppb iodide standard was injected eighteen times on different days with different eluents and different analysts and the RSD was found to be less than 2.5% (Figure 11, Peak Area (Peak response) values are shown in Table 5). Overall RSD of 36 inejctions (Day-1 and Day-2) were found to be less than 10%. This shows that method is highly reproducible.

Method Accuracy
Method accuracy was checked by undertaking spiking study. A known amount of iodide standard was spiked with urine sample and recovery value was calculated. 50 ppb of iodide standard was spiked with human urine sample and spiking study was carried out. The recovery value was found to be 97%. This shows that method is accurate (Figures 12 and 13).

Effect of Column Temperature
The column temperature was varied from room temperature 30°C to 40°C. Sensitivity was found to increase with increase in temperature from 30°C to 35°C and thereafter no further increase in response was found from 35°C to 40°C (Figures 14 to 17).

Method Ruggedness
10 ppb iodide standard was injected using different silver working electrodes as well as using different silver / silver chloride reference electrodes. No appreciable area difference was observed (Figures 18 and 19). Change of temperature between 35°C to 40°C does not alter the sensitivity. These data shows that method is rugged.

Discussion
This chromatographic method for the quantification of trace level iodide in human urine using ion exchange separation method with amperometric detection is suitable for human urine sample solution analysis. The limit of detection for iodide is well within the minimum expected level as per urinary iodine specifications. Sample matrix does not affect the method accuracy. The proposed method satisfies all the requirements for the determination of trace level iodide in human urine. This method does not require any derivatization. Sample can be analyzed directly after simple filtration. As samples are passed through the C-18 cartridge and filtered using a 0.2µm filter, most of the organic constituents and particulates are removed and thereby interferences are eliminated. In addition, the small quantity of organic modifier in the eluent helps to dissolve and remove any other organic molecules from the column. Presence of other inorganic constituents does not influence/interfere in the quantification of iodide. Detection method is also very selective and specific for the analyte iodide using the proposed column, electrode setup, applied potential

and the detector. Method accuracy is also confirmed by spiking study. The Colorimetric method using Sandell-Kolthoff scheme needs either chloric acid or persulfate digestion of the sample to remove the interferences, which results in toxic waste apart from iodine. Also the quantification is not direct but depends on its catalytic role of ceric ammonium sulfate in the presence of arsenious acid. Since this method uses digestion, one needs to analyse blank and hence is time consuming one. ICP MS is a good option for the analysis of iodine in urine, but the high cost of the equipment along with the running cost, use of plasma, liquid argon and its availability everywhere are the limitations. This ion chromatography method is simple, accurate and highly reproducible and can be easily automated for the regular analysis of iodide in urine samples.

Conclusions

A simple and rapid method has been optimized for the determination of trace level iodide in human urine by ion exchange chromatography with amperometric detection method. An Ion exchange column was used for the separation. This method is suitable for human urine which has a high concentration of alkali metals, chloride and organic waste. There is no special sample preparation or derivatization required prior to analysis. This method has a lot of advantages compared to other methods like spectrophotometry inductively coupled plasma mass spectrometry, microplate method, ion pair reverse phase chromatography etc.. This method can be used for a variety of urine samples like human urine, etc. animal urine etc. Detection limit is also well within the expected specification range of urinary iodine.

Acknowledgement

This work was supported by Metrohm India Private Limited, India and authors greatly acknowledge the support received.

References

1. Dr. Gro Harlem Brundtland, The Director-General of the World Health Organization, New York., May, **2002**, United Nations General Assembly Special Session on Children Sustained Elimination of Iodine Deficiency Disorders. [Google Scholar]
2. Harris, M.J., Jooste P.L. and Charlton K.E., 2003, *International Journal of Food Sciences and Nutrition,* **54,** 13-19.
3. Jooste, P.L., Weight M.J., Kriek J.A. et. al., 1999, *European Journal of Clinical Nutrition*, **53**, 8–12.
4. Pearce, E.N., Pino S., He X., et. al., 2004, *Journal of Clinical Endocrinology & Metabolism,* **89**, 3421–3424.
5. Haldimann, M., Alt A., Blanc K., et. al., 2005, *Journal of Food Composition and Analysis,* **18**, 461–471.
6. World Health Organization/United Nations Children's Fund/International Council for Control of Iodine Deficiency Disorders (WHO/UNICEF/ICCIDD), Assessment of the iodine deficiency disorders and monitoring their elimination, A guide for programme managers, 3rd ed., Geneva: World health Organization, 2007. WHO/NDH/01.1.
7. Zimmermann, M.B., Jooste P.L., and Pandav, C.S., 2008, *Lancet,* **372**, 1251-1262.
8. Metrohm Ion selective electrode Manual 8.109.8042EN / 2019-03-15
9. Haldimann, M.B., Zimmerli, C. Als and Gerber, H., 1998, *Clinical Chemistry,* **44**, 817.
10. Determination of iodide in urine by Ion-pair chromatography with electrochemical detection
11. *Fresenius Journal of Analytical Chemistry,* 2001, DOI: 10.1007/s002160101080· Source: PubMed.

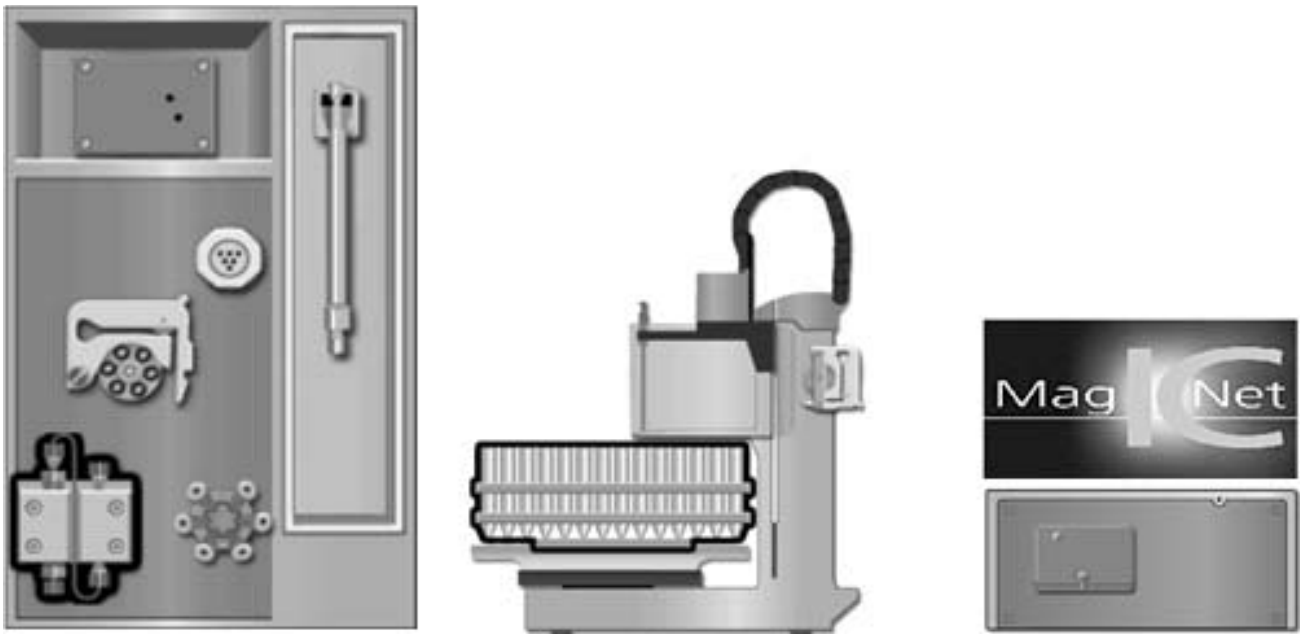

Fig. 1: Ion Chromatography Instrument setup

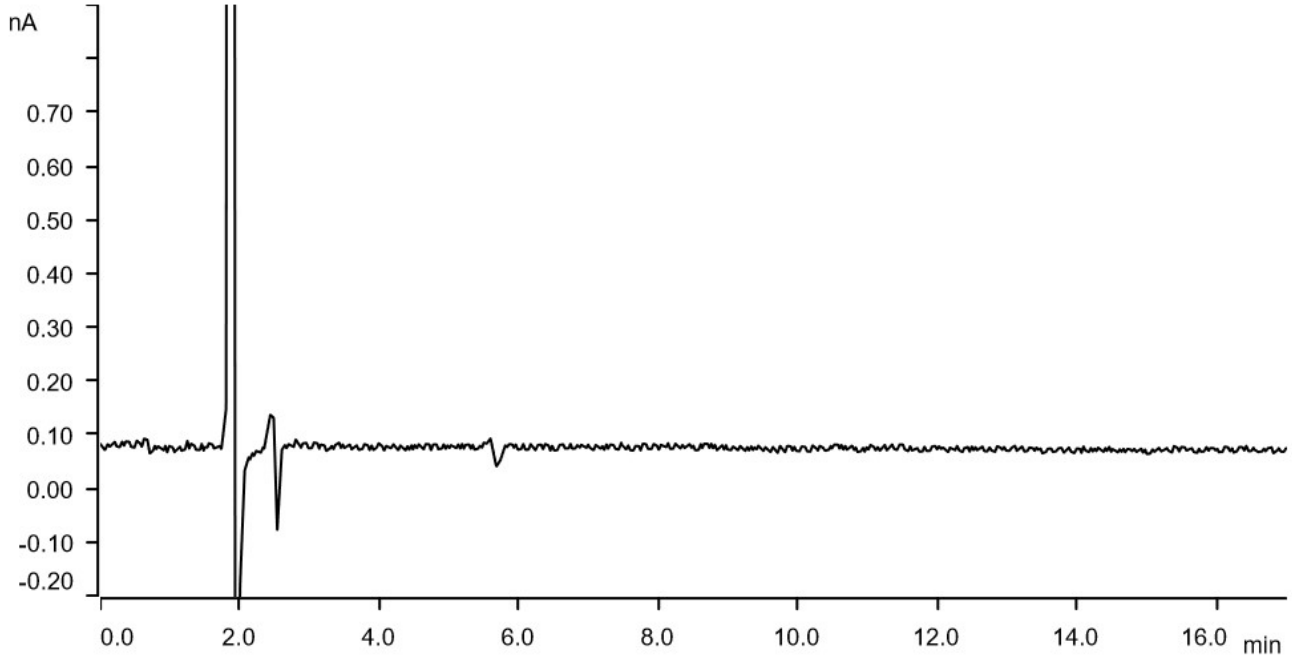

Fig. 2. Ion Chromatogram of blank diluent (Ultrapure water)

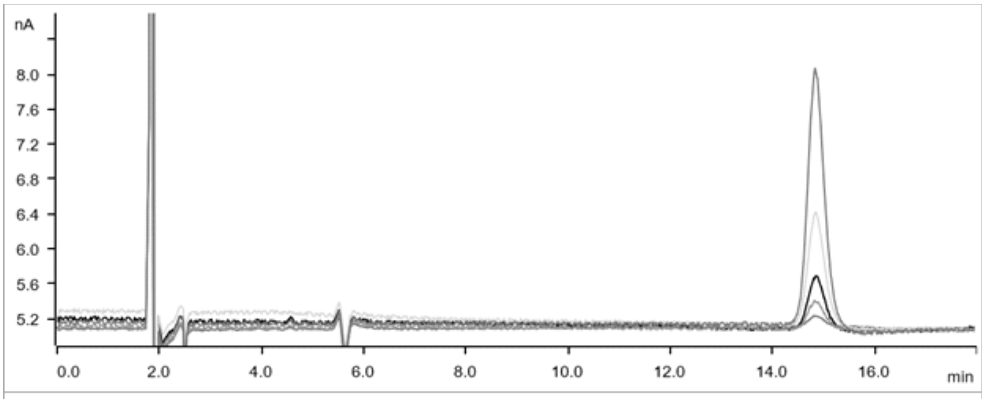

	Ident	Sample type	Volume	Legend	Display
1	2 ppb iodide	Standard 1	20.0		on
2	5 ppb iodide	Standard 2	20.0		on
3	10 ppb iodide	Standard 3	20.0		on
4	25 ppb iodide	Standard 4	20.0		on
5	50 ppb iodide	Standard 5	20.0		on

Fig. 3. Overlay of linearity chromatogram (iodide standards 2 to 50 ppb)

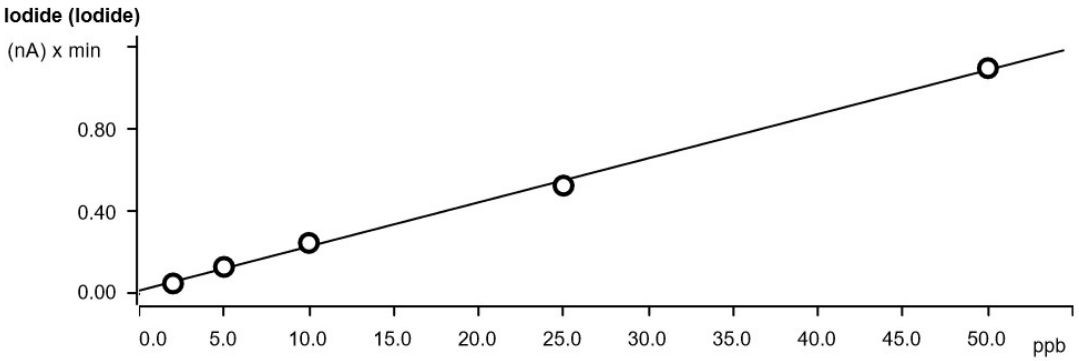

Function: . . . . . *A = 0.0158302 + 1.06779E-3× Q*

Relative standard deviation . . . . . *4.829499 %*

Correlation coefficient *0.999180*

Sample type	Index	Conc.	Volume	Dilution	Sample amount	Area	Ident
Standard 1	1	2.000	20.0	1.0	1.0	0.050	2 ppb iodide
Standard 3	1	10.000	20.0	1.0	1.0	0.247	10 ppb iodide
Standard 2	1	5.000	20.0	1.0	1.0	0.130	5 ppb iodide
Standard 4	1	25.000	20.0	1.0	1.0	0.524	25 ppb iodide
Standard 5	1	50.000	20.0	1.0	1.0	1.093	50 ppb iodide

Fig. 4. Linearity curve (2 ppb to 50 ppb iodide)

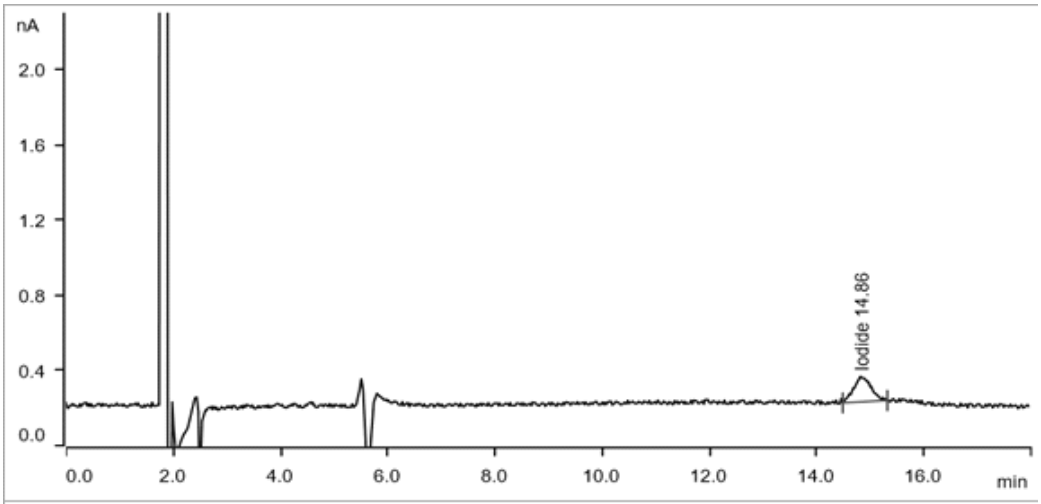

Component name	Retention time min	Height nA	Area (nA) x min	Concentration ppb	SNR
Iodide	14.855	0.133	0.05031	2.000	4.912

Fig. 5. Ion Chromatogram of 2 ppb iodide standard solution (LOD)

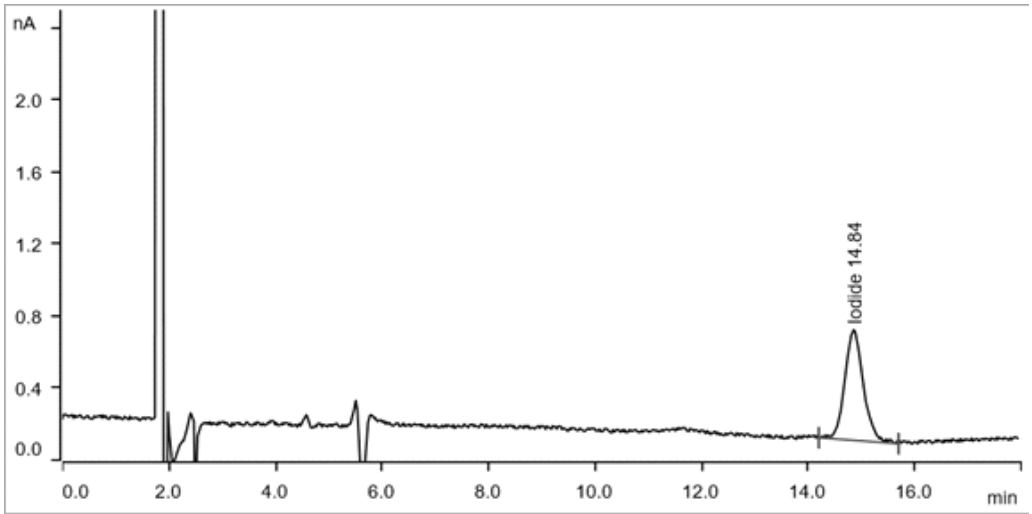

Component name	Retention time min	Height nA	Area (nA) x min	Concentration ppb	SNR
Iodide	14.835	0.614	0.24657	10.000	24.241

Fig. 6. Ion Chromatogram of 10 ppb iodide standard solution (LOQ)

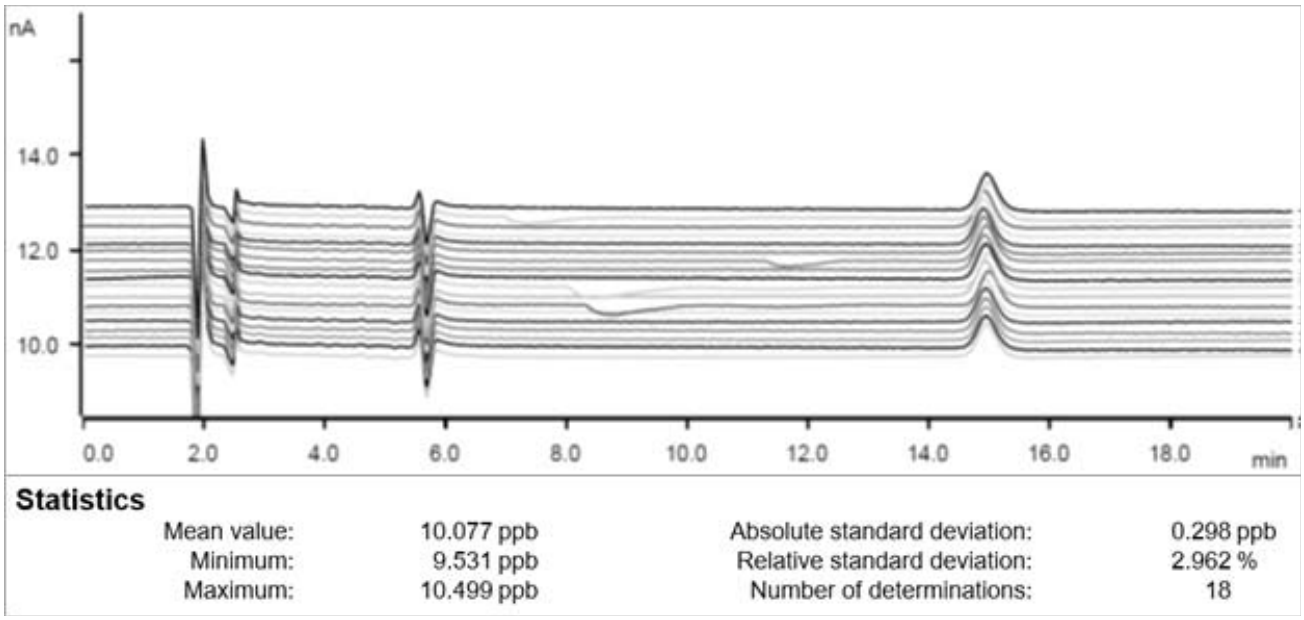

Fig. 7. Repeatability study (Overlay of 18 replicated injections of 10 ppb iodide standard)

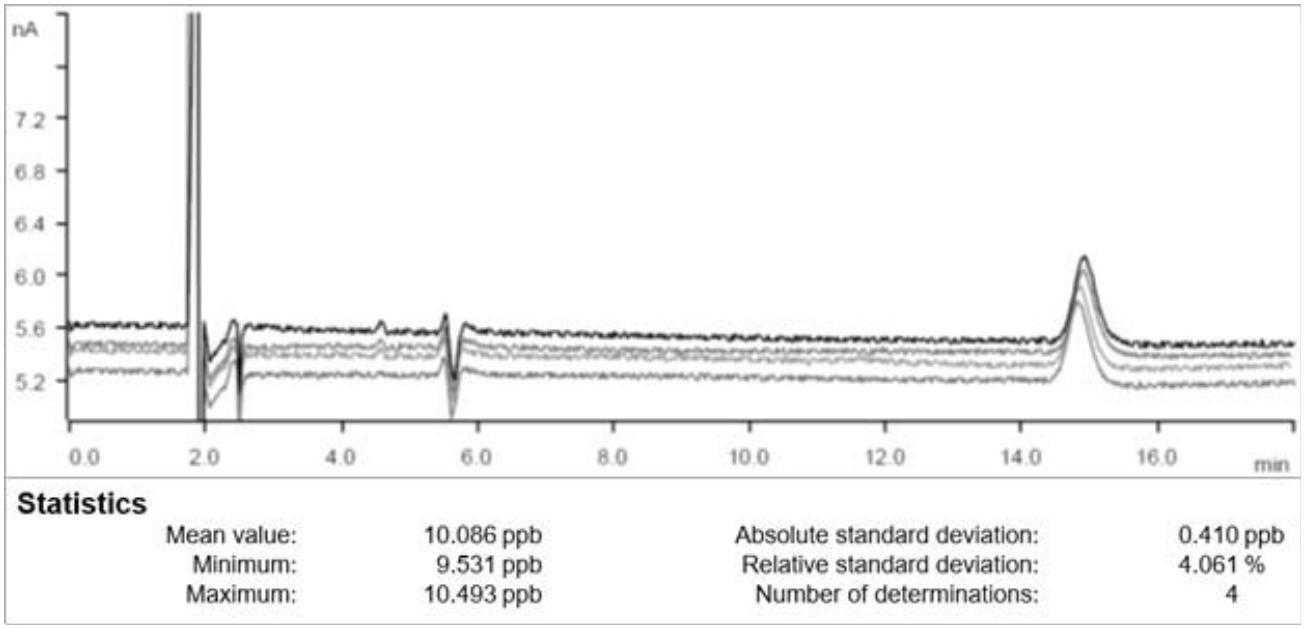

Fig. 8. Check standard stability for 12 hours (10 ppb iodide standard)

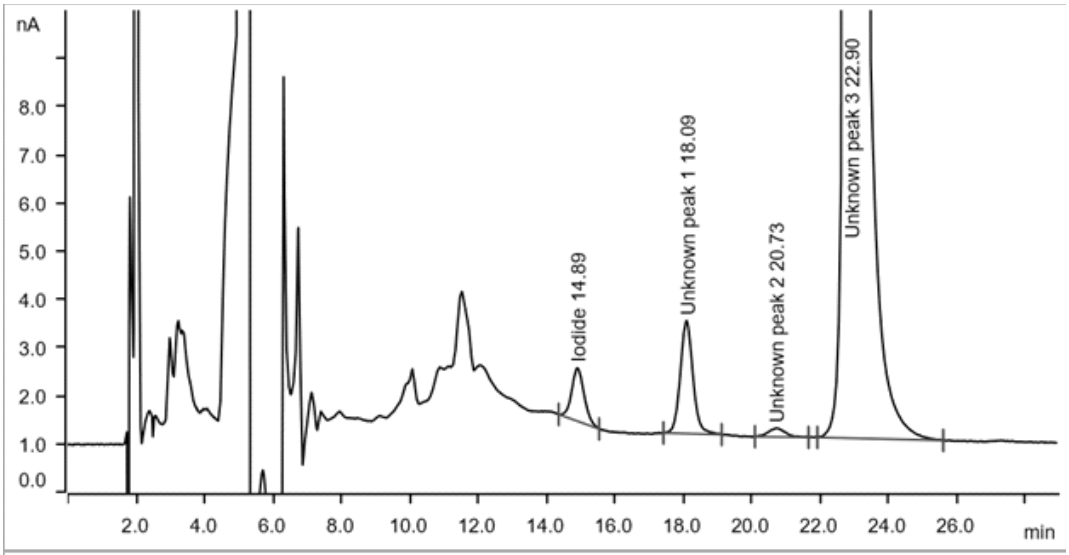

Component name	Retention time	Height	Area	Concentration	SNR
	min	nA	(nA) x min	ppb	
Iodide	14.888	1.103	0.46578	21.069	40.825

Fig. 9. Ion Chromatogram of Urine sample from a Volunteer

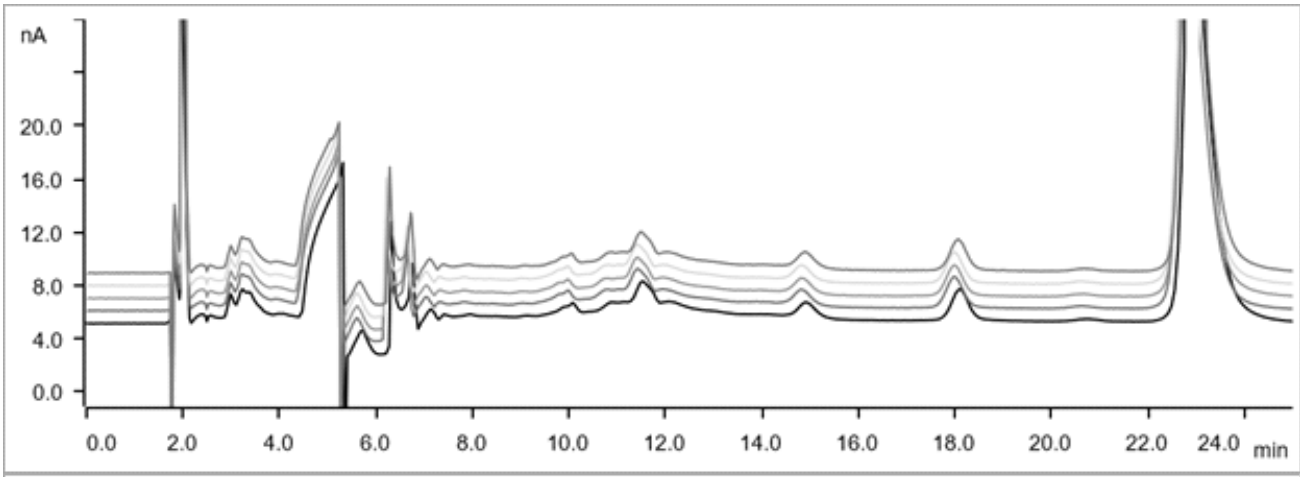

Statistics

Mean value:	21.333 ppb	Absolute standard deviation:	0.312 ppb
Minimum:	21.069 ppb	Relative standard deviation:	1.463 %
Maximum:	21.867 ppb	Number of determinations:	5

Fig. 10. Ion Chromatogram of Urine sample from a Volunteer (Overlay of 5 replicated injections and statistics data)

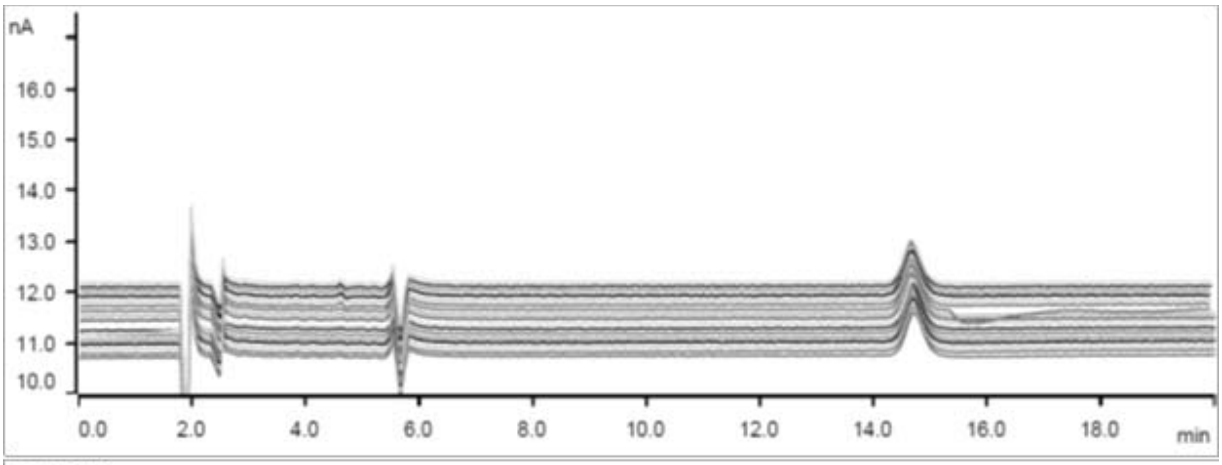

Statistics

Mean value:	10.218 µg/L	Absolute standard deviation:	0.209 µg/L
Minimum:	9.790 µg/L	Relative standard deviation:	2.048 %
Maximum:	10.493 µg/L	Number of determinations:	18

Fig. 11. Reproducibility study on different days using fresh eluent and with different persons (Overlay of 18 replicated injections of 10 ppb iodide standard)

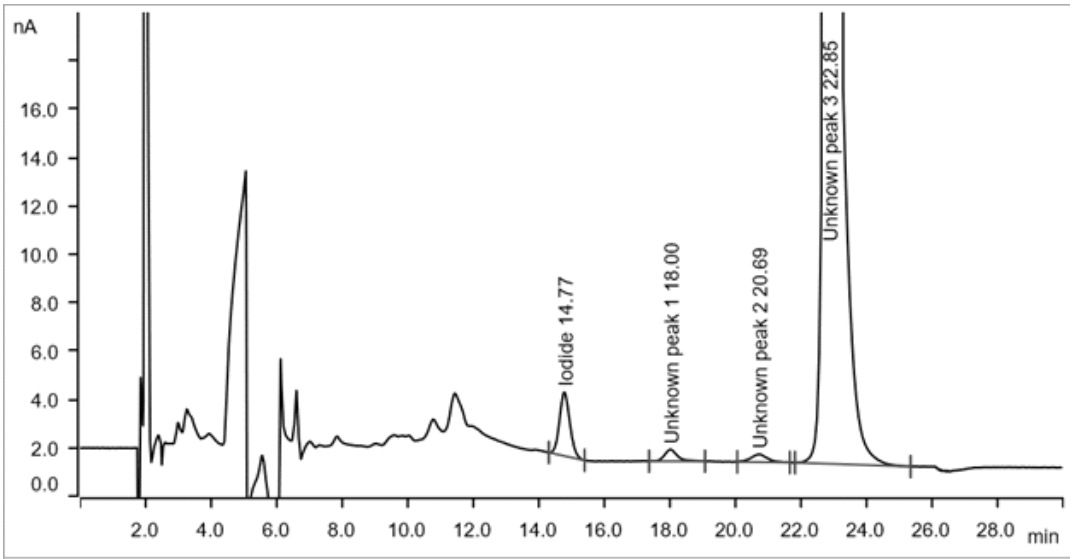

Component name	Retention time	Height	Area	Concentration	SNR
	min	nA	(nA) x min	ppb	
Iodide	14.768	2.640	0.96028	44.224	105.428

Fig. 12. Method accuracy study for anlaysis of urine sample

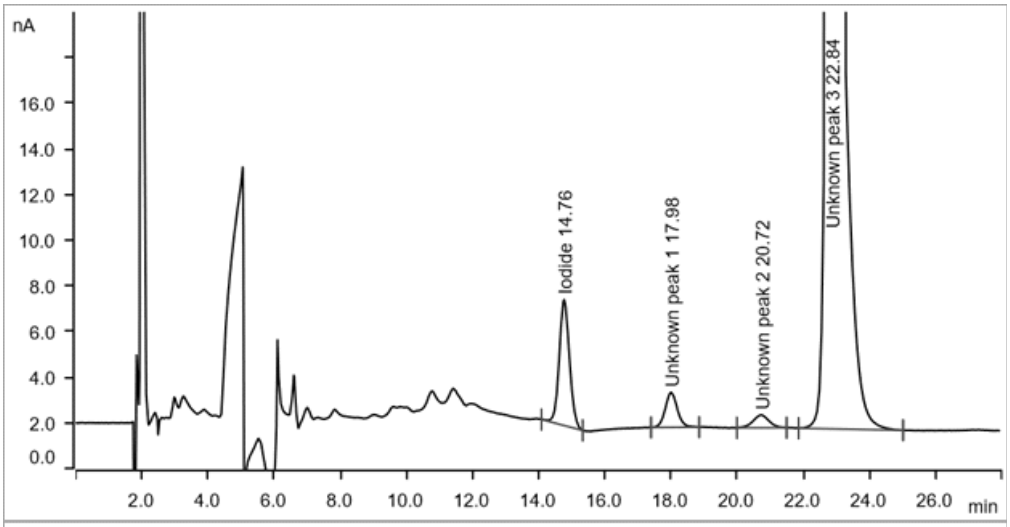

Component name	Retention time	Height	Area	Concentration	SNR
	min	nA	(nA) x min	ppb	
Iodide	14.760	5.513	1.97687	91.827	208.028

Fig. 13. Method of accuracy study for analysis of urine sample spiked with 50 ppb iodide standard

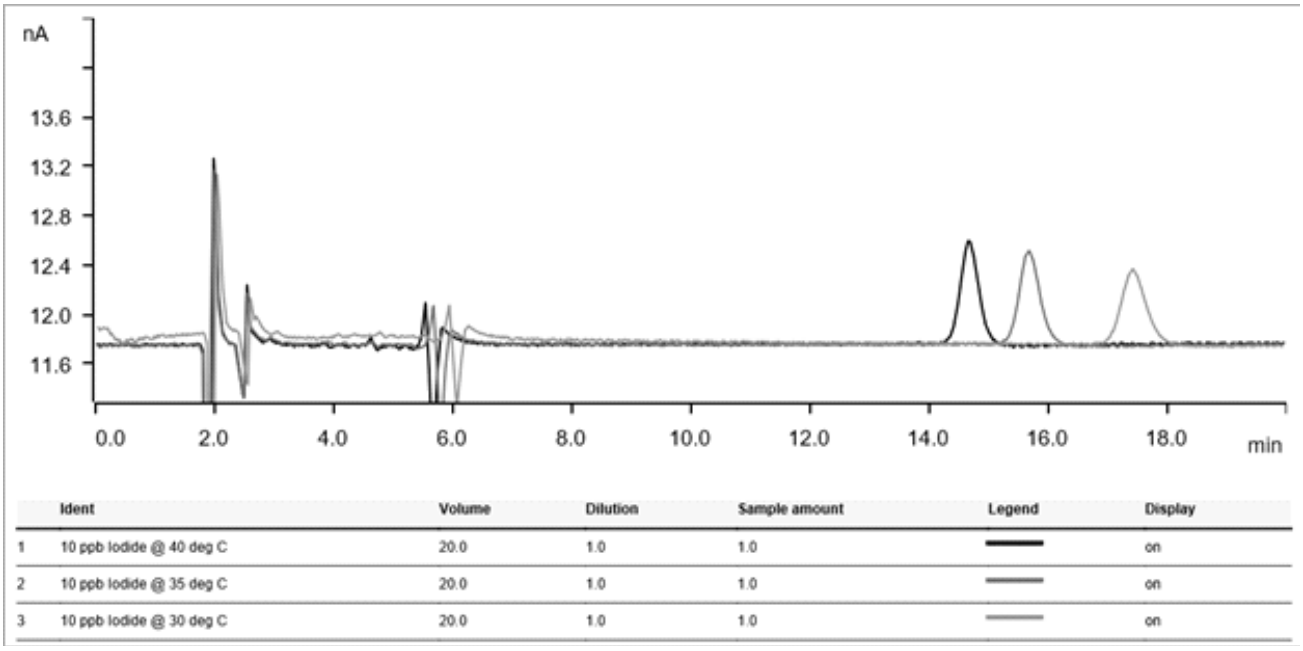

	Ident	Volume	Dilution	Sample amount	Legend	Display
1	10 ppb Iodide @ 40 deg C	20.0	1.0	1.0		on
2	10 ppb Iodide @ 35 deg C	20.0	1.0	1.0		on
3	10 ppb Iodide @ 30 deg C	20.0	1.0	1.0		on

Fig. 14. Overlay chromatogram for study of effect of temperature on Peak area

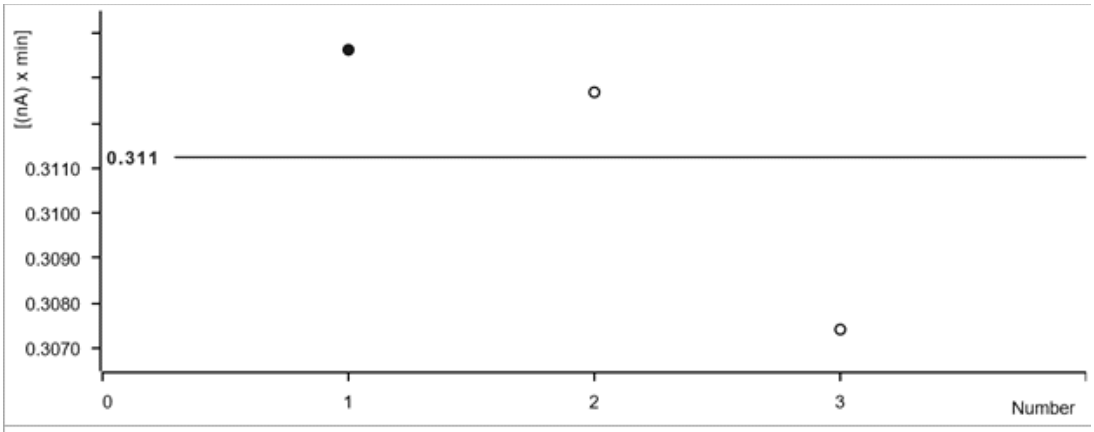

Result overview - Area

	Ident	Sample type	Iodide	Statistics
1	10 ppb Iodide @ 40 deg C	Sample	0.314 (nA) x min	on
2	10 ppb Iodide @ 35 deg C	Sample	0.313 (nA) x min	on
3	10 ppb Iodide @ 30 deg C	Sample	0.307 (nA) x min	on

Fig. 15. Statistics data for effect of temperature on peak area

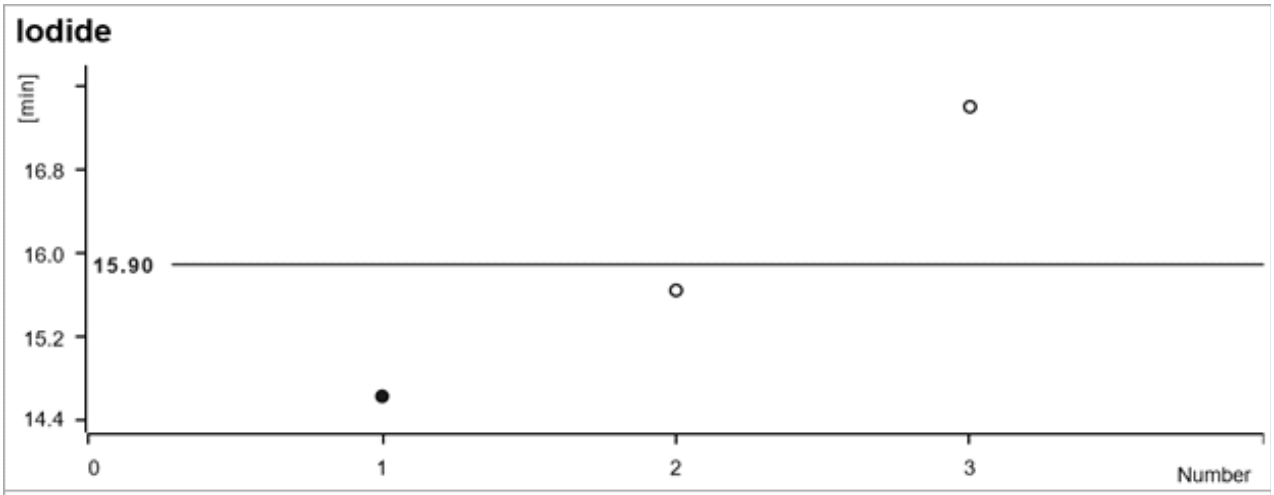

Result overview - Retention time

	Ident	Iodide	Statistics
1	10 ppb Iodide @ 40 deg C	14.64 min	on
2	10 ppb Iodide @ 35 deg C	15.65 min	on
3	10 ppb Iodide @ 30 deg C	17.40 min	on

Fig. 16. Statistics data for effect of temperature on Retention time

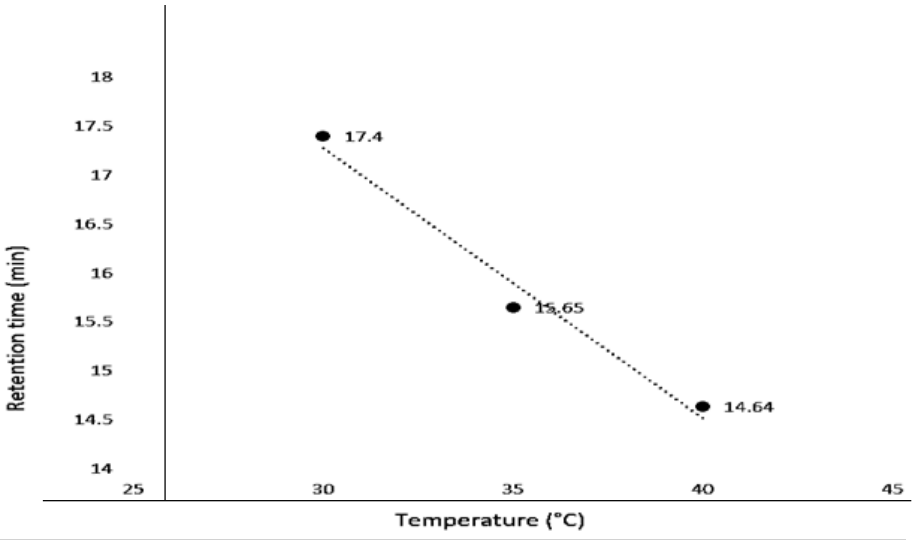

Fig. 17. Graphical data for Temperature vs Retention time

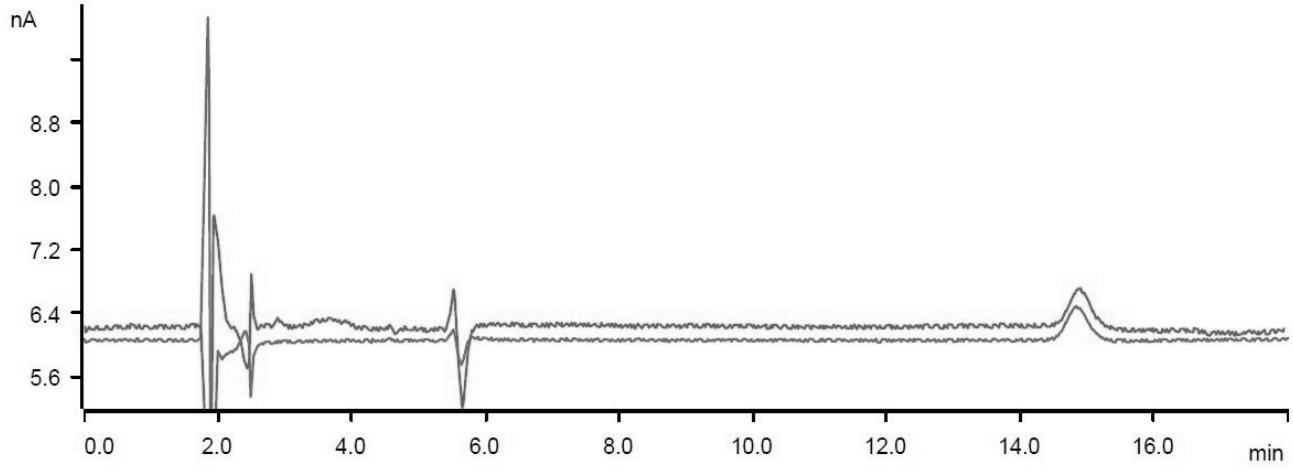

	Ident	Legend	Volume	Method	Sample amount	Dilution
1	10 ppb iodide		20.0	iodide in 896	1.0	1.0
2	10 ppb iodide (new Ag tip)		20.0	iodide in 896	1.0	1.0

Fig. 18. Comparison of ion chromatograms of two different silver working electrodes (new one vs used one)

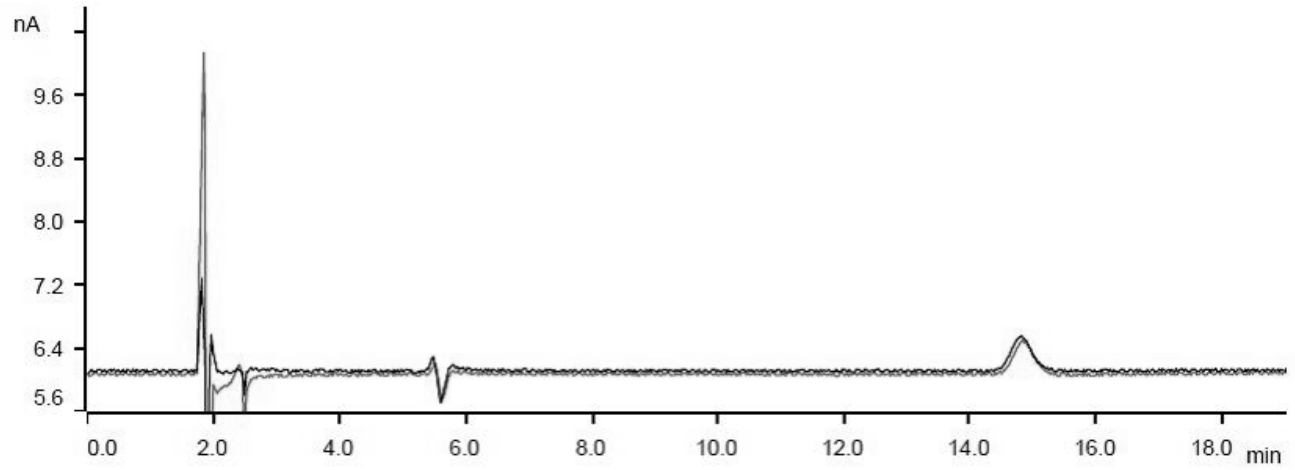

	Ident	Legend	Volume	Dilution	Sample amount
1	10 ppb iodide		20.0	1.0	1.0
2	10 ppb Iodide New Ag/AgCl reference		20.0	1.0	1.0

Fig. 19. Comparison of chromatogram of two different silver / silver reference electrode (new one vs used one)

Table 1. Iodine deficiency

Urine iodine µmol/L	Urine iodine µg/L	Iodine intake	Iodine nutritional status
0 – 0.15	< 20	Insufficient	Severe deficiency
0.16 – 0.38	20 - 49	Insufficient	Moderate deficiency
0.40 – 0.78	50 - 99	Insufficient	Mild deficiency
0.79 – 1.56	100 - 199	Adequate	Optimal
1.57 – 2.36	200 - 299	More than adequate	Risk of iodine – induced hyperthyroidism
≥ 2.37 µmol/L	≥ 300	Excessive	Risk of hyperthyroidism and autoimmune thyroid disease

Table 2. Repeatability study for standard (10 ppb iodide standard)

Sl.No	Standard Injections	Peak area [(nA) × min]	Mean area [(nA) × min]	RSD (%)
1	Injection 1	0.275	0.291	2.96
2	Injection 2	0.283		
3	Injection 3	0.281		
4	Injection 4	0.281		
5	Injection 5	0.279		
6	Injection 6	0.284		
7	Injection 7	0.288		
8	Injection 8	0.291		
9	Injection 9	0.290		
10	Injection 10	0.296		
11	Injection 11	0.290		
12	Injection 12	0.298		
13	Injection 13	0.301		
14	Injection 14	0.303		
15	Injection 15	0.296		
16	Injection 16	0.300		
17	Injection 17	0.294		
18	Injection 18	0.302		

Table 3. Repeatability study for urine samples

Sl.No	Sample injections	Concentration (ppb)	Mean concentration (ppb)	RSD (%)
1	Injection 1	21.07	21.33	1.46
2	Injection 2	21.24		
3	Injection 3	21.32		
4	Injection 4	21.17		
5	Injection 5	21.87		

Table 4. Consolidated Results – Iodide content in ppb for different voluenteers

Sample ID	Number of injections	Mean concentration (ppb)	RSD (%)
Volunteer 1	5	21.33	1.35
Volunteer 2	5	44.60	2.01
Volunteer 3	5	26.86	2.04
Volunteer 4	1	44.22	NA***

***NA = Not applicable

Table 5. Reproducibility study with standard (10 ppb iodide standard) on different days, fresh eluent & different analysts

Sl.No	Standard Injections	Peak area [(nA) × min]	Mean area [(nA) × min]	RSD (%)
1	Injection 1	0.320	0.327	2.05
2	Injection 2	0.320		
3	Injection 3	0.328		
4	Injection 4	0.323		
5	Injection 5	0.333		
6	Injection 6	0.328		
7	Injection 7	0.334		
8	Injection 8	0.331		
9	Injection 9	0.330		
10	Injection 10	0.331		
11	Injection 11	0.326		
12	Injection 12	0.330		
13	Injection 13	0.336		
14	Injection 14	0.335		
15	Injection 15	0.327		
16	Injection 16	0.314		
17	Injection 17	0.331		
18	Injection 18	0.314		

RNI No. MAHENG/2017/74063
ISSN No. (Print) 2581-5911
ISI Impact Factor 1.022 (2019-2020)

Efficient One-pot Green Synthesis of 2,3-Dihydroquinazolin-4(1*H*)-ones Derivatives by using $NiFe_2O_4$ Ferrite as Nanocatalyst under Microwave Irradiation Conditions

C.A. Ladole, A. M. Tade and A.S. Aswar*
Department of Chemistry
Sant Gadge Baba Amravati University Amravati 444 602, India
Email: aswaranand@gmail.com

Abstract
A microwave assisted synthesis of 2,3-Dihydroquinazolin-4(1H)-ones via the efficient one pot three component reaction of isatoic anhydride, aromatic aldehydes, and ammonium salts or primary amines under solvent free conditions in presence of nickel ferrite as an efficient heterogeneous catalyst is reported. The catalyst was prepared and characterized by P-XRD, FTIR, TG/DTA and SEM analysis. The XRD pattern of the catalyst conforms the phase purity of the material. The average crystallite size was calculated using Scherrer's formula as applied to the major intense peaks and the average particle size was found to be 25.10 nm. SEM images show tiny crystalline cubes with agglomeration. The FT IR spectrum of the catalyst can be ascribed to metal oxygen modes of tetrahedral and octahedral sites. This protocol offers several advantages including greenness with respect to mild reaction conditions, high yields and easy work-up and reusability of catalyst without loss of reactivity. The catalyst retained its activity for upto four cycles, hence it is considered as an attractive catalyst for multicomponent reactions. The catalytic activity of ferrite was checked as a function of amount of catalyst and recyclability of catalyst without loss of reactivity. This heterogeneous catalyst is easy to prepare, inexpensive and insoluble in most organic solvents and may be recycled during work up procedure. The synthesized compounds were confirmed using FT-IR, ^{1}H and ^{13}C NMR spectroscopic data and melting points compared with reported values.

Keywords: *2,3-Dihydroquinazolin-4(1H)-ones, $NiFe_2O_4$ ferrite, spectral data, microwave assisted synthesis.*

Introduction

Nanoparticles as heterogeneous catalysts have attracted a great deal of attention because of their high catalytic activity and applications in biotechnology, medicine, chemistry, material science, polymer science, biology and engineering[1-3]. Metal catalysed intramolecular hydroamination of alkynes has emerged in recent years as a useful synthetic tool for the preparation for various N-heterocycles, such as indoles, pyrroles, quinolones and isoquinolines. Multi-component reactions (MCRs) have recently been discovered to be a powerful method and an efficient tool for the synthesis of biologically important compounds[4]. Multicomponent reactions (MCRs) have some advantages over conventional methods, such as lower cost, shorter reaction time, and few side products[5, 6].

Heterocyclic chemistry occupies an important place in organic chemistry and forms the basis of many

pharmaceutical, agrochemical and veterinary products. In modern organic synthesis selective transformations using readily available, inexpensive and environmentally-benign recyclable catalysts and reagents are of great interest. Nowadays, the major goals of Green Chemistry are achieved by maximising the use of starting materials and reducing environmentally challenging reaction waste to achieve the objectives including the use of alternative reagents and catalysts, simplification of the purification steps, easy recovery and recycling of catalysts[7,8]. The catalytic ability of materials depends on their microscopic structure, selectivity, thermal and chemical stability[9]. Quinazolinone derivatives are a class of fused nitrogen containing heterocyclic compounds having potential biological and pharmaceutical activities including antifertility, antibacterial, antitumor and monoamine oxidase inhibitory activities[10,11]. Quinazoline ring is an aromatic benzopyrimidine, which oxidizes to quinazolin-4(3*H*)-ones moieties which are growth inhibitors in the treatment of leukemia cells and poly (ADP-ribose) polymerase-1 inhibitors, fungicides, bactericides, insecticides, and plant-growth regulators[12,13]. The group of quinazolinones have various biological activities and are key intermediates for the synthesis of quinazolin-4(3*H*)-ones which are diuretic, antitumor, antibacterial, anti-convulsant, anticancer and antihypertensive agents[14-20]. The procedure involves one pot three-component reaction of isatoic anhydride, aromatic aldehydes, and ammonium salts or primary amines for the synthesis of 2,3-dihydro- 4(1H)-quinazolinones. Various protocols have been developed for the synthesis of quinazolinone derivatives using supported ceric ammonium nitrate[21], Zeolite[22], Starch sulfate[23], Alumina (H_3PO_4-Al_2O_3)[24], Silica-supported zinc(II) chloride (SiO_2-$ZnCl_2$)[25], Aluminum methanesulfonate[26], Silica-bonded N-propylsulfamic acid[27], Montmorillonite K-10[28], Gallium(III) triflate[29] etc. Some of these procedures have drawbacks such as the use of hazardous organic solvents, separation of catalyst, long reaction time, expensive and tedious work-up procedure. Herein, we report a microwave assisted one pot synthesis of 2,3-dihydroquinazolin-4(1*H*)-ones derivatives by condensation of isatoic anhydride, aromatic aldehydes, and ammonium salts or primary amines in presence of reusable nickel ferrite as catalyst.

Materials and Metods

Analytical grade chemicals were used and distilled prior to use. Melting points were determined using a quality digital melting point apparatus. The IR spectra were recorded on Shimadzu FT IR spectrometer. NMR spectra recorded on a Bruker Avance (300 and 400 MHz) spectrometer using $CDCl_3$ and DMSO d_6 as solvents. Chemical shifts (ppm) were referenced to the initial standard tetramethylsilane (TMS). The structural and phase purity of the prepared samples were characterized by XRD measurement using Bruker AXS D8 advanced X ray powder diffractometer with CuK_∞ 10-90° line (λ = 1.54056 Å) in the 2θ range 10 90°. The morphology of prepared samples was examined by direct observation via Scanning Electron Microscope (SEM) model (JEOL Model JSM 6390LV). Thermogravimetric differential thermal analysis (TG/DTA) was carried out using a Perkin Elmer STA 6000 instrument in nitrogen atmosphere with the flowing rate 20 mL/min in the range room temperature to 720°C and heating rate of 10°C/min. Experiments under microwave irradiation were carried out in scientific microwave synthesizer system supplied by Ragatech Electronics India Pvt. Ltd., India, having maximum power output of 700 W and 2450 MHz frequency with 10 power levels (140 to 700 W). The reactions were monitored by thin layer chromatography using silica gel 60F254 aluminium sheets (Merck).

The nickel ferrite was prepared by known co-precipitation method with slight modification in the stoichiometry of the reaction[30]. The stoichiometric amount of nickel chloride was allowed to react with sodium hydroxide with continuous stirring. Ferric chloride in HCl was added with continuous stirring for

two hours. It was heated for half an hour at 60°C and allowed to cool to room temperature. The pH was adjusted to 7.5 by adding 2N sodium hydroxide. The product obtained was washed with distilled water and filtered and dried in an oven at 120°C. It was calcined at 500°C for 5 hours.

General procedure for preparation of 2,3-Dihydroquinazolin-4(1*H*)-ones

A mixture of isatoic anhydride, (1 mmol), primary amine or ammonium acetate (1.1 mmol), aromatic aldehyde (1 mmol) and $NiFe_2O_4$ ferrite (10 mol%) was placed in a 100 mL round bottom flask without solvent and irradiated in microwave (350 W) for the desired time. Upon comp-letion of the reaction (monitored by TLC using hexane: ethyl acetate (6:4, *v*:*v*) as eluent), the mixture was diluted with ethanol (3×10 mL), stirred and filtered to remove the catalyst. The solid residue was recrystallized from ethanol to give the pure product. All the products are known compounds and were characterized by IR and ^{1}H NMR Spectroscopic data and melting points were compared with the reported values.

Spectral data of some synthesized compounds

2-phenyl-2,3-dihydroquinazolin-4(1*H*)-one **(4a)**: ^{1}H-NMR (400 MHz, DMSO-*d*6, δ, ppm): 5.75 (d, 1H, CH), 6.64 (t, 1H, Ar-H), 6.75 (d, 1H, Ar-H), 7.01 (s, 1H, NH), 7.23 (t, 1H, Ar-H), 7.32-7.40 (m, 3H, Ar-H), 7.49-7.52 (m, 2H, Ar-H), 7.62 (d, 1H, Ar-H), 8.21 (s, 1H, NH); IR (KBr): ν 3301, 3181, 1650, 1609, 1506, 1480, 1283 cm^{-1}.

2-(4-methoxyphenyl)-2,3-dihydroquinazolin-4(1*H*)-one **(4b)**: ^{1}H-NMR (400 MHz, DMSO-*d*6, δ, ppm): 3.75 (s, 3H, OCH_3), 5.70 (s, 1H, CH), 6.66 (s, 1H, NH), 6.73 (d, 1H, Ar-H), 6.90 (m, 3H, Ar-H), 7.19 (t, 1H, Ar-H), 7.41 (d, 2H, Ar-H), 7.63 (d, 1H, CH), 8.12 (s, 1H, NH), ^{13}C NMR (400 MHz, DMSO-*d*6, δ, ppm): 55.04, 66.45, 78.85, 113.49, 113.82, 114.35, 114.93, 116.99, 127.28, 128.17, 133.06, 133.29, 147.98, 163.76; IR (KBr): ν 3297, 3176, 1650, 1608, 1504, 1484 cm^{-1}.

2-(2-hydroxyphenyl)-2,3-dihydroquinazolin-4(1*H*)-one **(4c)**: ^{1}H-NMR (400 MHz, DMSO-*d*6, δ, ppm): 5.98 (s, 1H, CH), 6.62-6.85 (m, 4H, Ar-H), 7.10-7.33 (m, 3H, Ar-H), 7.59-7.61 (d,1H, Ar-H), 7.92 (s, 2H, NH), 9.84 (s, 1H, OH); IR (KBr): ν 3409, 3281, 3200, 1645,1614,1576, 1438 cm^{-1}.

2-(3-nitrophenyl)-2,3-dihydroquinazolin-4(1*H*)-one **(4d)**: ^{1}H-NMR (400 MHz, DMSO-*d*6, δ, ppm): 7.23 (d, 1H, CH), 7.34 (t, 1H, Ar-H), 7.52 (t, 1H, Ar-H), 7.60 (s, 1H, NH), 7.82-7.89 (m, 2H, Ar-H), 8.0 (s, 1H, NH), 8.38-8.41 (m, 2H, Ar-H), 8.75 (t, 2H, Ar-H); IR (KBr): ν 3333, 3259, 3079, 1672, 1634, 1524, 1446 cm^{-1}.

2-(3,4-dimethoxyphenyl)-2,3-dihydroquinazolin-4(1*H*)-one **(4f)**: ^{1}H-NMR (400 MHz, DMSO-*d*6, δ, ppm): 3.76 (s, 6H, $2xCH_3$), 5.70 (s, 1H, CH), 6.65 (t, 1H, Ar-H), 6.74 (d, 1H, Ar-H), 6.92 (d, 1H, Ar-H), 6.94 (s, 1H, Ar-H), 6.99 (d, 1H, Ar-H), 7.01 (s, 1H, NH), 7.22 (t, 1H, Ar-H), 7.62 (d, 1H, Ar-H), 8.11 (s, 1H, NH); IR (KBr): ν 3353, 3331, 2966, 1666, 1608, 1494, 1412 cm^{-1}.

2-(2-hydroxy-3-methoxyphenyl)-2,3-dihydroquinazolin-4(1*H*)-one **(4h)**: ^{1}H-NMR (400 MHz, DMSO-*d*6, δ, ppm): 3.79 (s, 3H, OCH_3), 6.82 (s, 1H, CH), 7.11 (d, 1H, Ar-H), 7.48 (t, 1H, Ar-H), 7.73-7.85 (m, 5H, Ar-H), 8.1 (s, 2H, NH), 13.2 (s, 1H, OH); IR (KBr): ν 3197, 3060,2993, 2923, 2830, 1665, 1566, 1434 cm^{-1}.

2-(4-(dimethylamino)phenyl)-2,3-dihydroquinazolin-4(1*H*)-one **(4i)**: ^{1}H-NMR (400 MHz, DMSO-*d*6, δ, ppm): 2.89 (s, 6H, $2XCH_3$), 5.64 (s, 1H, CH), 6.63-6.74 (m, 4H, Ar-H), 6.83 (s, 1H, NH), 7.17 (t, 1H, Ar-H), 7.30 (d, 2H, Ar-H), 7.61 (d, 1H, Ar-H), 7.98 (s, 1H, NH); ^{13}C NMR (400 MHz, DMSO-*d*6, δ, ppm): 40.12, 40.17, 66.84, 78.50, 78.83, 111.77, 114.32, 114.96, 116.85, 127.27, 127.72, 128.43, 132.94, 148.19, 150.62, 163.91; IR (KBr): ν 3288, 3188, 2970, 1650, 1608, 1483 cm^{-1}.

2-(2-hydroxynaphthalen-1-yl)-2,3-dihydroquinazolin-4(1*H*)-one **(4j)**: ^{1}H-NMR (400 MHz, DMSO-*d*6, δ, ppm): 6.91 (d, 1H, CH), 7.33-7.38 (m, 2H, Ar-H), 7.52-7.66 (m, 4H, Ar-H), 7.76 (d, 1H, Ar-H), 7.89 (d, 2H, Ar-H), 8.02 (s, 1H, NH), 8.46 (d, 1H, Ar-H), 9.46 (s, 1H, NH), 15.07 (s, 1H, OH); ^{13}C NMR (400 MHz, DMSO-*d*6, δ, ppm): 60.22, 108.77, 119.02, 120.21, 123.09, 123.43, 125.51, 126.53, 128.13, 128.31, 128.98, 131.18, 133.54, 137.39, 141.90, 153.65, 169.12; IR (KBr): ν 3383, 3166, 2360, 1663, 1608, 1589, 1450 cm^{-1}.

2-(5-bromo-2-hydroxyphenyl)-2,3-dihydroquinazolin-4(1*H*)-one **(4k)**: ^{1}H-NMR (400 MHz, DMSO-*d*6, δ, ppm): 5.9 (s, 1H, CH), 6.41-7.86 (m, 7H, Ar-H), 8.82 (s, 1H, NH), 10.27 (s, 1H, NH), 12.59 (s, 1H, OH); IR (KBr): ν 3412, 3193, 2968, 2880, 1653, 1611, 1490 cm^{-1}.

2-(3-chlorophenyl)-2,3-dihydroquinazolin-4(1*H*)-one **(4l)**: ^{1}H-NMR (400 MHz, DMSO-*d*6, δ, ppm): 5.74 (s, 1H, CH), 6.63-6.73 (m, 3H, Ar-H), 7.07-7.25 (m, 2H, Ar-H), 7.33-7.69 (m, 3H, Ar-H), 8.32 (s, 2H, NH); IR (KBr): ν 3406, 3308, 2958, 1652, 1607, 1507, 1433 cm^{-1}.

2-(thiophen-3-yl)-2,3-dihydroquinazolin-4(1*H*)-one **(4m)**: ^{1}H-NMR (400 MHz, DMSO-*d*6, δ, ppm): 6.02 (s, 1H, CH), 6.68 (t, 1H, Ar-H), 6.75 (s, 1H, NH), 6.94 (t, 1H, Ar-H), 7.10-7.14 (m, 2H, Ar-H), 7.20 (t, 1H, Ar-H), 7.34 (d, 1H, Ar-H), 7.65 (d, 1H, Ar-H), 8.31 (s, 1H, NH); IR (KBr): ν 3293, 3180, 2936, 1654, 1611, 1517, 1441, 764 cm^{-1}.

2-(4-isopropylphenyl)-2,3-dihydroquinazolin-4(1*H*)-one **(4o)**: ^{1}H-NMR (400 MHz, DMSO-*d*6, δ, ppm): 1.2 (d, 6H, 2XCH_3), 2.89-2.92 (m, 1H, CH), 5.72 (s, 1H, NH), 6.64 (t, 1H, Ar-H), 6.72 (d, 1H, Ar-H), 6.92 (s, 1H, NH), 7.18-7.25 (m, 3H, Ar-H), 7.43 (d, 2H, Ar-H), 7.60 (d, 1H, Ar-H), 8.09 (s, 1H, NH); IR (KBr): ν 3293, 3192, 2954, 2871, 1772, 1726, 1655, 1511, 1387, 753 cm^{-1}.

Results and Discussion

Characterization of Catalyst

The catalyst nickel ferrite was prepared by co-precipitation method[30]. The phase composition of the sintered sample was analysed by X-ray diffraction pattern (at 500ºC for 2 hours). All peaks observed at 2θ = 27.48º, 31.81º, 35.72º, 43.37º, 45.53º, 53.87º, 56.55º, 62.99º, 66.30º, 75.34º clearly indicate the formation of the phase purity of $NiFe_2O_4$ (JCPDS card 89-7412). It was observed that, at high calcination temperature, XRD peaks become sharper as a result of shift towards greater crystallinity (Figure 1). The average crystallite size was calculated using Scherrer's formula as applied to the major intense peaks:

$$D = k\lambda/\beta\cos\theta \quad (1)$$

where, D is the average crystalline size, k the Scherrer constant (0.89), λ is the wavelength of CuK_{∞}, β is the full width at half-maximum (FWHM) of the diffraction peaks and θ is the Bragg's angle. The average particle size was found to be 25.10 nm.

The FT IR spectrum of catalyst shows bands in a low frequency region (750-500 cm^{-1}) due to the iron- oxygen stretching modes of tetrahedral and octahedral sites (Figure 2).

The thermogram shows continuous pyrolysis without any break except for 11.20% of the substance. The DTA curve shows endothermic reaction (Figure 3). The SEM images (Figure 4) show, tiny crystalline cubes with agglomeration. The higher SEM particle size as compared to XRD particle size can be attributed to agglomeration.

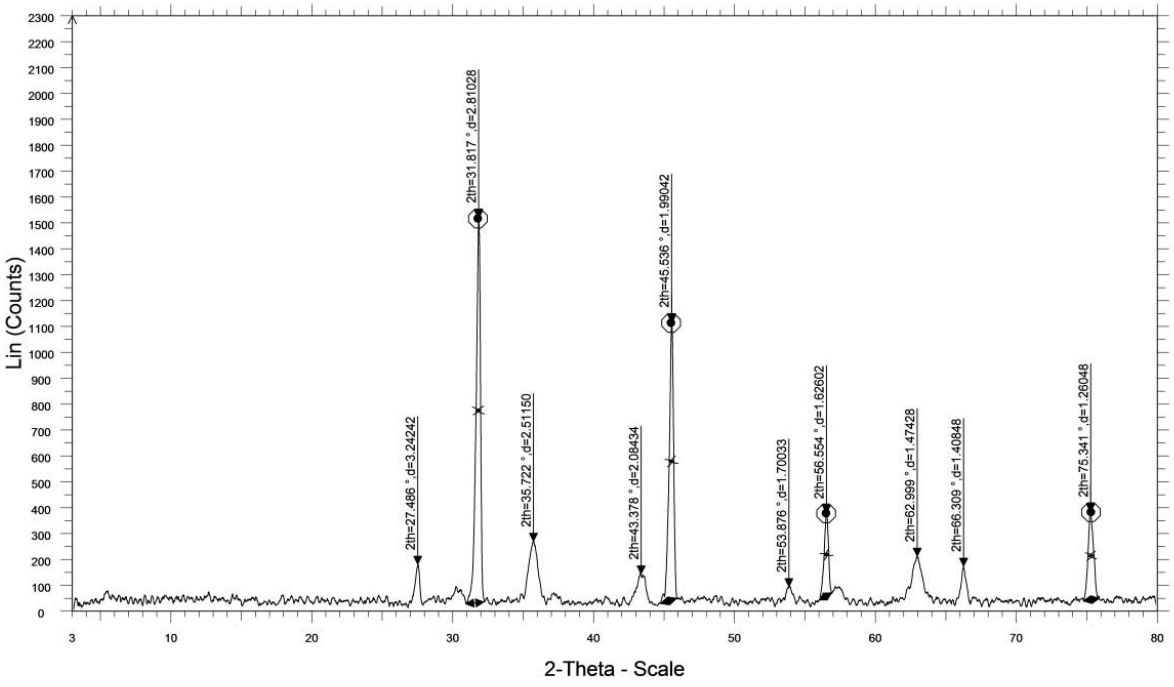

Fig. 1. Powder X-ray diffraction of $NiFe_2O_4$ ferrite

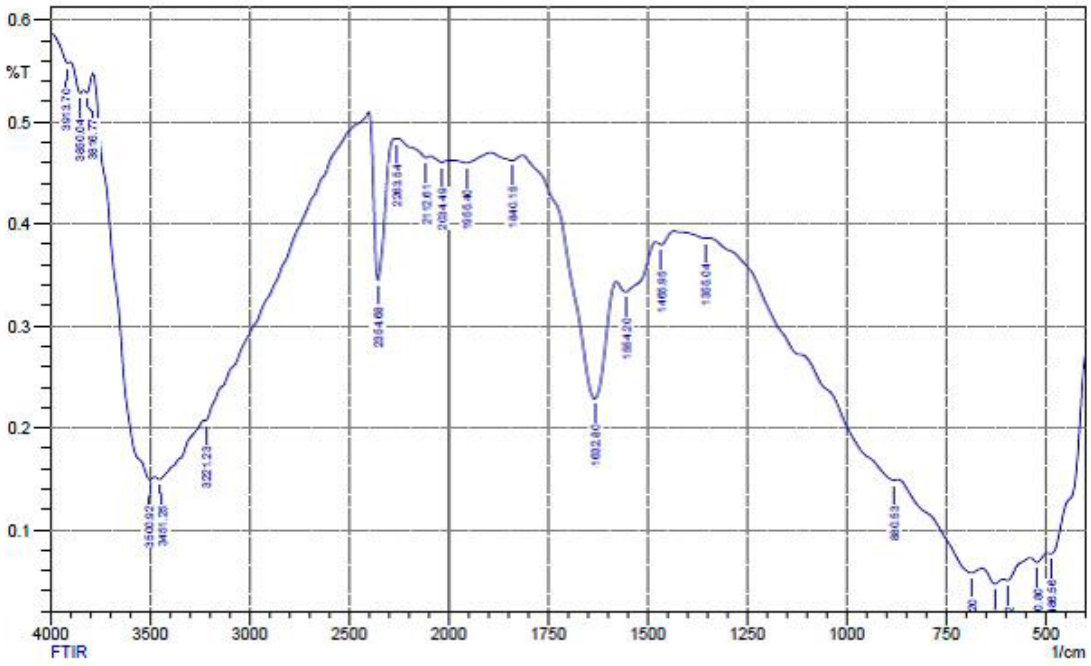

Fig. 2. FT-IR spectra of $NiFe_2O_4$ ferrite

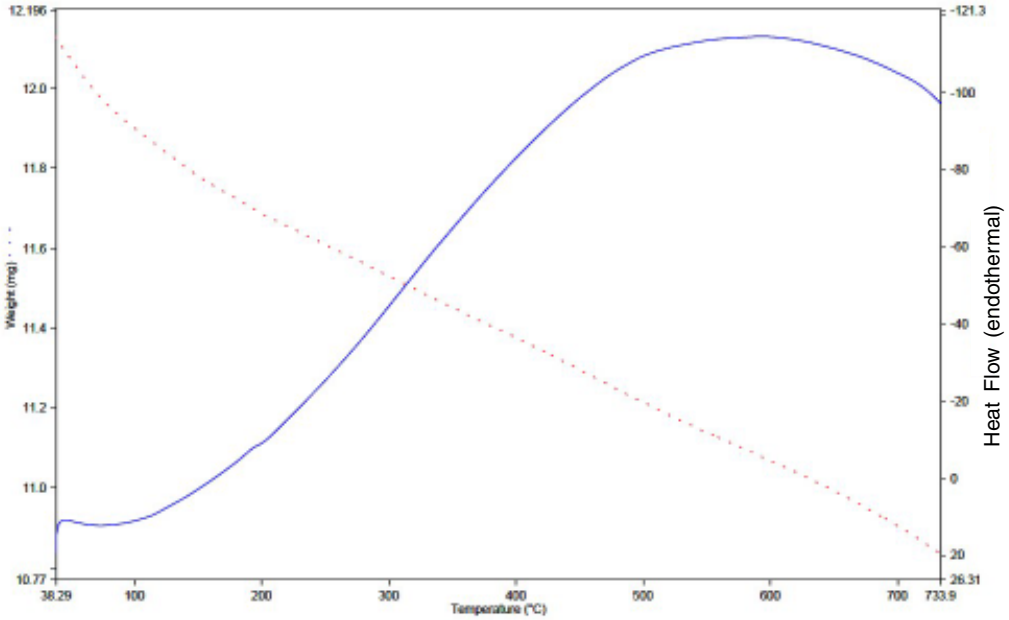

Fig. 3. Combined TG/DTA curves of $NiFe_2O_4$ ferrite

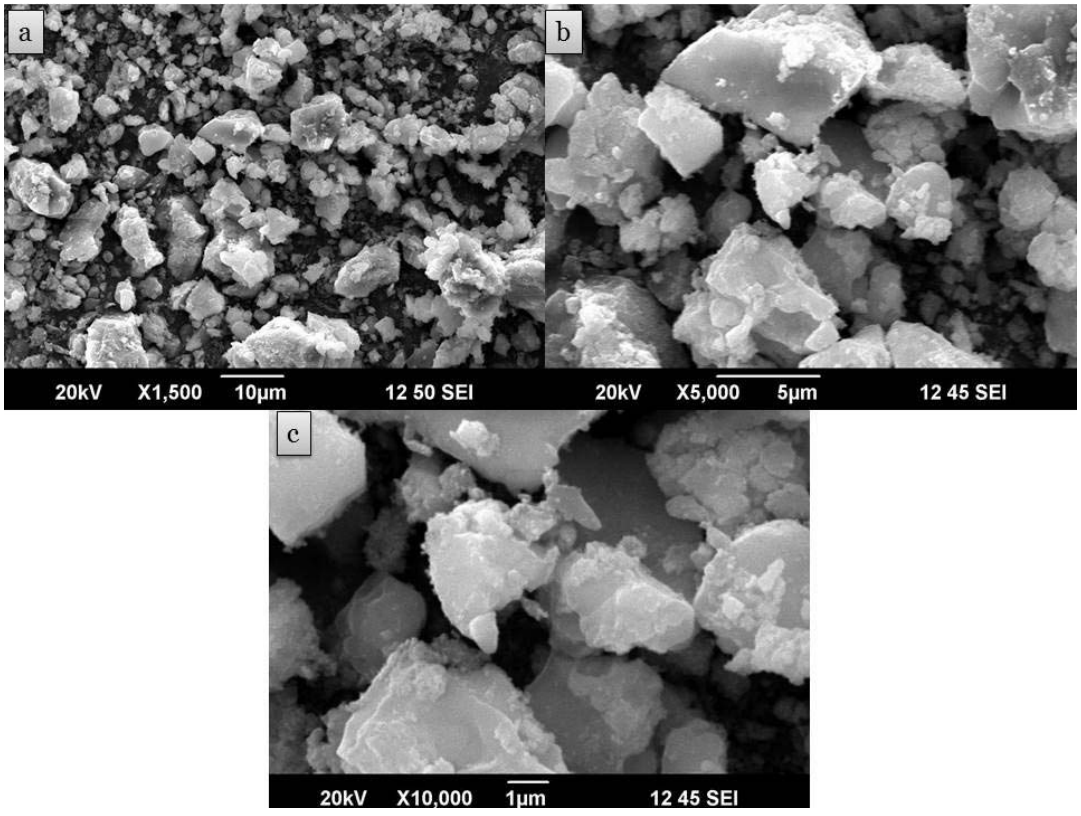

Fig. 4. SEM image of $NiFe_2O_4$ ferrite at different magnifications

To evaluate the efficiency of the catalyst, the synthesis of 2-phenyl-2,3-dihydroquinazolin-4(1*H*)-one (Scheme 1) was performed as a model reaction by condensation of isatoic anhydride, aromatic aldehydes, and ammonium salts or primary amines in the absence and presence of $NiFe_2O_4$ catalyst (Table 1).

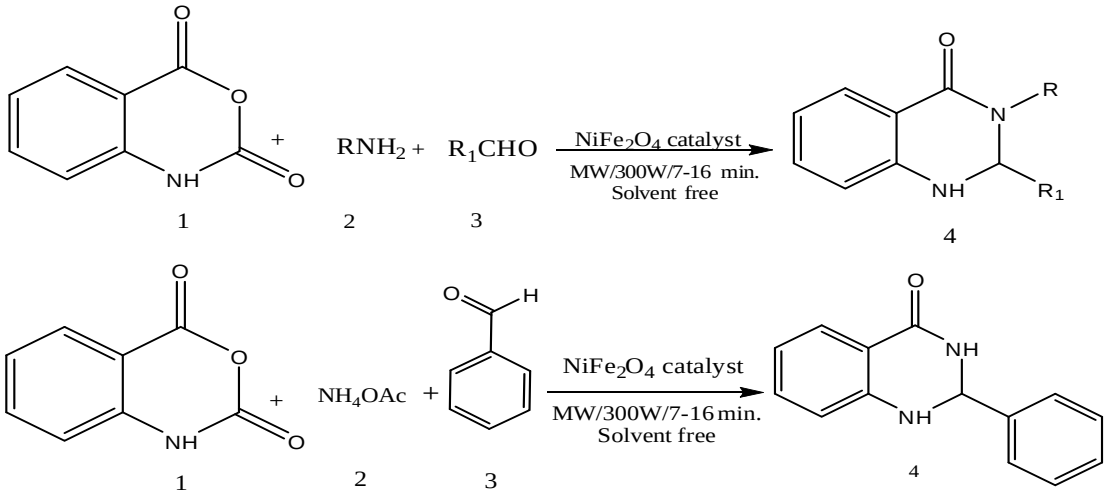

Scheme 1. Synthesis of 2,3-Dihydroquinazolin-4(1*H*)-ones using $NiFe_2O_4$ catalyst

Table 1. Effect of different amounts of $NiFe_2O_4$ and solvents on the formation of compound 4a [a]

Entry	Catalyst (mol%)	Condition/Solvents	Time(min)	Yield[b] (%)
1	Without catalyst	Microwave/solvent free	25	22
2	5	Microwave/solvent free	18	38
3	8	Microwave/solvent free	14	67
4	10	Microwave/solvent free	07	95
5	10	Reflux/ethanol	120	63
6	10	Reflux/water	120	73
7	10	Reflux/THF	120	36
8	10	Reflux/toluene	120	54

[a] Reaction conditions: isatoic anhydride, aromatic aldehydes, and ammonium salts or primary amines (1:1:1.5) in solvents and $NiFe_2O_4$ ferrite (10 mol%) as catalyst.
[b] Isolated yield.

Under microwave irradiation in the absence of catalyst, only 22% yield was obtained even with much longer reaction time (Table 1, Entry 1). Whereas in the presence of $NiFe_2O_4$ (5 mol %), the product yield was significantly enhanced (Table 1, Entry 2). Increasing the amount of catalyst up to 10 mol% improved the yield with complete reaction within 7 minutes (Table 1, Entry 4). Further, increasing the quantity of the catalyst did not increase the yield. The reaction performed in presence of ethanol, THF, toluene and water was slow (Table 1, Entries 5-8). At microwave irradiation below 350W, the reaction progressed slowly giving low yield and no improvement was observed above 350W microwave irradiation. Therefore, reactions were carried out at 350W. Moreover,

we have also compared reaction condition in terms of time and isolated yields with various solid catalysts such as Magnetic Fe_3O_4, cellulose-SO_3H, Ethylenediamine diacetate, [bmim]HSO_4, Bronsted acidic ionic liquids. It has been observed that $NiFe_2O_4$ is found to be a better catalyst as compared to others. Ethylenediamine diacetate (Table 2, Entry 3) shows slightly higher yield but it required longer reaction time.

Table 2. Comparative study of reaction yields with different catalysts

Entry	Catalyst	Amount (wt%)	Molar Ratio[a]	Condition/ Solvent	Time (min)/ Yield[b] (%)	References
1	Magnetic Fe_3O_4	15	1:1:1	Reflux/H_2O	120/80	31
2	Cellulose-SO_3H	05	1:1.2:1	Reflux/H_2O	28/90	32
3	Ethylenediamine diacetate	20	1:1:1	Reflux/H_2O	300/94	33
4	[bmim]HSO_4	25	1.1:1:1	Reflux/H_2O	180/85	34
5	Bronsted acidic ionic liquids	05	1:1.2:1	solvent free/80°C	09/91	35
6	$NiFe_2O_4$ ferrite	10	1:1:1.5	Microwave/ solvent free	7/95	Present work

[a] Molar ratio of isatoic anhydride, aromatic aldehydes, and ammonium salts or primary amines, [b] isolated yield

In order to explore suitable reaction conditions, one pot multicomponent reaction involving isatoic anhydride, benzaldehyde and NH_4OAc (Table 3, Entry 1) using $NiFe_2O_4$ ferrite was carried out under microwave irradiation for 7 minutes and the corresponding 2,3-dihydroquinazolin-4(1*H*)-one 4a was obtained in high yield (95%). The application of this procedure to a variety of substrates (aldehydes and amines) was investigated (Table 3). The aromatic aldehydes involving both electron-withdrawing and electron-donating groups such as OMe, Cl, Br, and NO_2, and heterocyclic were converted to give the corresponding 2,3-dihydroquinazolin-4(1*H*)-one products **4a to 4p** in good yields. These reactions proceeded smoothly and no undesirable side product was obtained. The experimental procedure is very simple, efficient, convenient, and can be used in the presence of variety of other functional groups. $NiFe_2O_4$ works well even with sensitive aldehydes such as furfural without the formation of any side product (Table 3, Entry 13). The reaction is comparatively faster with aldehydes containing *p*-hydroxy group. It required only 8 min to give excellent yields (Table 3, Entry 3). All the products obtained were characterized by spectroscopic methods such as IR, ^{1}H NMR, ^{13}C NMR and mass spectroscopy and melting points and compared with the reported values.

Table 3. Synthesis of 2,3-dihydroquinazolin-4(1*H*)-ones using $NiFe_2O_4$[a] as catalyst

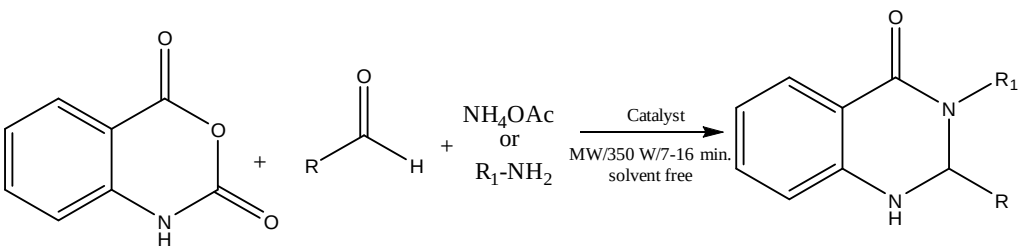

Entry	Product [b]	Substrate / Product		Time (min)	Yield [C] (%)	m.p. (°C)	
		Aldehyde (R)	Amine			Reported	Observed
1	4a	C_6H_5	NH_4OAc	7	95	225 -227	226-227
2	4b	4-OCH_3-C_6H_4	NH_4OAc	14	86	230-233	230-233
3	4c	2-OH-C_6H_4	NH_4OAc	8	94	212-214	212-214
4	4d	3-NO_2-C_6H_4	NH_4OAc	10	92	215-217	215-217
5	4e	4-Cl-C_6H_4	NH_4OAc	12	89	205-207	206-207
6	4f	3,4-OCH_3-C_6H_3	NH_4OAc	14	87	217-220	218-220
7	4g	4-NH_2-C_6H_4	NH_4OAc	15	88	220-221	219-221
8	4h	2-OH,3-OCH_3-C_6H_3	NH_4OAc	10	90	262-263	262-263
9	4i	4-$(CH_3)_2$-N-C_6H_4	NH_4OAc	11	91	206-208	206-208
10	4j	2-OH-Napthyl	NH_4OAc	10	92	222-224	223-224
11	4k	2-OH-5-Br-C_6H_3	NH_4OAc	15	87	233-235	234-235
12	4l	3-Cl-C_6H_4	NH_4OAc	15	89	189-190	189-192
13	4m	2-Furyl	NH_4OAc	9	91	165-167	166-168
14	4n	2-Thiophene	NH_4OAc	14	86	209-212	211-212
15	4o	4-$(CH_3)_2$-CH-C_6H_4	NH_4OAc	15	87	230-233	233-233
16	4p	3,4,5-OCH_3-C_6H_3	NH_4OAc	15	86	263-264	263-265

[a] Reaction conditions: isatoic anhydride, aromatic aldehydes, and ammonium salts or primary amines (1:1:1.5), $NiFe_2O_4$ (10 mol%).
[b]All products are known and were identified by their melting point, IR and ^1H and ^{13}C NMR spectra according to literature, [c] isolated yield.

In the present study, $NiFe_2O_4$ ferrite is used as an efficient catalyst and it's most important advantage is recyclability. The $NiFe_2O_4$ ferrite was magnetically separated from reaction medium and was reused four times (Fig. 5).

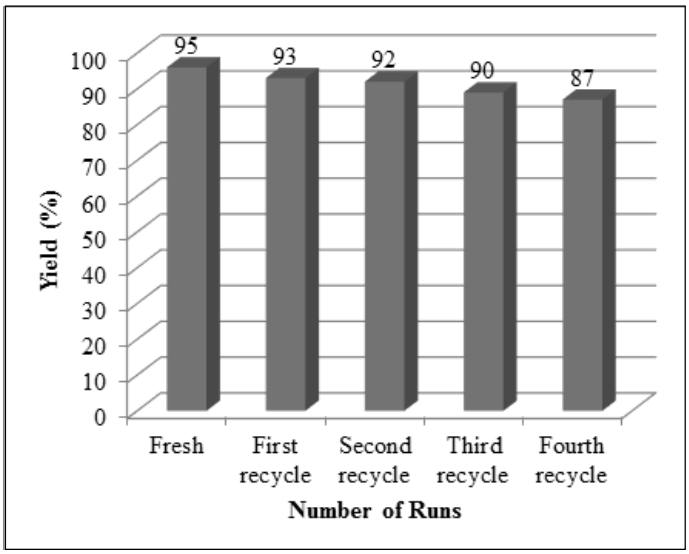

Fig. 5. Recyclability of $NiFe_2O_4$ ferrite

The probable mechanism for the synthesis of 2,3-dihydroquinazolin-4(1*H*)-ones derivatives has been outlined in Scheme 2. 2-amino-*N*-phenylbenzamide was prepared by the reaction of isatoic anhydride with aniline. 2-amino-*N*-phenylbenzamide reacted with benzaldehyde to give the corresponding product **4a** in presence of $NiFe_2O_4$ as catalyst. The reactions of isatoic anhydride with benzaldehyde and benzaldehyde with aniline did not proceed under the same conditions. The isatoic anhydride is first activated by $NiFe_2O_4$ ferrite particles followed by *N*-nucleophilic amine attacks on the carbonyl to form intermediate (**I)**. Then decarboxylation occurs resulting in generation of 2-amino-*N*-substitued benzamide **(II)**. Iron cations act as Lewis acid and increase the electrophilic character of the aldehydes. Subsequently, the reaction of activated aldehyde with **II** proceeds to give intermediate **III** that is converted to product **IV** via an intramolecular cyclization.

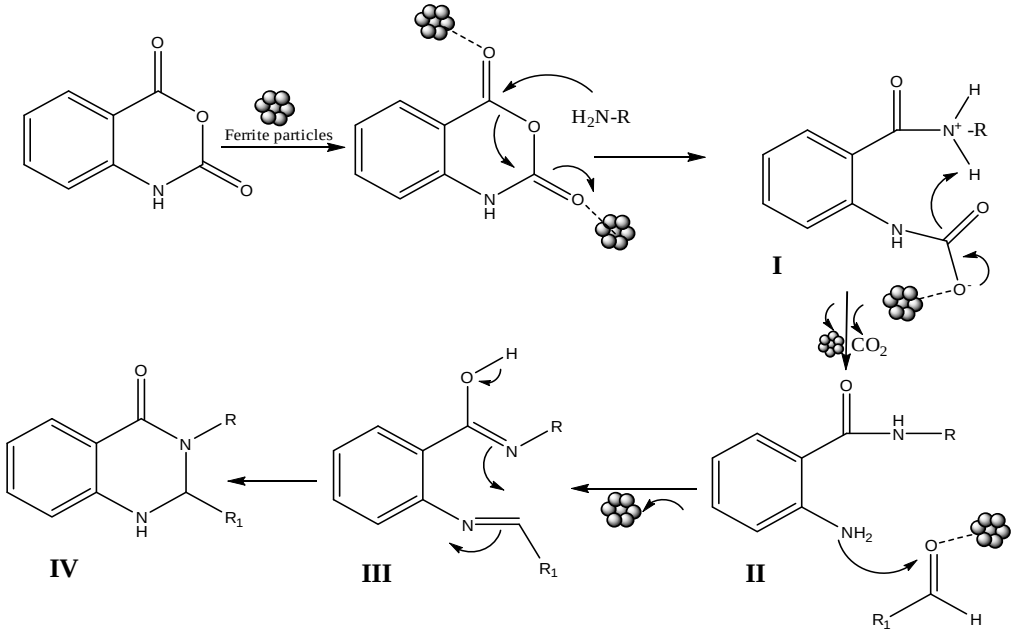

Scheme 2. Proposed mechanism for the synthesis of 2,3-Dihydroquinazolin-4(1*H*)-ones

Conclusions

$NiFe_2O_4$ ferrite nano-catalyst with high surface area has been synthesized by co-precipitation method and has been employed for the synthesis of 2,3-Dihydro-quinazolin-4(1H)-ones derivatives using a microwave reactor under solvent free conditions. By this new method, 2,3-Dihydroquinazolin-4(1*H*)-ones with varied substitution were synthesized. The catalyst was characterized by P-XRD, FTIR, TG/DTA and SEM analysis. The attractive features of this protocol offers several advantages including its greenness with respect to mild reaction conditions, high yields and easy work-up and reusability of catalyst without loss of reactivity.

Acknowledgements

The authors are thankful to 1) Sophisticated Test & Instrumentation Centre, Cochin, Kerala, India for providing Powder XRD, TG-DTA and SEM analysis. 2) Sophisticated Analytical Instrument Facility, Chandigarh, India for providing elemental analysis, IR

and ^{1}H NMR analysis and 3) Sant Gadge Baba Amravati University, Amravati, India for providing laboratory facilities.

References

1. Ikegami S. and Hamamoto, H., 2009, *Chem. Rev.*, **109,** 583.

2. Scheuermann, G.M., Rumi, L., Steurer, P., Bannwarth W. and Mulhaupt, R., 2009, *J. Am. Chem. Soc.*, **131,** 8262.

3. Polshettiwar V. and Varma, R.S., 2010, *Tetrahedron*, **66**, 1091.

4. Domling I. and Ugi., 2000, *Angew. Chem. Int. Ed.*, **39**, 3168.

5. Thirumurugan, P., Nandakumar, A., Muralidharan D. and Perumal, P.T., 2010, *J. Comb. Chem.*, **12**, 161.

6. Martinez, J., Romero-Vega, S., Abeja-Cruz, R., Alvarez-Toledano, C. and Miranda, R., 2013, *Int. J. Mol. Sci.*, **14**, 2903.

7. Dioos, B.M.L., Vankelecom I.F.J. and Jacobs, P.A., 2006, *Adv. Synth. Catal*., **348**, 1413.

8. Polshettiwar V. and Varma, R.S., 2010, *Green Chem.*, **12**, 743.

9. Astruc, D., Lu F. and Aranzaes, J.R., 2005, *Angew. Chem. Int. Ed.*, **44**, 7852.

10. Roshmi, A., Ashish, K., Gill N.S. and Rana, A.C., 2011, *Int. Res. J. Pharm.*, **2(12)**, 22.

11. Hour, M., Huang, L., Kuo, S., Xia, Y., Bastow, K., Nakanishi, Y., Hamel E. and Lee, K., 2000, *J. Med. Chem.*, **43**, 4479.

12. Kouji, H., Yoshiyuki, K., Hirofumi, Y., Junya, I., Kazunori, K., Kenji, M., Mitsuru, O., Takayoshi, K., Akinori, I., Kayoko, M., Syunji, Y., Nobuya, M., Yoshinori T. and Hiroshi, M., 2004, *J. Med. Chem.*, **47**, 4151.

13. Ouyang, G., Zhang, P., Xu, G., Song, B., Yang, S., Jin, L., Xue, W., Hu, D., Lu P. and Chen, Z., 2006, *Molecules*, **11**, 383.

14. Hour, M., Huang, L., Kuo, S., Xia, Y., Bastow, K., Nakanishi, Y., Hamel E. and Lee, K., 2000, *J. Med. Chem.*, **43(23)**, 4487.

15. Lopez, S.E., Rosales, M.E., Urdaneta, N., Godoy, M.V. and Charris, J.E., 2000, *J. Chem. Res.*, **6**, 258.

16. Connolly, D.J., Cusack, D., Osullivan T.P. and Guiry, P.J., 2006, *Tetrahedron*, **61(43)**, 10153.

17. Hour, M.J., Kuo, S.C., Xia, Y., Bastow, K., Nakanishi, Y., Hamel E. and Lee, K.H., 2000, *J. Med. Chem.*, **43**, 4489.

18. White, D.C., Greenwood, T.D., Downey, A.L., Bloomquist J.R. and Wolfe, J.F., 2004, *Bioorg. Med. Chem.*, **12**, 5711.

19. Cheng, X., Vellalath, S., Goddard R. and List, B., 2008, *J. Am. Chem. Soc.*, **130**, 15786.

20. Chinigo, G.M., Paige, M., Grindrod, S., Hamel, E., Dakshanamurthy, S., Chruszcz, M., Minor W. and Brown, M.L., 2008, *J. Med. Chem*., **51**, 4620.

21. Dindulkar, S.D., Oh, J., Arole, V.M., Jeong Y.T. and Chimie, C.R., 2014, **17(10)**, 971.

22. Takacs, A., Fodor, A., Nemeth J. and Hell, Z., 2014, *Synth. Comm*., **44(15)**, 2269.

23. Shaterian H.R. and Rig, F., 2015, *Research on Chemical Intermediates*, **41(2)**, 721.

24. Shaterian, H.R., Fahimi N. and Azizi, K., 2014, *Research on Chemical Intermediates*, **40(5)**, 1879.

25. Ghashang, M., 2012, *Oriental Journal of Chemistry*, **28(3)**, 1213.

26. Song, Z., Liu, L., Wang Y. and Sun, X., 2012, *Research on Chemical Intermediates*, **38(3-5)**, 1091.

27. Niknam, K., Jafarpour N. and Niknam, E., 2011, *Chin. Chem. Lett*., **22(1)**, 69.

28. Salehi, P., Dabiri, M., Baghbanzadeh M. and Bahramnejad, M., 2006, *Synth. Comm.*, **36(16)**, 2287.

29. Chen, J., Wu, D., He, F., Liu, M., Wu, H., Ding J. and Su, W., 2008, *Tetrahedron Lett*., **49(23)**, 3814.

30. Ladole, C.A., Salunkhe N.G. and Aswar, A.S., 2016, *J. Indian Chem. Soc.*, **93,** 1.

31. Zhang, Z.H., Lu, H.Y., Yang S.H. and Gao, J.W., 2010, *J. Comb. Chem.*, **12**, 643.

32. Shaterian H.R. and Rig, F., 2014, *Research on Chemical Intermediates*, **40(8)**, 2983.

33. Narasimhulu M. and Lee, Y.R., 2011, *Tetrahedron*, **67(49)**, 9627.

34. Darvatkar, N.B., Bhilare, S.V., Deorukhkar, A.R., Raut D.G. and Salunkhe, M.M., 2010, *Green Chem. Lett. Rev.*, **3(4)**, 301.

35. Toosi F.S. and Khakzadi, M., 2015, *Res. Chem. Intermed.*, **41(1)**, 311.

RNI No. MAHENG/2017/74063
ISSN No. (Print) 2581-5911
ISI Impact Factor 1.022 (2019-2020)

Analytical Method Development and Validation of Saroglitazar by RP-HPLC

Snehal P. Shingade*, Rajendra B. Kakde and Akansha B. Nagdeve
Department of Pharmaceutical Sciences, RTMNU, Nagpur, India
Email: snehal9177@rediffmail.com

Abstract
The present paper describes the development of a validated RP-HPLC method for the determination of Saroglitazar in presence of its degradation products or other pharmaceutical excipients. Stress studies were performed and it was found that it degrades in acidic and alkaline conditions. The separation was carried out at 40°C on a Princeton C18 (5 µg, 250×4.6 mm) column with 30mM Ammonium acetate: Acetonitrile (40:60 %v/v) as a mobile phase at a flow rate of 0.5mL min^{-1}. The wavelength of detection was 294 nm. The retention time of nearly 9.5 minutes was obtained. Analytical validation parameters such as specificity and selectivity, linearity, accuracy and precision were evaluated. The calibration curve was linear in the range of 2–20 µg/mL with a correlation co-efficient 0.9994. Relative standard deviation values for all key parameters, were less than 2.0%. The method was validated according to ICH guidelines and the acceptance criteria for accuracy, precision, linearity, specificity and system suitability were met in all cases.

Keywords: *Saroglitazar, RP-HPLC, Analysis, Validation.*

Introduction

Saroglitazar (trade name "Lipaglyn") is a drug used for the treatment of Type 2 diabetes mellitus and dyslipidemia. Chemically it is (2*S*)-2-Ethoxy-3-[4-(2-{2-methyl-5- [4-(methyl sulfanyl) phenyl] -1*H*-pyrrol-1-yl} ethoxy) phenyl] propanoic acid. The drug was approved for use in India by the Drug Controller General of India. Saroglitazar is used for the treatment of diabetic dyslipidemia and hypertrigly ceridemia with Type 2 diabetes mellitus not controlled by statin therapy. It is commercially available in tablet dosage form as "Lipaglyn" in India. Literature survey revealed that few analytical methods like stability indicating RP- HPLC method for the estimation of Saroglitazar in bulk and pharmaceutical dosage forms[1-5], UV spectrophotometric method [6] for estimation of Saroglitazar in bulk and tablet dosage form, Liquid chromatography/mass spectrometry (LC/MS)[7] method have been reported for the determination of Saroglitazar in human plasma. The present work describes an impurity profiling method for the determination of Saroglitazar in tablets using reverse phase HPLC. The proposed method was found to be suitable for routine determination of the drug in pharmaceutical formulations.

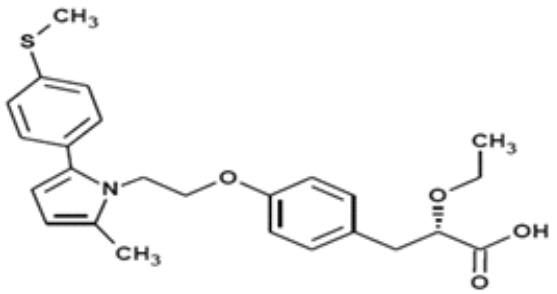

Fig.1. Chemical structure of Saroglitazar

Materials and Methods

Chemicals

A standard bulk drug sample of Saroglitazar was provided by Zydus Cadila Ahmedabad, India. Pharmaceutical dosage form used in this study was "**LIPAGLYN"** tablets labeled to contain 4 mg of the drug (Zydus Cadila, Ahmadabad, India). Acetonitrile (Merck), Methanol (Merck) and HPLC grade water (Merck) and Ammonium Acetate of HPLC grade were used. Hydrochloric acid, Sodium Hydroxide and Hydrogen peroxide of Analytical Reagent Grade (Loba Chemie Pvt. Ltd. Mumbai, India) were used for the study. The solvents were further filtered through nylon membrane filter (0.22µ) and vacuum degassed. The 0.22 µ nylon filter paper was purchased from Pall India Pvt. Ltd, Mumbai (India). All the glassware used during experimentation were of Analytical Grade-I.

Apparatus and chromatographic conditions

HPLC method development and validation was done on a Shimadzu (Japan) Liquid chromatograph equipped with (LC-20 AD pump), SPDM-20A prominence PDA detector, Rheodyne 7725i injection with 20µl loop and LC-Solutions software. Stationary phase used was Symmetry® C-18 5ìg Column (4.6 mm × 250mm) and the mobile phase used was 30mM Ammonium Acetate: ACN (40:60v/v). The mobile phase was filtered using 0.22 µ nylon filter paper purchased from Pall India Pvt. Ltd, Mumbai, India. The mobile phase flow rate was 0.5 mL min^{-1} and the injected volume was 20µL.

HPLC Method

Preparation of standard solution

Standard stock solution of Saroglitazar (100 µg mL^{-1}) was prepared in Acetonitrile and Water in the ratio of 6:4.

Preparation of Calibration graph

The stock solution was diluted with mobile phase to get a series of concentration ranging from 2-20 µg mL^{-1}. The chromatographic conditions were set as per the optimized parameters indicated and the mobile phase was allowed to equilibrate with stationary phase to get the steady baseline. Standard solutions of different concen-trations were injected separately and the chromatograms were recorded. A graph was plotted of peak area vs. concentration of drug (µg mL^{-1}).

Preparation of sample solution

Twenty tablets were weighed and the average weight was calculated. A quantity equivalent to 10 mg of Saroglitazar was transferred into a 10 mL volumetric flask, 4 mL water was added and then sonicated for a minimum period of 30 min. with intermittent shaking. Then the contents was brought back to ambient temperature and diluted to volume with water. The sample was filtered through 0.45 µ nylon syringe filter. 100 µL of this solution was pipetted out and diluted to 10 mL using diluents to obtain concentration 10 µg mL^{-1} of Saroglitazar (10 ppm).

Validation

The developed method was validated according to ICH guidelines. The linearity was evaluated by linear regression analysis. The calibration graph was plotted for the HPLC method (2-20 µg mL^{-1}).

Precision studies were done in terms of repeatability (intra-day precision) and intermediate (inter-day precision) and was expressed as relative standard deviation (RSD) of a series of measurements. Intra-day precision was calculated from six replicate readings at 3 concentration levels within the linearity range. Inter - day precision was studied by comparing the results on three different days.

To study the accuracy of the method, recovery studies were carried out by addition of standard drug solution to the pre-analyzed sample at 3 different levels i.e. 80, 100 and 120%. The resultant solutions were then

reanalyzed by the proposed method.

LOD and LOQ was calculated using single-to-noise (S/N) ratio method. LOD was taken as a concentration of analyte where S/N is 3 and LOQ was taken at a concentration of analyte where S/N is 10.

Robustness was evaluated by studying the influence of small deliberate changes in the analytical parameters on the retention times and peak shapes. The method should be robust enough with respect to all critical parameters so as to allow routine laboratory use. The specificity of the method towards the drug was studied by determination of purity for drug peak in a mixture of stress samples using a UV detector.

Degradation Studies

Acidic conditions

The solution was prepared by dissolving the drug substance in water and the drug was subjected to accelerated degradation under acidic condition by refluxing with 0.5 N HCl at 70°C for 2 hrs and the sampling was done at intervals of five minutes till sufficient degradation was achieved. The resulting solution was neutralized, appropriately diluted and the chromatograms were recorded.

Alkaline conditions

The drug substance was dissolved in water and the drug was subjected to accelerated degradation under alkaline condition by refluxing with 1N NaOH at 70° C for 4 hrs and the sampling was done at intervals of five minutes till sufficient degradation was achieved. The resulting solution was neutralized, appropriately diluted and the chromatograms were recorded.

Neutral condition

For forced degradation study in neutral conditions, the drug was dissolved in water and heated at 70°C. The samples were withdrawn at appropriate time intervals and subjected to HPLC analysis after suitable dilution.

Oxidative studies

Oxidation studies were performed in 10% H_2O_2 at room temperature for 24 hrs. The resultant solution was appropriately diluted and the chromatograms were recorded.

Photolytic studies

For photolytic stress studies, the samples of the drug and drug product were exposed to sunlight during daytime for 3 days. Samples were withdrawn at appropriate time intervals and subjected to HPLC analysis after suitable dilution. Appropriate controls were also prepared and injected for each degradation study.

Results and Discussion

For RP-HPLC studies, chromatographic conditions were optimized to get best resolution and peak shape. The selection of mobile phase was based on the peak parameters i.e. symmetry, theoretical plates and capacity factor, ease of preparation and cost. Symmetrical peaks with good separation (retention time for Saroglitazar was 9.50 ± 0.05 min.) was obtained with C18 column and the mobile phase consisting of Acetonitrile: 30mM Ammonium Acetate (60:40 v/v) was used at flow rate of 0.5 mL min^{-1}. A typical chromatogram obtained for the analysis of drugs using the developed method is shown in Fig. 2.

The optimum wave length for detection and quantification was 294 nm, at which good detector response for both drugs were obtained. There was no interference from the diluents and excipients present in the pharmaceutical formulation.

To check linearity, the standard calibration curve for the drug was constructed by plotting ratios of standard drug peak area to internal standard peak area vs. concentration of standard solutions and the curve showed good linearity

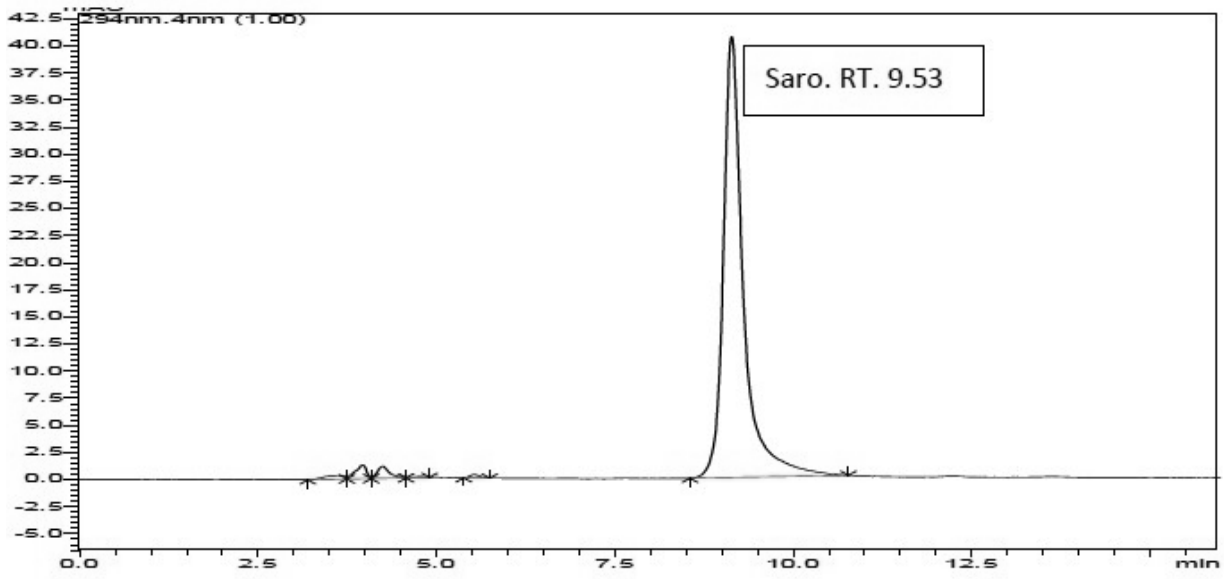

Fig.2: Chromatogram of Saroglitazar

over a concentration range of 2-20 μg mL^{-1}. The regression equations for the drugs were found by plotting peak area vs. concentration μg mL^{-1}. Table 1 summarizes the linearity range and the linear regression equation for the drug.

The LOD and LOQ values of Saroglitazar were found to be 0.3559 μg mL^{-1} and 1.0786 μg mL^{-1} respectively. The precision of the method was determined by repeatability (intra-day) and intermediate precision (inter-day).

Table 1: Linearity range and the linear regression equation for the drug.

Parameter	**Saroglitazar**
Linear Dynamic range (μg/mL)	2-20 μg/mL
Slope	80579
Intercept	12356
Correlation Coefficient	0.9994
LOD (μg/mL)	0.3559
LOQ (μg/mL)	1.0786

The precision was expressed as the RSD of the results. The values obtained for the precision studies, presented in Table 2, indicate good repeatability and low inter-day variability.

Table 2: Precision Studies

Sr. No.	Observation	% Labelled claim		
		Intra-day	Inter-day	Different Analyst
1.	I	99.69	99.64	100.06
2.	II	99.85	99.91	99.84
3.	III	100.50	99.98	100.01
Mean		100.13	99.81	99.98
SD		0.4289	0.1700	0.1153
%RSD		0.4289	0.1703	0.1153

The robustness of the proposed method was evaluated by slight modification in the organic composition of mobile phase and flow rate. During these studies, it was found that there was not much change in retention time, area and symmetry of peak.

The recovery results in the range 98-99% show the accuracy of the method (Table 3).

Table 3: Recovery studies

Accuracy Level (%)	% Recovery*
80%	98.13
100%	99.19
120%	99.83
Mean	99.05
±SD	0.8586
%RSD	0.8668

***** Mean of three reading

Degradation Studies

HPLC studies of samples obtained on stress testing of Saroglitazar under different conditions using 30mM Ammonium Acetate : ACN (40:60v/v) as mobile solvent system suggested the following degradation behavior:

Forced degradation studies

Acidic conditions

The drug was subjected to 0.5 N HCl for 2 hrs at 70°C and formed degradation products at retention time 4.3 min (Fig. 3a). The rate of hydrolysis in acid was faster as compared to that in alkali or water.

Alkaline conditions

The drug was subjected to 1 N NaOH for 4 hrs at 70°C (Fig. 3b).

Neutral Condition

In neutral condition, significant degradation of the drug was achieved after heating the drug at 70°C for 24 hrs (Fig. 3c).

Oxidative studies

In oxidative condition, significant degradation of the drug was obtained after exposure to 10 % H_2O_2 for 24 hrs (Fig. 3d).

Photolytic studies

Sufficient degradation was achieved by exposing the drug product to sunlight during day time for 3. Days (Fig. 3e).

In forced degradation studies, the molecular weight of Saroglitazar was found to be 325 in acidic medium and 387 in basic medium. It was thus confirmed that the drug was degraded and the fragmentation pattern was predicted by the fragments obtained in ESI-LC/MS/MS study of Saroglitazar and forced degradation samples (acidic, basic and oxidation).

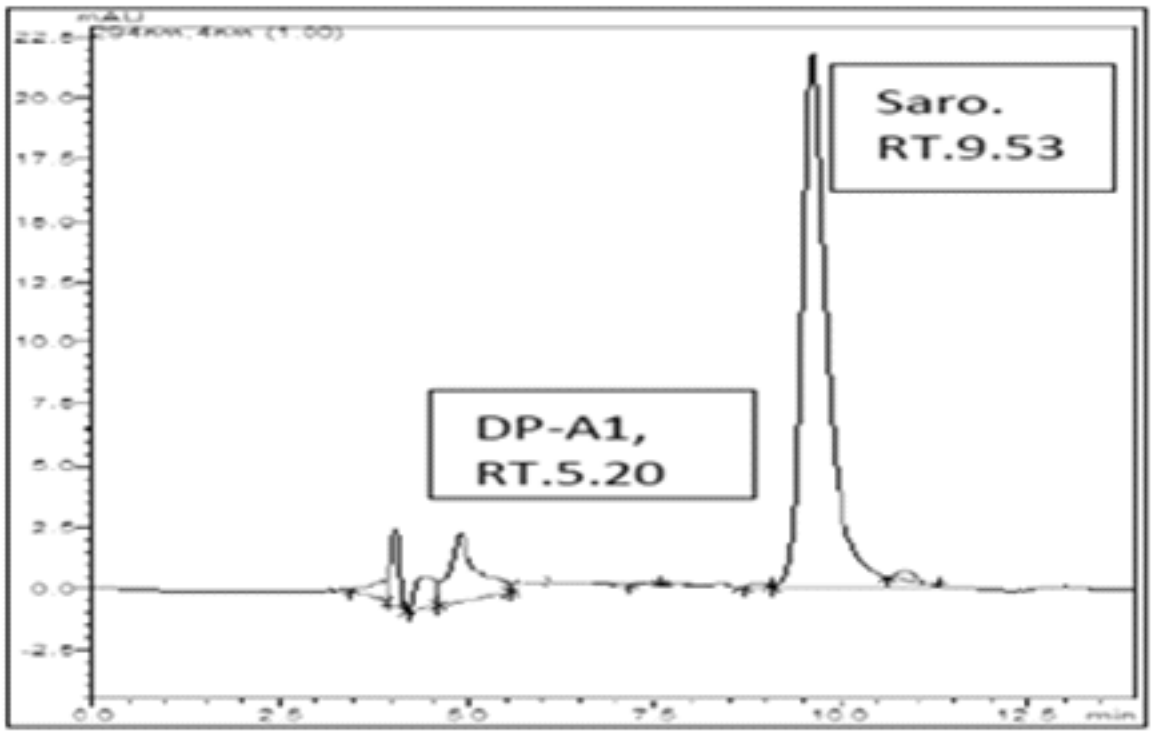

Fig 3a. Chromatogram of sample degraded in 0.5N Hydrochloric acid

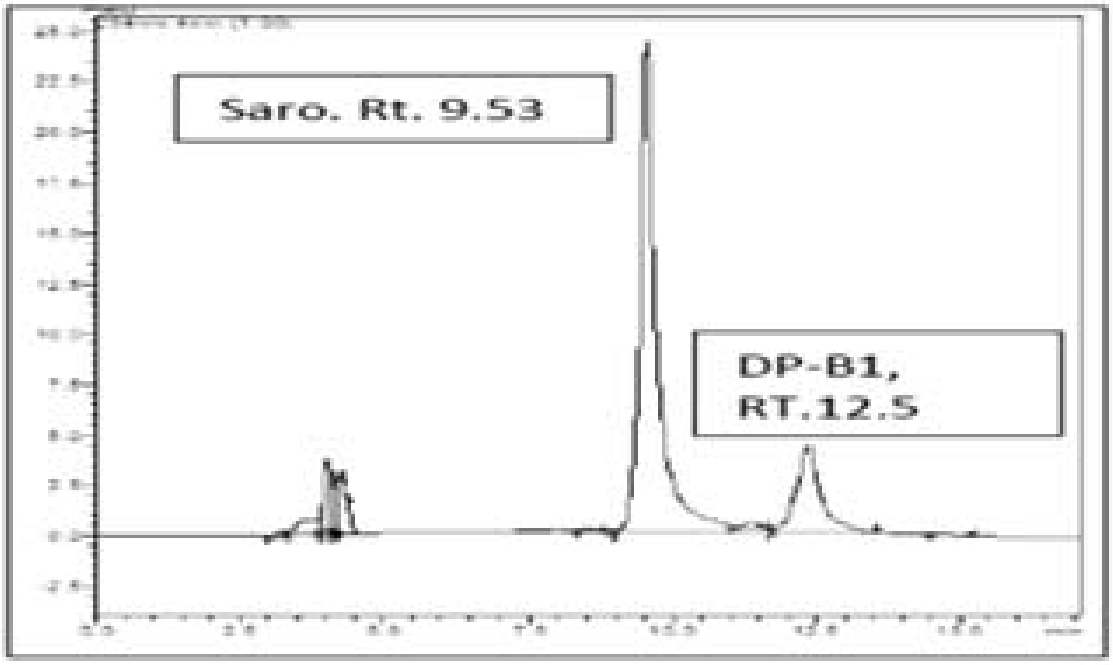

Fig 3b. Chromatogram of sample degraded in 1 N Sodium Hydroxide

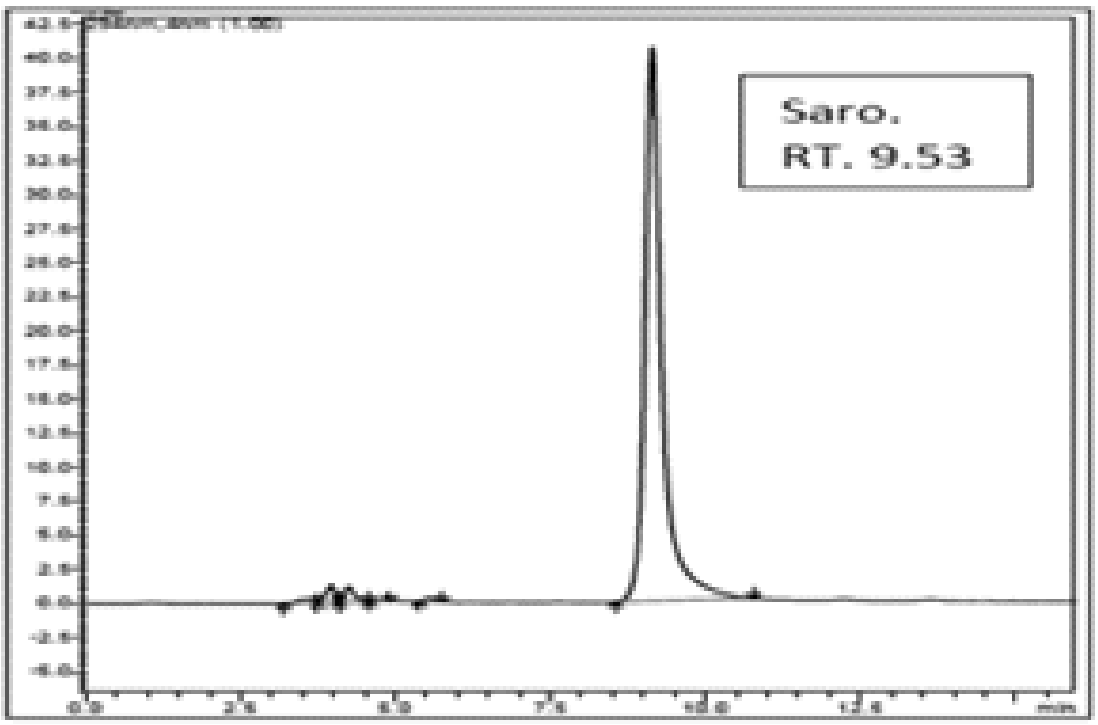

Fig 3c. Chromatogram of sample subjected to Neutral degradation

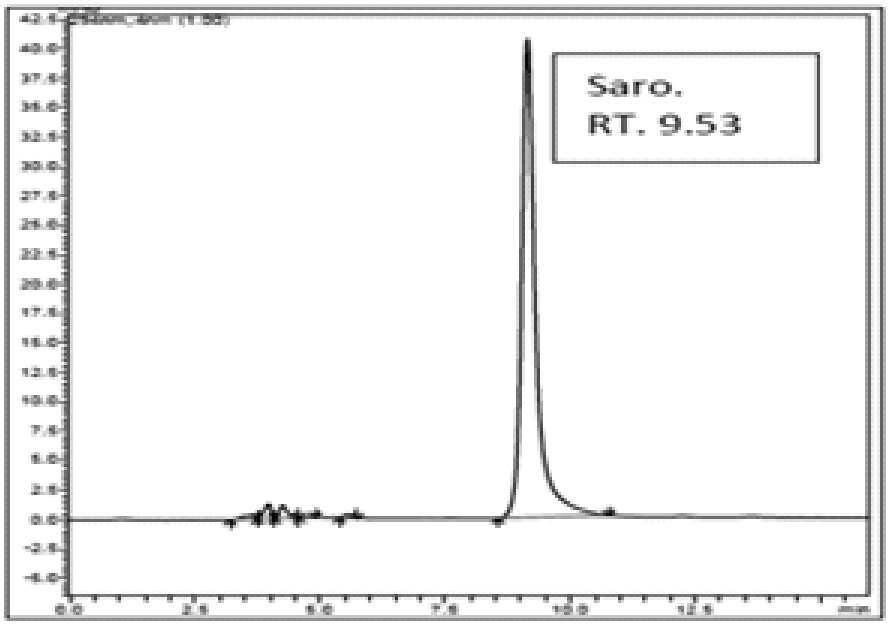

Fig 3d. Chromatogram of sample subjected to Oxidative degradation

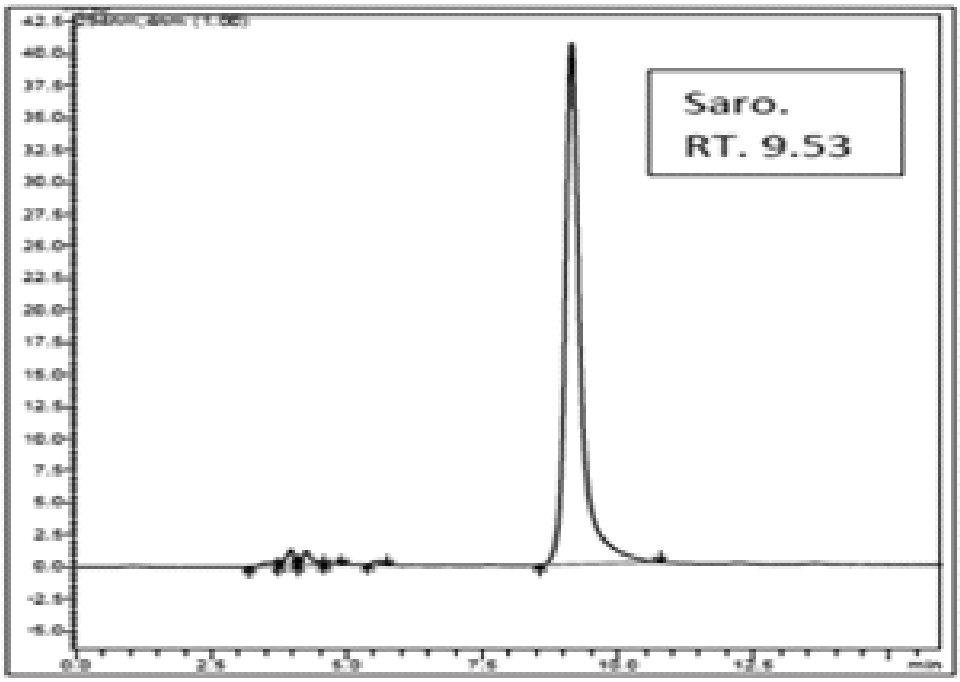

Fig 3e. Chromatogram of sample subjected to Photolytic degradation

Table 4: Forced Degradation and Stability assay

Condition	% Assay
Normal	99.89
Acid	85.56
Base	80.12
Oxidation	99.15
Heat	99.52
Photolytic	98.87

The developed method was used for the assay of commercially available tablets and six replicate determinations were performed. Experimental values obtained for the determination of tablets are given in Table 5. The interference of excipients was studied by comparing the chromatograms of standards and formulations. Similar shapes and retention times of peaks showed that there was no interference from the excipients.

Table 5: Analysis of formulation assay

Sr. No.	Wt. of Sample (mg)	% Assay
1.	323.122	99.43
2.	322.124	99.85
3.	3232.101	99.62
4.	323.051	99.63
5.	323.108	99.68
6.	323.123	99.62
Mean		**99.63**
±SD		**0.1346**
%RSD		**0.1351**

The system suitability test of the chromatographic system was performed before each run. Six replicate injections of standards were done and peak asymmetry, theoretical plate number and RSD of peak areas were determined. For all system suitability tests, performed, asymmetry was < 1.5, theoretical plate number was > 5000 and RSD of peak areas was < 1%.

Conclusions

A simple, accurate, precise and economical method was developed for analysis of Saroglitazar. The method was validated according to ICH R2 guidelines. In Impurity Profiling study, drug was forcefully degraded in acidic medium (0.5 N HCl, 2hr reflux), basic medium (1N NaOH, 4hrs reflux) and oxidation mode (10%) at room temperature for 24 hrs. In oxidation, neutral and thermal conditions, the drug was found to be stable.

Acknowledgement

The authors extend their sincere thanks to Zydus Cadila Ahmadabad, India for providing gift samples of Saroglitazar.

References

1. Kealey, D. and Haines, J.P., 2002, UK, Analytical Chemistry, BIOS Scientific Publishers Limited, p.1-2.

2. Srinivasan, N., 1979, Chemical Testing and Analytical Chemistry, Department of Industries and Commerce, Government of Tamilnadu, Chennai, p.55.

3. Skoog, D.A. and West, D.M., 1980, Principles of Instrumental Analysis. 2nd edition, Holt Saunders Golden Sunburst Series, p.667.

4. Pavia, D.L., Lampman, G.M. and Kriz, G.S., 2006, Introduction to Spectroscopy, 3rd ed., Harcourt College Publishers, p.353.

5. Jeffery, G.H., Besset, J., Mendham, J. and Denney, R.C., 1989, Vogel's Text Book of Quantitative Chemical Analysis, 5th ed. English Language Society/Longman, p.216.

6. Beckett, H. and Stenlake, J.B., 1997, Practical Pharmaceutical Chemistry, 4th ed., Part II, CBS Publisher and Distributor, New Delhi, p.277.

7. Prathap, B., Dey A., Rao, G.S., Sundarrajan, T. and Hussain, S., A Review on Impurity Profile in Pharmaceutical Substances, *Journal of Pharmacy and Pharmaceutical Sciences*.

8. ICH Q1A (R2), 2003, Stability Testing of Drug Substances and Products, International Conference of Harmonization, IFPMA, Geneva.

9. ICH, Q2 (R1), 2005, Validation of Analytical Procedures: Text and Methodology, Proceedings of the International Conference on Harmonization, IFPMA, Geneva.

10. Snyder, R.L., 1997, Practical HPLC Method Development, 2nd edition, p.292.

RNI No. MAHENG/2017/74063
ISSN No. (Print) 2581-5911
ISI Impact Factor 1.022 (2019-2020)

Natural Product based Alkyd Resin for Water Thinnable Coatings

Bharati C. Burande[1] and Pravin A. Dhakite[2]
[1]Department of Chemistry, Priyadarshini Indira Gandhi College of Engineering, Nagpur, India
[2]S.N. Mor Arts, Commerce and Smt. G.D. Saraf Science College, Tumsar, Dist. Bhandara, India
Email: bharati.pigce@gmail.com

Abstract
The interest in the improvement of waterborne paints has lately increased due to the toxicological effect of certain ingredients of paint on human health, environment and the escalation in prices of petroleum based raw materials. Alkyd resin is one of the most common types of binders in the paint and coating industry, prepared from reagents such as petroleum products, phthalic anhydrides and organic solvents. However, the excessive use of these reagents harms the environment. Therefore, the concerned industries are trying to replaces these hazardous chemicals with alternative resources which are of vegetative nature. In the present paper, we have reported the use of vegetable oils, herbs, plant extracts as alternative substitutes for petroleum products. The main intention of using these substitutes in the synthesis of products is because they are primarily nonhazardous and degradable in nature. We have prepared alkyd resin with less than 15% of petroleum ingredients and 80-90% renewable plant products like castor oil, rosin, etc. It has been thoroughly analyzed for its physicochemical and spectroscopic properties. Alkyd resin with desirable properties has further been used for the formulation of water thinnable paints. In the composition of paints, we have successfully replaced maximum amount of organic solvents with water without sacrificing the technical performance of the final products. All paint samples have been analysed for their physicochemical and film properties. Further, the properties of these samples have been compared with the commercial samples and shows good to excellent results. Our main focus was on the use of less amounts of organic solvents and petroleum based raw materials. The present research on water thinnable paints is technically sound, economic and environment friendly with more emphasis on low volatile organic compounds (VOCs) emission.

Keywords: *Alkyd resin, Castor oil, Rosin, volatile organic compounds, water thinnable paints*

Introduction

Paint, surfactant, ink and germicide industries depend mainly on petroleum products. A large number of petroleum products are used as solvents in these industries. The excessive use of these solvents creates a global pressure on extraction and prices of petroleum products. It also causes several environmental problems. Recent development shows that the plant products and extracts are suitable alternatives for petroleum products[1]. In India, we have very vast renewable sources of vegetative nature such as oilseeds, herbs, plant extracts, etc. We can use these raw materials as substitutes for vinyl and other petroleum products[2].

Keeping all these aspects in mind, we have developed alkyd resin using castor oil and resin as raw materials. Alkyd resin is a short length polymer which is the base for useable products such as paints[3], detergents[4] and surfactants[4].

Castor oil[5,6] is a triglyceride of fatty acids, containing 87-90% Ricinoleic acid, cis-12 hydroxyoctadec-9-enoic acid ($C_{18}H_{34}O_3$), derived from the beans of castor plant, *Ricinus Communis L.* of the family *Eurphorbiaceae*. The chemical structure of castor oil is

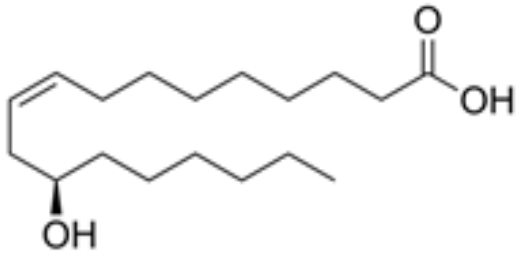

Castor is found widely in tropical and semi tropical countries, either wild or cultivated. It is non edible oil and has enormous applications in industries. It is well documented that reaction of castor oil with maleic anhydride and monobasic alcohol gives a configuration suggesting a new type of alkyd with alcohol coupled to the acid chain through maleic acid. This resin composition acts as an excellent softener in lacquer varnishes[7].

Rosin[8] is the residue obtained from the distillation of pine exudate. Rosin acids are monocarboxylic acids having molecular formula $C_{20}H_{30}O_2$. The residue contains 90% rosin acid and remaining are esters, aldehyde and alcohol.

Rosin is a monobasic acid which controls the polymerisation reaction as a chain stopper. It has a natural tendency of forming an excellent emulsion for development of water based compositions. It is also abundantly available and widely used in a large number of industrial products like paints, detergents, cosmetics and pharmaceuticals. Alkyds obtained from Rosin have good water. Rosin and its derivatives[9] have some inherent properties such as excellent film forming property, ability to form moisture protective films, resistance to acids, excellent binding ability, non conductor of electricity, etc. The chemical structures of a typical rosin is:

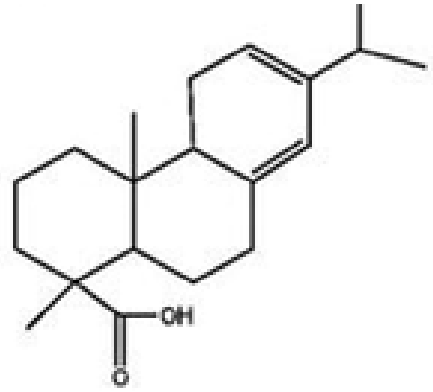

Special alkyds based on castor oil, rosin, maleic anhydride, phthalic anhydride, pentaerythritol and sorbitol have been developed by Gogte and Agrawal[10]. The paints and primers based on these special alkyds have excellent resistance to water, xylene and mineral turpentine.

Alkyd Resin

Alkyd resin[11] is a polyester of polyhydroxyl alcohols and polycarboxyl acidsn chemically combined with the acids of various drying, semidrying, non drying oils in different proportions. All these alkydss possess most of the desirable properties which are required for protective coatings. They are ideal riders for pigmented coatings because they have good wetting and dispersing properties. The coatings prepared from alkyd resins are comparatively low in cost, have excellent properties such as durability, flexibility, toughness, gloss retention and color retention. They also act as good solvents and exhibit remarkable heat resistance property.

Water Thinnable Coatings

Although, the coating thinned with organic solvents gives desirable results, it later poses some serious problems, viz.

(a) solvents are volatile, may easily catches fire,
(b) they are toxic and lead to atmospheric pollution,
(c) they are expensive,
(d) they do not form part of the final film.

These problems are overcome when paints are thinned using water[12,13].

In the context of the growing emphasis on preservation of petrochemical substances, water soluble binders play an important role in the surface coating industry[14]. Current research is mainly focused on synthesis and characterization of alkyd resins (Polymer) using various types of polybasic acids, polyhydric alcohols and fatty acids and their application in water thinnable paints.

Materials and Methods

Synthesis of Alkyd Resins (Polymers)

Synthesis of alkyd resin based on compositions like castor oil, rosin, glycerol, Pentaerythritol, sorbitol, maleic anhydride, phthalic anhydride and benzoic acid were carried out in a glass reactor.

Four different compositions (Table I) were prepared by batch process and the addition of ingredients. The reaction and temperatures used are detailed below in three steps:

First Step: The castor oil along with rosin, maleic anhydride, glycerol and catalyst were heated for nearly 2 hours at 160^{0}C to 275^{0}C. In this step, dehydration of castor oil takes place. Herein, we have used some portion of maleic anhydride (approximately 50% of actual requirement) and the remaining was used at a later stage.

Second Step: Pentaerythritol was added at a slightly higher temperature (200^{0}C to 260^{0}C) and then the mixture was heated for 4 to 5 hours. In this stage, OH groups of pentaerythritol react with acidic groups of rosin and maleic anhydride. This process permits bodying and polymerization of oil.

If sorbitol is used as an ingredient, then it is added at a lower temperature (100-110^{0}C) and the heating is continued for 4 to 5 hours.

Third Step: The remaining maleic anhydride, phthalic anhydride, benzoic acid and 5% solvent was added and reaction was continued for 4 to 6 hours so that acids can react with OH group of pentaerythritol or glycerol. This step was carried out to get polymerization reaction in a controlled manner.

The presence of maleic adducts and rosin esters are expected to make the reaction product more viscous and give exceptional durability. The main chemical reaction involved in the formation of alkyd resin is the polymerization of monoglyceride of castor oil with phthalic and maleic anhydrides, as shown below:

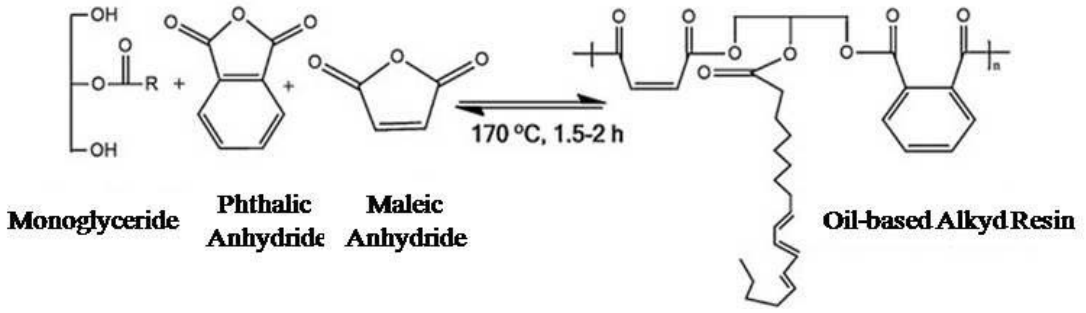

The extent of the reaction was determined by checking the acid value and viscosity periodically. After attaining the desired acid value, the sample was cooled to 80^0C. At this temperature, the sample was thinned with solvent, filtered and stored in an air tight container. The results of the analysis are tabulated in Table II.

The requisite parameters of alkyd resin such as acid value[15], iodine value[16], peroxide value[17] and hydroxide value[18] were obtained by physicochemical analysis.

Preparation of Water Thinnable paints from Alkyd Resin

The water thinnable paint was prepared in a laboratory pot mill of 10 dm^3 capacity. First the pot mill was charged with pigment (TiO_2, ZnO), extender (polyvinyl alcohol), binder (alkyd resin) and solvent (xylene, turpentine and butanol). A thick paste of the mixture was maintained in the ball mill. 50% volume of the ball mill was occupied by steel balls of 1.27cm (1/2") diameter. The ball mill was run for 8 hours and then the paint was tested for fineness of grind. The expected thickness should be 1-2 micrometer for final application. The grinding was continued to get the desirable thickness. The sample was removed from the mill. Additional alkyd resin was added and the viscosity was adjusted by adding solvent. The sample was filtered through wire mesh and stored in airtight containers.

The prepared paints were studied for physicochemical properties like viscosity[19], density[20], volatile content[21] and solid content [22]. The film properties, hiding power[23], drying time[24], finish (gloss)[25], scratch hardness[26], adhesion[27] and rub resistance test[28] were determined. Further, resistive tendencies of the paint films to water, seawater, chemicals, detergent[29,30] and various solvents[31] have been tested.

Results and Discussion

Alkyd Resins

(a) The prepared alkyd resin contained 35-39% of castor oil and 37-40% of rosin.

(b) In conventional short oil alkyd, a high percentage of anhydrides is used (40-50%). These anhydrides are mainly based on petroleum based products. In our product, only 6-15% of phthalic anhydride has been used. Hence, we have successfully reduced the petroleum based phthalic anhydride by 75% and substituted it with renewable rosin without affecting the performance characteristics.

(c) Dehydration of Castor Oil (DCO) with very high quantity of anhydride is risky and sometimes goes out of control. We have easily controlled the reaction by using rosin, smaller quantity of anhydride and chain stopper benzoic acid. It was observed that benzoic acid effectively regulates the polymerization.

(d) In the final best formulation **A4**, the quantity of polyol was 10% (including pentaerythritol 4% and glycerol 6%), which is less than in the conventional resins (15-20%). Moreover, pentaerythritol is very expensive. Therefore, the use of smaller quantity of pentaerythritol is cost effective.

(e) The catalysts, sodium bisulphate (1.5%) and sodium bisulphate (0.5%) gave better performance characteristics. The proportion of catalysts has been fixed by repeated experimentation and analysis of products. With these proportions of catalysts, the yield of resin is 94 to 95%.

(f) In commercial practices, 16-20 hours are required for the synthesis of a short oil alkyd. In our case, the reaction time was found to be 12-13 hours.

(g) IR spectra of alkyd resin indicate the presence of carboxylic group, OH group, aliphatic group and aromatic ring in the structure of polymer. UV spectrum of alkyd resin shows the presence of conjugated double bond, aromatic or heteroaromatic system. NMR predicts the presence of aromatic protons, aliphatic protons and hydroxyl proton.

Analysis of Alkyd Resins

The analysis of alkyd resin is shown in Table II. It is

observed that the prepared resin with a lower acid number is not very suitable for conversion into water thinnable coatings. For getting water thinnable compositions, the acid value should be slightly higher than 30. Therefore, we have designed our formulation in such a way so as to get acid value around 30 in the final product **(A4)**. The higher acid value products are soluble in water by reaction with ammonia.

Thus, in our formulation the acid values are on higher side i.e. 10 to 38. The iodine value of the samples indicate dehydration of castor oil. The peroxide value is very low indicating that all available peroxide groups have been utilized in oxidative polymerisation reaction. The higher hydroxide value (77 to 120) ensures excellent adhesive nature of the samples.

Water Thinnable Paints

Several formulations of water thinnable paints based on alkyd resin **(A4)** have been studied. Few remarkable properties of the water thinnable paints are listed below:

(a) Paints based on combination of alkyd resin and polyvinyl alcohol have been formulated successfully. The resin content in paints is in the range 12-20%.

(b) The useful pigment binder ratio for paints is 1.25 to 3.12. Thus, the prepared alkyd resin can be used over a range of pigment binder ratio.

(c) The incorporation of PVA (about 3%) improves water intake. We have successfully prepared paints with water intake upto 50% and binder 8-10%.

(d) Addition of water upto 10 to 35% reduces the cost of paint without affecting the performance characteristics.

(e) The solvent content in paint varies from 25-50% while water content varies from 10 to 50%. Thus, the organic solvent is reduced by approximately 50%.

(f) The fire hazard and the toxicity of the paint has also been reduced due to the water intake.

(g) The water thinnable paints have excellent hiding power, hardness, adhesion, stability and resistance to water, seawater and chemicals.

(h) All paint samples surface dry within 5-10 minutes, while their hard drying time is less than one hour.

(i) In all the paint formulations, no driers have been used. This will further reduc the raw material cost of paint and make the paint free from toxic metals such as lead, cobalt, calcium, etc.

(j) The main features of these formulations are their excellent hardness and film properties which are obtained even at lower resin content of 10 to 25%. Normally, 35 to 50% binder is required for getting useful technical properties. Thus, in our composition, we have saved 10 to 15% binder.

(k) The stability of paints is excellent. Generally water thinnable coatings are unstable. However, we have obtained stable products with stability period of more than six months.

(l) We have developed a paint which is lower in cost, excellent in technical performance compared to commercial samples and thinnable with water as solvent.

(m) E2, E3, and E4 formulations were compared with commercial samples for all physico-chemical and film properties and can be adjudged as good compositions from the technical performance view point.

Acknowledgements

Authors are highly indebted to Dr. B.B. Gogte, Former-Professor, LIT, Nagpur, India for his valuable guidance and suggestions. Authors gratefully acknowledge the financial support by M.S. Jotun A/S, Norway Government for this research work.

Table 1. Composition of alkyd resins based on Castor oil (Composition % by weight)

Ingredients	A1	A2	A3	A4
Castor Oil	39.44	39.04	35.45	35.89
Rosin	39.36	38.98	40.55	37.62
Glycerol	6.60	6.53	1.00	6.00
Pentaerythritol	4.67	4.62	-----	4.25
Sorbitol	-----	-----	16.01	-----
Maleic Anhydride	3.94	3.90	3.26	5.40
Phthalic Anhydride	5.99	5.93	3.73	9.84
Benzoic acid	-----	1.00	1.00	1.00
Sodium bisulphate	0.50	0.50	0.50	1.50
Sodium bisulphite	0.10	0.10	0.10	0.50
% Yield	**95.5**	**96.3**	**93.6**	**95.0**

Table 2. Analysis of Alkyd resins

Alkyd Resin	Acid Value	Iodine Value	Peroxide Value	Hydroxide Value	% Solids
A1	11.35	39.22	0.37	64.28	94.03
A2	8.18	44.41	0.58	94.47	90.93
A3	9.11	51.32	0.51	44.50	93.10
A4	30.00	42.00	1.02	120.30	95.14

Table 3. Composition (% by weight) of water thinnable paints based on Alkyd resin (A4)

Component	E1	E2	E3	E4	E5	E6
TiO_2	28.17	21.98	20.0	18.39	11.41	7.33
ZnO	2.58	2.02	1.83	1.67	1.05	0.66
Alkyd (A4)	19.55	15.25	13.87	12.76	8.00	5.08
Polyvinyl alcohol (PVA)	-----	1.21	1.65	2.02	3.50	2.20
Ammonia	-----	0.55	0.50	0.46	0.30	0.20
Xylene	35.28	30.77	30.32	30.06	28.05	24.57
Mineral Turpentine	14.11	12.31	12.13	12.02	11.22	9.83
Butanol	1.01	0.87	0.86	0.85	0.80	0.70
Water	-----	15.67	18.18	21.73	35.67	50.00
Pigment Binder ratio	1.573	1.574	1.574	1.572	1.557	1.573

Table 4. Physicochemical and film properties of water thinnable paints based on Alkyd resin (A4)

Analysis	E1	E2	E3	E4	E5	E6	Asian paint	Nerolac Paint
Viscosity	60	60	60	60	60	60	130	160
Density (g/mL)	1.18	1.15	1.13	1.11	1.01	1.006	1.112	0.928
Hiding power (m^2/L)	18.80	17.04	16.26	14.80	11.23	10.01	14.43	14.28
% Solids	50%	45.08%	39.17%	37.40%	26.13%	18.29%	59.02%	48.03%
Surface Dry(In min)	5	5	5	5	10	10	180	120
Hard Dry (In min)	10	15	18	20	35	55	480	360
Scratch Hardness (g)	>1000	>1000	>1000	>1000	>1000	900	>1000	>1000
Finish	Matt	Matt	Matt	Matt	Matt	Matt	Gloss	Gloss
Adhesion Test	Excellent	Excellent	Excellent	Excellent	Excellent	Excellent	Excellent	Excellent
Stability Test (90 days)	Excellent	Excellent	Excellent	Excellent	Excellent	Excellent	Excellent	Excellent

Table 5. Film resistance properties of water thinnable paints based on Alkyd resin (A4)

Analysis		E1	E2	E3	E4	E5	E6	"Asian paint"	"Nerolac paint"
Water	15 Days	Excellent	Excellent	Excellent	Excellent	Excellent	Excellent	Excellent	Excellent
	1 Month	Excellent	Excellent	Excellent	Good	Good	Good	Excellent	Good
Sea-water	15 Days	Excellent	Excellent	Good	Good	Good	Good	Excellent	Poor
	1 Month	Good	Good	Good	Good	Poor	Poor	Good	Poor
3% NaOH (30min)		Excellent	Excellent	Excellent	Excellent	Excellent	Excellent	Excellent	Excellent
3% H_2SO_4 (48 hrs)		Excellent	Excellent	Excellent	Good	Poor	Poor	Excellent	Excellent
3% Detergent (30 min)		Excellent	Excellent	Excellent	Excellent	Good	Good	Excellent	Excellent
Xylene (15min)		Good	Good	Good	Good	Good	Good	Excellent	Excellent

References

1. Burande, B., 2017, *IJRAET*, **5(9-10),** 12-16.
2. Burande, B., Dhakite, P.A. and Gogte B.B., 2017, *IJAIR*, **4(1),** 132-134.
3. Phate, B. and Gogte, B.B., 2005, *Paint India*, 71-76.
4. Dhakite, P.A., Burande, B.C. and Gogte, B.B., 2014, *IJRBAT*, **1(2),** 239-249.
5. Joshi, A., 1991, *Paint India*, **41(3)**, 41-46.
6. Kirk and Othmer, 1979, John Wiley and Sons, Inc. New York, **3(5)**, 1-12.
7. Ullman H.M., 1946, U.S. **2**, 396, 763, C.A. **40**, 36277.
8. Kirk and Othmer, 1979, Encyclopedia of Chemical Technology, John Wiley and Sons, Inc. New York 3rd edition, **8**, 135-137.
9. Sudhra, S., Fould, I.S., Gray, C.N., Koh, D. and Gardiner, K., 1994, *Ann. Occup. Hyg.*, **38**, 385.
10. Gogte, B.B. and Agrawal, A., 1994, *Paint India*, **44(10)**, 51.

11. Payne, H.F., 1954, Organic Coatings Technology, Vol. 1, John Wiley and Sons, Inc. New York, 279-280.

12. Taylor, C.J. and Marks, S., 1972, Paint Technology Manual - Part III Convertible Coatings, Chapman and Hall Publications, London, 92-94.

13. http.//web umr. edu /jstoffer/CHEM 381/ Chap.33.html.

14. Paul Lucas, 1994, *Paint India*, **44(5)**, 39.

15. ASTM Standard Method, 1981, 6.01, D 1639-70, (For Acid Value of Organic Coating Materials), American Society for Testing Materials, Philadelphia.

16. ASTM Standard Method, 1979, 6.03, D 1959-69, (For Iodine Value of Drying Oils, Varnishes, Resins).

17. AOCS, 1946, Official and Tentative Methods of the American oil Chemist's Society, 2nd edition Cd 8-53, (For Peroxide Value of Fatty Oils and Acids).

18. ASTM Standard Method, 1979, 6.03, D. 1957-63, (For Hydroxyl Value of Fatty Oils and Acids).

19. ASTM Standard Method, 1982, 6.01, D 1200-82, (For Viscosity of Paint, Varnishes and Lacquers by Ford Cup Method).

20. ASTM Standard Method, 1982, 6.03, D 1963-74, (For Specific Gravity of Drying Oils, Varnishes, Resins).

21. ASTM Standard Method, 1981, 6.01, D 2369-81, (For Volatile Content of paints).

22. ASTM Standard Method, 1980, 6.02, D 1259 -61, (For Non-Volatile Content of Resin).

23. ASTM Standard Method, 1980, 6.01, D 280580, (For Hiding Power of Paint).

24. ASTM Standard Method, 1974, 6.01, D, 1640-69, (For Drying or Film Formation of Organic Coating at Room Temperature).

25. ASTM Standard Method, 1980, 6.01, D. 523-80, (For Determination of Gloss).

26. Morgan, W.M., 1996, Outlines of Paint Technology (3rd Edition), CBSW Publishers and Distributors, New Delhi, 438.

27. Taylor and Marks, 1965, Paint Technology Manuals: The Testing of Paints, B.S. 391, Performance test for protective Coatings, 80.

28. Indian Standard Specification I.S. 1969, 428, (For Dry Rub Resistance Test).

29. Indian Standard specifications, 1964, I.S. 101, (For Water Resistance).

30. ASTM Standard Method, 1981, 6.01, D1647-70, (For Resistance of Water and Chemicals of Dried Films of Varnish and Paint).

31. Indian Standard Method, 1980, 6.01 D 2792-69 (For Solvent and Fuel Resistance of Paints).

RNI No. MAHENG/2017/74063
ISSN No. (Print) 2581-5911
ISI Impact Factor 1.022 (2019-2020)

Design, Synthesis and Biological Evaluation of some Novel Imidazole Derivatives for Anti-Inflammatory and Antibacterial Activity

Kundlik S. Khandare[1*], Laxman A. Chate[2], Suraj N. Wanjari[2], Megha P. Ambatkar[2] and P.B. Khedekar[2]

[1] Department of Pharmaceutical Sciences,
Rastrasant Tukadoji Maharaj Nagpur University,
Nagpur 440033, Maharashtra, India

[2] Department of Pharmaceutical Chemistry, UDPS RTMNU Campus,
Nagpur 440033, Maharashtra, India

E-mail*: kundlikkhandare77@gmail.com
laxmanchate1234@gmail.com; wanjarisuraj9@gmail.com
megha_bodhe@rediffmail.com; pbkhedekarudps@gmail.com

Abstract

In the present research, 1, 2, 4-Trisubstituted-1H-imidazoles were synthesized by using nitrophenyl glyoxal with various substituted aryl aldehydes. The objective behind the research was to design and synthesize substituted imidazole derivatives and evaluate them for Invitro and Invivo anti-inflammatory and antibacterial activity. The purity and homogeneity of all the synthesized compounds were confirmed by their melting points, thin layer chromatography, UV spectrophotometry and IR spectroscopy. Invitro anti-inflammatory activity of the newly synthesized imidazole derivatives was carried out by protein denaturation method and Invivo anti-inflammatory activity was carried out by carrageenan induced rat paw edema method. Antibacterial activity was carried out by the cylinder (cup) plate method.

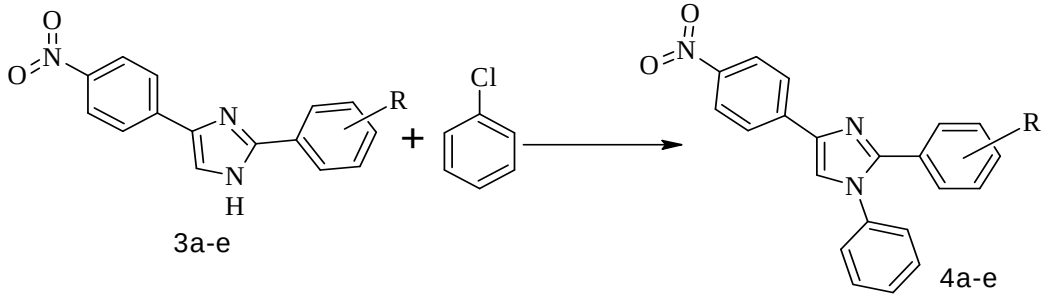

Keywords: *Anti-inflammatory activity, antibacterial activity, Imidazole, substituted aryl aldehydes.*

Introduction

Inflammation is a process which occurs when the tissues are injured by foreign organisms such as bacteria, viruses, trauma, toxins, heat, or by any other cause[1-3] It is a local response of mammalian tissue to injured cells or harmful stimuli such as pathogens, damaged cells and irritants as well as the healing of damaged tissue by protective response of immune cells, blood cells and molecular mediators. Inflammation is also one of the keys to detect autoimmune diseases, such as multiple sclerosis, rheuma-toid arthritis, Crohn's disease and Type I diabetes.[4] The generation of prostaglandins is one of the most important factors in the inflammatory process because they are produced within the body cells by the cyclooxygenase (Cox) enzyme. Both Cyclooxygenase-1(COX-1) and Cyclooxygenase-2(COX-2) enzymes produces prosta-glandins that promote inflammation pain and fever.[5-7]

Inflammation can be caused by a number of factors that can damage cells and are mainly categorised into:[8]

Physical: It can be mechanical as in a car accident injury or assault or ailments like severe cold and heat (burns), stress etc.

Chemical: Acid burns, drugs, venom, ionizing radiation, Infection due to bacteria, viruses, fungi and other parasites.

Ischemia: lack of or restricted blood supply which may eventually lead to death of tissue (necrosis) known as an infarct.

Autoimmune disorder: Autoimmune conditions, trauma and allergies.[9]

Symptoms of inflammation can vary according to whether the reaction is acute or chronic such as swelling, redness, immobility, pain and heat.[10-11]

There are two basic types of inflammation – acute inflammation and chronic inflammation.

Acute inflammation: It is of short duration, which could be anything from a few minutes to a few days. Such inflammation is caused by foreign substances entering the body, or by physical damage. A viral infection may also precipitate acute inflammation.[12]

Chronic inflammation: It is long lasting. It may persist for weeks, months or even years. Chronic inflammation may be brought on by acute inflammation or it may be the result of an auto immune disease.[13-14]

Non-steroidal anti-inflammatory drugs (NSAID) are drugs which are used as analgesic and antipyretic agents and at higher doses produce anti-inflammatory effects. Non-steroidal anti-inflammatory drugs block the Cox enzymes, which are involved in the formation of prostaglandins and thromboxanes from arachidonic acid (AA) contained in cellular membranes, and reduce the prostaglandins throughout the body.[15] As a consequence, on-going inflammation, pain and fever are reduced. So, it is necessary to discover safe and effective anti-inflammatory compounds.[16-20]

Mostly NSAIDs are prescribed in acute inflammatory conditions such as sports injuries, fractures, sprains, soft tissue injuries, postoperative, dental and menstrual pain, and also headaches and migraine.[21]

Some NSAIDs have emerged as a part of a new class of cancer chemotherapeutics and chemo preventive agents.[22] As several NSAIDs are available over the counter, they are often taken without prescription for other types of minor aches and pains.[23]

AA is the most abundant polyunsaturated fatty acid found in the phospholipid cell membranes. Activation of the phospholipase A_2 (PLA_2), in response to various stimuli, releases AA, which can be further metabolized by two major enzymatic pathways: Cyclooxygenase and 5-Lipoxygenase (5-LOX), leading to pro-inflammatory mediators, prostanoids and leukotrienes (LTs), respectively.[24]

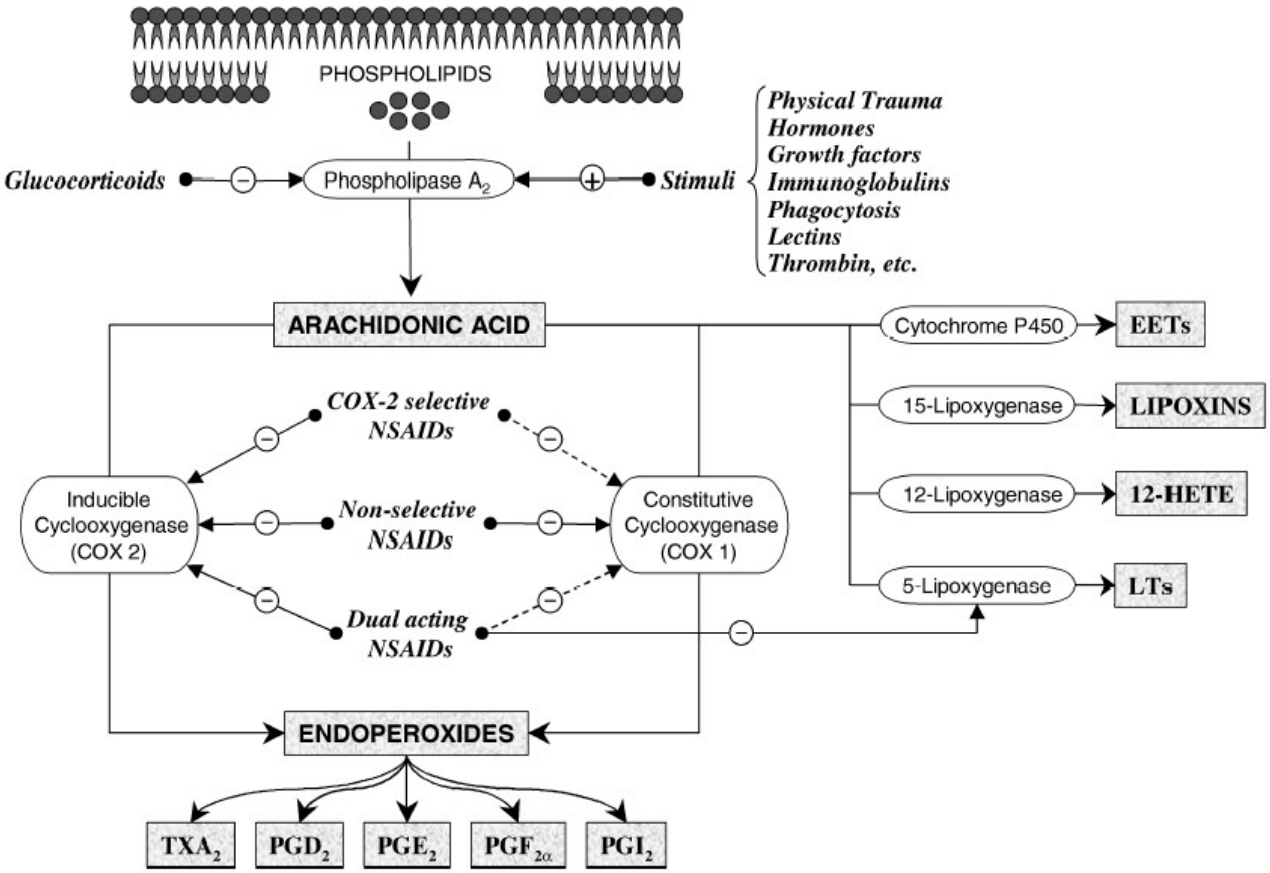

Fig. 1. Biosynthesis of eicosanoids and possible drug targets

Prostaglandin endoperoxide H synthase, colloquially known as Cyclooxygenase or COX has two distinct catalytic activities (Fig. 1): (1) Cyclooxygenase oxidizes AA to hydroperoxy endoperoxide PGG_2 and (2) peroxidase which subsequently reduces PGG_2 to the hydroxy-endoperoxide PGH_2. Afterwards, the unstable PGH_2 is transformed by diverse tissue-specific synthases and isomerises into prostanoids. This includes the prostaglandins (PGD_2, PGE_2 and PGF_{2a}), prostacyclin (PGI_2) and thromboxane A_2 (TXA_2).

There are two types of cyclooxygenases namely COX-1 and COX-2.[25] Each type of cyclooxygenase lends itself to producing different types of PGs.

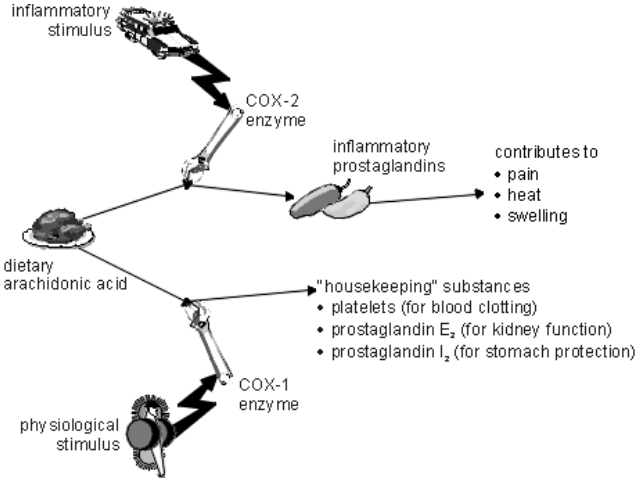

Fig. 2. Cyclooxygenase Pathway

Different mechanisms stimulate the two types of cyclooxygenases. COX-1 is stimulated continuously by normal body physiology.[26] (Fig. 2)

It is present in most tissues and converts arachidonic acid into PGs. These PGs in turn stimulate normal body functions, such as stomach mucus production and kidney water excretion, as well as platelet formation. For example, COX-1 in the stomach wall produces PGs that stimulate mucous production. In contrast, the COX-2 enzyme is induced.[27] It is not normally present in cells but its expression can be increased dramatically by the action of macrophages, the scavenger cells of the immune system. COX-2 is involved in producing PGs for an inflammatory response. COX-1 is stimulated continuously, and COX-2 is stimulated only as a part of an immune response.[28]

An antibacterial is an agent that interferes with the growth and reproduction of bacteria. These agents kill or prevent bacteria by fighting against bacterial infection. Heat, chemicals such as chlorine, and all antibiotic drugs have antibacterial properties.[29]

An antibiotic is a type of antimicrobial substance active against bacteria and is the most important type of antibacterial agent for fighting bacterial infections. Antibiotic medications are widely used in the treatment and prevention of such infections.[30-31] They may either kill or inhibit the growth of bacteria. A limited number of antibiotics also possess antiprotozoal activity.[32-33]

Various classes of Antibacterial agents

Antibiotics are generally used to treat bacterial infections. Antibacterial agents act by interfering with[34] (Figure 3)

1. Cell wall synthesis: Penicillin, Cephalosporin, Carbapenams, Monobactum.
2. Protein synthesis: Aminoglycoside, Chloramphenicol, Macrolides, Tetracycline, Streptogrmins.
3. Nucleic acid synthesis: Quinolone, Fluoroquinolone.
4. Ribosomal function: Rifampin
5. Folate synthesis: Sulfonamide, Trimetoprim,

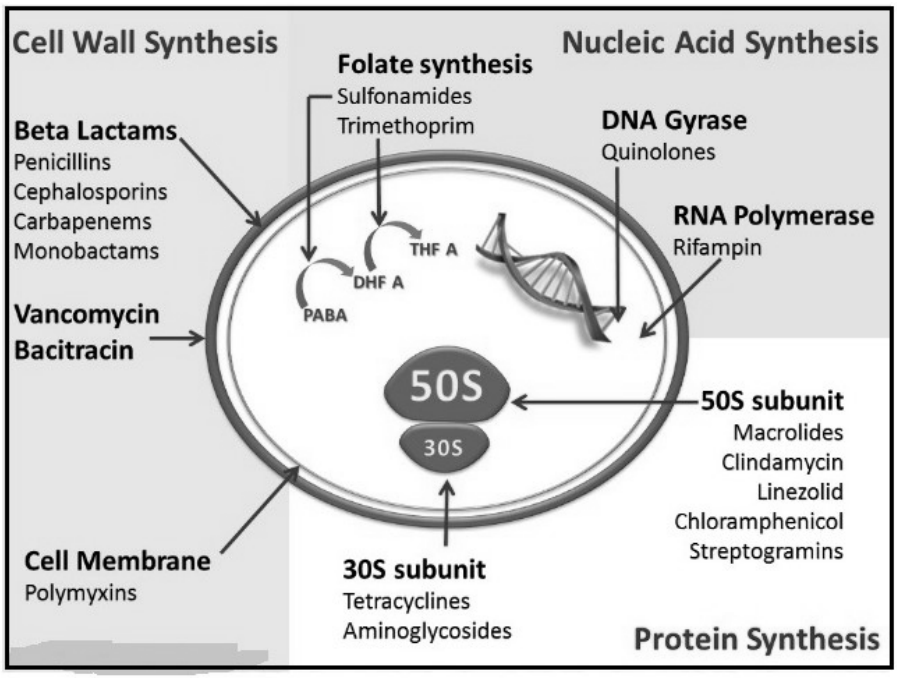

Fig. 3. Site of action of antibacterial agents

Imidazole as a heterocyclic moiety

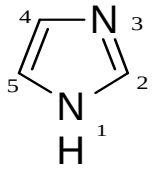

Imidazole moiety is an important heterocyclic organic compound. Imidazole is a 5-membered planar ring containing two nitrogens at one and three position. Imidazoles are generally poorly soluble in water but can be dissolved in organic solvents such as chloroform, propylene glycol, and polyethoxylated castor oil for IV use (Table 1). An exception is fluconazole. Imidazoles are weak dibasic agents. Alterations in the side chain structure determine antifungal activity as well as the degree of toxicity.[35]

Imidazole derivatives have scope in medicine such as antibacterial, antifungal[36-37], anti-inflammatory agent[38-40], antiprotozoal[40-41], anticancer[42-44] and anthel-mintic activity[45]. Several distinct phenylimidazoles are therapeutically useful antifungal agents with a wide spectra of activity against yeasts and filamentous fungi responsible for either superficial or systemic infections. The anthelmintic thiabendazole is also an imidazole with antifungal properties. Clotrimazole, miconazole, econazole, ketoconazole, itraconazole, and fluconazole are the most clinically important members of this group.

Table 1: Physicochemical properties of Imidazole

Sr. No.	Physicochemical parameters	Imidazole
1.	Structural formula	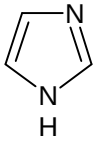
2.	Molecular formula	$C_3H_4N_2$
3.	IUPAC name	1*H*-Imidazole
4.	Other name	1,3-Diazole
5.	Molecular weight	68.077 g/mol
6.	Solubility in water (g/100mL)	Soluble in water
7.	Appearance	White crystals
8.	Melting point	89-91^{0}C
9.	Boiling point	256 -258°C

The present research work focusses on the synthesis of 1, 2, 4-trisubstituted-1*H*-imidazole derivatives by using nitrophenyl glyoxal with various substituted aryl aldehydes. The purity and homogeneity of all the synthesized compounds were confirmed by their melting points, thin layer chromatography, UV spectrophotometry, and IR spectroscopy. Invitro and invivo anti-inflammatory activities of the newly synthesized imidazole derivatives were studied by protein denaturation method and by carrageenan induced rat paw oedema method respectively.

Synthetic Scheme

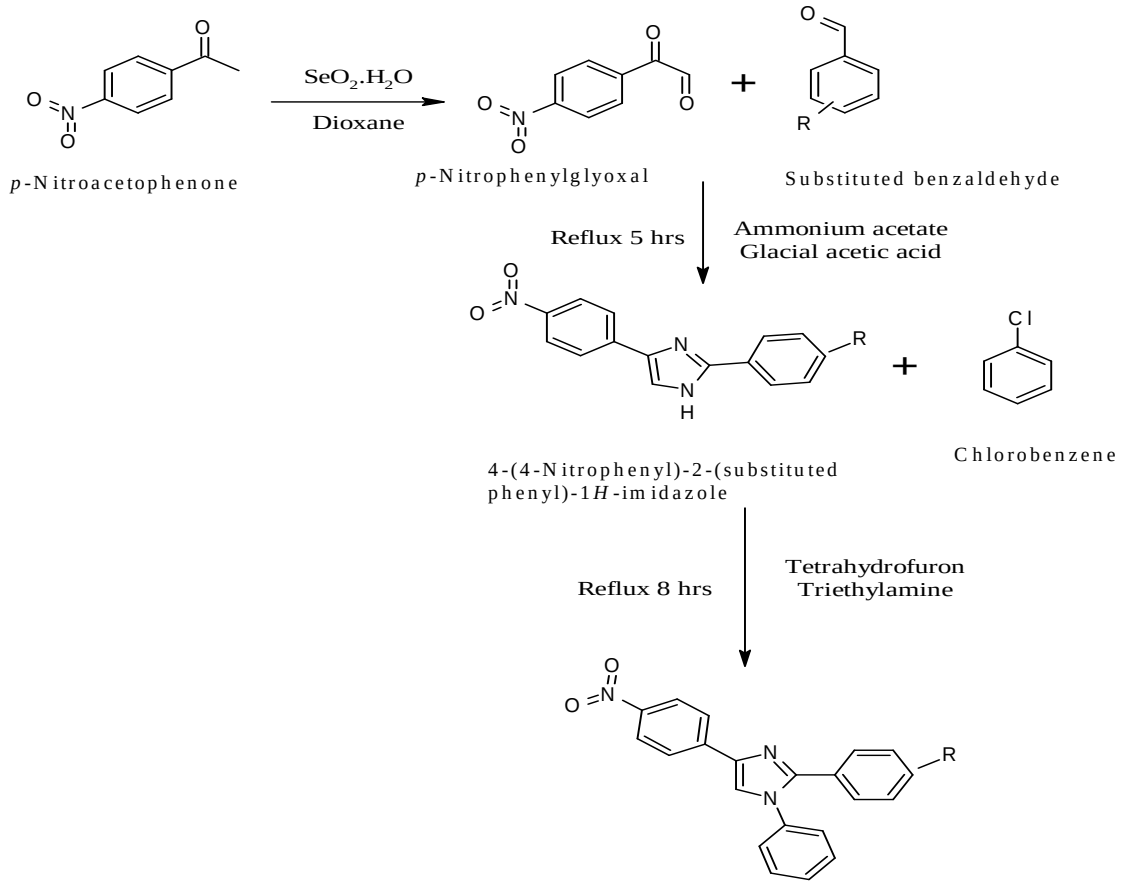

4-(4-Nitrophenyl)-2-(substituted phenyl)-1-phenyl imidazole

Materials and Methods

All solvents and chemicals employed for the synthetic work were of laboratory grade and all chemicals and solvents were procured from SD Fine Chemicals, E. Merck, Loba Chemie and were used without further purification. Melting points (M.P.) were determined by using melting point apparatus. λ_{max} values of compounds were determined by UV spectrophotometry. IR spectra of synthesized compounds were recorded using KBr powder on FTIR spectrophotometer IR Affinity-1S Shimadzu A219652 (Shimadzu, Japan) make from Department of Pharmaceutical Sciences, Rashtrasant Tukadoji Maharaj Nagpur University, Nagpur, India.

General Procedure

Synthesis of *p*- nitrophenylglyoxal

p-nitrophenylglyoxal was synthesized by heating a mixture of pure selenium dioxide (2.77g, 0.025 mol), water (1mL) and dioxane (15 mL) in a round bottom flask at 50-55^{0}C with stirring till a clear solution was obtained. To the above solution, *p*-nitro acetophenone (4.12 g, 0.025 mol) was added in one lot. The mixture was further refluxed with stirring for 4 hours and during refluxing, small amount of selenium precipitated out. The reaction mixture was decanted to remove the precipitate. The clear solution so obtained was distilled to remove excess dioxane and water. TLC of compound

was performed by using mobile phase, Chloroform: Acetone, 9:1, v/v. Yield: 58% M.P.: 66-68, R_f 0.45

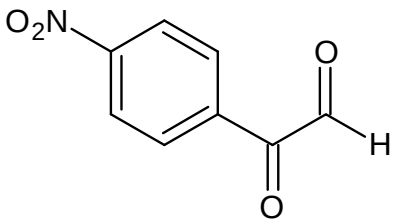

General structure of different N-substituted Imidazole derivatives

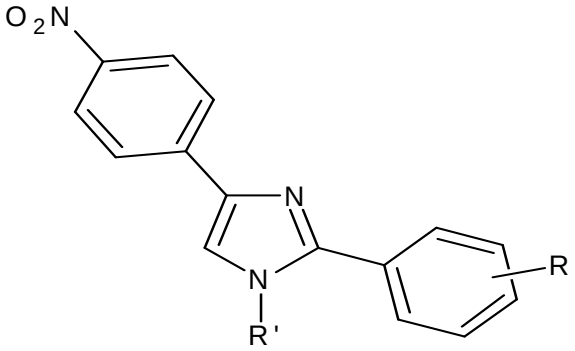

Synthesis of 4-(4-nitrophenyl)-2-substituted phenyl-1 *H*-imidazole

A mixture of *p*-nitrophenyl glyoxal 2 (2.23 g, 0.0125 mol), substituted benzaldehyde (1.32 g, 0.0125 mol) and ammonium acetate (5 g) in glacial acetic acid (25 mL) was refluxed in a round bottom flask for 5 hours. After refluxing, the mixture was cooled to room temperature and then poured into cold water (200 mL). A precipitate separated out, which was filtered, washed, dried and crystallized from acetone. TLC of compound was performed using mobile phase, Chloroform: Acetone, 9:1, (v/v).

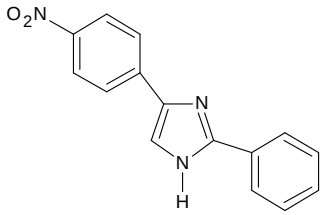

Table 2: Different N-substituted Imidazole derivatives

Sr. No.	R	R^1
1.	H	H
2.	*o*-NO_2	H
3.	*p*-Cl	H
4.	*p*-OH	H
5.	*p*-OCH_3	H
6.	H	C_6H_5
7.	*o*-NO_2	C_6H_5
8.	*p*-Cl	C_6H_5
9.	*p*-OH	C_6H_5
10.	*p*-OCH_3	C_6H_5

Synthesis of 4-(4-nitrophenyl)-2-phenyl-1 *H*-imidazole (3a)

A mixture of *p*-nitrophenyl glyoxal 2 (2.23 g, 0.0125 mol), substituted benzaldehyde (1.32 g, 0.0125 mol) and ammonium acetate (5 g) in glacial acetic acid (25 mL) was refluxed in a round bottom flask for 5 hours. After refluxing, the mixture was cooled to room temperature and then poured into cold water (200 mL). A precipitate separated out, which was filtered, washed, dried and crystallized from acetone. TLC of compound was performed using mobile phase, Chloroform: Acetone 9:1, (v/v).

Molecular Formula: $C_{15}H_{11}N_3O_2$, Molecular Weight: 265.26 , Yield: 62.22% (1.40g), m.p. 110-112^{0}C, λ_{max} 271.5 (Methanol), R_f 0.42, IR (KBr): 3481cm^{-1} (N-H Stretching), 1330 cm^{-1} (C-N Stretching), 1670 cm^{-1} (C=N Stretching); 3080 cm^{-1} (C-H Stretching); 1474 cm^{-1} (C=C Stretching), 1400,1550 cm^{-1} (N-O Stretching).

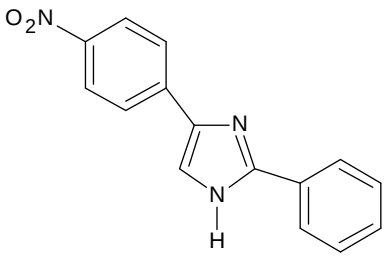

Synthesis of 2-(2-nitrophenyl)-4-(4-nitrophenyl)-1 *H*-imidazole (3b)

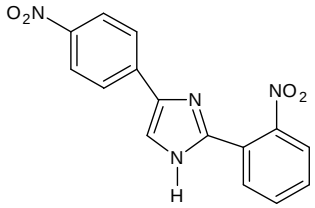

Molecular Formula: $C_{15}H_{10}N_4O_4$, Molecular Weight: 310.26, Yield: 42.22% (0.95g), m.p. 162-164^{0}C, λ_{max} 280.5 (Methanol), R_f 0.48, IR (KBr): 3419cm^{-1} (N-H Stretching), 1288cm^{-1} (C-N Stretching), 1687cm^{-1} (C=N Stretching), 3107cm^{-1} (C-H Stretching), 1450cm^{-1} (C=C Stretching), 1520-1350cm^{-1} (N-O Stretching).

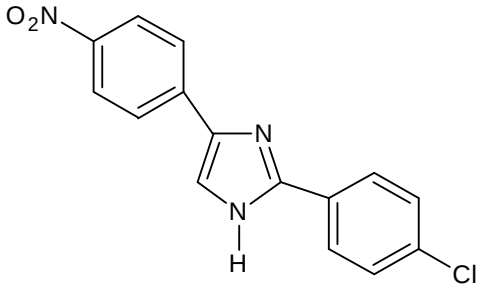

Synthesis of 2-(4-chlorophenyl)-4-(4-nitrophenyl)-1 *H*-imidazole (3c)

Molecular Formula: $C_{15}H_{10}N_3O_2Cl$, Molecular Weight: 299.71, Yield: 66.66% (1.5g), m.p. 136-138^{0}C, λ_{max} 265.5 (Methanol), R_f 0.41, IR (KBr): 3417cm^{-1} (N-H Stretching), 1296 cm^{-1} (C-N Stretching), 1597 cm^{-1} (C=N Stretching), 3049 cm^{-1} (C-H Stretching), 1596, 1450 cm^{-1} (C=C Stretching), 688 cm^{-1} (C-Cl Stretching), 1346-1523 cm^{-1} (N-O Stretching).

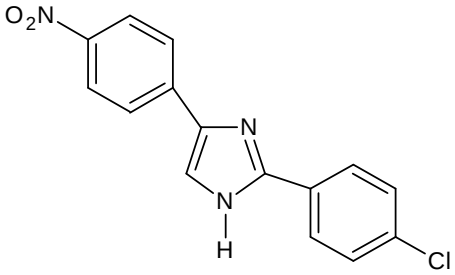

Synthesis of 2-(4-hydroxyphenyl)-4-(4-nitrophenyl)-1 *H*- imidazole (3d)

Molecular Formula: $C_{15}H_{11}N_3O_3$, Molecular Weight: 281.26, Yield: 44.44% (1.0g), m.p. 178-180^{0}C, λ_{max} 275 (Methanol), R_f 0.57, IR (KBr): 3419 cm^{-1} (N-H Stretching 1240 cm^{-1} (C-N Stretching), 1600 cm^{-1} (C=N Stretching), 3049 cm^{-1} (C-H Stretching), 1450 cm^{-1} (C=C Stretching), 3676 cm^{-1} (O-H Stretching) 1338, 1550 cm^{-1} (N-O Stretching).

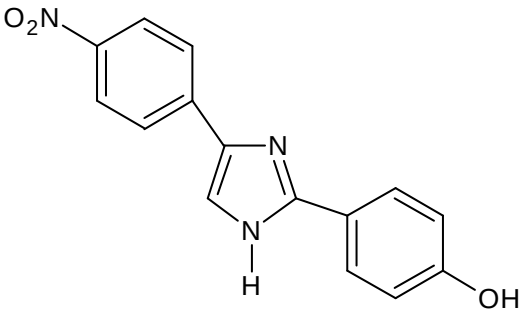

Synthesis of 2-(4-methoxyphenyl)-4-(4-nitrophenyl) -1 *H*-imidazole (3e)

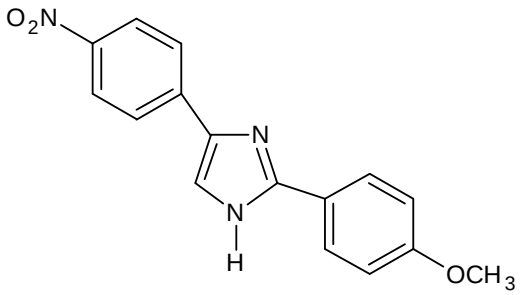

Molecular Formula: $C_{16}H_{13}N_3O_3$, Molecular Weight: 295.29, Yield: 48.88% (1.10g), m.p. 240-244^{0}C, λ_{max} 270.5 (Methanol), R_f 0.35, IR (KBr): 3417 cm^{-1} (N-H Stretching); 1213 cm^{-1} (C-N Stretching); 1598 cm^{-1} (C=N Stretching); 3049 cm^{-1} (C-H Stretching); 1410 cm^{-1} (C=C Stretching); 2845 cm^{-1} (C-O Stretching), 1338, 1515 cm^{-1} (N-O Stretching).

Synthesis of 4-(4-nitrophenyl)-1,2-diphenyl-1 *H*-imidazole (4a)

Compound **3a** (2.65 g, 0.01 mol) was suspended in

tetrahydrofuran (20 mL) and refluxed with chlorobenzene (2 mL) in the presence of 2-3 drops of triethylamine for 8 hours. The completion of reaction was confirmed by TLC. After refluxing, acetone was added to the reaction mixture and it was kept overnight at room temperature. The precipitate formed was filtered and recrystallized from ethanol. TLC of compound was performed using mobile phase, Benzene: Acetone, 8:2 (v/v).

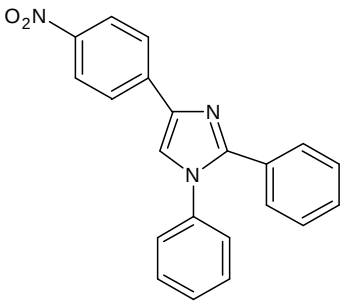

Molecular Formula: $C_{21}H_{15}N_3O_3$, Molecular Weight: 341.36, Yield: 60.60% (0.80g), m.p. 180-184^{0}C, λ_{max} 220.5 (Methanol), R_f 0.52, IR (KBr): 3417 cm^{-1} (N-H Stretching), 1350 cm^{-1} (C-N Stretching), 1600 cm^{-1} (C=N Stretching); 3049 cm^{-1} (C-H Stretching); 1448 cm^{-1} (C=C Stretching), 1334, 1529 cm^{-1} (N-O Stretching).

Synthesis of 2-(2-nitrophenyl)-4-(4-nitrophenyl)-1-phenyl imidazole(4b)

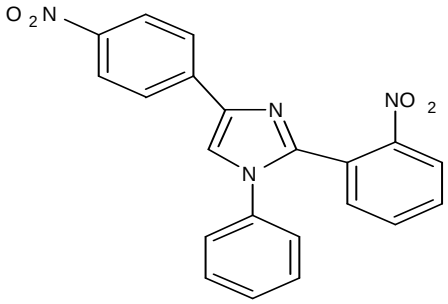

Molecular Formula: $C_{21}H_{14}N_4O_4$, Molecular Weight: 386.36, Yield: 60% (0.5g), m.p. 114-118^{0}C, λ_{max} 221 (Methanol), R_f 0.64, IR (KBr): 3429 cm^{-1} (N-H Stretching), 1350 cm^{-1} (C-N Stretching), 1610 cm^{-1} (C=N Stretching), 3055 cm^{-1} (C-H Stretching), 1410 cm^{-1} (C=C Stretching), 1360, 1506 cm^{-1} (N-O Stretching).

Synthesis of 2-(4-chlorophenyl)-4-(4-nitrophenyl)-1-phenyl imidazole(4c)

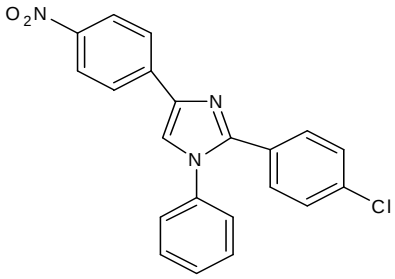

Molecular Formula: $C_{21}H_{14}N_3O_2Cl$, Molecular Weight: 375.80, Yield: 40% (0.40g), m.p. 118-120^{0}C, λ_{max} 295 (Methanol), R_f 0.28, IR (KBr) : 3360 cm^{-1} (N-H Stretching), 1261 cm^{-1} (C-N Stretching), 1600 cm^{-1} (C=N Stretching), 3000 cm^{-1} (C-H Stretching), 1487 cm^{-1} (C=C Stretching), 746 cm^{-1} (C-Cl Stretching), 1346, 1525 cm^{-1} (N-O Stretching).

Synthesis of 2-(4-hydroxyphenyl)-4-(4-nitrophenyl)-1-phenyl imidazole (4d)

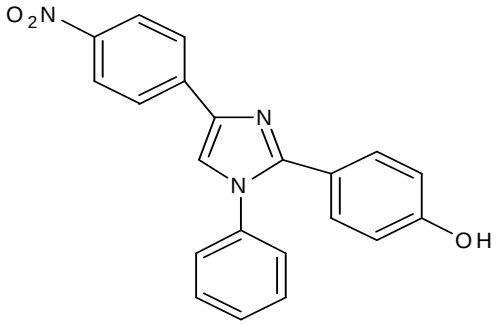

Molecular Formula: $C_{21}H_{15}N_3O_3$, Molecular Weight: 357.36, Yield: 50% (0.70g), m.p. 82-84^{0}C, λ_{max} 219.5 (Methanol), R_f 0.38, IR (KBr) (cm^{-1}): 3360(N-H Stretching), 1240(C-N Stretching), 1602(C=N Stretching), 3049(C-H Stretching), 1448(C=C Stretching), 3417(O-H Stretching), 1350(N-O Stretching).

Synthesis of 2-(4-methoxyphenyl)-4-(4-nitrophenyl)-1-phenyl imidazole (4e)

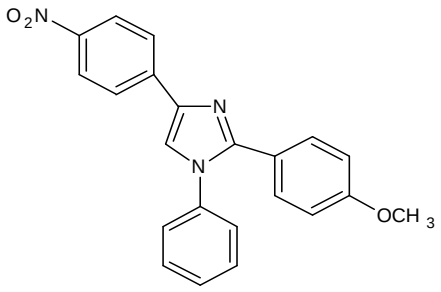

Molecular Formula: $C_{22}H_{17}N_3O_3$, Molecular Weight: 371.38, Yield: 42.85% (0.30g), m.p. 208-210^{0}C, λ_{max} 229.5 (Methanol), R_f 0.45, IR (KBr)$^{cm-1}$: 3323(N-H Stretching); 1190(C-N Stretching); 1600(C=N Stretching); 3012(C-H Stretching); 1450(C=C Stretching); 2848(C-O Stretching), 1300, 1580(N-O Stretching.

Anti-inflammatory activity[46]

***Invitro* anti-inflammatory activity**

The synthesized compounds were screened for *Invitro* anti-inflammatory activity by using inhibition of albumin denaturation technique of Muzushima and Kabayashi with slight modification.[47] The reaction mixture (5 mL) consisted of 0.2 mL of egg albumin (from fresh hen's egg), 2.8 mL phosphate buffered saline (pH: 6.4) and 2 mL of varying concentrations of test compounds. A similar volume of double distilled water served as control. Then the mixtures were incubated at 37±2°C in an incubator for 15 minutes and then heated at 70ºC for 5 minutes. After cooling, their absorbance was measured at 660 nm by using vehicle as blank. Diclofenac of final concentration of 50 ppm was used as standard drug and treated similarly for determination of absorbance. The percent inhibition of protein denaturation was calculated as follows and the results are shown in Table 3 and Figure 4.

Percentage inhibition = $[A_{control} – A_{sample}) / A_{control}] X 100$

Table 3: % Inhibition of protein denaturation of *N*-substituted imidazole derivatives

Compounds	Absorbance (660 nm)	Inhibition of Protein Denaturation (%)
Control	**0.7850**	**-**
3a	0.3109	60.39
3b	0.2159	72.49
3c	0.4000	49.04
3d	0.1196	84.76
3e	0.2473	68.49
4a	0.5024	36.00
4b	0.4732	39.71
4c	0.4301	45.21
4d	0.4130	47.38
4e	0.5100	35.03
Diclofenac (standard)	**0.1050**	**85.82**

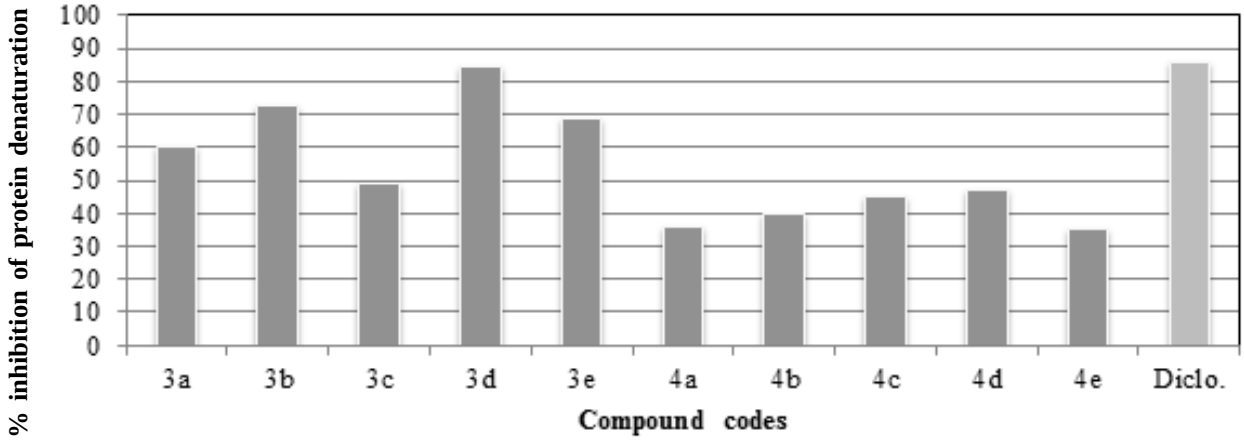

Fig. 4. % inhibition of protein denaturation of synthesized compounds compared with standard diclofenac

***Invivo* anti-inflammatory activity[48, 49]**

All the newly synthesized compounds **(3a-e, 4a-e)** were subjected to pharmacological screening to determine *invivo* anti-inflammatory activity. Male Sprague-Dawley rats (200-300 g) were used in the study. The animals were housed in the animal facility under standard conditions of temperature (25±2ºC) and 12 hr light / 12 hr dark cycles. The animals were kept under laboratory conditions for one week before the start of the experiments and allowed free access to food and water.

The anti-inflammatory activity of *N*-substituted 1, 2, 4-triaryl imidazole was determined using a carrageenan-induced rat paw edema method. Thirty male Sprague-Dawley rats (200-300 g) were randomly divided into 5 groups (6 animals in each group) consisting of 1 control group, 1 standard group and 3 test groups. Test compounds (10 mg/kg) suspended in 0.5% carboxy-methylcellulose solution (CMC) were administered orally. The control group received an equivalent volume of vehicle (0.5% CMC in distilled water) and the standard group received indomethac dissolved in 0.5% CMC solution (10 mg/kg, i.p.) one hour before subcutaneous injection of carrageenan (1% w/v in NSS) into the plantar surface of the left hind paw. After carrageenan injection, the paw thickness was measured at 0 hr, 1 hr, 2 hr and 3 hr in the individual animals of control, test and standard group using Digital Vernier caliper (Table 4). % inhibition of inflammation by experimental compounds was compared with standard Indomethacin. (Fig. 5)

The percentage inhibition of edema (Table 5) was calculated by the following equation:

% Inhibition (%I) = $[1- (D_t/D_c)] \times 100$

where,

D_t = Mean relative change in paw thickness in test group/ standard group.

D_c = Mean relative change in paw thickness in control group.

Table 4: Average rat paw thickness (mm) after carrageenan injection at different hours

Sr. No.	Group	Dose mg/kg	Average rat paw thickness after carrageenan injection (mm)			
			0 h	1 h	2 h	3 h
1.	**Control**	-	4.60	4.56	4.48	4.21
2.	**Indomethacin**	10 mg/kg	4.61	2.98	2.91	1.99
3.	**3a**	10 mg/kg	4.20	2.43	2.12	2.05
4.	**3b**	10 mg/kg	4.76	3.28	3.10	2.10
5.	**3c**	10 mg/kg	4.18	2.61	3.35	3.10
6.	**3d**	10 mg/kg	4.73	3.82	3.71	2.20
7.	**3e**	10 mg/kg	4.28	3.32	2.48	2.07
8.	**4a**	10 mg/kg	4.18	3.43	3.32	3.05
9.	**4b**	10 mg/kg	4.19	2.59	2.95	2.89
10.	**4c**	10 mg/kg	4.30	2.83	2.62	2.15
11.	**4d**	10 mg/kg	4.88	3.92	3.73	2.80
12.	**4e**	10 mg/kg	4.20	3.88	2.92	2.95

Table 5: % inhibition (%I) of inflammation by carrageenan induced rat paw edema

Sr. No.	Group	Dose mg/kg	% inhibition of rat paw edema			
			0 hr	1 hr	2 hr	3 hr
1.	**Control**	-	-	-	-	-
2.	**Indomethacin**	10 mg/kg	-	34.64	35.04	52.73
3.	**3a**	10 mg/kg	-	32.71	34.67	51.30
4.	**3b**	10 mg/kg	-	28.07	30.80	49.88
5.	**3c**	10 mg/kg	-	18.76	21.98	26.36
6.	**3d**	10 mg/kg	-	16.22	17.18	47.74
7.	**3e**	10 mg/kg	-	27.19	44.64	50.11
8.	**4a**	10 mg/kg	-	24.78	25.89	27.20
9.	**4b**	10 mg/kg	-	37.93	41.51	48.50
10.	**4c**	10 mg/kg	-	29.20	30.88	31.35
11.	**4d**	10 mg/kg	-	14.03	16.74	33.05
12.	**4e**	10 mg/kg	-	26.84	27.27	29.36

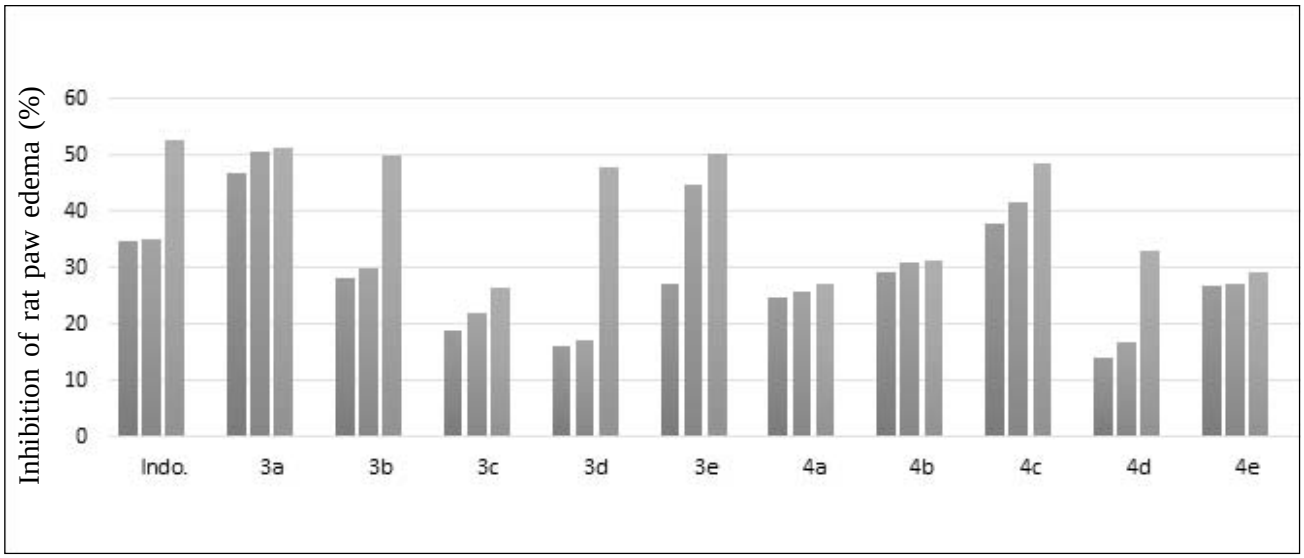

Fig. 5. % inhibition of inflammation by experimental compounds compared with standard indomethacin

Antibacterial activity

Antibacterial assay is based on a comparison of inhibition of growth of bacteria by measured concentrations of test compounds with that produced by known concentration of a standard antibiotic. The cylinder (cup) plate method depends upon diffusion of antibiotic from a vertical cylinder through a solidified agar layer in a Petri dish or plate to such an extent that growth of added bacteria is prevented entirely in a zone around the cylinder containing the solution of the antibiotics. The cup-plate method is simple and measurement of inhibition of bacteria is also easy. We have used this method for antibacterial screening of the test compounds.[50, 51]

Name of organisms used for antibacterial activity

Gram +Ve microorganisms

- *Staphylococcus aureus* (MTCC No. 96)
- *Bacillus subtilis* (MTCC No. 121).

Gram -Ve microorganisms

- *Escherichia coli* (MTCC No. 521).

Working standards: Stock solutions of synthesized compounds and standard drug were prepared in methanol (1000µg/mL). Further dilution was made to get concentrations of 50µg/mL, 100µg/mL, 150µg/mL and 200µg/mL.

Preparation of medium: Nutrient agar 2%, Peptone 1%, Beef extract 1%, Sodium chloride 0.5% and distilled water. All the ingredients were weighed and added to water. This solution was heated in a water bath for about one and half-hours till it became clear. This nutrient media was sterilized in an autoclave at 121°C for 15 minutes at 15 psi.

Apparatus: All the apparatus like Petri dishes, pipettes, glass rods, test-tubes etc. were properly wrapped with papers and sterilized in an hot air oven at 160°C for 3 hours.

Culture: *S.aureus* and *B.subtilus* were used as gram-positive bacteria and *E.coli* were used as gram negative bacteria for our study. The master culture was prepared on agar slant of the above nutrient media and kept in a refrigerator. The working culture was prepared from it by weekly transfer in nutrient agar medium.

Preparation of inoculum: In aseptic conditions, small amount of culture was transferred from the working

culture to about 10-15 mL of sterile normal saline (0.9% NaCl solution). This solution was gently mixed and used for antibacterial activity studies About 0.5 mL of inoculum was added to the sterilized Petri dish along with cooled melted agar, mixed gently and then allowed to solidify. Wells were bored in the agar plate and constant volumes of solutions of the compounds were filled in the bores. The solution was allowed to diffuse for a period 90 minutes. The Petri dishes were then incubated at 37°C for 24 hours after which zones of inhibition were measured.

The MIC was determined as the lowest concentration of compound that completely inhibits organism growth.
Preparation of test solution: Specified quantity (100 mg) of the compound was accurately weighed and dissolved in 100mL of methanol and further dilution was made to get the concentrations 50µg/mL, 100µg/mL, 150µg/mL, and 200µg/mL.

Antibacterial screening method: All the petri dishes were sterilized in an oven at 160^0C for 1hr. Agar media filter discs and test solutions were sterilized in an autoclave at 121^0C, 15 lbs/sq. inch. Molten sterile agar was poured in sterile Petri dishes aseptically and cooled at room temperature. Bacterial suspensions were poured in Petri dishes aseptically. The sterile paper discs were placed in the four quadrants of Petri dishes aseptically after soaking in the sterile test solutions. The petri dishes were incubated at 37^0C for 24 hrs and the zones of inhibition were observed. (Table 6)

Table 6: *Invitro* antibacterial screening data 3a-e, 4a-e (MIC in µg/mL)

Compounds	MIC (µg/mL) Gram positive bacteria		MIC (µg/mL) Gram negative bacteria
	B. Subtilis	***S. Aureus***	***E. Coli***
3a	100	100	200
3b	100	100	150
3c	150	150	200
3d	100	100	200
3e	150	200	150
4a	100	100	200
4b	50	50	100
4c	200	150	200
4d	100	50	50
4e	100	150	100

Molecular docking studies: The molecular docking tool, VLife MDS 4.6 software was used for ligand docking studies into the enzymes, selective COX-2, with PDB code (4COX) having co-crystallized ligand Indomethacin and glucosamine 6-phosphate synthase with PDB code (1MOQ).[52] Results of molecular docking studies for *N*-substituted 1, 2, 4-triaryl imidazoles with 4COX are given in Table 7.

Molecular docking protocol: The structures of compounds were sketched using the 2D structure draw application Vlife2Ddraw and converted to 3D structures. All the structures were minimized and optimized with the MMFF method taking the root mean square gradient (RMS) of 0.01 kcal/mol A^0 and the iteration limit to 10,000. Conformers for each structure were generated using Monte Carlo by applying MMFF force field

method and the least energy conformer was selected for further study. The molecules chosen from docking studies were used for synthesis purposes. Among them, the first ten compounds showed very good dock score. These molecules were again selected for 3D-QSAR method. The following steps were undertaken for Molecular docking studies:

A. Ligand preparation: Structures of the *N*-substituted 1,2,4-triaryl-*1H*-imidazole ligands were sketched using Chem Sketch 2D draw and converted to 3D structure taken in .mol format. The 3D structure in mol format were then optimized and saved in mol 2 format. MMFF force field with default settings were used for the ligand optimization.

B. Protein preparation: The PDB structures [4COX, 1MOQ] were downloaded from Protein Data Bank. All the bound water molecules, ligands and other moieties were removed from the proteins and saved in pdb format. Cavity No. was 1 selected. The tool neutralised the side chains that were not close to the binding cavity and did not participate in the salt bridge. This step was then followed by restrained minimization of co-crystallized complex, with reoriented side chain hydroxyl group and alleviated potential side steric clashes. The minimization was terminated after either completion of 5,000 steps or energy gradient convergence below 0.05 kcal/mol.

C. Docking methodology: Docking study was performed on VLife MDS version 4.6 on Acer PC, with Windows 7 operating system. To pre-asses the anti-inflammatory and antibacterial behaviour of the designed ligands on a structural basis, automated docking studies were carried out and scoring functions, their binding affinities and orientation of these compounds at the active sites of cox-2 and glucosamine 6-phosphate synthase were found out. The GA-based ligand docking with genetic algorithm approximated a systematic search of positions, orientations and conformations of the ligand in the receptor binding pocket. The minimum dock score is not reproducible because this is a Genetic Algorithm (GA) based run. The input parameters such as number of cycles, Rotation limits, Translation, Convergence etc. affect the dock score. The comparative docking experiments of designed compounds with celecoxib and chloramphenicol were carried out. MDS was successfully employed to dock the ligands into the catalytic site of receptor and correlated to obtain the binding score with inhibitory activity of compounds.

D. Viewing docking results: The H-bonds, charge interaction, hydrophobic and Van der Waals contacts to the receptor were visualized using default settings to analyse the binding modes of the ligands to receptor. Dock score and Binding energy was calculated and lowest dock scores were selected to study their binding interaction with the Cavity No. 1 of the receptors (4COX, 1MOQ).

3D QSAR Studies

A Quantitative Structure-Activity Relationship (QSAR) is a study of the dependence upon chemical structure of some observable property or activity for a series of chemical compounds. This dependence enables predictions to be made about the activity of previously unseen chemical compounds.

Procedure for 3D QSAR

The Modules >>QSARPlus>> 3DQSAR from the main menu of MDS was selected to launch the worksheet. By default, all the molecules in a directory were considered for QSAR. QSAR tool was chosen from which molecules were opened and the subfolder containing set of anti-inflammatory and antibacterial molecules was selected. Activity data which was stored as activity.txt was inserted by selecting File >> Insert Data. The field parameters electrostatic, hydrophobic and steric, were computed by selecting QSAR Tools >> Compute Field window. The Gasteiger-Marsili charge was selected for the computation and invariable columns were removed.

Table 7: Results of molecular docking studies for *N*-substituted 1, 2, 4-triaryl imidazole with 4COX

Compounds	Dock score (KJ/mol)	Hydrogen bonds	Hydrophobic bonds	Van der Waals
3a	-5.093617	-	-	74 ASN, TYR, THR, SER, PHE, GLU, LYS, ILE
3b	-5.879297	01 TYR	-	82 ASN, TYR, THR, SER, PHE, GLU, LYS, ILE
3c	-4.831735	-	-	78 ASN, TYR, THR, SER, PHE, GLU, LYS, ILE
3d	-5.650273	-	-	79 TYR, THR, SER, PHE, GLU, LYS, ILE
3e	-4.516323	-	11 ASN, PRO, TYR, THR, ILE, ASP	91 ASN, TYR, THR, SER, PHE, GLU, LYS, ILE, ASP
4a	-5.064331	-	-	99 ASN, TYR, THR, SER, PHE, GLU, LEU, MET, ALA, ILE
4b	-3.719436	-	-	115 TYR, THR, SER, PHE, GLU, LEU, ALA, ILE
4c	-3.811562	-	-	115 TYR, THR, SER, PHE, GLU, LEU, ALA, ILE
4d	-4.300615	-	-	105 TYR, THR, SER, PHE, GLU, ALA, LEU, ILE
4e	-3.576725	-	12 ASN, PRO, TYR, THR, ILE, ASP	142 ASN, THR, TYR, SER, PHE, GLU, LEU, MET, ALA, LYS, ILE, ASP
Indomethacin	-4.986063	-	29 TYR, SER, PHE, LEU, THR, LYS, GLU,MET, ALA, ILE	150 TYR, THR, SER, PHE, GLU, LEU, LYS, MET, ALA, ILE

The data selection was done by choosing QSAR Tools >> Data Selection. Training data set selection method was applied to create training and test set for this random selection was done. The data was selected in the range of 65% to 85%. Finally, Variable Selection and Model Building Wizard tool was selected for the application of statistical methods like kNN, PLSR, MLR and PCR from Advanced Methods >> Method. The statistical data was generated which results in coefficient of determination r^2, coefficient of regression q^2, cross validated r^2, fitness plot and points of distribution.

Model validation: The results were in terms of r^2, q^2, F-test, and predicted r^2 values. The QSAR models having significant values were selected for the design of compounds. The standard model is explained in Tables 8-10.

Table 8: Regression analysis details

Sr. No.	TERM	MEANING	RANGE
1	K	No. of descriptors in model	Statistically n/5
2	Df	Degree of freedom (n-k-1)	Higher is better
3	r^2	Co-efficient of determination	>0.7
4	q^2	Cross validated r^2	>0.5
5	Pred r^2	r^2 for external test set	>0.5
6	SEE	Standard error of estimate	Smaller is better
7	F-test	Statistical significance of the model	Higher is better

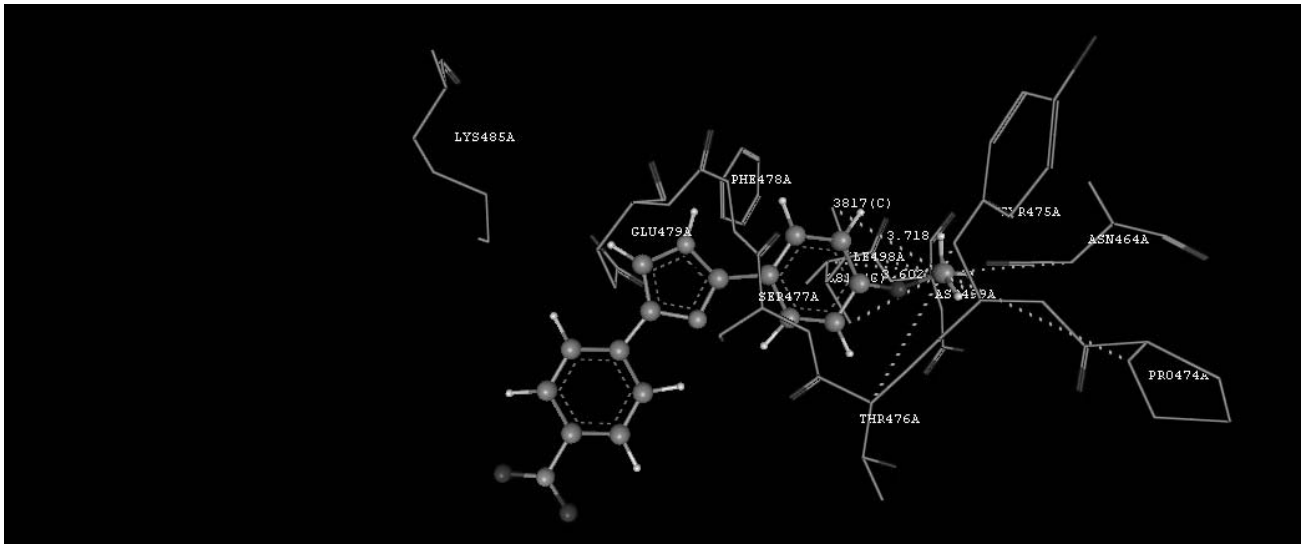

3D QSAR Anti-inflammatory model

Table 9: Unicolumn statistics analysis of the training and test sets for 3D QSAR anti-inflammatory model (3a-3e, 4a-4e)

Data Set	Average	Maximum	Minimum	Standard deviation	Sum
Training Set	83.3713	95.1400	70.0800	9.5799	666.9700
Test Set	92.5150	94.0200	91.0100	2.1284	185.0300

Table 10: Comparative results of 3D QSAR methods for compounds (3a-3e, 4a-4e) as anti-inflammatory agents

Sr. No.	Method	r^2	q^2	F-test	Pred_ r^2	Pred_r^2se
1.	**MLR**	0.9957	0.9556	172.6955	0.8864	4.4180
2.	**PLSR**	0.7439	0.4665	14.5241	0.9350	2.3460
3.	**PCR**	0.8016	0.5593	20.2022	0.7021	5.0236
4.	**Knn**	-	0.7062	-	0.8570	4.9552

Among these methods, MLR showed good results with r^2 0.9991 (99.57%) and the statistical significance of the model is 172.6955. This statistical data along with distribution points and fitness plot was used for design of new compounds. Results of 3D QSAR analysis of *N*-substituted 1, 2, 4-triaryl-*1H*-imidazole for anti-inflammatory model (Figure 6) and Data set used for 3D QSAR analysis with actual and predicted activities of anti-inflammatory compounds (3a-e, 4a-e) are given in Table 10.

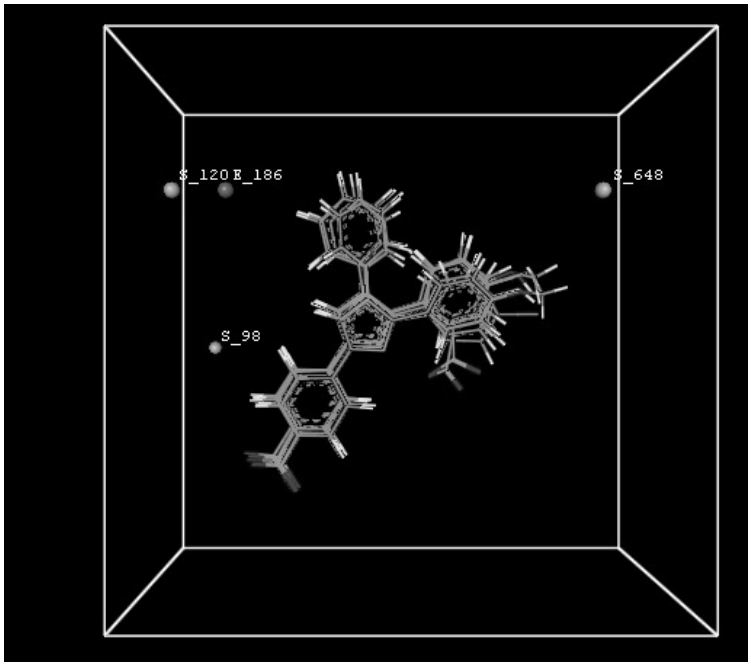

a) 3-D Graphical representation

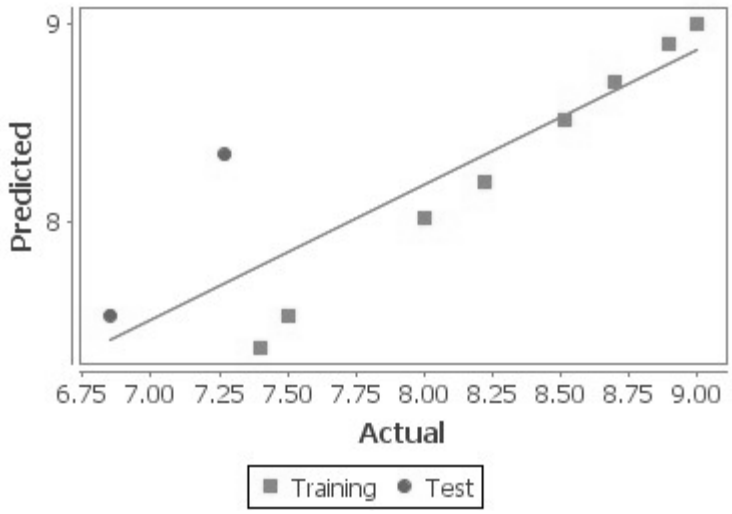

b) Graph of Predicted activity vs Actual activity

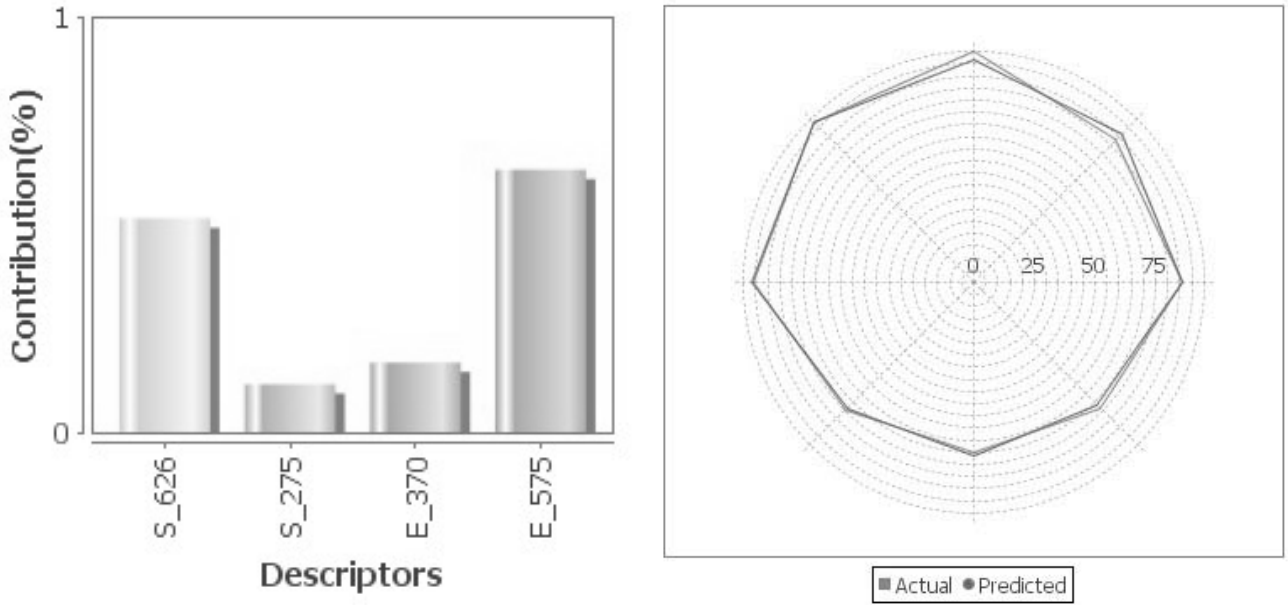

c) Contribution plot **d) Training set**

Fig. 6. Results of 3D QSAR analysis of *N*-substituted 1, 2, 4-triaryl-*1H*-imidazoles for anti-inflammatory model: a) Graphical representation for descriptors, b) Graph of Predicted vs Actual activity, c) Contribution plot for descriptors, d) Training set.

Table 11: Data set used for 3D QSAR analysis with actual and predicted activities of anti-inflammatory compounds (3a-e, 4a-e)

Compound No.	Actual activity	Predicted activity	Residual
3a	49.56	45.91	3.65
3b	36.25	43.78	7.53
3c	22.36	31.26	8.9
3d	27.04	25.37	1.67
3e	40.64	38.02	2.62
4a	25.95	29.01	3.06
4b	30.47	27.53	2.94
4c	42.64	40.00	2.64
4d	21.27	32.87	11.6
4e	27.82	29.94	2.12

3D QSAR antibacterial model

The results obtained from antibacterial activity studies were employed for carrying out the 3D QSAR studies and the minimum inhibitory concentrations (MIC) of ten compounds employed for statistical analysis on the basis of various descriptors such as steric, electrostatic and hydrophobic were calculated and used as independent variables. Unicolumn statistical analysis of the training and test sets for 3D QSAR antibacterial model (3a-3e, 4a-4e) **(**Table 12) and comparative results of 3D QSAR methods for compounds **(3a-3e, 4a-4e)** are shown in Table 13.

Table 12: Unicolumn statistics analysis of the training and test sets for 3D QSAR antibacterial model (3a-3e, 4a-4e)

Data Set	Average	Maximum	Minimum	Standard deviation	Sum
Training Set	8.0567	9.0000	6.8500	0.8481	48.3400
Test Set	8.0050	8.9000	7.4000	0.6996	32.0200

Table 13: Comparative results of 3D QSAR methods for compounds (3a-3e, 4a-4e) as antibacterial

Sr. No.	Method	r^2	q^2	F-test	Pred_ r^2	Pred_r^2se
1.	**MLR**	0.9991	0.9916	809.3574	0.8774	2.3988
2.	**PLSR**	0.9953	0.5785	1270.8739	0.3863	1.3715
3.	**PCR**	0.9178	0.8303	66.9768	0.2842	1.6086
4.	**Knn**	-	0.7483	-	0.6580	0.4106

Conclusions

The molecular docking and 3D-QSAR studies were performed for compounds **(3a-e & 4a-e).**

Both the biological activity studies and QSAR results are in agreement. It was found that compounds **3a, 3b, 3d** and **3e** show good activity as compared to the standard drug indomethacin. In future, these compounds could be used as good anti-inflammatory agents. The QSAR model provided actual and predicted values which were plotted in terms of fitness and activity training graph. The model obtained for QSAR suggests that removal of bulky groups, reduction of hydrophobicity and electropositive groups from the phenyl ring will increase anti-inflammatory activity.

For antibacterial activity, the electronic and steric descriptors play an important role. It was found that increasing both steric hindrance and electrostatic potential at both substituted phenyl rings increases the anti-bacterial activity. Compounds **3a, 3d**, **4a, and 4b** were found to be most potent when compared to chloramphenicol as a standard drug.

Acknowledgements

The authors thanks Department of Pharmaceutical Sciences, RTMNU Nagpur, India for constant support in conducting the research work and also thank to SD Fine Chemicals, E. Merck and Loba Chemie for providing all chemicals and solvents.

References

1. Medzhitov, R., 2008, *Nature*, **454**, 428-435.

2. Chin, L., Deng, H., Cui, H., Fang, J., Zuo, Z., Deng, J., Li, Y., Wang, X. and Zhao, L., 2018, *Oncotarget*, **9**, 7204-7218.

3. Tasneem, S., Liu, B., Li, B., Choudhary, M.I. and Wang, W., 2018, *Pharmacological Research*, **139**, 126-140.

4. Aggarwal, R., Bansal, A., Rozas, I., Kelly, B., Kaushik, P. and Kaushik, D., 2013, *Eur. J. Med. Chem.*, **70**, 350-357.

5. Kaur, M., Singh, M. and Silakari, O., 2013, *Eur. J. Med. Chem.*, **67**, 434-446.

6. Chen, G.Y. and Nuñez, G., 2010, *Nature Reviews Immunology,* **10(12)**, 826-837.

7. Goldring, M.B., 2011, *Current Opinion in Rheumatology,* **23(5)**, 471-478.

8. Cotran, K. and Robbins, 1998, Pathologic Basis of Disease, Philadelphia, W. B. Saunders Company. ISBN 0-7216-7335-X.

9. https://www.healthline.com/health/chronic-inflammation#causes

10. https://www.medicalnewstoday.com/articles/248423

11. Malefyt, D., Abrams, J., Bennett, B. and Figdor, C., 1991, *J. Exp. Med.,* **5**, 12-20.

12. Andrew W., "Chronic inflammation- An American Epidemic". www.mnwelldir.org assessed on 20-8-12.

13. https://www.medicalnewstoday.com/articles/248423#inflammation-helps-wounds-heal.

14. Sever, B., Altýntop, M.D., Kus, G., Ozkurt, M., Ozdemir, A. and Kaplanckl, Z.A., 2016, *Eur. J. Med. Chem.,* **113**, 179-186.

15. Grover, J., Kumar, V. Singh, V., Bairwa, K., Sobhia, M.E. and Jachak, S.M., 2014, *Eur. J. Med. Chem.,* **80**, 47-56.

16. Aggarwal, R., Bansal, A., Rozas, I., Kelly, B., Kaushik, P. and Kaushik, D., 2013, *Eur. J. Med. Chem.,* **70**, 350–357.

17. https://www.livescience.com/52344-inflammation.html.

18. Chennamaneni, S., Zhong, B., Lama, R. and Su, B., 2012, *Eur. J. Med. Chem.,* **56**, 17-29.

19. https://en.wikipedia.org/wiki/Anti-inflammatory #Immune_selective_anti-inflammatory_ derivatives_ (ImSAIDs).

20. Madhukar, M., Sawraj, S. and Sharma, P.D., 2010, *Eur. J. Med. Chem.,* **45**, 2591–2596.

21. Antman, E., Bennett, J. and Daugherty, A., 2007, *Circulation,* **12**, 1634-1642.

22. Siddiqui, A. and Siddiqui, S., 2008, Textbook of Medicinal Chemistry**,** 1st Ed., Birla Publication Pvt. Ltd., p.54-56**.**

23. Barar, F., 2005, Non-narcotic analgesics and antipyretic essentials of pharmacotherapeutics, S. Chand and Company Ltd., New Delhi**,** 3rd Ed., p.117.

24. Leval, D., Julemont, X., Delarge, F., Pirotte, J. and Dogne, D., 2002, *Curr. Med. Chem.,* **9**, 941-962.

25. Abdelall, *Bioorganic Chemistry*, 2019, doi: https://doi.org/10.1016/j.bioorg. 2019.103441.

26. Gierse, J., 1996, *J. Biol. Chem.,* **271**, 1510-1514.

27. Abramson, S. and Weismann, G., 1989, *Arthritis Rheum.,* **32**, 1-9.

28. Cryer, B. and Feldman, M., 1998, *Am. J. Med.,* **104**, 413-421.

29. Block, J., John, B., Wilson and Grisvold's Textbook of Organic Medicinal and Pharmaceutical Chemistry." 11th Ed., Lippincott Wiliams and Wilkins, Philadelphia, p.299-360.

30. "Antibiotic." NHS.5 June 2014. Retrieved 17 January 2015.

31. Factsheet for experts, European Centre for Disease Prevention and Control, Archived from the original on 21 December 2014, Retrieved 21 December 2014.

32. Metronidazole, The American Society of Health System Pharmacists, Retrieved 31 July 2015.

33. John Wiley & Sons, 2012, Chemical Analysis of Antibiotic Residues in Food, Inc., 1-60 ISBN 978-1-4496-1459-1.

34. Stanier, R., Doudorof, M. and Adelberg, E., 1963, "General microbiology." 2nd Ed. Macmillan, New York, p.254-256.

35. Bhatnagar, A. L., Sharma, P. K. and Kumar, N., 2011, *Int. J. Pharmtech Research.,* **3**, 268-282.

36. Mani Chandrika, K.V.S. and Sharma, S., 2020, *Bioorg. Med. Chem.,* doi: https://doi.org/10.1016/j.bmc.2020.115398.

37. Kathiravan, M.K., Salake, A.B., Chothe, A.S., Dudhe, P.B., Watode, R.P., Mukta M.S. and Gadhwe, S., 2012, *Bioorg. Med. Chem.,* **20**, 5678-5698.

38. Aggarwal, R., Bansal, Anshul., Rozas, Isabel., Kelly, B., Kaushik, P. and Kaushik, D., 2013, *Eur. J. Med. Chem.,* **70**, 350-357.

39. Mandolesi Sá, M. and Dalmarco, E.M., 2019, *Biomedicine & Pharmacotherapy,* **111**, 1399-1407.

40. El-Shitanya, N.A. and Eida, B.G., 2019, *Biomedicine & Pharmacotherapy*, **120**, 109567.

41. Pérez-Villanueva, J., Hernández-Campos, A., Yépez-Mulia, L., Méndez-Cuesta, C., Méndez-Lucio, O., Hernández-Luis, F. and Castillo, R., 2013, *Bioorg. Med. Chem.Lett.,* 2**3(14)**, 4221-4224.

42. De Vita, D., Moraca, F., Zamperini, C., Pandolfi, F., Di Santo, R., Matheeussen, A., Maes, L., Tortorella, S. and Scipione, L., 2016, *Eur. J. Med. Chem.*, doi: 10.1016/j.ejmech.2016.02.028.

43. Izabella Krezel, 1998, *II Farmaco*, **53**, 342-345.

44. Ding, H.W., Yu, L., Bai, M. X., Qin, X.C., Song, M.T. and Zhao Q.C., 2019, *Bioorganic Chemistry*, **93**, 103283.

45. Ling L., Dongling Q., Jingxuan C., Jiahao D., Jinwu Z., Lin L. V. and Jianjun C., 2019, *Eur. J. Med. Chem.,* **184**, 111732.

46. Dahiya, R. and Pathak, D., 2007, *Eur. J. Med. Chem.*, **42**, 772-798.

47. Silverstein, R.M. and Bassler, C.G., 1968, Inc., New York., p.71.

48. Beals, R., Sheridan, C.M. and Turck, C.W., 1997, *Crabtree. Science*, **275**, 1930-33.

49. Husain, A., Drabu, S., Kumar, N., Alam, M. and Bawa, S., 2013, *J. Pharm. Bioall. Sci.,* **5**, 154-61.

50. Parmar, N.S. and Prakash, S., 2006, Screening Methods in Pharmacology, 1st Ed., Narosa Publishing House, p.213, 214.

51. Xavier, D., Jacques, D., Fabian, S., Pascal, D., Yves, H., Bernard, P. and Jean- Michel, D., 2000, *Curr. Med. Chem.*, **7**, 1041-1062.

52. Nawwar, Galal and Nabil, Grant., 2013, *Der. Pharma. Chemica.,* **5**, 241-255.

53. Tomi, I.H.R., Al-Daraji, A.H.R., Abdula, A.M. and Al-Marjani, M.F., 2016, *Journal of Saudi Chemical Society*, **20**, 509-516.

RNI No. MAHENG/2017/74063
ISSN No. (Print) 2581-5911
ISI Impact Factor 1.022 (2019-2020)

Development and Validation of Analytical Method by RP-HPLC for Simultaneous Estimation of Rosuvastatin Calcium and Fenofibrate in Pharmaceutical Dosage Form

Awdhut Pimpale* and Rajendra Kakde
Department of Pharmaceutical Sciences, R.T.M. Nagpur University,
Nagpur - 440033, India.
***Email: adityapimpale@gmail.com**

Abstract

A simple, precise, and accurate stability-indicating reversed-phase HPLC method has been developed for the simultaneous estimation of Rosuvastatin calcium and Fenofibrate in combination in tablet formulation. The chromatographic separation was performed on reverse phase Princeton (C18) (250 mm x 4.6 mm, 5 µ) column with mobile phase as a mixture of water (pH adjusted to 3.0 with orthophosphoric acid) and acetonitrile in the ratio (40:60 v/v) at the flow rate 1.0 mL/min. Detection was carried out at wavelength 240 nm. The retention times under the optimized condition of Rosuvastatin calcium and Fenofibrate were found to be 2.485 and 3.905 minutes respectively.

The developed method was validated as per ICH guidelines for specificity, linearity, accuracy, precision, and system suitability. The new RP-HPLC method was successfully applied to market formulations without any interference from the excipients.

Keywords: *Rosuvastatin calcium, Fenofibrate, RP-HPLC, Method validation.*

Introduction

Rosuvastatin calcium (RSV) is chemically (3R,5S,6E)-7-[4-(4-fluorophenyl)-6-(1-methylene)-2[methyl (methyl sulphonyl amino)]-5pyrimidinyl]-3,5-dihydroxy-6-heptenoic acid calcium[1] (Figure 1). It is a synthetic lipid-lowering agent that blocks the production of cholesterol in the body, and a competitive 3-hydroxy-3-methyl-glutaryl coenzyme-A reductase inhibitor effective in lowering LDL cholesterol and triglycerides which has been developed for the treatment of dyslipidemia[2]. Fenofibrate (FEN), is chemically propane-2-yl 2-{4-[(4-chlorophenyl) carbonyl] phenoxy} methyl propanoate[1] (Figure 2). It is a class of medications known as antilipemic and fibric acid. It works by breaking down fats and thus helping the body eliminate triglycerides, is effective at reducing triglyceride levels and increases HDL cholesterol levels. It is used to treat primary hypercholesterolemia, mixed dyslipidemia, severe hypertriglyceridemia[3]. Literature survey revealed that several HPLC methods have been reported for the estimation of rosuvastatin calcium and fenofibrate in isolation or in combination tablet dosage formulation[4-17]. The reported method has the drawbacks of long runtime and the use of a large proportion of organic phase. Hence, an attempt was made to develop

reversed-phase high performance-liquid chromatography (RP-HPLC) which is a simple, rapid, accurate, precise, specific, economical, and sensitive method for the estimation of rosuvastatin calcium and fenofibrate in combined tablet and bulk dosage form.

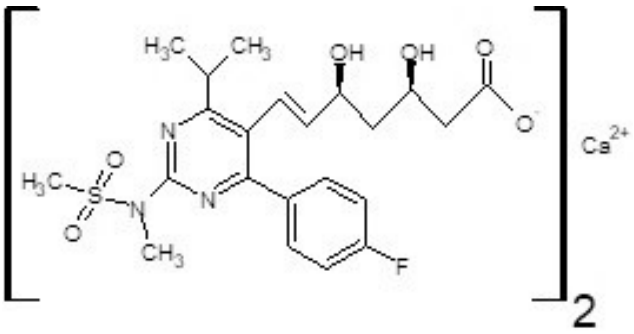

Fig. 1: Chemical structure of Rosuvastatin calcium

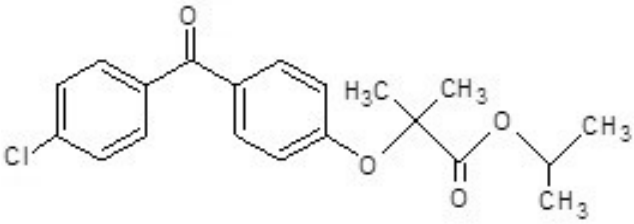

Fig. 2: Chemical structure of Fenofibrate

Materials and Methods

Chemicals and Reagents

Pharmaceutical grade Rosuvastatin Calcium and Fenofibrate were procured as a gift sample from Cadila Pharmaceuticals Ltd., Ahmedabad, India. Zyrova F-10, a tablet formulation, obtained commercially.

Acetonitrile, methanol, orthophosphoric acid, hydrochloric acid, sodium hydroxide, and hydrogen peroxide 30% of analytical grade were used throughout the work.

Instrumentation

Shimadzu HPLC system and PDA detector with Lab Solution software were used.

Chromatographic Conditions

Chromatographic separation was achieved on a reverse-phase column Princeton C18 (250 mm × 4.6 mm, 5 ì) at ambient temperature using a mobile phase consisting of a mixture of buffer (pH 3.0, adjusted with orthophosphoric acid) and acetonitrile in the ratio of (40:60 v/v) at a flow rate of 1.0 mL/min. Detection was carried out at 240 nm. The mobile phase system after preparation was filtered through a membrane filter (0.22 µm) and sonicated for 10 minutes. The pH of the mobile phase was set at 3.0. The injection volume was 10 µl. The results of the optimized chromatographic condition are shown in Table 1. Typical chromatographs of a mixture of standard and sample rosuvastatin calcium and fenofibrate are shown in Figures 3 and 4 respectively.

Table 1: Optimized chromatographic conditions

Chromatographic conditions	
Mobile phase	Water (pH adjusted to 3.0 with ortho phosphoric acid):Acetonitrile (40:60 v/v)
Flow rate	1.0 mL/min.
Column	Princeton C18 (250 mm × 4.6 mm, 5 µ)
Detector wavelength	240 nm
Column temperature	30°C
Injection volume	10 µL
Runtime	20 minutes
Diluent	Acetonitrile: Water (50:50)
Retention time	About 2.485 minutes for Rosuvastatin calcium peak and 3.905 minutes for Fenofibrate peak

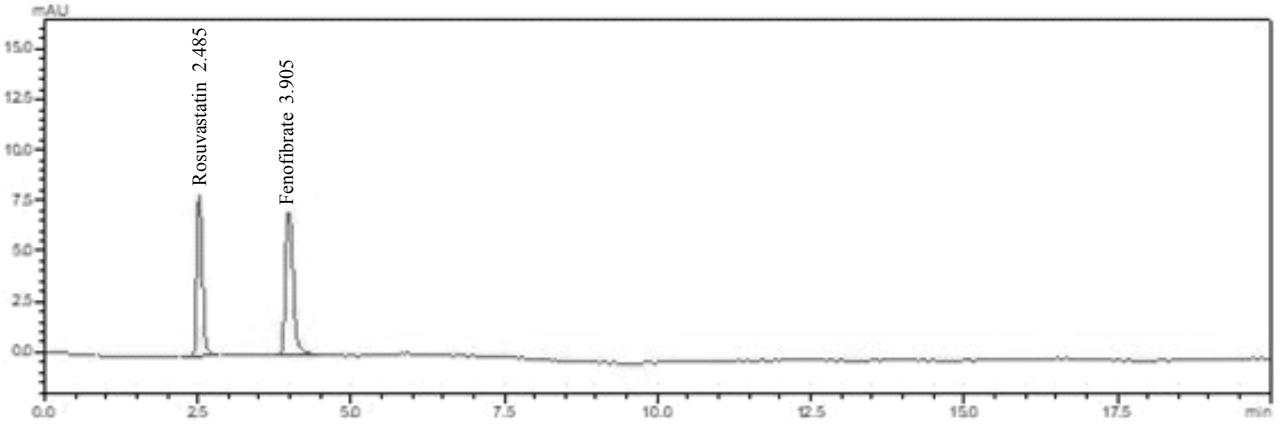

Fig. 3: A typical Chromatograph of a mixture of standard Rosuvastatin calcium and Fenofibrate

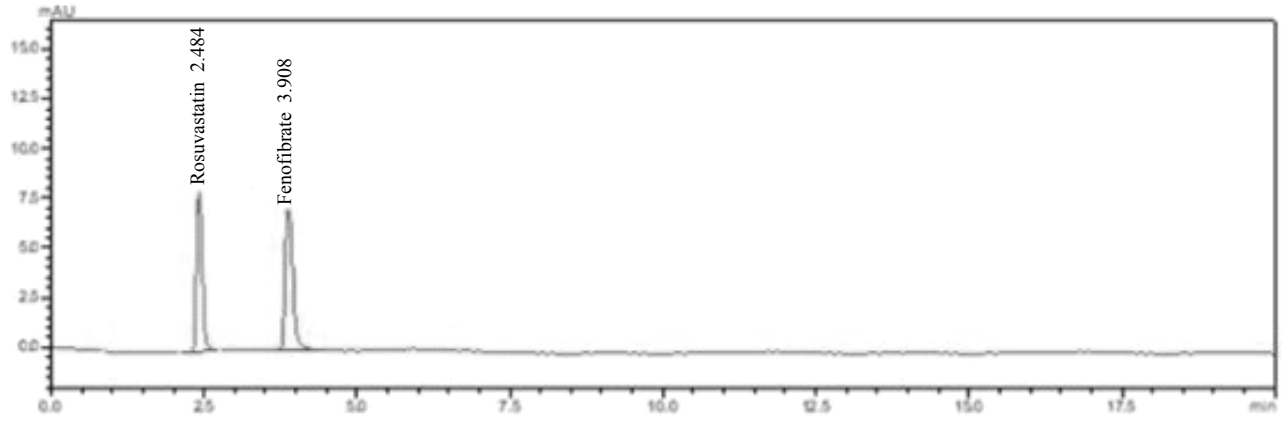

Fig. 4: A typical Chromatograph of a mixture of sample Rosuvastatin calcium and Fenofibrate

Preparation of standard solution of RSV and FEN
For RSV, an accurately weighed 1.0 mg of RSV was transferred into a 10.0 mL volumetric flask and dissolved in 5 mL of diluent, and diluted to 10 mL with diluent. One milliliter of the resulting solution was pipetted out in 10 mL volumetric flask and the volume was made up to 10 mL with diluent to obtain a solution of concentration 10 µg/mL of RSV.

For FEN, an accurately weighed 14.5 mg of FEN was transferred into a 10 mL volumetric flask and dissolved in 5 mL of diluent. The volume was made up to 10 mL with diluent. One milliliter of the resulting solution was pipetted out in 10 mL volumetric flask and the volume was made up to 10 mL with diluent to obtain a solution of concentration 145 µg/mL of FEN.

For the working mixed standard solution, an accurately weighed 1.0 mg of RSV and 14.5 mg of FEN were transferred into a 10 mL volumetric flask and dissolved in 5 mL of diluent. The volume was made upto 10 mL with diluent. One milliliter of the resulting solution was pipetted out in 10 mL volumetric flask and the volume was made up to 10 mL with diluent to obtain a solution of concentration 10 µg/mL and 145 µg/mL of RSV and FEN respectively.

Preparation of sample solution of RSV and FEN

Twenty tablets were weighed and finely powdered. An accurately weighed amount of powder equivalent to 1.0 mg of RSV and 14.5 mg of FEN was transferred into a 10 mL volumetric flask. Then 5.0 ml of diluent was added in it. The flask contents were sonicated for 10 minutes to make the contents homogeneous. This solution was then diluted up to the mark with diluent. The resultant solution was filtered through Whatman Grade I filter paper. One milliliter of the filtrate was transferred into a 10 mL volumetric flask, and then the volume was made up to the mark with diluent to obtain a sample solution containing 10 µg/mL of RSV and 145 µg/mL of FEN.

Six replicate of tablet powder equivalent to 1.0 mg of RSV and 14.5 mg of FEN were transferred into six 10 mL volumetric flask and homogeneous sample solutions were prepared.

Method Validation

Specificity

Specificity is the ability of the method to measure the responses of the analyte in the presence of related substances. The results of system suitability are shown in Table 2.

Table 2: System suitability results

Parameter	RSV	FEN
Theoretical Plate	3636	4997
Retention Time	2.485	3.905
Tailing factor	1.30	1.45
% RSD	0.6	0.4

LOD and LOQ

The LOD is the lowest analyte concentration that can be detected. LOQ is the lowest analyte concentration that can be quantified with acceptable accuracy and precision. The limits of detection (LOD) and quantification (LOQ) were calculated from the standard deviation of the response and the slope of the calibration plot. LOD and LOQ were established, following ICH definitions, by use of the equations LOD = 3.3σ/S and LOQ = 10σ/S, where σ is the standard deviation of the regression line and S is the slope of the calibration plot.

Linearity

Linearity test solutions of RSV and FEN were prepared at concentration levels of 6-16 µg/mL and 116-174 µg/mL respectively. Linearity test solutions were prepared by diluting the stock solution to the required concentrations. Linearity was established by the least-squares linear regression analysis of the calibration data. The results of linearity are shown in Table 3.

Peak areas were plotted against the respective concentrations and linear regression analysis was performed on the resulting curves. The linearity curves for RSV and FEN are shown in Figures 5 and 6 respectively.

Table 3: Linearity results

Parameter	RSV	FEN
Concentration Range (µg/ml)	6-16	116-174
Slope (m)	44776	415.83
Intercept	40116	557.22
Coefficient correlation (r^2)	0.9999	0.9994

Precision

The system precision was evaluated by measuring the area of six qualified working standards for RSV and FEN and calculating the percentage of relative standard deviation (RSD). The assay method precision was evaluated by conducting six independent assays of test samples of RSV and FEN against qualified working standards and calculating the percentage of relative standard deviation (RSD). The intermediate precision of the method was also verified by different analysis on different days.

Accuracy

The accuracy of an analytical procedure expresses the

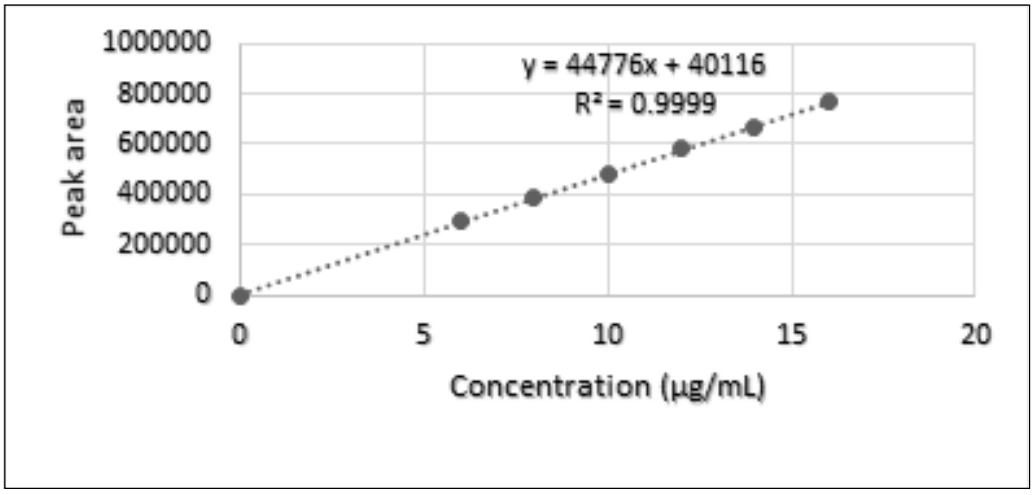

Fig. 5: Linearity curve for Rosuvastatin calcium

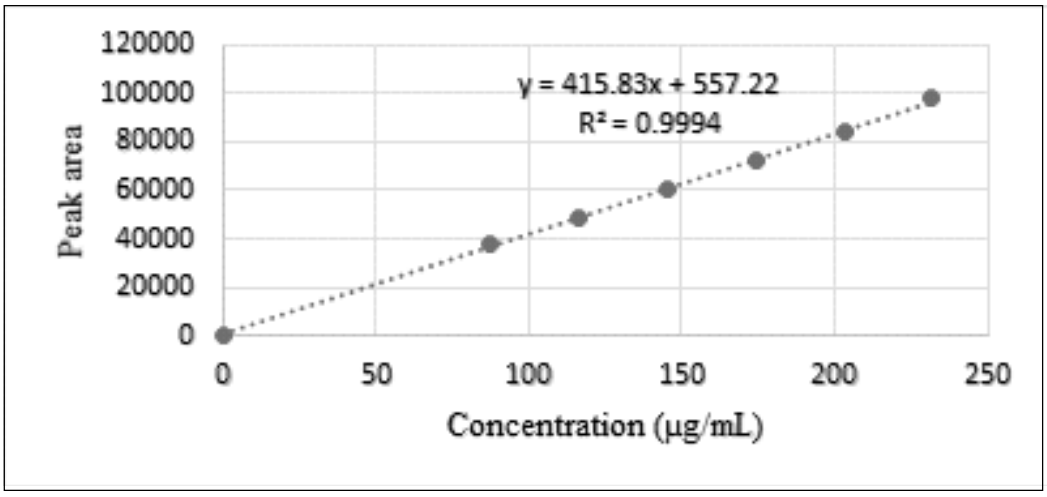

Fig. 6: Linearity curve for Fenofibrate

Table 4: Recovery results

Drug	Spiked level (%)	Amount taken (µg/mL)	Amount found (µg/mL)	% Recovery
RSV	80	8	7.97	98.87
	100	10	10.03	100.30
	120	12	11.96	99.66
FEN	80	116	116.86	100.74
	100	145	145.05	100.04
	120	174	171.65	98.65

closeness of agreement between the value accepted as reference and the value found. It was computed at three different levels, i.e., 80, 100, and 120% of the label claim. Standard addition and recovery experiments were conducted to determine the accuracy of RSV and FEN for the quantification of drugs in the samples. The results of recovery are shown in Table 4.

Robustness

To evaluate the robustness of the developed method, the chromatographic conditions were deliberately altered and the resolution between RSV and FEN was evaluated. To study the effect of wavelength on the estimation, the wavelength was altered by ±2 nm, i.e., 238 and 242 nm from the actual wavelength, 240 nm. To study the effect of flow rate on estimation, the flow rate was altered by ±0.1 mL/min. i.e., 0.9 and 1.1 mL/min. from the actual flow rate, 1.0 mL/min. The results of robustness are shown in Table 5.

Table 5: Robustness results

Conditions		RSV		FEN	
		Amount estimated [%]	RSD [%]	Amount estimated [%]	RSD [%]
Change in wavelength (240±2 nm)	238 nm	97.28	0.5698	100.16	0.0900
	242 nm	98.21	0.5733	100.08	0.1417
Change in flow rate (1.0±0.1 ml/min)	0.9 mL/min	99.55	0.6381	99.37	0.2068
	1.1 mL/min	99.24	0.5078	99.56	0.2009

* Each value is a mean of three observations

Results and Discussion

HPLC method development and optimization

Initially, the pure drug solution was chromatographed using a mobile phase consisting of a mixture of buffer (pH 3.0, adjusted with orthophosphoric acid) and acetonitrile in the ratio of (40:60 v/v) at a flow rate of 1.0 mL/min. Well-resolved peaks of drug were obtained. Detection was carried out at 240 nm. The retention times, under optimized conditions of Rosuvastatin calcium and Fenofibrate were found to be 2.485 and 3.905 minutes respectively. The total run time of the chromatogram was about 20 minutes.

Validation of the method

LOD and LOQ

The LOD values of RSV and FEN were 0.29 and 23.12 respectively. The LOQ values of RSV and FEN were 0.89 and 70.08 respectively.

Linearity

Linearity was established by the least-squares linear regression analysis of the calibration data. Calibration plots were linear over the concentration range of 6-16 µg/mL for RSV and 116-174 µg/mL for FEN. Peak areas were plotted against the respective concentrations and linear regression analysis was performed on the resulting curves. The equation for the calibration plots of RSV was Y= 44776x + 40116, with a correlation coefficient of 0.9999. The equation for the calibration plots of FEN was Y= 415.83x + 557.22, with a correlation coefficient of 0.9994.

Precision

The results of intraday precision and interday precision were 0.6 and 0.9 for RSV. The results of intraday precision and interday precision were 0.4 and 0.8 respectively for FEN. The percentage RSD was well within ±2.0%, indicating that the method was precise.

Accuracy

The percentage of recoveries was 98.69±1.337 % and 100.15± 0.5016% for RSV and FEN respectively.

Robustness

To evaluate the robustness of the developed method, the chromatographic conditions were deliberately altered, and the resolution between RSV and FEN was evaluated. The effect of wavelength and flow rate on the estimation was determined.

The summary of the validation parameters is shown in Table 6.

Table 6: Summary of validation parameters

Parameter	RSV	FEN
Calibration range (µg/mL)	6-16	116-174
Optimized wavelength (nm)	240	240
Retention Time	2.485	3.905
Regression equation (Y)	Y = 44776x + 40116	Y= 415.83x + 557.22
Slope	44776	415.583
Intercept	40116	557.22
Coefficient correlation (r^2)	0.9999	0.9994
Precision (% RSD)		
Intraday	0.6	0.4
Interday	0.9	0.8
% Assay	98.69	100.15
LOD (µg/mL)	0.29	23.12
LOQ (µg/mL)	0.89	70.08

% RSD: Percentage relative standard deviation

Conclusions

The method enables simple, rapid, accurate, precise, specific, economical, and sensitive analysis of Rosuvastatin calcium and Fenofibrate in combined tablet and bulk dosage form. This method was validated as per ICH guidelines. The method can, therefore, be used for routine quality-control analysis of Rosuvastatin calcium and Fenofibrate in combined tablet and bulk dosage form.

Acknowledgments

The authors thank Cadila Pharmaceuticals Ltd, Ahmadabad, India for providing gift samples of pure Rosuvastatin calcium and Fenofibrate, and the Head of Department, Department of Pharmaceutical Sciences, RTM Nagpur University, Nagpur, India for providing the necessary facilities.

References

1. The Merck Index, 2004, 13th Edn., Merck Research Laboratories, Merck & Co., White House Station, NJ, USA. p.3949.

2. Martin P.D., Warwick M.J., Dane A.L., Hill S.J., Giles P.B., Phillips P.J. and Lenz E., 2003, *Clin Ther*., **25**, 2822.

3. Sweetman S.C., 2002, Martindale, Pharmaceutical Press.

4. Rajput P., Shah, D.B. and Maheshwari, D.G., 2018, *Int, J, Res, Pharmacy Pharm, Sci.*, **3**, 28-31.

5. Thammera, R.K., Shitut, N.R., Pasikanti, K.K., Menon, V.C.A., Venkata, V.P.K. and Mullangi, R., 2006, *Biomed Chromatography*, **20**, 881-887.

6. Hassouna, M.E. and Salem, H.O., 2017, *Int. J. Appl. Pharm., Biol., Res.,* **2**, 11-27.

7. SirishaMulukuri, N.V., Srinivasarao, T. and Raveendra, B.G., 2017, *J. Pharm. Res.,* **11**, 257-260.

8. Fathy, M.M., Salama, Mohamed, W.I., Nassar, Mohie, M.K., Sharaf, El-Din., Khalid, A.M., Attia and Mohamed, Yousri Kaddah, 2011, *American J, Anal. Chem.*, **2**, 332-343.

9. Moinuddin, M., Rahaman, S.A., Yadav, B.R. and Battu, R.K., 2012, *Int. J. Pharm. Sci.,* **4**, 150-154.

10. Rao, B.K., Rao, M.N., Ramu, G. and Rambabu, C., 2015, *ACAIJ*, **15**, 160-168.

11. Sailaja, B. and Sravan Kumari, K., 2019, *Asian J. Pharm. Clin. Res.,* **12**, 251-256.

12. Hasumati, A.R., Rajput, S.J., Dave, J.B. and Patel, C.N., 2009, *Int. J. Chem. Tech. Res.*, **1**, 677-689.

13. Gosula, V.R.R., Bobba, V.R., Syed, W.H., Haum, D.G. and Poonam, K., 2011, *Quim. Nova.*, **34**, 250-255.

14. Trivedi, H.K. and Patel, M.C., 2012, *Scientica Pharmaceutica*, **80**, 393-406.

15. Jain, N., Jain, R., Jain, S. and Jain, D.K., 2011, *J. Pharma. Res.*, **10**, 16-20.

16. Singh, S.S., Sharma, K., Patel, H., Jain, M., Shah, H. and Gupta, S., 2005, *J. Braz. Chem. Soc.*, **16**, 944-950.

17. Dujuan, Z., Jing, Z., Xiaoyan, L., Chunmin, W., Rui, Z., Haojing, S., Han, Y., Guiyan, Y., Benjie, W. and Ruichen, G., 2011, *Pharmacol. Pharm.*, **2**, 341-346.

18. ICH Harmonised Tripartite Guideline. Validation of Analytical Procedures: Text and Methodology, Q2(R1), 2005.

19. ICH Harmonised Tripartite Guideline. Stability Testing of New Drug Substances and Products, Q1A(R2), 2003.

RNI No. MAHENG/2017/74063
ISSN No. (Print) 2581-5911
ISI Impact Factor 1.022 (2019-2020)

Analytical Method Development and Validation of Ezetimibe by RP-HPLC

Himani A. Kawale* and Rajendra B. Kakde
Department of Pharmaceutical Sciences,
R.T.M. Nagpur University, Nagpur 440 033, India

Email: khimani1996@gmail.com; drkakde@yahoo.com

Abstract
The present study describes the development of a validated RP-HPLC method for the determination of Ezetimibe drug. The separation was carried out at 40°C on a Princeton C18 (5 µg, 250×4.6 mm) column with Methanol: Acetonitrile (25: 75%v/v) as a mobile phase at a flow rate of 0.8 mL/min. The wavelength of detection was 232nm. Retention time of nearly 3.8 minutes was obtained. Analytical validation parameters such as specificity and selectivity, linearity, accuracy and precision were evaluated. The calibration curve was linear in the range of 2–20 µg/mL with a correlation co-efficient 0.999. Relative standard deviation values for all key parameters, was less than 2.0%. The method was validated according to ICH guidelines and the acceptance criteria for accuracy, precision, linearity, specificity and system suitability were met in all cases.

Keywords: *Ezetimibe, RP-HPLC, room temperature, Methanol.*

Introduction

The drug Ezetimibe (EZT), (3R, 4S)-1-(4-fluorophenyl)-3-[(3S)-3-(4-fluorophenyl)-3-hydroxypropyl]-4-(4-hydroxyphenyl) azetidin-2-one (Fig. 1) marketed as Ezetrol, is used as a cholesterol absorption inhibitor. It is a white powder soluble in methanol and acetronitrile.

A variety of chromatographic methods based on HPLC have been developed to resolve drugs and their related impurities. In the drug industry, UV detection is commonly used.

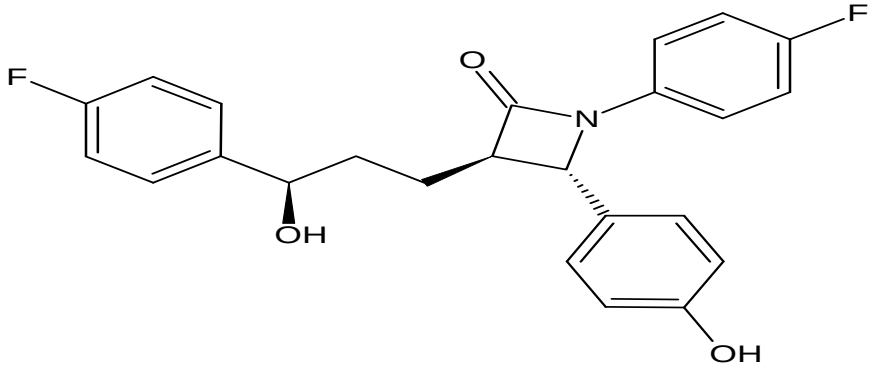

Fig. 1: Structure of Ezetimibe

Materials and Methods

EZT was received as a gift sample from Glenmark Pharmaceuticals, Mumbai, India. All chemicals of HPLC grade were used throughout the experiment. Hydrochloric acid, Sodium hydroxide and Hydrogen peroxide of Analytical Reagent Grades purchased from Loba Chemie Pvt. Ltd., Mumbai, India were used for the study.

Instrumentation and analytical conditions

HPLC system (Shimadzu) consisted of LC-20AD with LC Solution Software, SPD-M20A prominence PDA detector, DGU-20A_5 prominence degasser and Rheodyne injector 7725i with 20µL loop. The separation was carried out using Princeton C18 (250mm × 4.6 mm, 5µg), at the flow rate of 0.5 mL/min. The wavelength of detection was 294 nm.

Ultra-Violet Visible Spectrophotometric method

JASCO UV VIS SPECTROPHOTOMETER (Model Name- V-630, serial no. C280261148) was used for the wavelength determination.

Sample Preparation

Preparation of stock solution (Solution A)

10 mg EZT was dissolved in 10 mL of Methanol to give 1000 µg/mL of EZT.

Preparation of working standard solution (Solution B)

1 mL from solution A was pipetted out and diluted up to 10 mL with diluent to give 100 µg/mL of EZT.

Preparation of working standard solution (Solution C)

1 mL of solution B was pipetted out and diluted up to 10 mL with diluent and sonicated for 15 min. to give 10 µg/mL of EZT.

Optimization of Chromatographic conditions

Chromatographic studies were performed on trial and error basis, after using different mobile phases and columns. The retention of EZT was found to be adequate on Princeton C18 column in Methanol: Acetonitirile (25:75 v/v) at flow rate of 0.8 mL/ min with a retention time of 3.851 ± 0.05 min. with sharp peak, good peak symmetry and minimum tailing factor.

Results and Discussion

Determination of working wavelength (λ_{max})

The working standard solution was scanned in the UV range (400-200 nm) in 1.0 cm quartz cell against solvent blank. The λ_{max} was found to be 232 nm. The UV absorption spectrum of the drug is shown in Figure 2.

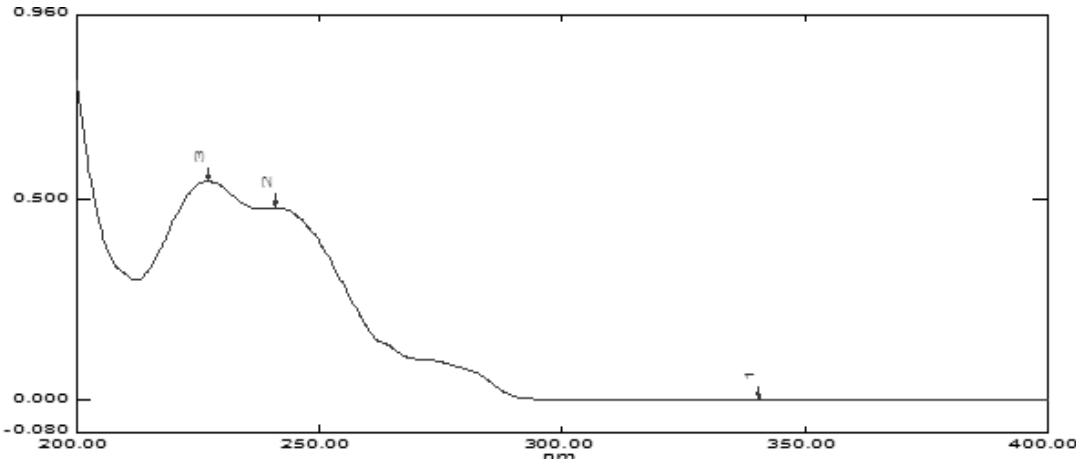

Fig. 2: UV Absorption Spectrum of EZT at 400-200 nm

Chromatographic conditions for drug on analytical HPLC

The following chromatographic parameters were established on the basis of literature review and chemistry of compound and column and were kept constant during experimentation (Table 1).

Table 1: Optimized Chromatographic Conditions for EZT on HPLC

Column	**PRINCETON, C18, 4.6 mm × 150 mm 5µ**
Detection wavelength	232 nm
Injection volume	25 µL
Pump mode	Gradient
Flow rate	0.8 mL/min
Temperature	40°C
Mobile phase	ACN : Methanol (75:25 v/v)
Retention time	3.89 minutes

The Chromatographic column conditions were set as per the established parameters and the mobile phase was allowed to equilibrate with the stationary phase. The working standard solution was injected and the resulting chromatograms are reproduced in Figure 3.

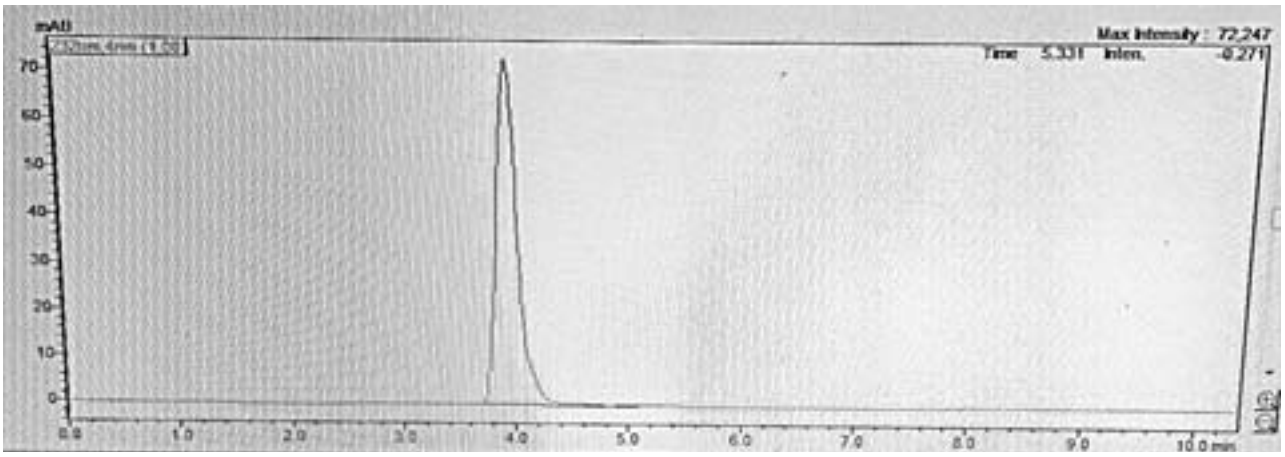

Fig. 3: Chromatogram of EZT

Validation Studies:

System Suitability Parameters:

System suitability is an integral part of method validation to evaluate the parameters like tailing factor, theoretical plates, resolution and % RSD for replicate injections. The results were within the limits (Table 2).

Table 2: Study of System Suitability parameters

Sr. No.	Retention Time	No. of Theoretical Plates	Peak Area	Tailing Factor
1	3.89	2781	385301	1.731
2	3.90	2759	387689	1.688
3	3.88	2727	397600	1.659
4	3.89	2776	382689	1.678
5	3.90	2668	390159	1.704
6	3.88	2779	380390	1.738
MEAN	3.89	2748.33	387304.66	1.6996
S.D.	0.0089	44.2613	6122.42	0.0307
%RSD	0.2299	1.6104	1.5807	1.8094

Linearity of Response:

Linearity was evaluated by measuring mean peak areas at different concentrations of the standard solutions of SGT. The calibration curve was constructed by plotting concentration of standard solutions against mean peak areas and the regression equation was computed. The summary of the parameters is shown in Table 3 and in Figure 4.

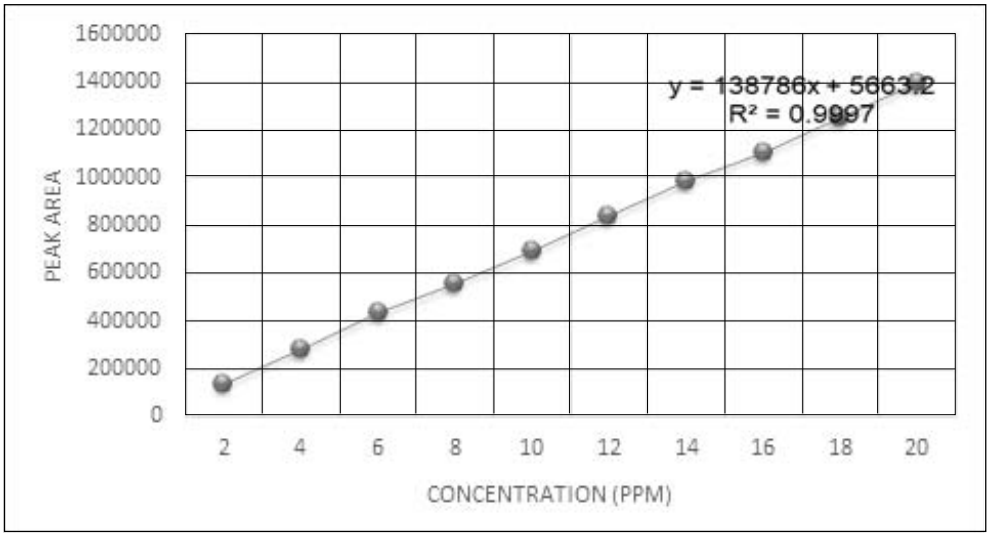

Fig. 4: Linearity Study of EZT

Table 3: Data for Regression Analysis

Parameters	Ezetimibe
Linear dynamic range (µg/mL)	2-20
Slope	138786
Intercept	5663.2
Correlation coefficient (R^2)	0.9997

Accuracy:

Three independent samples (80%, 100%, and 120%) were prepared for each level. Three replicate injections of each of the sample solutions were made separately and chromatograms were recorded. The accuracy was calculated as percentage recovery as depicted in Table 5.

Table 5: Results of Accuracy Study by HPLC

Ezetrol tablets (Avg. Wt. 105.35 mg for 10 mg of Ezetrol)						
Level	Weight of sample taken (mg)	Amount of standard added (mg)	Area		Total estimated weight of drug(mg)	% Recovery
			Sample	standard		
80%	105.35	8	1835117	818645	17.93	99.16
100%	105.34	10	1633237	818645	19.95	99.50
120%	105.36	12	1498978	818645	21.97	99.77
				Overall	Mean	99.54
					± SD	0.3202
					% RSD	0.3216

*Mean of 3 readings

Precision:

Intraday precision (Repeatability) was performed by analysis of six independent samples within a day. Three replicate injection of each of sample solutions were made separately and chromatograms were recorded. Similarly three replicate injections were made daily for six days on six independent samples for interday precision. Table 6 represents the results of intermediate precision. The System precision was determined by analysis of the same sample over a time interval. Results of precision were expressed as% recovery and are tabulated in Table 6.

Table 6: Results of Precision Study by HPLC

Sr. No.	Observations	% DRUG ESTIMATION		
		Intra-day*	Inter-day*	Different Analyst*
1	I	99.21	99.87	99.67
2	II	99.43	99.12	100.01
3	III	99.35	100	99.52
4	IV	99.36	98.97	99.3
5	V	99.62	99.74	99.13
6	VI	98.14	99.62	99.12
Mean		**99.1850**	**99.553**	**99**
SD		**0.5291**	**0.4164**	**0.346**
%RSD		**0.5335**	**0.4183**	**0.348**

*Mean of 3 readings

Specificity Studies:

After stipulated time of stress conditions, the samples were analyzed and the absorbance of each of the resulting solutions was measured at 251 nm using solvent blank and the drug content was estimated (Table 7).

Table 7: Results of Specificity Study

Sr. No	Treatment	Time	Weight of tablet powder (mg)*	Concentration (µg/ml)	%Drug estimation*
1.	Neutral	24hrs	105.3	10	99.89
2.	0.1N Acid	24hrs	105.3	10	79.44
3.	0.1N Alkali	24hrs	105.3	10	71.77
4.	6% Peroxide	3hrs	105.3	10	74.83
5.	Thermal	8hrs	105.3	10	94.52
6.	Photo	24hrs	105.3	10	93.25

*Mean of observation

Limit of detection (LOD) and Limit of quantitation (LOQ)

The estimation of detection limit (DL) and quantitation limit (QL) were determined using the acceptable signal-to-noise ratios 3:1 and 10:1, respectively. LOD and LOQ were determined using the method based on standard deviation of the response and the slope of calibration curve as shown below:

$$LOD = \frac{3.3\sigma}{S} \text{ and } LOQ = \frac{10\sigma}{S}$$

where,

σ is Standard deviation of response

S is Slope of calibration curve

Table 8: Results of LOD & LOQ Study by HPLC

LOD (µg/mL)	0.4071
LOQ (µg/mL)	1.2337

Robustness:

The robustness of the method was not affected when small and deliberate changes in flow change, mobile phase composition, column temperature were made at 100% test concentration. The parameters and results are shown Tables 9 and 10.

Table 9: Parameters for Robustness study

Parameter	- Level	Nominal	+ Level
Change in Acetonitrile content in total mobile phase	73.00 mL	75.00 mL	77.00 mL
Change in flow rate	0.6mL/min	0.8mL/min	1.0mL/min

Table 10: Results of Robustness Parameters by HPLC

Ezetrol (Avg. Wt. 105.35 mg for 10 mg of Ezetimibe)				
% Estimation	Acetonitrile content in mobile phase [Acetonitrile: MeOH(75:25v/v)]		Flow Rate (0.8 mL/min ± 0.2)	
	73mL Acetonitrile	77mL Acetonitrile	0.6 mL/min	1.0 mL/min
Mean	99.8	100.07	99.12	100.15
SD	0.2193	0.365	1.2581	0.6392
%RSD	0.2197	0.3647	1.2693	0.6382
Retention Time			5.932	3.015

*Mean of 3 readings

Assay of pharmaceutical formulations:

Standard solution: Solution C was used as the working standard.

Sample solution:

For sample preparation, methanol was used as diluent for experiments. Twenty tablets were weighed and finely powdered. An accurately weighed tablet powder equivalent to 10 mg of EZT was transferred into a 10 mL volumetric flask. About 5 mL of methanol was added and the mixture was sonicated for 15 min. Then the solution was diluted up to the mark with methanol (1000 µg/mL). The resultant solution was filtered through Whatmann Grade I filter paper. 1mL of filtrate was transferred to a 10 mL volumetric flask and then volume was made up to the mark with methanol to obtain a concentration of 100 mg/mL. Six independent samples were prepared by diluting 1ml of 100µg/mL to get the final concentration of EZT 10µg/mL.

Procedure:

After equilibration of stationary phase, three replicate injections of each of the sample solutions were made separately and chromatograms were recorded. % assay was calculated using the formula,

$$\%\text{Assay} = \frac{A_{sam} \times C_{std} \times DF \times \text{Avg.Wt.}}{A_{std} \times \text{Wt. taken} \times LC}$$

where,

A_{sam} = Area of Sample taken
A_{std} = Area of Standard taken
C_{std} = Concentration of standard, µg/ml
DF = Dilution Factor
Avg. Wt. = Average weight of tablets
Wt. taken = Weight of tablet powder taken
LC = Labeled Claim

The results of percentage assay are shown in Table 11.

Table 11: Analysis of Marketed Formulations by HPLC

Sr. No.	Wt. of Sample (mg)	Area of Sample	Area of Standard	% Assay
1	101.23	695633	698544	99.22
2	101.13	695634		99.56
3	101.25	695651		99.86
4	101.24	695673		99.22
5	101.24	695664		99.56
6	101.25	695664		99.86
			Mean	**99.48**
			SD	**0.3038**
			%RSD	**0.3054**

Conclusions

The proposed RP-HPLC method was found to be simple, accurate, precise and rapid and was found suitable for the estimation of Ezetimibe in tablet dosage form. All the parameters met the criteria of ICH guidelines for method validation. The reported method is more economical and can find practical applications and may be recommended for QC analysis.

Acknowledgement

The authors are thankful to Glenmark Pharmaceuticals, Mumbai, India for providing drug samples and Department of Pharmaceutical Sciences, RTMNU, Nagpur, India for providing facilities to carry out this work.

References

1. Anonymous, ICH Q1A (R2), Stability Testing of Drug Substances and Products, International Conference of Harmonization, IFPMA, Geneva, 2003.

2. Anonymous, ICH Q1B, Stability Testing: Photo Stability Testing of New Drug Substances and Products; In Proceedings of the International Conference on Harmonization, IFPMA, Geneva, 1996.

3. Anonymous, ICH, Q2 (R1), Validation of Analytical Procedures: Text and Methodology In Proceedings the International Conference on Harmonization, IFPMA, Geneva, 2005.

4. Sreedhar B., Pavani P., et al., 2015, *International Journal of Pharmaceutical Sciences and Research*, **6(3)**, 1066–77.

5. D. Swathi, S., T. Hemant, K., K. Vara, P.R. and Y. Srinivasa, R., 2015, *International Journal of Pharmacy and Pharmaceutical Research*, **7(4)**.

6. Cansel, K.O., Ozgur, E., Sevinc, K. and Ayhan, S., et. al., 2015, Development of a Suitable Dissolution Method for the Combined Tablet Formulation of Atorvastatin and Ezetimibe by RP-LC Method.

7. Kumar, P., Ghosh, A. and Chaudhary, M., 2012, *Pharmaceutica Analytica Acta.*, **3(6)**.

8. Gurram, S.C., 2015, *Biochemistry & Analytical Biochemistry*, **4(2)**, 8-11.

9. Mukthinuthalapati, M.A., Bukkapatnam, V., Pavan, S. and Bandaru, K., 2014, Stability Indicating Liquid Chromatographic Method for the Simultaneous Determination of Rosuvastatin and Ezetimibe in Pharmaceutical Formulations. 4(4), 405-11.

10. Goel, A., Baboota, S., Sahni, J.K., Srinivas, K.S., Gupta, R.S. and Gupta, A., et. al., 2013, Development and Validation of Stability-Indicating Assay Method by UPLC for a Fixed Dose Combination of Atorvastatin and Ezetimibe, p.222-8.

11. Choudhari, V.P. and Nikalje, A.P., 2010, *Pharmaceutica Analytica Acta.*, **1(2)**, 1-5.

Conference Alerts

1) The 6th International Conference on Chemical Materials and Process (ICCMP 2020)
July 2-4, 2020, Warsaw, Poland
Website : http://www.iccmp.org

2) 5th International Conference on Water Pollution and Treatment (ICWPT 2020)
July 14-16, 2020, Frankfurt, Germany
Website : http://www.icwpt.net

3) 5th International Conference on Green Chemistry and Sustainable Engineering (GREEN -20)
July 22-24, 2020, Rome, Italy
Website : https://greenchem-20.chem

4) Medical Conference on Pharmaceutical Science and Chemistry
August 10-11, 2020, London, UK
Website : http://pharma.averconferences.com/

5) International Conference on Chemistry and Catalysis
August 10-12, 2020, Prague, Czech Republic
Website : http://chemistry.deligoninternational.com/

6) Global Meeting on Nanotechnology
August 19-20, 2020, Boston, Massachusetts, USA
Website : mecglobalevents.com/conferences/nanotechnology/

7) 1st Malaysia International Conference on Nanotechnology and Catalysis
August 25-27, 2020, Langkawi Island, Malaysia
Website : https://umevent.um.edu.my/MICNC2020

8) 9th International Conference on Environment,Chemistry and Biology (ICECB 2020)
September 8-10, 2020, Helsinki, Finland
Website : http://www.icecb.org

9) 11th International Conference on Green Chemistry and Environment (Webinar)
September 19, 2020
Enquiries : sustainablechemistry@annualmeetings.net

10) 3rd International Conference on Oil & Gas Chemistry and Additives
September 24-25, 2020, Ahmedabad, India
Website : http://oilfieldchemistry.org/

11) The 2nd International Conference on Green Energy and Environment 2020 (ICoGEE 2020)
October 8, 2020, Pangkai Pinang, Bangka Belitung, Indonesia
Website : http://icogee.org

12) 11th International Conference on Biology, Environment and Chemistry (ICBEC 2020)
October 22-24, 2020, Lisbon, Portugal
Website : http://www.icbec.org

13) SQU International Chemistry Conference 2020: Natural Products Chemistry and Herbal Medicine
November 10-12, 2020, Muscat, Oman
Website : http://conferences.squ.edu.om/icc2020/

14) 8th International Symposium on Energy from Biomass and Waste
November 16-19, 2020, Venice, Italy
Enquiries : info@venicesymposium.it

15) 9th International Conference on Chemical Science and Engineering (ICCSE 2020)
November 20-22, 2020, Macau, China
Website : http://www.iccse.org/

16) International Conference on Environment 2020
December 8-10, 2020, Putrajaya, Malaysia
Website : http://chemical.eng.usm.mu/ICENV2020/

17) 2nd International Conference on Functional Materials and Applied Technologies (FMAT2020)
December 15-17, 2020, Tokyo, Japan
Website : http://www.fmat.org/

18) International Conference on Environmental Science and Applications (ICESA'20)
December 15-18, 2020, Seoul, South Korea
Website : https://esacconference.com/

RNI No. MAHENG / 2017 / 74063
VOLUME 4 (Issue I) July - Dec 2020

ISSN No. 2581-5911
BI-ANNUAL SUBSCRIPTION : Rs. 2000/-

G P GLOBALIZE
RESEARCH JOURNAL OF CHEMISTRY

VOLUME 4 (Issue I) July - Dec 2020
BI-ANNUAL 2020

GAURANG PUBLISHING

GAURANG PUBLISHING GLOBALIZE
PRIVATE LIMITED
1, Plot-72, P.M.M.M. Marg, Tardeo, Mumbai-400034. **Tel.:** 022 23522068 **(M) :** +91 9969392245
Email : gpglobalize@gmail.com | **Web :** www.gpglobalize.in

CIN No. U22130MH2016PTC287238 | UAN - MH19D0008178